CANADIAN THESES ON MICROFICHE

THÈSES CANADIENNES SUR MICROFICHE

National Library of Canada
Collections Development Branch

Canadian Theses on
Microfiche Service

Ottawa, Canada
K1A 0N4

Bibliothèque nationale du Canada
Direction du développement des collections

Service des thèses canadiennes
sur microfiche

NOTICE

The quality of this microfiche is heavily dependent upon the quality of the original thesis submitted for microfilming. Every effort has been made to ensure the highest quality of reproduction possible.

If pages are missing, contact the university which granted the degree.

Some pages may have indistinct print especially if the original pages were typed with a poor typewriter ribbon or if the university sent us an inferior photocopy.

Previously copyrighted materials (journal articles, published tests, etc.) are not filmed.

Reproduction in full or in part of this film is governed by the Canadian Copyright Act, R.S.C. 1970, c. C-30. Please read the authorization forms which accompany this thesis.

AVIS

La qualité de cette microfiche dépend grandement de la qualité de la thèse soumise au microfilmage. Nous avons tout fait pour assurer une qualité supérieure de reproduction.

S'il manque des pages, veuillez communiquer avec l'université qui a conféré le grade.

La qualité d'impression de certaines pages peut laisser à désirer, surtout si les pages originales ont été dactylographiées à l'aide d'un ruban usé ou si l'université nous a fait parvenir une photocopie de qualité inférieure.

Les documents qui font déjà l'objet d'un droit d'auteur (articles de revue, examens publiés, etc.) ne sont pas microfilmés.

La reproduction, même partielle, de ce microfilm est soumise à la Loi canadienne sur le droit d'auteur, SRC 1970, c. C-30. Veuillez prendre connaissance des formules d'autorisation qui accompagnent cette thèse.

THIS DISSERTATION
HAS BEEN MICROFILMED
EXACTLY AS RECEIVED

LA THÈSE A ÉTÉ
MICROFILMÉE TELLE QUE
NOUS L'AVONS REÇUE

NL 339 (r. 85/09)

Canada

Ottawa, Canada
K1A 0N4

190

87440

ISBN 0-315-19532-0

CANADIAN THESES ON MICROFICHE SERVICE – SERVICE DES THÈSES CANADIENNES SUR MICROFICHE

PERMISION TO MICROFILM – AUTORISATION DE MICROFILMER

• Please print or type – Écrire en lettres moulées ou dactylographier

AUTHOR – AUTEUR

Full Name of Author – Nom complet de l'auteur

PETER EVAN ASHMORE

Date of Birth – Date de naissance	Canadian Citizen – Citoyen canadien
28 FEB. 1956	☐ Yes / Oui ☑ No / Non
Country of Birth – Lieu de naissance	**Permanent Address – Résidence fixe**
UNITED KINGDOM	FARNHAM HOUSE, HESKET NEWMARKET, WIGTON, CUMBRIA, ENGLAND

THESIS – THÈSE

Title of Thesis – Titre de la thèse

PROCESS AND FORM IN GRAVEL BRAIDED STREAMS: LABORATORY MODELLING AND FIELD OBSERVATIONS

Degree for which thesis was presented – Grade pour lequel cette thèse fut présentée	Year this degree conferred – Année d'obtention de ce grade
Ph. D.	1985
University – Université	**Name of Supervisor – Nom du directeur de thèse**
UNIVERSITY OF ALBERTA	Dr. J. SHAW Dr. R. B. RAINS

AUTHORIZATION – AUTORISATION

Permission is hereby granted to the NATIONAL LIBRARY OF CANADA to **microfilm** this thesis and to **lend** or **sell copies of the film.**

The author reserves other publication rights, and neither the thesis nor extensive extracts from it may be printed or otherwise reproduced without the author's written permission.

L'autorisation est, par la présente, accordée à la BIBLIOTHÈQUE NATIONALE DU CANADA de **microfilmer** cette thèse et de **prêter** ou de **vendre des exemplaires du film.**

L'auteur se réserve les autres droits de publication; ni la thèse ni de longs extraits de celle-ci ne doivent être imprimés ou autrement reproduits sans l'autorisation écrite de l'auteur.

ATTACH FORM TO THESIS – VEUILLEZ JOINDRE CE FORMULAIRE À LA THÈSE

Signature	Date
Peter Ashmore	27 March 1985

Canada

THE UNIVERSITY OF ALBERTA

PROCESS AND FORM IN GRAVEL BRAIDED STREAMS: LABORATORY MODELLING AND FIELD OBSERVATIONS

by

PETER EUAN ASHMORE

A THESIS

SUBMITTED TO THE FACULTY OF GRADUATE STUDIES AND RESEARCH IN PARTIAL FULFILMENT OF THE REQUIREMENTS FOR THE DEGREE OF DOCTOR OF PHILOSOPHY.

DEPARTMENT OF GEOGRAPHY

EDMONTON, ALBERTA

SPRING, 1985

THE UNIVERSITY OF ALBERTA

RELEASE FORM

Name of Author: PETER EUAN ASHMORE

Title of Thesis:

PROCESS AND FORM IN GRAVEL BRAIDED STREAMS: LABORATORY MODELLING AND FIELD OBSERVATIONS

Degree for which Thesis was presented: DOCTOR OF PHILOSOPHY

Year this degree granted: 1985

Peter Ashmore

PERMANENT ADDRESS:

FARNHAM HOUSE,
HESKET NEWMARKET
WIGTON
CUMBRIA,
ENGLAND

DATED

25 March 1985

THE UNIVERSITY OF ALBERTA

FACULTY OF GRADUATE STUDIES AND RESEARCH

The undersigned certify that they have read, and recommend to the Faculty of Graduate Studies and Research, for acceptance, a thesis entitled

PROCESS AND FORM IN GRAVEL BRAIDED STREAMS: LABORATORY MODELLING AND FIELD OBSERVATIONS

submitted by PETER EUAN ASHMORE

in partial fulfillment of the requirements for the degree of Doctor of Philosophy.

John Shaw

R C Kellerhals

Supervisors

David Cunningham

D. Lister

Gerald L. Smith

External Examiner

Date March 8 1985

Abstract

Aspects of sediment transport, channel morphology and sedimentary processes in gravel braided streams were examined using Froude number modelling to produce small-scale laboratory streams, augmented by field data from Sunwapta River, Alberta.

Ten laboratory runs, each of 60 hours duration, were carried out at seven different combinations of slope and discharge. Mean bedload transport rate is positively correlated with discharge and stream power index. When adjusted for the critical conditions of motion, dimensionless sediment transport rates in the model runs compared closely with measured rates in published studies of several field gravel rivers and laboratory streams, and with the empirical and theoretical relationships of Meyer-Peter and Muller (1948), Einstein (1950) and Parker (1978).

Absolute confluence scour depth is largely a function of total discharge and confluence angle. Scour depth relative to the depth of the confluent channels varies from about 2 to 7 in the laboratory and field data. This depth is primarily a function of confluence angle and secondarily of the proportion of the total discharge carried in each confluent channel. Field and laboratory data for these relationships are closely comparable. Scour holes do not become armoured during their formation; the flow in the scour hole has a slightly greater competence than that in the confluent channels. The confluences exert considerable influence on the location of aggradation and channel division immediately downstream of scour holes.

Braiding may be initiated from a straight channel by one of three mechanisms; cut-off of meanders developed from alternating bars, mid-channel

aggradation, and incision of "proto-channels" into the bed of steep, shallow ($h/D_{50}<4$) flows. The occurrence of the first of these can be partly predicted using existing criteria for the occurrence of alternating bars. Cut-offs result in the formation of zones of flow convergence (confluences) and divergence (medial bar deposition) whose spacing is similar to that of the wavelength of the prior meanders. The occurrence of alternating bars and the development of avalanche faces on migratory unit bars is subject to control by flow depth and bed shear stress.

Braiding intensity, bed relief and the abundance of avalanche-face bars are all positively correlated with stream power. Greater stream power in excess of the critical value for sediment motion produces a progression from 'proximal' braided stream morphology to one more characteristic of 'distal' braided streams.

Braiding intensity and avalanche-face bar development are also related to regular fluctuations in the sediment transport rate that occur at the scale of a few hours. An increase in the sediment delivery rate to an area of the channel causes aggradation, increased braiding and the formation of a greater number of avalanche faces. A given area of the stream undergoes repeated cycles of aggradation and degradation resulting in the transfer of sediment in a series of steps along the channel. Smaller-scale fluctuations in the sediment transport rate, in the form of diffuse sheets and unit bars, are responsible for the step-by-step construction of complex bars and fluctuations in scour depth at confluences. Thus, the process of sediment transport and the morphology of the braided stream are intimately linked.

Acknowledgements

I have many people to thank for their contributions over the past few years which enabled me to complete this work. Dr. John Shaw supervised the work throughout. I am grateful for his time freely given on so many occasions, his advice and encouragement, his thorough reading and criticism of this, and earlier, drafts and for his example. Dr. Bruce Rains acted as nominal supervisor from September 1982 onwards and was a great help in seeing the thesis through the final stages. Dr. Gary Parker has been involved in the project from the outset. The thesis owes much to his teaching and assistance.

Research funding was provided by the Natural Sciences and Engineering Research Council of Canada through grants to Dr. Shaw and Dr. Parker. Additional support for field work was granted by Alberta Research Council and the Department of the Environment of the Province of Alberta. For three years I received personal funding through an Izaak Walton Killam Doctoral Scholarship, for which I am grateful. The Geography Department at Queen's University at Kingston provided me with a Teaching Assistantship for four months, and the work was completed while I was employed in the Geography Department at the Memorial University of Newfoundland. I am grateful to the latter for covering the cost of some of the photographic work.

I am indebted to the Civil Engineering Department of the University of Alberta for allowing me prolonged use of their Hydraulics Laboratory, and to Sheldon Lovell for his technical help. David Sands of the Technical Services Division of the University of Alberta advised me on the production of the time-lapse films and supplied the camera and timing device. Data analysis was assisted

by Dr. John Honsaker who wrote the Apple II particle-size digitizing and analysis program.

Carolyn King and Martin Dawson ably assisted in the field. I am grateful to Parks Canada for granting permission to work in Jasper National Park and to the Canadian Hostelling Association who allowed the use of Beauty Creek Hostel in July and August, 1981.

Loreto Mortimer and Trevor Bell typed, formatted and printed the text. Joan Ellsworth drafted the majority of the diagrams; the remainder are the work of John Howley, Sandra Halliday and Henry Butler. Gary McManus and Charlie Conway of the Memorial University Cartography Laboratory, ETV Photography at Memorial University, and Randi Pakan and Jack Chesterman in the Geography Department at the University of Alberta all contributed to the photographic work. Joan Ellsworth prepared the list of references. Thanks to all of these people for their work on my behalf.

The support of my friends in Edmonton, Kingston and St. John's is greatly appreciated; likewise that of Alick and Eileen who have always been interested in our education.

Table of Contents

List of Tables

List of Figures

Notation

SYMBOL	VARIABLE	UNITS	DIMENSIONS
A	Total cross-section area of confluent anabranches	m^2	L^2
B	Channel width	m	L
d	Mean channel depth of braided stream	m	L
D	Particle diameter	mm,m	L
D_i	Diameter of the ith percentile of the particle size distribution (D_{50}, D_{90}, etc.)	mm,m	L
F	Froude number	--	--
F_o	Densimetric Froude number	--	--
g	Acceleration due to gravity	$m\ s^{-2}$	LT^{-2}
G_b	Mass rate of sediment transport	$kg\ s^{-1}$	MT^{-1}
g_b	Mass rate of sediment transport per unit width	$kg\ s^{-1}$	$MT^{-1}L^{-1}$
h	Flow depth	m	L
$\overline{h}$	Mean depth of confluent channels	m	L
h_s	Absolute scour depth	m	L
h_r	Relative scour depth	m	L
I	Bed relief index	mm	L
k	Roughness height	mm	L
L	Characteristic length	--	L
M	Mean number of avalanche-face bars per flume length	--	--
N	Mean number of active channels per flume transect	--	--
P	Mean number of active channel segments per flume length	--	--
Q	Discharge	m^3s^{-1}	L^3T^{-1}
Q_b	Bedload discharge	m^3s^{-1}	L^3T^{-1}
Q^*_b	Dimensionless bedload discharge	--	--
q_b	Bedload discharge per unit width	m^2s^{-1}	L^2T^{-1}

SYMBOL	VARIABLE	UNITS	DIMENSIONS
q^*_b	Dimensionless bedload discharge per unit width	--	--
Q_{bf}	Bankfull discharge	m^3s^{-1}	L^3T^{-1}
Q_m	Mean annual discharge	m^3s^{-1}	L^3T^{-1}
R	Submerged specific gravity of sediment	--	--
Re	Reynolds number	--	--
Re*	Particle Reynolds number	--	--
S	Channel or water surface slope	--	--
U	Mean velocity	$m\ s^{-1}$	LT^{-1}
u^*	Shear velocity	$m\ s^{-1}$	LT^{-1}
ϵ	Relative discharge of confluent channels	m^3s^{-1}	L^3T^{-1}
θ	Angle of confluence	degrees	--
λ_i	Scale ratio for parameter i	--	--
λ	Wavelength	m	L
μ	Dynamic viscosity	$kg\ m^{-1}s^{-1}$	$ML^{-1}T^{-1}$
ν	Kinematic viscosity	m^2s^{-1}	L^2T^{-1}
ρ	Water density	$kg\ m^{-3}$	ML^{-3}
ρ_s	Sediment density	$kg\ m^{-3}$	ML^{-3}
τ_o	Bed shear stress	$N\ m^{-2}$	$ML^{-1}T^{-2}$
τ_c	Critical bed shear stress	$N\ m^{-2}$	$ML^{-1}T^{-2}$
τ^*	Shields stress	--	--
τ^*_c	Critical Shields stress	--	--
ϕ	Einstein's bedload parameter	--	--
ψ	Einstein's sediment mobility parameter	--	--
Ω	Stream power	$W\ m^{-2}$	MLT^{-3}
Ω'	Stream power index	m^3s^{-1}	L^3T^{-1}
$\overline{\Omega'}$	Dimensionless stream power index	--	--
ω	Stream power per unit width	m^2s^{-1}	L^2T^{-1}
ω'	Stream power index per unit width	$W\ m^{-2}$	MT^{-3}
$\overline{\omega'}$	Dimensionless stream power index per unit width	--	--
$\overline{\omega'}_c$	Critical dimensionless stream power index per unit width	--	--

Chapter 1 : Introduction

Braiding constitutes a distinct category of river channel pattern among what Leopold and Wolman (1957) considered to be a continuum of pattern types. Braided streams are characterized in particular by the presence of numerous, largely unvegetated, mid-channel bars whose form and location are constantly changing along with the numerous channels that surround them (Kellerhals, Church and Bray, 1976). In the past their characteristics have been examined by sedimentologists eager to understand the origin and nature of braided river deposits and by geomorphologists attempting to explain the occurrence of a range of channel pattern types and the causes of braiding. Unlike meandering streams, braided streams have only recently been subjected to scrutiny from the point of describing and understanding the fluvial processes responsible for their form. Lewin (1978) and Carson (1984 a & b) have urged that greater understanding of "meso-scale" channel changes (Lewin, 1978) and the description of the details of the process of braiding are required to explain the occurrence of braiding and the evolution of braided river floodplains. Recent work by Bluck (1979), Ashmore (1982) and Ferguson and Werritty (1983), along with earlier investigations of unit bar accretion by Hein (1974) and Smith (1974) have begun to contribute to a fund of knowledge about braided rivers.

However, many aspects of braided river mechanics remain poorly documented and a synthesis of sedimentary processes of the kind that is available for meandering rivers is lacking although Miall (1977) has summarised many of their sedimentary and morphological characteristics. The mechanisms of flow division and the variables that control the occurrence of each, the rate of

sediment transport under conditions of increasing slope and discharge, the controls of confluence scour form and the role of such features in sedimentation, and the influence of slope and discharge on braiding intensity, channel dimensions and unit bar types are all examples of aspects of braided river morphology and processes that remain incompletely documented and understood and, as yet, unrelated to one another. This thesis examines these aspects of braided stream form and process and draws them together into a synthesis of the sedimentary mechanics of braided streams.

It is the contention here that braided river form can only be fully understood by examining the processes of sediment transport, and particularly the spatial and temporal variations in sediment transport rate. This is also true of meandering streams although the situation there is simpler than that in braided streams. Recent measurements of and speculation about the sediment transport rate in braided streams (Griffiths, 1979; Kang, 1982; Southard and Smith, 1982) have indicated that periodic fluctuations in transport rate occur at a variety of time scales but as yet only tentative suggestions about the origin and physical form of these fluctuations have been made. Such unsteadiness in the sediment transport rate is potentially very important in explaining the location and form of braid bars and the morphology and sedimentary characteristics of braided streams as a whole.

An investigation of this kind requires conditions in which documentation and observation of sedimentary processes are possible along with measurement of channel form and sediment transport rate. In theory such observations and measurements could be made, with much difficulty, in the field, but this study

adopts a different approach. Engineers have for many years made use of small-scale hydraulic models for design purposes and consequently the principles of hydraulic similarity are well known and published in numerous textbooks on hydraulics. More detailed treatises such as those of Allen (1947) and Yalin (1971) provide further information on the subject, particularly the principles of similarity for movable bed models. The principles for producing a small-scale model of a gravel braided stream are therefore well known and recent work by Ashmore (1982) and Southard and Smith (1982) has shown that some aspects of channel form can be reproduced quantitatively and that the qualitative similarity of sedimentary processes and forms is quite striking. This thesis takes this approach further and an integral part of the thesis is the verification of various aspects of the model braided streams by reference to the author's own field observations and other published data on gravel braided streams.

The model approach has several advantages, particularly the ease of recording channel changes and sedimentation (by the use of time-lapse cinematography), the simplicity of monitoring the sediment transport rate, and the rapidity with which topographic surveys of channel cross-sections can be made. In addition, the fact that the time scale, as well as the geometric scale, is reduced, means that processes occurring over long periods of time in the field can be observed in a fraction of the time in the laboratory. Further, the ability to impose values of the principal independent variables (discharge, slope and particle size) is advantageous because it eliminates the problem of simultaneous variation of slope, discharge and grain-size encountered in the field.

Apart from the general thesis that braided river form can be understood as

the product of spatial and temporal fluctuations in the sediment transport rate, and that this approach provides the basis for a synthesis of braided river mechanics, the following specific aspects of braided river form and process are examined :

1. The increase of sediment transport rate with increasing slope and discharge in braided streams, the nature of fluctuations about the mean sediment transport rate and their role in braided stream morphology.

2. The morphology of confluence scour holes, the main controls on scour depth and the role of confluences in braided stream sedimentation.

3. The response of braided river form to changes in slope and discharge, in particular braiding intensity, mean channel width and depth, the form of unit bars, and the rapidity of channel changes.

4. The details of the processes of flow division and the conditions controlling the occurrence of each. Related to this is an examination of unit bar height in relation to flow conditions.

Much of the discussion is based on laboratory observations and data but in most cases field data collected as part of the study, on the Sunwapta River, Alberta, or other published information is used to support the conclusions reached from examination of the laboratory streams.

Chapter 2 : Form and Process in Gravel Braided Rivers : A Review

2-1 The Causes of Braiding

For a number of years it has been recognised that river channel pattern types form a continuum but for convenience it has been common to recognise a few distinct patterns. Although the basis for such classifications differ (Leopold and Wolman, 1957; Schumm, 1963; Kondratyev and Popov, 1967; Kellerhals, Church and Bray, 1976) braided streams are generally recognised to be multi-thread rivers whose individual channels (anabranches) constantly migrate across the floodplain. This rapid lateral movement helps distinguish them from anastomosed streams in which lateral migration of individual channels is much slower (Smith and Smith, 1980).

Braided streams flow on steep valley gradients and have a large bedload, easily eroded banks and often a rapidly fluctuating discharge (Richards, 1982, p.211). Each of these characteristics may be important in producing braiding. However, there is some doubt about the importance of fluctuating discharge even though Wright, Coleman and Erickson (1974) showed statistically that braided streams have higher flood peakedness, higher total discharge range and higher monthly discharge variability than single channel streams. A number of flume experiments (Friedkin, 1945; Leopold and Wolman, 1957; Schumm and Khan, 1972; Hong and Davies, 1980; Ashmore, 1982) have produced braiding with a constant discharge. These results suggest that under certain conditions a fluctuating discharge is not necessary to produce braiding yet considerable importance has been attached to it by some authors (Doeglas, 1951; Fahnestock,

1963; Gupta, 1975). Doeglas (1951) considered discharge fluctuation to be much more important than gradient or availability of sediment in producing a braided pattern and, similarly, Gupta (1975) saw stream regime as a primary factor explaining differences in channel pattern between north and south flowing streams in Jamaica. The seasonal rainfall regime of the south-draining basins contrasts with the more uniform temporal rainfall distribution of the north side of the island and Gupta (1975) suggested that this could account for the occurrence of braiding in the south-flowing streams. Fahnestock (1963) is dubious of the necessity of rapidly varying discharge for the formation of braids but does suggest that rapid increase in discharge might mobilize large amounts of sediment which some channel reaches may be incapable of transporting. The result would be deposition of mid-channel bars. A more gradual increase in flow might give these reaches time to adjust their form to carry the imposed load without any in-channel deposition. Perhaps the uncertainty about the role of varying discharge can be removed by regarding it as a factor encouraging braiding but not necessary for braiding when other variables such as valley gradient already favour its occurrence.

The importance of flow regime, bank erodibility and bedload aside, the channel gradient is most frequently cited as the primary cause of braiding. Lane (1957) identified two types of braiding; one due to aggradation and the other the consequence of high stream gradient. In the case of the latter, he was able to discriminate between channel patterns on the basis of gradient and mean annual discharge. Braided channels were those in which :

$$S > 0.004\, Q_m^{-0.25}$$

where S is channel gradient and Q_m is mean annual discharge (m^3s^{-1}). Similarly Leopold and Wolman (1957) proposed a discrimination based on channel gradient and bankfull discharge. Braiding occurred when :

$$S > 0.033\, Q_{bf}^{-0.44} \qquad 2-2$$

where Q_{bf} is bankfull discharge (m^3s^{-1}). Both of these relationships are based on field data. Laboratory experiments by Schumm and Khan (1972) confirmed the role of slope in channel pattern adjustment. Note that the control by valley slope necessitates viewing slope as an independent variable but this is true only over a limited time span (Schumm and Lichty, 1963). As Richards (1982, p.214) pointed out, the use [by Lane (1957) and Leopold and Wolman (1957)] of channel slope instead of valley slope confuses the issue because channel gradient will change with adjustments in channel pattern.

Henderson (1961) realised that the channel pattern was the result of the interaction between sediment and water and that any explanation of braiding ought to incorporate the role of sediment size. His re-analysis of Leopold and Wolman's (1957) data gave the following relationship for the channel slope at which braiding occurs :

$$S = 0.002\, D_{50}^{1.15}\, Q_{bf}^{-0.46} \qquad 2-3$$

where D_{50} is median grain size (mm) and Q_{bf} is bankfull discharge (m^3s^{-1}). This indicates that as grain size increases a higher threshold slope is needed to produce braiding. Kellerhals (1982) was more equivocal on this point. His analysis of published data, augmented by his own river surveys in western Canada, showed that grain size appeared to have only a minor effect on the threshold slope for braiding.

A recent development in attempts to identify the causes of braiding has been the analysis of data in terms of stream power or energy rather than on the slope/discharge plane. Since stream power is directly proportional to the product of slope and discharge, the use of stream power allows grain size to be incorporated as the second rather than the third variable. Analysis of this kind was attempted by Begin (1981) who showed, for a data set of 359 streams, that the braided streams had higher bed shear stress in excess of that necessary for initiation of sediment transport than meandering or straight streams. Richards (1982) analysed the threshold problem using the discharge-slope product as an index of power expenditure per unit length of channel [his Figure 7.12(d)] and demonstrated that single and multi-thread channels can be discriminated on a plot of D_{50} versus stream power index. The discriminant expression is:

$$\Omega' = 0.011 D_{50}^{0.77} \qquad 2-4$$

where Ω' is the stream power index (m^3s^{-1}) and D_{50} is in millimetres. Thus for a given grain size braiding occurs at higher values of stream power, and as grain size increases greater power is needed to produce braiding. Similarly Ferguson (1981, Figure 4-19) shows that active braiding occurs only at high values of stream power (greater than 100 Wm^{-2}) in the coarse grained, mountain streams of Britain. The corresponding value from Leopold and Wolman's (1957) threshold is about 50Wm^{-2} which probably reflects the sandy nature of most of Leopold and Wolman's streams (Ferguson, 1981, p.114).

Carson (1984a) has recently questioned the basis of several studies of the channel pattern thresholds reviewed above, pointing out that in some cases the distinction by discharge and slope is unsatisfactory not only as a result of the

failure to consider particle size but in addition because the discrimination is actually illusory owing to the use of channel slope (which is a function of sinuosity and therefore of channel pattern) instead of valley slope. Carson (1984a) also showed that the sample characteristics (particularly the range of particle sizes in the data set used) influence the form of the threshold curve. Carson (1984a) accepts that in principle a greater propensity towards braiding should be favoured by higher stream power (higher slope and discharge) for a given particle size but suggests that the role of other factors, particularly the ability of the stream to supply bedload calibre sediment from its banks at a rate in excess of the stream's capacity, may be the direct causes of braiding and this may explain why the slope-discharge discrimination is unsatisfactory in many cases. In addition, Carson (1984a) questioned the validity of Begin's (1981) physical explanation of the braiding threshold and suggested that while an alternative interpretation in terms of a threshold specific power (Ferguson, 1981) may be more promising, a more thorough investigation of braiding mechanisms is required before "explanations" of the origin of braiding can be attempted.

It is interesting to note Carson's (1984a) reference to bank erosion as a contributory factor in braiding because of its frequent mention in previous attempts to explain the occurrence of braiding (Mackin, 1956; Fahnestock, 1963; Brice, 1964). The fact that braided streams have high excess stream power means that such streams have relatively large amounts of energy available for bank erosion. Braiding is preceded by the development of wide shallow channels (i.e. by an increase in the width/depth ratio) which tend to occur in easily eroded material. Banks in cohesive sediment (high silt and clay content) offer greater

resistance to erosion than non-cohesive sediment (Schumm, 1960; Ferguson, 1973; Miller and Onesti, 1979) thus, for a given stream power, braiding is more likely in non-cohesive sediment than in cohesive sediment. At the same time, in a given sediment type, braiding is more likely at high stream power when more energy is available for bank erosion. Braiding may therefore be viewed as a response to the development of high width/depth ratios in easily eroded sediments and at high stream power. The theoretical stability analyses of Engelund and Skovgaard (1973) and Parker (1976) distinguish braided and meandering channels on this basis. Many criteria for the formation of alternating bars also rely on width/depth ratio which is important in the light of recent observations of braiding mechanisms that show braiding to be initiated via alternating bar formation (Parker and Anderson, 1975; Ashmore, 1979; Hong and Davies, 1979).

The above has served to elaborate the initial statement that braiding occurs on steep gradients in rivers with easily eroded banks (and hence high width/depth ratio) and large bedload. It should be added that Howard, Keetch and Vincent (1970) and Parker (1976) have shown empirically and theoretically that the further a stream is above the braiding threshold (however defined), the more braided (the greater the number of bars and anabranches) it becomes. This is discussed further in Section 2-3.

2-2 Braiding Mechanisms

The conditions under which braiding occurs have been identified but a complete explanation of the phenomenon requires a description of the mechanism of channel division itself. This has most frequently been observed in laboratory experiments but descriptions of the process based on field observations also exist.

Friedkin (1945) was apparently the first to describe the process by which a braided channel develops from an initial single channel. By doubling the discharge of the original meandering channel a braided channel developed when, "Each of the former convex bars was swept downstream and the former (meandering) pattern was completely destroyed." (Friedkin, 1945, p.259). A detailed description of this process was not presented by Friedkin (1945), and a number of years passed before Leopold and Wolman (1957) provided the first detailed step by step account of braiding. Because of the absence of any subsequent work for several years that of Leopold and Wolman (1957) became widely quoted and the process they described was often tacitly assumed to be the process by which all streams braid despite the fact that the circumstances under which braiding occurred and the braiding process itself were quite different from Friedkin's (1945) earlier account.

The essence of Leopold and Wolman's (1957) account is that for the transport of poorly sorted sediment a slight loss of competence by the stream results in the deposition of some of the larger particles in transport. This initial nucleus then encourages trapping and deposition of more sediment and begins to divert the flow to either side, although in the initial stages of bar development the principal zone of sediment movement is across the top of the bar. Deflection of the flow by the bar causes local scour of the channels and the lowered water surface results in exposure of the bar. Continued movement of the channels gradually builds a bar consisting of patches of material of different sizes and degrees of sorting. In places, particularly at the toe of the bar, well-sorted fine material is deposited as delta-like foreset beds.

Some later descriptions of braiding in poorly sorted gravel (Krigstrom, 1962; Fahnestock, 1963; Ore, 1964; Knighton, 1976) resemble Leopold and Wolman's (1957) but in others the course of events during braiding seems to be different. This is particularly true in well-sorted sediment such as sand (Friedkin, 1945; Kinoshita, 1957; Brice, 1963; Ore, 1964; Smith, 1970, 1971a; Boothroyd and Ashley, 1975; Cant and Walker, 1978; Blodgett and Stanley, 1980) but also in poorly sorted gravel and in gravel river models (Wolman and Brush, 1961; Hein, 1974; Parker and Anderson, 1975; Lewin, 1976; Rundle, 1976; Ashmore, 1982; Ferguson and Werritty, 1983). In these cases braiding occurred by dissection of slip-face bars either on a falling stage or following diversion of the flow, or as the result of meander cut-offs.

In shallow sandy streams the bed consists of a profusion of approximately equally spaced lobes of sediment usually referred to as linguoid bars (Allen, 1968; Collinson, 1970) or transverse bars (Sundborg, 1956; Ore, 1964; Smith, 1971a). Their downstream margins are bounded by avalanche faces the progradation of which, together with erosion on the stoss side, result in migration of the bar downstream. Similar features are referred to as "dunes" by Kinoshita (1957) but the distinction between the bars and dunes, if it exists, has not been established. Most accounts of braiding under these circumstances simply refer to falling stage resulting in a change from conditions in which the flow determines the nature of the bedforms to one in which the bedforms begin to emerge and to direct the flow. Smith (1971a) suggested that dissection of these bars may not require a reduction in the discharge across the bar (bar discharge measured at the bar head) but may occur if the bar grows to a size which the bar discharge can no longer

sustain. He was able to derive an approximate relationship between bar discharge and the surface area above which dissection would occur. These lobate slip-face bars are also present in some gravel streams although they are fewer and usually isolated (Hein, 1974; Smith, 1974; Lewin, 1976, 1978; Rundle, 1976; Martini, 1977; Gustavson, 1978; Ashmore, 1979). Hein (1974) and Rundle (1976) have described braiding by falling-stage dissection of these lobate features and Rundle (1976) insists that this fall in stage (at least locally) is necessary for braiding to occur. Ashmore's (1979) description of braiding in model gravel rivers, which is similar to an earlier description for a sandy river (Cant and Walker, 1978), showed that channel division could occur atop one of these lobes by the central part of its margin becoming inactive and the flow diverting to either side; a mechanism reminiscent of that described by Leopold and Wolman (1957). The migration of the two new channels away from the initial bar resulted in it becoming exposed and no reduction in discharge was necessary.

Braiding as a result of meander cut-offs has also been frequently observed, particularly in laboratory streams. There are numerous laboratory studies of the formation of alternating dunes or bars in an initially straight channel. Many of these involve channels with non-erodible banks (Kinoshita, 1957, 1980; Einstein and Li, 1958; Einstein and Shen, 1964; Chang, Simons and Woolhiser, 1971; Ikeda, 1973; Nakagawa, 1983; Jaeggi, 1984) which do not allow the development of channel sinuosity but they do indicate that, in general, alternating bars are to be expected in relatively wide, shallow channels with high bed shear stress. Kinoshita (1955) was able to show that when the channel was sufficiently wide more than one bar developed in some cross-sections giving the bed a fish-scale like

appearance of overlapping bars with the flow diverging over the bar tops and converging downstream. When the banks of these channels are erodible a sinuous channel develops because of bank erosion produced by deflection of the flow associated with the alternating bars. The result is the development of "pseudomeanders" (Wolman and Brush, 1961) or "point-dunes" (Hickin, 1969) which, under certain circumstances, may be cut off to form a braided channel (Schumm and Khan, 1972; Parker and Anderson, 1975; Hong and Davies, 1980; Ashmore, 1982). Lewin (1976) and Ferguson and Werritty (1983) have documented such features from gravel rivers in the field and noted the presence of incipient or actual cutoffs in these rivers, classified by Lewis and Lewin (1983) as mobile bar cutoffs. Detailed descriptions of the precise course of events during these cutoffs are lacking but they apparently occur by overtopping the upstream end of the point bar at the outside of the next bend upstream (perhaps in association with erosion at this point, and hence migration of the bend) and the diversion of flow across the upstream end of the bar into the slough channel (Bluck, 1974, 1976) on the bankward margin of the point bar.

Thus, it is possible to identify three apparently different braiding mechanisms from the literature. The Leopold and Wolman (1957) mechanism and the cutoff mechanism first described by Friedkin (1945) are clearly quite different although both are seen to occur in initially straight laboratory channels. The dissection of slip-face bars, as mentioned previously, has affinities with the Leopold and Wolman (1957) mechanism in some cases but also with the cutoff process. If these three mechanisms are regarded as essentially distinct from one another the obvious question is what factors determine the occurrence of these mechanisms ?

In the light of later laboratory studies discussed above, Leopold and Wolman's (1957) experiments are unusual in producing one short braided reach in an otherwise straight laboratory channel. Since the reach downstream of the braided reach was apparently unmodified it seems that the shear stress on the bed of the channel was only marginally above that necessary for sediment transport and the braiding was the result of local aggradation perhaps induced by the manner in which the flow was introduced to the flume. This supposition is not supported by calculation of the Shields stress which has values in the range 0.07 to 0.10 for Leopold and Wolman's (1957) experiments when D_{50} is used as the characteristic sediment size. However, in poorly sorted sediments it may be more appropriate to choose a larger percentile of the sediment size distribution in the calculation of Shields stress (Yalin, 1977, p.84-87). Thus, for example, replacing D_{50} by D_{90} in the Shields stress calculation gives values of only 0.03 - very close to critical. This argument supports the idea that the Leopold and Wolman (1957) mechanism occurs at relatively low values of excess shear stress (shear stress above that necessary for sediment movement). One can approach this problem in a slightly different way by considering flow depth rather than shear stress. For a given water surface slope and sediment size a lower bed shear stress results when depth is reduced. Since grain size is given, this can be interpreted as a decrease in relative depth (h/D_{90}, where h is the flow depth) and the implication is that the relative depth might determine the type of bars and flow division mechanism to be expected. Again the choice of grain size affects the result but most resistance equations for gravel streams use a roughness size equal to a grain size near the coarse end of the size range, often D_{84} or D_{90} (Bray, 1982). Church and Jones

(1982) suggested that bar development would be unlikely if depth was less than D_{50} (or about equal to $0.3\ D_{90}$) and at low slopes indicated that the limiting value of h/D_{90} is closer to 3 or more. It is suggested that as relative depth increases so does the likelihood of the development of lobate bars and perhaps alternating bars. If so we would expect Leopold and Wolman's (1957) initial channel to have comparatively low relative depth. The value of h/D_{50} is about 9 in their braided run 6b. This is about the same as the value (that produced alternating bars) for Ashmore's (1982) experiment. However, when h/D_{50} is replaced by h/D_{90} Leopold and Wolman's (1957) run 6b has a lower value (less than 4) than Ashmore's (1982) experiment where h/D_{90} is about 6. This agrees with the suggestion that bar type and therefore the division mechanism varies with relative depth, but the difference in h/D_{90} is small and the two experiments are not strictly comparable because of the slight difference in channel slope (0.016 and 0.013 for Leopold and Wolman (1957) and Ashmore (1982) respectively).

Regardless of whether flow division occurs by deposition of a nucleus of coarse material on a plane bed, or by division round the inactive portion of a prograding bar, both are the result of the loss of competence near the centre of the bed. Church and Gilbert (1975) considered the situation as one in which stream power falls below that necessary to move the sediment load through the channel or, looked at another way; an increase in channel resistance to a value which prevents passage of the imposed load. Shen and Vedula (1969) showed that excessive channel widening could lead to this result, by a reduction in bed shear stress through a decrease in depth. Bar building would have the same effect. Henderson (1966, p.449) shows that where the width of a channel increases,

sediment deposition occurs because of a reduction in the discharge per unit width and that this deposition results in an increase in channel slope to restore the balance between water discharge and sediment discharge. Such deposition could lead to braiding. The situation for the cutoff mechanism is apparently rather different and is analogous to the process of avulsion which is common in braided streams (Ashmore, 1982) and also anastamosing streams (Smith and Smith , 1980).

The experiments of Moss, Walker and Hutka (1980) and Moss, Green and Hutka (1982) demonstrate that a fourth braiding mechanism exists. In shallow (1-3mm) flows over a steep (0.02 - 0.09) plane sand bed, small channels develop spontaneously provided the flow can disturb the bed material. These "proto channels" eventually develop into an integrated braided channel, apparently by headward growth of small "proto channel" tributaries. The tributary junctions are areas of pronounced scour and the concomitant deposition immediately downstream divides the flow which then either feeds into adjacent channels or is reunited. In either case further scour and deposition results and eventually a braiding channel develops. Subsequent development simplifies this initial network through capture of smaller channels by larger ones. The number of channels thus declines during each run although the stream remains braided. In this case braiding is the result of secondary currents in the shallow, supercritical flow causing local scour which lead eventually to channel formation. The concentrated flow is capable of transporting sediment, at least over short distances, and is therefore more efficient than the initial sheet flow.

This observation of changes in flow competence as a result of braiding draws attention away from the sedimentological aspects of braiding mechanics discussed

so far, towards the hydraulic aspects. It has been suggested that, from a hydraulic point of view, braiding is an adjustment in channel form and flow geometry that allows continuity of sediment transport in the face of rapidly declining competence in a single channel due to rapid aggradation and consequent reduction in flow depth and channel slope. This is clearly the view of Stebbings (1964) and Shen and Vedula (1969) and has been echoed by Church and Gilbert (1975). The experiments of Moss et al. (1982) demonstrate that there are circumstances under which channel division is the only means of maintaining sediment transport. This greater competence in the divided channel is achieved through local increases in slope caused by aggradation within the single channel (Leopold and Wolman, 1957). The meander cutoff mechanism seems to be a good example of this process as the flow favours the locally advantageous hydraulic gradient across the bankward face of the point bar into the slough channel.

Apart from increasing slope other modifications of the hydraulic geometry downstream of a flow division, although the empirical evidence is radictory. Rubey (1952) and Briee (1964) reported a decrease in total width nd an increase in mean depth downstream of a flow division while Leopold and Wolman (1957) and Nordseth (1973) found the exact opposite; an increase in total width and decrease in mean depth. One can argue (Richards, 1982, p.213) on the basis that width increases as the square root of discharge, that total width ought to be higher downstream of the division and this agrees with Leopold and Wolman's (1957) and Nordseth's (1973) findings. Specifically, the total width of two equal sized distributaries should be 1.41 times the width of the undivided parent channel. Cheetham's (1979) data indicate that the distributary channels

have lower width/depth ratios than the undivided channels, although Church (1972) concludes that the equilibrium shape is roughly the same for both parent and distributary channels.

There is also disagreement on the nature of the velocity variation downstream of a channel division. Church (1972) found the velocity exponent in the hydraulic geometry equations (Leopold and Maddock, 1953) in the steeper distributaries to be higher than in the undivided channels but Cheetham (1979) found the reverse and suggested that this could explain the nature of the braiding mechanism. He proposes that, at low flow, velocity in the distributaries exceeds that in the main channel but as discharge increases a higher velocity exponent in the main channel is responsible for its velocity eventually exceeding that in the distributaries. Therefore at high stage the areas of channel division are bottlenecks for sediment transport and it is at the head of these distributary channels that deposition and bar accretion occur. This suggestion actually runs counter to the original notion (Church and Gilbert, 1975) that braiding is a hydraulic adjustment to maintain sediment transport in a situation where sediment transport capacity is decreasing downstream. In fact deposition at the head of the distributaries is inevitable under these circumstances but it does not follow that the hydraulic conditions observed by Cheetham (1979) are stable, and as the braid develops one might expect the situation to be modified. Initially the distributaries may be less efficient than the main channel in order for bar accretion to occur, but at some stage the channels flanking the bar apparently incise themselves (Leopold and Wolman, 1957). It is possible that this is an equilibrium condition in which the distributary channels are just able to transfer

all the sediment supplied from upstream; something that the pre-existing single channel was incapable of doing. Since few braids remain morphologically unchanged for long this equilibrium situation is apparently easily upset. This instability distinguishes braided channels from other channel patterns. Thus, any statements about the nature of hydraulic adjustments in the vicinity of a flow division should be qualified by noting the dynamic nature of the process and the stage of the process at which the measurements were made. It is also possible that the conditions obtaining in a stable divided reach of a stream are very different from those of a division in an active braided stream showing rapid channel migration, abandonment and avulsion. Some of the confusion about the nature of hydraulic adjustments in flow divisions may be attributable to a failure to consider these factors, emphasising the importance of observation of the processes as a pre-requisite for their comprehension.

It is apparent from this discussion that braiding may develop by one of at least four different mechanisms. Two of them [those described by Leopold and Wolman (1957) and Ashmore (1982)] have much in common and are the result of a downstream decrease in bed shear stress causing in-channel deposition. Morphological differences in these two cases may be the result of differences in relative depth. The other two processes (the cutoff mechanism and the "proto channel" development) have different basic causes. Cutoffs occur where flow overtops the upstream end of point bars which develop from the initial alternating bar pattern, while "proto channels" are a product of incision of the bed in steep, shallow sheet flows. Thus the widely quoted braiding mechanism of Leopold and Wolman (1957) is prevalent only under certain flow conditions. Detailed

descriptions of the braiding mechanisms and the conditions under which they occur are essential for a thorough understanding of the hydraulics of braided streams and the causes of braiding.

2-3 Braided Channel Form and Sedimentary Processes

2-3-1 Channel Pattern

Given that braided rivers are multiple channel streams subject to frequent channel migration and avulsion, and continual bar erosion and deposition, it is possible to identify a series of forms and processes characteristic of such streams. It should be recognised that braiding grades into other channel pattern types so that, for example, "wandering" streams (Kellerhals et al., 1976) may display many of the characteristics of braided streams (Ferguson and Werritty, 1983).

In any reach it is typical for the multiple channel network to be dominated by one or two main channels and a series of secondary ones (Fahnestock, 1963; Williams and Rust, 1969; Krumbein and Orme, 1972; Cheetham, 1979; Pickup and Higgins, 1979). Williams and Rust (1969) suggested a heirarchy of channels which they limited to third order but which presumably could be extended to higher orders. Such a scheme may be useful in describing the degree of braiding but contributes little to the understanding of stream mechanics. The main channel or channels visible in one reach are usually only traceable downstream for a fairly short distance until they disappear in areas where the main channel fragments into many minor channels, all of which feed back into another main channel segment a short distance downstream. Such features are referred to as "breakups" by Rundle (1976), a term acquired from jet boating enthusiasts in New Zealand. This alternation of highly braided sections (breakups) and

collection areas (nodes) has been recognised frequently. In some cases the nodes are the result of natural or artificial constrictions (Chien, 1961) but in many cases are obviously a product of the stream itself (Coleman, 1969; Church, 1972; Rundle, 1976; Griffiths, 1979). There has been some speculation that the nodes may be regularly spaced and that their spacing is in some way analogous to meander wavelength (Rundle, 1976; Rust, 1978a). In view of the complex interaction of channels of various discharges in braided streams it seems unlikely that this relationship could be established except for streams with only a low degree of braiding (two or three channels per cross-section). The potential importance of these nodes in braiding mechanics is discussed in section 2-3-3.

Braiding develops in non-cohesive sediment which results in individual anabranches being relatively wide and shallow (Schumm, 1960). Church and Gilbert (1975) present data from Baffin Island sandar (Church, 1972) and White River, Washington (Fahnestock, 1963) which show width/depth ratios of individual anabranches to be from 10 to 300 but typically in the range 15 to 80. Pickup and Higgins (1979) found similar values for the Kawerong River, Papua-New Guinea. This tendency to develop wide, shallow channels is intimately linked with the development of braiding as discussed previously.

The intensity of braiding varies considerably but investigation of this variation is hampered by the problem of defining a quantitative measure of braiding intensity (Brice, 1964; Rust, 1978a). The theoretical analysis of Parker (1976) indicates that as the slope and/or the width/depth ratio increase the number of braids increases. This is difficult to confirm, at least from field data, because of the tendency for slope, grain size, discharge and braiding intensity to

co-vary along a reach of, say, braided glacial outwash and because of potential variability introduced by historical factors. Howard, Keetch and Vincent (1970) attempted to tackle the question using data derived from maps and air photographs. They were unable to control for variations in braiding due to differences in the river stage at which the photographs were taken, or for the potentially important effects of grain size and bank resistance, but were still able to show a positive correlation between slope and discharge (and hence stream power), and the excess segment index used to denote the degree of braiding. (The excess segment index is the average number of segments bisected by lines drawn across the river perpendicular to the flow direction, at several points along a section of river). Maizels (1979) showed that aggradation of a proglacial valley train, and the resultant increase in slope (particularly in the proximal section), coincided with an increase in the number of channel segments in the valley train despite glacier advance shortening the reach. In other words, the mean number of segments per valley cross-section increased considerably. This indicates that if experiments were conducted in which grain size was constant and slope and discharge varied independently, one would expect a positive correlation between braiding intensity and both slope and discharge.

2-3-2 Bars and Sedimentary Processes and Structures

The nature of the sedimentary forms and processes in braided streams has been touched on in the discussion of braiding mechanics. That discussion showed that the processes and forms may vary with the character of the flow; in other words there is a considerable variety in bar morphology. The bewildering array of bar morphologies visible in rivers has caused considerable confusion about the

terminology and classification of these features which is at least in part due to a poor understanding of the genesis of bars (Smith, 1978; Ashmore, 1982; Crowley, 1983). The term 'bar' itself has been applied to an enormous variety of features (Smith, 1978) varying in scale from a few metres to several hundreds of metres. It is now generally recognised (Bluck, 1974, 1979; Smith, 1974, 1978; Cant and Walker, 1978; Church and Jones, 1982; Ashmore, 1982) that the large exposed sand and gravel flats in braided streams (Krigström's (1962) "spool islands" or Allen's (1968) "braid bars") owe much of their external form to post-depositional modification and are actually composed of a large number of small features which gradually accrete in a complex manner. The large features are variously termed compound or mosaic bars (Bluck, 1974, 1979), complexes (Church and Jones, 1982; Ashmore, 1982) or flats (Cant and Walker, 1978) and the smaller, primarily depositional units of which they are composed are referred to as unit bars (Smith, 1974) or units of size segregation (Bluck, 1974). The presence of these unit bars has since been recognised in other studies (Rundle, 1976; Hein and Walker, 1977; Ashmore, 1982) as well as in single channel streams (Galay, 1967; Lewin, 1976, 1978; Bluck, 1979; Martini, 1977). They have a variety of forms but Smith (1974) originally recognised four types; longitudinal, transverse, diagonal and point bars. The longitudinal bar closely resembles the mid-channel bar developed in Leopold and Wolman's (1957) experiments; a stream-lined mound of gravel in the centre of the channel. The unit point bar is a simple sheet of sediment deposited on the inside of many bends. (Note that this unit point bar is different from the point bars discussed previously which are actually complex bars.) The transverse and diagonal bars are rather different in character from the other two. They are

essentially tongues of sediment the downstream margins of which are either symmetrical with respect to the flow (transverse bar) or asymmetrical or skewed (diagonal bar). In some cases, particularly the transverse bars, the downstream margin is an avalanche face which in the field may be on the order of one metre or more high. The diagonal and transverse bars, in contrast to the other two types, are mobile in the sense that the margins of the tongues grow downstream and change in shape and height in response to the local flow conditions and channel form.

The discussion of braiding initiation indicated that mobile tongues of sediment could be a product of the interaction of unsteady flow over a bed of erodible sediment. Their pattern is then related to the pattern of the velocity perturbations in the flow. The unit bars in braided rivers may occur in this way occasionally, but usually their location is determined by local flow expansion (Krigström, 1962; Hein, 1974; Smith,1974; Rundle, 1976; Cant and Walker, 1978; Ashmore, 1982; Church and Jones, 1982). A common association is that between an area of local scour such as a channel junction, and the channel immediately downstream where the scouring action is absent and material may be deposited (Rundle, 1976; Hein and Walker, 1977; Bluck, 1979; Ashmore, 1982; Moss et al., 1982).

Hein (1974) and Hein and Walker (1977) proposed that these transverse and diagonal bars developed from "diffuse gravel sheets". These are thin (a few grains thick) pulses in the bedload composed of a wide range of grain sizes, which migrate downstream. Such features have been noted by several workers (Church, 1972; Hein, 1974; Rundle, 1976; Bluck, 1979) although the term 'diffuse gravel

sheet' is due to Hein (1974). The diffuse gravel sheet model of bar deposition suggests that when such sheets stall in the channel at a local expansion (or during a fall in stage) finer material is winnowed out and deposited immediately downstream as a bar with or without a slip face. Hein and Walker (1977) suggested that the development, or otherwise, of the downstream slip face depends on the water and sediment discharge. If these are high the bar would grow rapidly downstream and would not develop an avalanche face. Only if water and sediment discharge are low would an avalanche face develop. This explanation in terms of water and sediment discharge is not particularly satisfactory. One would expect flow depth to be one important factor in determining bar morphology (see section 2-2) but it is not explicitly included in Hein and Walker's (1977) model. One could argue that since depth is positively correlated with discharge the implication of Hein and Walker's (1977) model is that flow depth is associated with low angle bar margins and the absence of avalanche faces; the converse of the argument presented in section 2-2 concerning the initiation of braiding.

Jopling's (1964) account of the deposition of small laboratory deltas provides insights to this problem particularly since many of the bars formed in braided rivers resemble small lobate deltas. Jopling (1964) showed that given sufficient time at a stable base-level (water surface elevation) the surface of the delta topsets graded to an equilibrium profile for the imposed flow conditions. This equilibrium profile can be altered in two ways, firstly by changing the base-level and secondly by introducing sediment to the upstream end of the flume in excess of the capacity of the flow. In the first situation, a rise in base-level, the delta

surface aggrades to a new equilibrium profile. It does this by the progressive downstream migration of a step on the delta surface which Jopling (1964) termed a 'rheologic micro-front'. The height of this front is directly related to the magnitude of the rise in base-level. When the base-level rise is extremely small the rheologic front is replaced by what Jopling (1964) described as a zone of attenuating particle concentration which spearheaded the deposition of the bedload. Thus the extra depth made available by the rise in base-level has a direct influence on the form of the aggradation front. When excess sediment was dumped into the flume the resultant aggradation process was very similar to that occurring for small changes in base-level but in order to distinguish the two Jopling referred to the former as a 'saltation front'. Transferring these observations to bar deposition in braided streams suggests that Hein's (1974) and Hein and Walker's (1977) 'diffuse gravel sheets' may be analogous to Jopling's (1964) 'saltation fronts' and, like the saltation fronts, may be the result of local overloading of the stream. Alternatively they may represent 'micro-fronts' formed under slight increases of depth. Similarly, the formation of avalanche faces may be controlled by the available depth and in particular by downstream changes in depth which may provide areas of relatively deep, slack water into which avalanche faces can build (Fahnestock and Bradley, 1973).

A further refinement may be offered by Yalin and Karahan's (1979) observations of bedform steepness (height/wavelength ratio) in flows of low relative roughness. Yalin and Karahan (1979) showed that steepness increases with increasing bed shear stress above critical until a maximum steepness value is reached, beyond which steepness declines again. The maximum steepness, and

the value of excess shear stress at which it is reached, vary with relative depth. If the unit bars of gravel rivers behave in the same way then bed shear stress, as well as relative depth, could also have a significant influence on bar form. This approach seems to be more promising than Hein and Walker's (1977) rather vague suppositions about control by sediment and water discharge. In particular, this approach explains how bars may change in form as they migrate downstream, independent of changing discharge; the sort of metamorphosis reported from braided streams by Bluck (1979) and Ashmore (1982).

The superimposition of successive diffuse gravel sheets to form a unit bar is one possible origin for the horizontal stratification that is so common in gravel braided stream deposits (Hein and Walker, 1977). It appears that the horizontal stratification may also be formed by the migration of depositional fronts with avalanche faces. Jopling (1964) and Smith (1971b) both report the development of horizontal stratification within such structures despite the presence of avalanche faces which one might expect to produce inclined foreset beds. Smith (1971b) observed this horizontal stratification even when the height of the avalanche face was ten times D_{90}. Thus in the shallow flows associated with gravel braided streams cross-bedding would be quite rare even where avalanche-face bars form, unless these are quite high relative to the prevailing grain size. Hein (1974) reported cross-bedding in only about 10 per cent of the excavations she made on the floodplain of the North Saskatchewan River. While the origin of stratification types may be understood in terms of bar development it is more difficult to identify the bars themselves in braided river deposits. Eynon and Walker (1974) attempted to do so with some success and as more refined criteria

are made available (Bluck, 1979) the task is becoming easier, as recent investigations by Bluck (1980) and Steel and Thompson (1983) indicate.

The processes by which the unit bars accrete to form compound or complex bars are enormously variable but Bluck (1974, 1979) and Ashmore (1982) have described some of the most common processes in gravel streams and likewise Cant and Walker (1978) for sandy streams. Bluck (1974, 1979) pointed out that in many rivers, particularly single channel streams where lateral migration is slow, it is rarely possible to identify the individual units comprising a complex bar although the manner of its growth may be discernible from its relation to the channel and its sedimentary structure. In contrast, the rapid lateral channel movements characteristic of braided streams commonly result in the preservation of the individual unit bars, at least in part. This is because the lateral migration rarely allows reworking of the bar by subsequent flood stages. The processes producing medial (those with channels on both sides) complexes are apparently the same as those responsible for lateral complexes (those attached to one bank) except that the former are the product of two bends migrating downstream and away from one another while the latter are the result of the lateral and downstream migration of a single bend. Ashmore's (1982) Figures 17 and 18 show the stages in the development of a lateral bar by accretion of successive unit bars and these compare closely with Bluck's (1974) Figure 7. In fact many medial and lateral complexes have a much more complicated history than this. Specific field examples are given by Bluck (1979) in which some individual unit bars are identified during their initial formation and their contribution to the final complex is traced (his Figures 16, 17 and 18). The implication, at least from

Bluck's (1974, 1979) descriptions, is that the morphologically and sedimentologically discrete components of complex bars are each the product of one migratory unit bar. Compound bar accretion is therefore episodic, related to the formation of each unit bar. Accretion of each unit bar is presumably accompanied by some adjustment of the adjacent channel to accommodate the increase in size of the complex. The complexes also display numerous post-depositional modifications such as small chutes cut by minor flows across the bar surface and small deltas deposited at the downstream end of such chutes where they issue into slack water areas. Bluck (1979) gives details of the morphology and structure of a variety of such features.

There has been some discussion of the relative abundance of longitudinal (*sensu* Smith, 1970, 1974) and diagonal and transverse unit bars in different kinds of braided streams. The result of a greater abundance of transverse bars may be an increasing amount of cross-bedding in the floodplain deposits. Most sandy braided streams are dominated by such transverse (linguoid) bars and therefore have abundant tabular cross-bedding (Ore, 1964; Smith, 1970; Boothroyd and Ashley, 1975; Cant and Walker, 1978; Walker and Cant, 1979). In gravel braided streams, cross-bedding is rare and examples of large scale cross-bedding in braided stream deposits are very unusual although Eynon and Walker (1974) report 3-4m high cross-beds in Pleistocene braided river gravels which they assume to be the product of avalanche-face transverse bars. Such large features require flow depths much greater than is common in most present day braided streams but it is conceivable that local scour could reach such depths allowing the deposition of a delta-like bar with large-scale foresets. There is therefore a transition from steep,

coarse-grained braided streams in which avalanche-face bars are rare and deposits are dominated by crude horizontal bedding, to fine-grained rivers where cross-bedding is abundant. Various studies of braided river sedimentology have recognised this transition (Ore, 1964; Smith, 1970; Boothroyd and Ashley, 1975; Miall, 1977, 1978; Rust, 1978b) although the emphasis has always been on grain size alone, rather than grain size relative to flow depth, in these proximal-distal transitions. Smith (1970) described the decrease in the number of longitudinal bars and increase in transverse bars downstream along the Platte River as sediment size and slope declined, and discharge increased. He defined bed relief as the average difference in height between successive high and low points on each transect across the stream, noting a decrease in relative relief of the bed along the proximal-distal transition. However, in terms of the average grain size, bed relief is much higher in the distal reaches than the proximal reaches of the Platte River. Hein (1974) and Hein and Walker (1977) also described in the Kicking Horse River the change in bar form downstream with the decrease in grain size and slope. In this case the transition occurred much more rapidly than in the Platte River and the change did not progress as far into the transverse bar regime. Even so, they (Hein, 1974; and Hein and Walker, 1977) were able to identify a decrease in the number of non-migratory longitudinal bars and an increase in the number of mobile transverse or diagonal bars downstream. The number of channels also increased downstream; a common observation on glacial outwash. Fahnestock (1969), Gustavson (1974), and Boothroyd and Ashley (1975) provide further examples of these downstream trends in bar type on outwash surfaces.

The control on bar type is presumably, as indicated previously, exerted

through the relative depth. The co-variation of slope, discharge and grain size on o[redacted]rfaces makes it impossible to infer which is most responsible for the c[redacted]rphology but it would be expected that at a constant grain size an in[redacted]scharge or a decrease in slope would both lead to increased flow dep[redacted]d hence a greater relative abundance of mobile, slip-face bars.

[redacted]rom a rather different standpoint Church and Jones (1982) argue that [redacted] a single upstream source of sediment in a gravel channel, activity will be [redacted]test close to the source and will become more stable with fewer migratory [redacted]s downstream in a finer grained, paved channel. The abundance of migratory [redacted] is therefore related to both the availability and the mobility of the sediment a[redacted]ll as the more immediate controls on bar form such as flow depth. The influence of sediment supply on channel form is considered further in section 2-3-[redacted]

2-3 [redacted]al Scour

The close association of bar deposition and local scour was pointed out earlier in the discussion. The presence of scour in braided channels has been mentioned in passing in several studies (Smith, 1973; Fahnestock and Bradley, 1973) but rarely has any systematic study of their form been attempted. Ashmore (1979) identified three types of local scour in braided streams; scour in bends or alongside asymmetric unit bars, waning flow scour on exposed complexes and channel confluence scour. Of these the most pronounced is the confluence scour and it is these areas that are often cited as controlling deposition in the channel downstream (Smith, 1973; Rundle, 1976; Moss et al., 1982). Scour at bends or alongside asymmetric bars may contribute to lateral complexes downstream but in

view of the generally shallow channels and low sinuosity such scour is rarely significant. Confluence scour may, however, produce local depths several times greater than the associated channels (Fahnestock and Bradley, 1973; Smith, 1973; Mosley, 1976) and the following discussion relates solely to this type of scour.

Scour depth and form at confluences varies considerably. Rarely are confluences in braided streams a simple case of the joining of two straight channels of approximately equal size; most commonly junctions are complex with several channels, some of which have very poorly defined margins, converging in one area. The most detailed analysis of confluence scour to date investigated the ideal Y-shaped confluence of two channels (Mosley, 1976, 1977). Mosley's (1976) experiments showed that, for constant total discharge, the angle of confluence of the two channels to be the dominant control on scour depth with some other variables exerting a secondary influence; of these the relative discharge of the two channels was most important. For a given angle of confluence, depth was greatest when the channels had equal discharge and decreased as one channel increased in size relative to the other. Increase in sediment load also reduced scour depth slightly (by about 25 per cent for a four-fold increase in sediment load). Mosley (1976) noted that these scour holes were lens-shaped in plan with the maximum depth upstream of centre so that in three dimensions they resemble the bowl of a spoon. Dying the water in one channel revealed that the circulation in the scour hole consisted of two secondary flow cells with water plunging to the bed over the centre of the scour where the two flows met and diverging at the bed downstream (Mosley, 1976; Ashmore, 1982). When the angle of incidence is high there is very little mixing in the confluence of the water from the two contributory channels.

Mosley (1981) has recently reported the results of a brief field study of nine confluence scours and suggests that, for engineering design purposes, a relationship between scour depth and total discharge is the most useful. A thorough investigation of confluence scour comparing field data with laboratory data for comparable sediment characteristics still remains to be attempted in order to confirm Mosley's (1976, 1977) findings.

The scour is an adjustment to the strong secondary currents set up in the confluence. Downstream of the scour hole the channel begins to adjust to the larger discharge; in low angle confluences this occurs almost immediately. The hydraulic geometry of confluences has been investigated to a limited extent by Miller (1958) who demonstrated that channel width increases in accordance with the standard relationships for hydraulic geometry, that is, as the square root of discharge. Just as adjustment to channel division results in channels with width/depth ratios similar to the original undivided channel (Church, 1972) so it would be expected that the downstream channel would adjust to a geometry similar to anabranches free of deepening by the strong secondary currents and turbulence present at confluences. This means that as distance downstream from the confluence increases, the channel may become progressively wider and shallower and hence show a greater propensity for braiding. The literature on braiding suggests that there is a direct relationship between local scour and the presence of bars and braids immediately downstream (Smith, 1973; Hein, 1974; Rundle, 1976; Ashmore, 1979; Moss et al., 1982). However, there is a lack of direct evidence to show that the material scoured from the bed acts as a nucleus stimulating the development of bars downstream. Rundle (1976) describes the

scour holes as a 'trigger' for deposition and braiding but detailed investigations of the role of confluences in braiding are lacking. However, the relatively deep water immediately downstream of scour holes is one obvious location for the development of avalanche faces which may be destroyed as the bar migrates downstream into shallower water.

The orientation of the scour hole, and hence the locus of deposition downstream, are controlled by the relative discharges of the two channels. If the discharges are about equal the long axis of the scour bisects the angle between the two channels. If not the long axis tends to parallel the larger channel. Thus a change in the discharge of one of the confluent channels would result in re-orientation of the scour hole and a change in the position of the locus of deposition.

2-3-4 Sediment Transport and Channel Form

Earlier discussion emphasised that braiding is limited to streams with a large bedload and showed that this is to be expected given the conditions necessary for braiding. This bedload is responsible for the depositional forms on the bed which are a product of the spatial non-uniformity in sediment transport rate. Local scour and deposition are a necessary result of this spatial variability in sediment transport rate. Thus, if bedload transport rate were recorded at one cross-section of a braided stream we would expect there to be considerable variation in that rate through time and between adjacent cross-sections. In view of the number of individual channels involved the pattern of this variation might be so complex as to preclude the recognition of regularities in transport rate due to, for example, the approximately equal spacing of unit bars or diffuse gravel sheets along the channel.

Attempts to measure bedload transport in braided streams have been few (Pickup and Higgins, 1979; Kang, 1982) and only Pickup and Higgins (1979) have attempted to compare measured rates with those predicted by various published sediment transport equations. This situation is hardly surprising given the complexities of flow in braided rivers and the problems of measuring the transport rate of coarse gravel. Only in circumstances such as natural constrictions in the channel, the deposition of sediment at an aggradational site or on rivers amenable to artificial constriction can measurements be made. At the same time the application of standard sediment transport equations is frustrated by the difficulty of measuring the channel geometry of a river undergoing rapid morphological changes. Pickup and Higgins (1979) devised a method of deriving probability distributions of the relevant channel and flow variables for the application of sediment transport formulae and concluded that the Meyer-Peter and Muller (1948) equation gave the most reliable results. Kang (1982) simply demonstrated that the relationship between water discharge and bedload transport rate obeyed a power law with an exponent of approximately 2. There is thus an obvious lack of data, and hence analysis, of the bedload transport rate in gravel braided streams. A reliable hydraulic model may go some way towards rectifying this situation.

At the same time little research has been directed towards fluctuations about the mean rate of sediment transport. Some recent investigations of these fluctuations in sediment transport rate in braided streams have been attempted. Sediment transport rate in a steep, braided mountain stream (Hilda Creek, Alberta) has been shown to fluctuate regularly (Kang, 1982). These fluctuations

occurred on the order of several minutes and Kang identified two modal values; 13 and 30 minutes. In this case little attempt was made to relate the bedload fluctuations to the changes (if any) in channel form, but Smith and Southard (1982) and Southard and Smith (1982) have suggested that the Hilda Creek bedload fluctuations are related to braiding processes such as bar erosion and deposition and channel avulsion, and have identified similar fluctuations in a laboratory model of Hilda Creek. This model also produced much longer-term fluctuations equivalent to a few tens of hours in the field and related to longer-term aggradation and degradation. Smith and Southard (1982, p.52) noted that the rate of sediment input had "little effect on the qualitative character of braided patterns" but they did note an increase in the rate at which channel changes occurred, and a decrease in bed relief during aggradation.

On a larger scale Griffiths (1979) noted fluctuations in bed elevation over several years on the braided Waimakariri River, New Zealand and speculated that bedload moved downstream as waves with a wavelength of perhaps 1km and an amplitude of about 1m. Bedload transport rate was therefore seen as having two components; the plane bed rate predicted from equilibrium transport formulae, plus the fluctuations from this wave-like movement. Griffiths (1979) suggested that the waves of aggradation may appear as groups of bars with avalanche faces migrating downstream. Church (1972) and Church and Gilbert (1975) noted the presence of zones of increased braiding complexity on sandar on Baffin Island and suggested that the treads in the stepped profiles of these streams corresponded to these "sedimentation zones". Church and Jones (1982) recognised the presence of similar features on some largely single-channel gravel streams in British Columbia

and noted that the Soviet literature also contains some reference to regularly spaced aggradational zones on this fairly large scale (Romashin, 1967, cited in Church and Jones, 1982). In order to understand the presence of these sedimentation zones Church and Jones (1982) speculated on the fate of a slug of sediment introduced at one point along a river channel. They suggested that intermittent removal of sediment from this point during floods could result in approximately regularly spaced aggradational zones downstream in which sediment would be trapped temporarily. The result would be a series of steps in the profile where deposition is prominent and braiding of the single channel occurs. It is possible that local controls on the stream long profile, such as bedrock exposures or moraines, could interfere with this pattern by interposing depositional sites. In addition, there is no reason why successive floods would be of the same magnitude and transport the same volume of sediment the same distance.

Whether a slug of sediment delivered to a stream results in one or several bed-level perturbations is an interesting question but the important point seems to be that the channel must respond to the sudden change in sediment supply and that aggradation, and possibly an increase in channel activity or degree of braiding, are the results. Fahnestock (1963), in discussing variations in the degree of braiding with river stage, pointed out the role of sediment supply in the relationship, saying that an aggrading section upstream would deprive the downstream section of sediment and result in degradation, and so on downstream. This link between sediment transport and channel morphology is clearly important to braided river form. Maizels (1979) has shown on a larger scale that

aggradation results in more intense braiding and this also seems to apply to small-scale variations in bedload. Hence there is evidence to indicate that local aggradation in braided streams may occur in response to internal or external sediment supply factors and that in either case more pronounced braiding and, possibly, the presence of a larger number of migratory bars are the results. In this connection it is worth reiterating Lane's (1957) observation that braiding may be the result of a steep valley slope or of aggradation.

2-4 Conclusions

At several places in this review some aspects of braided stream mechanics that are in doubt and worthy of further investigation have been identified. This thesis is aimed at furthering understanding of these aspects and integrating them into a picture of braided river mechanics. In particular the following themes have been identified and are pursued in the succeeding chapters:-

1. The nature of fluctuations in sediment load and the morphological effects of such fluctuations is an aspect of braided river mechanics that has surfaced recently. The origin of these pulses and their physical form remain in question. At the same time the measurement of mean bedload transport rates at a given slope and discharge and the comparison of these rates with other gravel rivers and with sediment transport equations is an area that requires considerable attention.

2. The influence of external variables such as discharge and slope on braided river form and process are known to some extent but there are no generally applicable quantitative relationships for sediment transport rate in braided streams and the influence of these variables on the intensity of braiding and on bar morphology still remain to be investigated in detail. This leads to

consideration of the conditions responsible for the braiding mechanisms described in section 2-2.

3. The controls of bar morphology and the presence of sediment pulses are both elements in explaining the processes of bar deposition and accretion. The role of diffuse gravel sheets and unit bars in these processes are of particular interest.

4. Mosley's (1976, 1977) analysis of confluence scour was conducted under controlled laboratory conditions. A detailed investigation of such features in the field and under 'natural' conditions in the laboratory is lacking as is a comparison of the two. An examination of the role of these confluences in generating bars and controlling the location of deposition is also important in understanding braided stream mechanics.

Chapter 3 : Modelling Principles

3-1 Models in Fluvial Geomorphology

Small-scale hardware models of geomorphic phenomena have several advantages over field study. They allow direct observation of forms and processes that are inaccessible in the field. For example, the nature of bedload movement may be obscured by turbid water in the field but a simple laboratory model using clear water would enable the processes to be described in detail. Scale models compress the time over which processes take place. This speeds up data collection; data that may take years to collect in the field may be collected in a few days or weeks in the laboratory. The experimental approach also allows the independent control of variables because experiments can be conducted in which the governing variables are changed one at a time. In the field it is rarely possible to conduct controlled experiments of this kind although statistical techniques may be used to isolate the influence of each variable. Mosley and Zimpfer (1978) give a more exhaustive list of the potential advantages of hardware models but the most important have been covered here. There are, of course, disadvantages to their use and again, Mosley and Zimpfer (1978) present a list of these. These can be reduced to one basic problem : that of oversimplification or abstraction from reality, in other words the extent to which the model reproduces nature. The degree of abstraction will vary from model to model and in each case both theory and field data can be used to assess the validity of the model. This chapter discusses the validity of the modelling technique employed in this study, and later chapters will discuss some field results which allow further model verification. It should be noted that simplification is not necessarily a disadvantage, in the initial

stages of investigation it may be advantageous to isolate those variables considered important and exclude the less important ones.

In spite of their potential value in fluvial geomorphology and the fact that the principles of hydraulic similitude have been in practical use by engineers for many years, fluvial geomorphologists have apparently been reluctant to use scale models in research in alluvial stream form and process. This does not mean that laboratory studies have been rare. There are many examples of such investigations (Lewis, 1944; Leopold and Wolman, 1957; Wolman and Brush, 1961; Schumm and Khan, 1972; Hooke, 1975), but attempts to relate the laboratory results directly to the field using hydraulic scaling criteria are rare. The tendency has been to regard laboratory streams as analogues, or process models (Hooke, 1968) of larger rivers, or as small streams in their own right (Leopold and Wolman, 1957). This approach is responsible for the scepticism often expressed about the usefulness of laboratory models.

Analogue models reproduce some aspects of a particular natural phenomenon but the materials used, and processes involved, may be quite different from those in nature. For example, several studies of meanders exist in which meanders are reproduced by a thread of water running down a glass plate (Tanner, 1960; Gorycki, 1973; Davies and Tinker, 1981). These surface tension meanders may provide some observations on meander form and behaviour which are useful in the study of river meanders (Davies and Tinker, 1981), but must be treated with caution because of the degree of abstraction involved.

Process models represent the next stage towards dynamically similar models in what is really a continuum of model types. In response to a paper by Bruun

(1967) on the application of hydraulic similarity theory to alluvial stream studies, Hooke (1968) suggested that, rather than using site-specific engineering models, geomorphologists may find a more general kind of modelling more valuable. This was partly motivated by Hooke's doubt that the knowledge of the mechanics of alluvial streams was sufficiently advanced to "specify exactly the conditions necessary for hydraulic similarity" (Hooke, 1968, p.392). A process model is based on simpler criteria that : 1) "gross scaling relations" (Hooke, 1968, p.392) be met (these were not defined by Hooke); 2) the model reproduce some morphologic characteristic of the prototype and; 3) the processes producing this characteristic in the model have the same effect in the prototype. Such a model would use the same materials in the model as in the natural feature but the results would be of purely qualitative application. Thus, Schumm and Khan's (1972) study of the influence of channel slope on channel pattern may be considered a process model. As with analogue models, the results from process models have some applicability to natural phenomena but are unlikely to be of quantitative use because of the absence of any strict scaling criteria.

Mosley and Zimpfer (1978) suggest that 'process-similar' models may point out previously unsuspected aspects of river channel behaviour, or factors which had previously been considered unimportant. In this case, they may be extremely valuable guides to the design of field experiments and observations.

Leopold and Wolman's (1957) argument that the laboratory stream should be considered to be a small natural stream really goes little beyond process modelling. If the stream is not a model the results are of limited applicability (they can only be used to predict the behaviour of small natural streams). The

extension of the results to large streams is in effect using the laboratory stream as a model, and in the absence of any scaling criteria, it can only be considered a process model. In fact, as will be seen later, it is likely that Leopold and Wolman's (1957) streams in poorly-sorted sand and with steep, shallow channels, may be fairly good quantitative models of natural gravel streams.

This study is based on the contention that it is possible, in certain cases, to go beyond process modelling and produce a laboratory stream which, while not a hydraulic model in the site-specific engineering sense, does yield quantitative results for some forms and processes that can be applied directly to the field. This applies particularly to gravel streams and Parker and Anderson (1975), Parker (1979), Southard, Smith, Drake and Kuhnle (1981) and Ashmore (1982) have demonstrated this theoretically and experimentally, particularly for gravel braided streams.

3-2 The Principles of Hydraulic Similarity

A discussion of the modelling criteria used in this study requires a brief introduction to hydraulic similarity theory. Complete expositions of the theory appear in several engineering texts (Allen, 1947; Henderson, 1966; Yalin, 1971; Shen, 1979;) and the reader is referred to these for a comprehensive discussion.

The prototype is the large-scale field feature to be modelled. Exact modelling requires the fulfillment of dynamic similarity of model and prototype. This means that all quantities involving the principal dimensions of mass, length and time (for example force, pressure, dynamic viscosity) should be scaled down by the same amount. Thus, for example, the relative magnitude of all forces should be the same in model and prototype. The satisfaction of dynamic

similarity necessarily satisfies geometric similarity (all lengths are scaled by the same amount) and kinematic similarity (all quantities involving the dimensions of length and time, for example velocity, are scaled by the same amount). A variable in the model is given the subscript m, in the prototype p, and the ratio of the two is denoted λ. Thus, if h is the depth of flow, h_m is the model depth, h_p the prototype depth and λ_h equals h_p/h_m.

3-2-1 Scaling Fully Turbulent Flows

Standard dimensional analysis of steady, open channel flow uses seven independent parameters, chosen by physical intuition, to describe the flow characteristics : μ dynamic viscosity, ρ fluid density, h mean depth (which is approximately equal to the hydraulic radius), k the roughness height, u the average velocity, S the water surface slope and g the acceleration due to gravity (Yalin, 1971). These can be combined into four dimensionless variables : S, h/k (relative roughness), uh/ν (Reynolds number, Re, where $\nu = \mu/\rho$) and $u/(gh)^{0.5}$ (Froude number, F). Dynamic similarity is given by $\lambda_S = 1$, $\lambda_{h/k} = 1$, $\lambda_{Re} = 1$, $\lambda_F = 1$. Given that $\lambda_g = 1$, $\lambda_\mu = 1$, and $\lambda_\rho = 1$, it proves impossible to satisfy $\lambda_{Re} = 1$ and $\lambda_F = 1$ simultaneously. (A formal proof of this can be arrived at by dimensional analysis (Yalin, 1971) or by showing that if $\lambda_F = 1$ then $\lambda_u = \lambda_L^{0.5}$, while if $\lambda_{Re} = 1$ then $\lambda_u = \lambda_L^{-1}$ where λ_L is the scale ratio for any length). Note, however, that this is true only if λ_μ and $\lambda_\rho = 1$, that is, if the fluid viscosity and density are the same in the prototype and model. One way of avoiding this impasse is to change fluid viscosity and/or density by, for example, changing the temperature of the fluid. The alternative is to relax the criterion of exact dynamic similarity and allow either λ_F or λ_{Re} to be different from unity. The

latter is the common approach in open-channel flow models. Where the prototype flow is fully turbulent the effect of viscosity on flow characteristics becomes relatively unimportant, particularly when the channel boundaries are rough. For example, Shields' curve of critical conditions for sediment movement shows the critical Shields stress to be independent of particle Reynolds number, Re*, provided Re* exceeds about 100. Yalin (1971) suggests a value of 70 as the lower limit.

In fully turbulent flow, at low ratios of h/k, flow resistance is largely independent of Reynolds number (Re) when it exceeds 5×10^3 (Henderson, 1966, Fig. 4.3). Thus, provided a model can be run at a scale which produces Reynolds numbers in excess of these values ($Re \geq 5000$ and $Re^* > 100$), the exact scaling of Reynolds number is unnecessary and the model can be based on Froude similarity alone. Manipulation of the Froude number gives the scales for the various parameters necessary for Froude similarity. Such a model has the following properties :

1. the grain size and flow dimensions are all scaled down by the same amount,
2. the model bed material has the same density and specific weight as the prototype,
3. the bed slope is identical to that of the prototype, and
4. the velocity scale is equal to the square root of the length scale, i.e. $\lambda_u = \lambda_L^{1/2}$. From this it follows that $\lambda_Q = \lambda_L^{5/2}$ (where Q is discharge).

The reliability of the Froude model rests on the assumption that the Reynolds number is unimportant in the properties of the model to be studied. For this reason Froude modelling is particularly convenient for modelling steep rivers where grain Reynolds numbers are large and relative roughness is

small (Yalin, 1971, 110-115). In low slope sand rivers where grain Reynolds numbers are much smaller the type of bedforms present is influenced by, amongst other variables, the value of the Reynolds number (through water temperature and concentration of suspended sediment) making careful Reynolds modelling very important. In addition, a small-scale model of a sand-bed prototype would run into the problem that the bed material may be cohesive.

3-2-2 Application of Froude Modelling to Gravel Braided Streams

It is possible to apply the principles of Froude modelling to a specific stream by obtaining information on its grain size, channel dimensions, slope and discharge, and scaling accordingly. Alternatively, a generalised model of braiding can be obtained by making use of the grain size and specific weight, and channel slope similarity, and simply setting the flume to a slope and discharge at which it is expected that braiding will occur. Information on channel pattern thresholds for such small streams is rare and an alternative is, given a grain-size scale, to select a value of slope and discharge from a diagram based on larger streams (e.g. Leopold and Wolman, 1957; Kellerhals, 1982), and scale down these values according to Froude modelling criteria. All calculations need to take into account the limitations of size and discharge imposed by the experimental equipment. This more general model requires field verification of at least some aspects of morphology and process to assess the validity of the model. In the case of a dynamically similar model, if one aspect of the flow can be shown to be modelled accurately, then the same must be true for all other aspects. This also applies to a Froude model as long as Reynolds number is not a significant influence on the processes being considered. This generalised approach to Froude modelling is

somewhere between the process model approach proposed by Hooke (1968) and the strict site-specific model employed in engineering studies.

As an example of this general approach consider a braided stream with a slope of 0.015, a discharge of $10 m^3 s^{-1}$, and D_{50} of 45mm. Such a stream would be braided according to Leopold and Wolman's (1957) diagram and Kellerhals' (1982) more recent graph of discharge versus slope and grain size. Because the stream is self-formed the only length scale to be chosen is the grain size. Suppose the model has D_{50} of 1.5mm, then $\lambda_L = 30$ and $\lambda_Q = 30^{5/2} \simeq 5000$ giving a model discharge of $0.002 m^3 s^{-1}$. Froude modelling criteria dictate that slope remains the same and if the prototype is braided it is expected that the model will also be braided. The relative depth (h/D_{50}) and Froude number should be the same in the model and prototype and this could be verified by reference to field data from gravel braided streams. The grain Reynolds number in the prototype (u^*D_{50}/ν) would be about 9000 (assuming a depth of 30 cm) and in the model 57.5. A grain Reynolds number of about 60 is a little below the limit suggested above for fully turbulent flow and this may have some effect on the model results. A slightly lower scale factor (say, $\lambda_L = 20$) would avoid this problem (Re^* would then be about 105, and Q_m would be about $0.005 m^3 s^{-1}$). This gives an indication of the grain size, slope and discharge necessary to produce small-scale braided streams which obey the rules outlined in the previous section.

Thus far the scaling has used a single grain size for the bed material. How should natural gravel with a range of sizes be modelled ? The bed material is the major component of flow resistance where there are no bedforms. The movement of the bed material is a complex phenomenon involving several processes including

the hiding of small particles by large ones, the rolling of large particles over small ones, the detachment of grains and the nature of rolling and saltation. Different properties of the grains and the flow may be important in each of these transport processes and in flow resistance, making it difficult to decide how the bed material ought to be scaled down. For small prototype grain sizes or large scale ratios it is common to scale grain size using fall velocity similarity (Dodge, 1978). In a Froude model, velocity scale is equal to the square root of the length scale so that grain size distribution in the model would be a distorted version of the prototype distribution (the smaller grains would be larger than if they were scaled geometrically). For large prototype grains and a small scale ratio the difference between fall velocity and geometric scaling is quite small. For example, with a scale of 1:16 and a prototype grain size of 24mm, fall velocity scaling gives a model diameter of 1.75mm while geometric scaling gives 1.50mm (Dodge, 1978). Yalin (1971) recommends that, in view of the fact that different grain properties are important in different aspects of resistance and sediment transport, the simplest and most reliable approach is to use geometric scaling. A further consideration is that for the general modelling used here it is impossible to know precisely what is the prototype grain size distribution, in which case the minor differences between fall velocity and geometric scaling are irrelevant. Therefore, geometric scaling was used so that :

$$\frac{D_{50m}}{D_{50p}} = \frac{D_{90m}}{D_{90p}} = \frac{D_{im}}{D_{ip}} \qquad 3\text{–}1$$

where D_i is the grain size of any percentage, i, of the cumulative grain size distribution. This is discussed further in Chapter 4.

One further criterion is necessary. The model should have bed shear stress high enough to produce sediment transport. In the case of grain Reynolds number greater than 100, the value of critical Shields stress is about 0.04. The Shields stress is a dimensionless number similar in form to the Froude number and if the scaling has been carried out correctly it should have the same value in prototype and model. For example, a prototype channel with slope 0.01, depth 0.3m, and D_{50}=36mm would have a Shields stress of about 0.05. A Froude model with $\lambda_L = 30$ would also have a Shields stress of 0.05. Some preliminary calculation of Shields stress can be carried out, but only when the model is run can the criterion be checked.

This relates to a more general point about the similarity of sediment transport which has already been mentioned in connection with modelling grain size distributions. Sediment transport is composed of a series of processes each of which is governed by different variables. There is no way of predicting whether a model which reproduces the total bedload will be an accurate model of the dimensions of bedforms, the length of saltation, the mode of movement, the rate of attachment and detachment of particles or some other component of sediment transport. Hooke (1968) had this in mind when he made his comments about the impossibility of accurate hydraulic modelling. Without careful verification it would be impossible to assess the validity of the model with respect to sediment transport, but, with a foundation on the principles of hydraulic modelling, there is good reason to assume that it is at least a process model, and in some respects may be more reliable than that.

One further problem is the potential effect of surface tension in the model.

The earlier discussion of modelling criteria used Froude and Reynolds similarity as the primary aims of modelling. At small scales, where inertial forces are small, the surface tension may be relatively much more important than in the prototype. Surface tension at the banks of a narrow channel may affect the velocity distribution by retarding the flow at the boundaries and may influence sediment entrainment at the banks. Henderson (1966) states that as long as channel widths and depths are greater than about one inch (25mm), capillary effects would be unimportant for flow characteristics. In the model used here this criterion is not always satisfied in the smaller channels. Unfortunately, the modelling texts contain no systematic discussion of the effects of relatively large surface tension on channel processes such as sediment entrainment. In the larger channels the turbulence is probably large enough to break up the surface tension and render it unimportant. Maxwell and Weggel (1969) pointed out that the surface tension may influence propagation and amplitude of gravity waves. However, at high Froude numbers (>0.5) they showed this effect to be negligible.

To summarise, the main modelling criteria to be satisfied are :

1) the same fluid is used in model and prototype, and sediment density is identical in model and prototype; however, suspended sediment is absent from the model,
2) the dimensionless size distribution of the bed material of the model and prototype should be the same; in other words, all sizes are scaled down by the same amount,
3) slope is the same in model and prototype,
4) relative roughness (h/D_{50}) should be in the same range in model and prototype,
5) Froude number should have the same range of values in the model and prototype,
6) grain Reynolds number (Re^*) should be greater than 70, and flow Reynolds number (Re) greater than 2000,
7) sediment movement should be present in the model, i.e. Shields stress should exceed critical (about 0.04).

It should be emphasised that this is a general model whose characteristics ought to be similar to any gravel stream of approximately the same slope and relative roughness. Whether there is exact modelling of all forms and processes is impossible to establish, but, as pointed out previously in connection with sediment transport, it is unlikely. In some cases there may be adequate quantitative modelling, in others only process modelling.

3-3 Preliminary Model Verification

Various comparisons will be made between model and field observations in later chapters but an indication of the success and limitations of the modelling can be gained from analysis of the dimensions and flow characteristics of the braid anabranches measured as part of the confluence scour study (see Chapter 6 for details of the measurement procedures). The data are tabulated in Appendix 1. Froude number based on cross-sectional average depth and velocity ranged from 0.41 to 1.08 in the field and from 0.56 to 0.93 in the laboratory. On average, Froude numbers are slightly higher in the model so that Froude similarity is only approximate, but in both cases Froude numbers are in the range where standing waves and antidunes might be expected in parts of the flow. The densimetric Froude number, Fo, is defined as (Ashmore and Parker, 1983) :

$$Fo = u^2/(RgD_{50}) \qquad 3-2$$

where u is the average velocity in the two channels, R is the submerged specific gravity of the sediment (≈ 1.65), g is the acceleration due to gravity, and D_{50} the average grain size of the surface layer in the two channels for each pair of confluent channels, and gives an idea of the relative sediment mobility in the

model and the field. For the field data, Fo ranged from 1.21 to 1.90 with an average of 1.42. In the model, values ranged from 1.02 to 1.76 with an average of 1.40. The similarity between the two data sets is therefore very close.

Using overall flume slope as an approximation to local anabranch slope in the model, it is possible to calculate values of Re* for the channels. These fall in the range 35.7 to 103.2 with a mean of 62.8 which is on the border line for fully rough flow. It may be argued that D_{90} is a more reasonable roughness size to use. Since the model grain size distribution was designed so that $D_{90} = 2D_{50}$, the Re* values would double. Thus, there may be some slight influence of the relatively high viscous forces on sediment transport and flow resistance.

The relative roughness (h/D_{50}) is a useful measure of the flow geometry and indicates whether geometric similarity is obeyed. In the field it ranged from 1.9 to 12.2 with an average of 5.2, while in the model the range is from 3.2 to 13.4 with an average of 6.9. Thus, the two sets of anabranches have very similar relative roughness and hence geometric similarity is obeyed. Much of the resistance to the flow in gravel streams without bedforms is due to the grains on the bed. Indeed, many empirical or semi-empirical resistance equations for gravel streams give velocity as a function of some form of relative roughness (Bray, 1982). It is therefore reasonable to assume that similarity in relative roughness is indicative of similarity in resistance also.

It is apparent from this preliminary analysis that the general rules for dynamic similarity outlined above have been obeyed in the model experiments and from a hydraulic point of view, therefore, the model is a reasonable one. Later chapters will illustrate the geomorphological validity of the model.

Chapter 4 : Data Collection

4-1 Laboratory Procedure

The experiments were carried out in a river tray 10m long and 2.3m wide filled to a depth of 0.1m with poorly sorted sand. Flume slope could be adjusted by four jacks driven by an electric motor. Water was pumped to the flume from the laboratory sump and discharge to the head of the flume was measured by a magnetic flow meter in the delivery line. The flow meter could be read at a digital display calibrated to give the discharge in litres per second. The water discharged vertically down into the wooden head section of the flume, with part of its energy being dissipated by a 0.04m thick fibre cushion. The wooden head section, positioned in the centre of the flume against the upstream end, was 0.8m wide and 0.6m long with 0.08m high walls on either side. Its bed was flush with the sand bed and parallel with the floor of the flume.

Sediment delivered to the tail of the flume was washed to the bottom of the tail box by two submerged water jets. A compressed air diaphragm pump removed the sediment plus some water and returned it to the head of the flume through a 0.025m diameter plastic pipe. There the pipe was divided into four nozzles by a series of elbows. Each of the nozzles discharged vertically down into the head section immediately downstream of the main water supply. The pressure of the compressed air supply could be regulated and the pump was calibrated to give the discharge of water to the flume through the sediment return line. Sediment discharge was measured by placing four fine-mesh sieves under the input pipes and measuring the sediment accumulated on the sieves over a given length of time. This recirculating system was chosen primarily for ease of

singlehanded operation. A sediment feed system may take several hours to reach an equilibrium slope and requires careful monitoring throughout to ensure that equilibrium is maintained. The recirculating system is self-regulating and no trial and error is needed to arrive at a suitable sediment feed rate for the imposed slope and discharge.

The water level at the tail of the flume was controlled by an overflow pipe with an adjustable plastic sleeve. Bed elevation at the downstream end of the flume could be changed by tilting the frame of wire mesh that retained the bed material. The top of the frame than acted as the base-level below which the stream could not erode. The water surface elevation in the tail box was set so that there was a slight drawdown to avoid backwater influencing sedimentation in the flume. The experimental equipment is illustrated in Figures 4-1 and 4-2.

Measurements of bed and water surface topography were made with a point gauge mounted on a trolley. The trolley was moved up and down the flume on rails bolted on top of each side of the flume. The gauge could be moved across the width of the flume by sliding it along the trolley, and vertically by means of a ratchet. Thus measurements could be made on a three-dimensional grid. Two photographic platforms were positioned in the laboratory ceiling about 3m vertically above the flume. These were used for still photography. A time-lapse 16mm motion picture camera mounted above the upstream end of the flume gave an oblique view of the channel changes. The camera exposed one frame every 30 seconds.

Selecting a suitable grain size distribution for the model was problematic. As stated in Chapter 3, the geometric scaling criteria require that every fraction

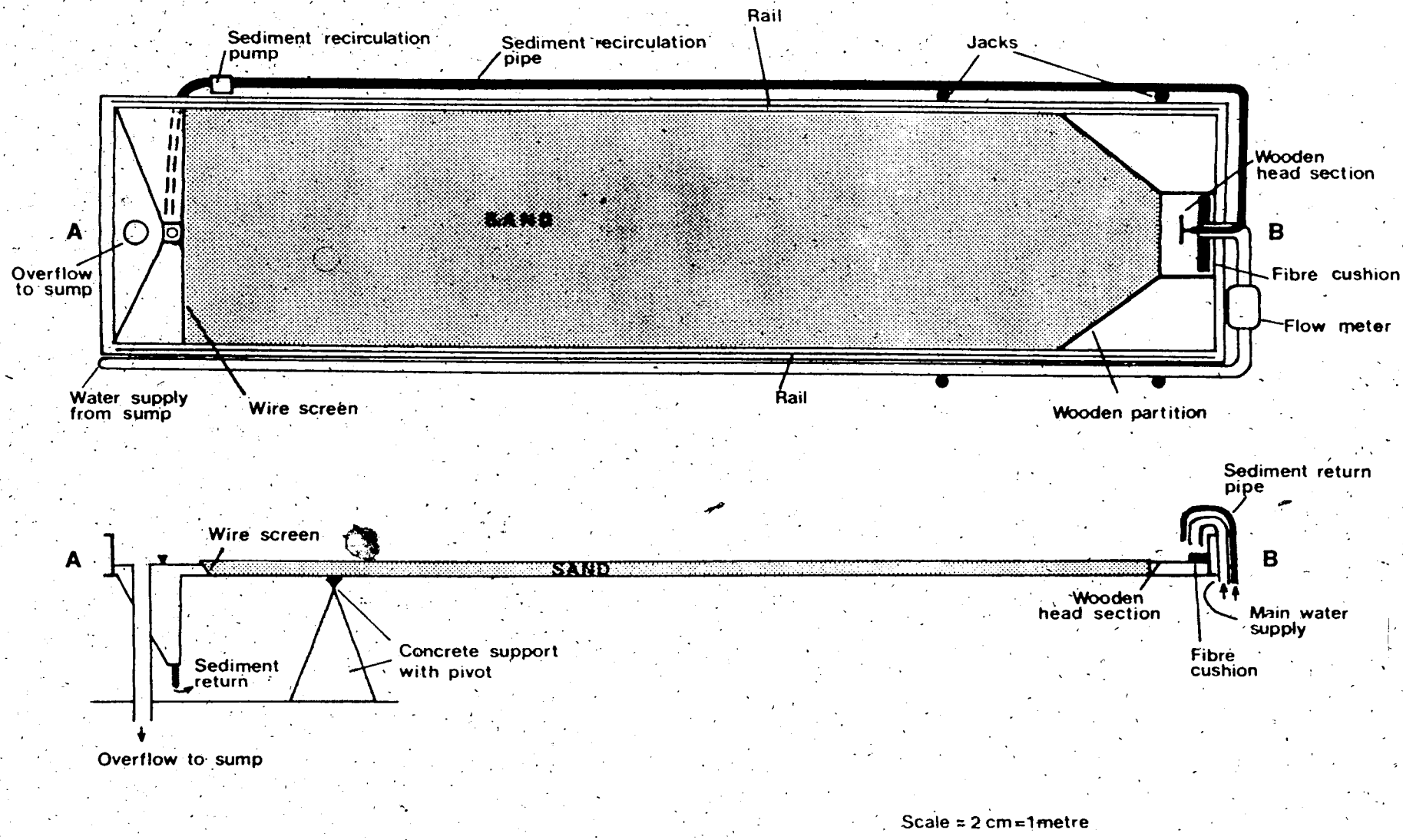

Figure 4-1 Plan and section of the flume showing its principal features.

Figure 4-2 View of the head arrangement of the flume showing the sediment input pipe (narrow, black pipe) with four nozzles and the main water input pipe (wide, grey pipe).

of the size distribution of the prototype be scaled down by the same amount. In a site-specific model the grain size distribution to be modelled is given. However, in a more generally applicable model of the type used here where no specific prototype is used, the prototype grain size distribution is not specified. The best solution in this case is to summarise information from typical prototype streams (i.e. gravel braided streams) and manufacture a distribution similar to those prototype distributions. Unfortunately, very few data of the kind required are available and there are some differences in the sampling methods used. The most useful data are from Kicking Horse River, British Columbia (Smith, 1974 and pers. comm. 1981), Ekalugad Sandur, Baffin Island, N.W.T. (Church, 1972) and Sunwapta River, Alberta (Rice, 1979). In addition, two data sets from single channel gravel rivers in Alberta (Kellerhals, Neill and Bray, 1972) and Britain (Charlton, Brown and Benson, 1978) were used.

The equivalence of the various methods employed in sampling gravel streams has been the subject of some discussion (Leopold, 1970; Kellerhals and Bray, 1971a and b; and Klingeman and Emmett, 1982). In this case the main problem is the equivalence (or otherwise) of grid-by-number samples of the surface layer used by Church (1972), Kellerhals et al. (1972) Charlton et al. (1978) and the sieved bulk sample of surface and subsurface material used by Smith (1974) and Rice (1979). One would expect the inclusion of the matrix from the subsurface sample to increase the size range of the sample compared to the surface pavement sample, and to give a smaller average size. Surprisingly, Kellerhals and Bray (1971b) report little difference between the mean grain size of samples taken from the same site using the two different methods, provided

material finer than 8mm is removed from bulk samples before analysis. However, Kellerhals and Bray (1971b) did not analyse differences in sorting due to the two different procedures.

From the point of view of the present study the bulk sieved samples provide the best estimate of typical size distributions of fluvial gravel. Analysis of the Kicking Horse and Sunwapta River data showed that there is an improvement in sorting with a decrease in grain size so that the correct value of sorting depends on whether the model is to represent coarse, medium or fine gravel. It was decided to use an intermediate value representing gravel with D_{50} of about 30-40mm. Not all the curves had sufficiently well defined tails to give values of ϕ_{95} and ϕ_5 for calculation of graphic standard deviation, therefore a cruder estimate of sorting, D_{90}/D_{10}, was used. This parameter had a mean value of 5.83 for 30 samples of varying D_{50} (10 each from coarse, medium and fine gravel reaches) from Sunwapta River and 5.71 for 9 samples from Kicking Horse River. The grid-by-number samples have very similar values; Ekalugad Sandur has an average value of 5.87 for 30 samples varying in D_{50} from 32mm to 107mm, while the British rivers have values of 3 to 5. The Alberta (Kellerhals, Neill and Bray, 1972) study only quotes values of D_{90} and D_{50} but assuming a symmetrical distribution the ratio D_{90}/D_{10} ranges from 3.5 to 7.5 with typical values of 4 to 5. The overall pattern indicates that a distribution with D_{90} about five times greater than D_{10} would be representative of medium gravel. Recently Bathurst (1982) has published data from gravel beds streams showing that values of D_{84}/D_{50} are usually in the range 1.6 to 2.8. The sorting of the bed material used here is therefore at the upper end of the range of Bathurst's (1982) data. Some of the

distributions are slightly skewed but in view of the crudeness of the analysis this was ignored in preparing the bed material.

The bed material was manufactured by mixing proportions of a selection of industrial sands of known size distribution and coarse granules (2 to 8mm) sieved from street sand used by the City of Edmonton. This material is well-rounded silica sand apart from the street sand which contains more angular fragments. The flume sand was mixed volumetrically, necessitating some experimentation with small samples of various mixtures before the correct volumetric combination of the component sands needed to give a suitable size distribution by weight was arrived at. The final distribution is plotted in Figure 4-3 along with composite curves from Kicking Horse River and Ekalugad Sandur for comparison. This size distribution has D_{90}/D_{10} of 6.4 and a D_{50} of 1.16mm. Five percent by weight is coarser than 4mm (-2ϕ) and five percent is finer than 0.345mm ($+1.5\phi$).

At a length scale of 1:20, 0.345mm is equivalent to about 7mm, and at 1:30 it is equivalent to about 10mm. Thus, the sand fraction of the prototype distribution is not represented in the model. Sand is usually a significant component of the prototype bed material. For example, Rice (1979) reported that sand composed from 10 to 30 percent by weight of bed material samples from the braided Sunwapta River, Alberta. In the field it is evident that the sand is important as a matrix in the gravel, helping to maintain steep (and sometimes overhanging) banks which could not be reproduced in the model. Beyond this the role of the sand in processes such as sediment transport is unknown. The absence of the sand equivalent in the model is a necessary simplification since scaling the sand fraction would give cohesive material which would not reproduce the essentially non-cohesive nature of the prototype material.

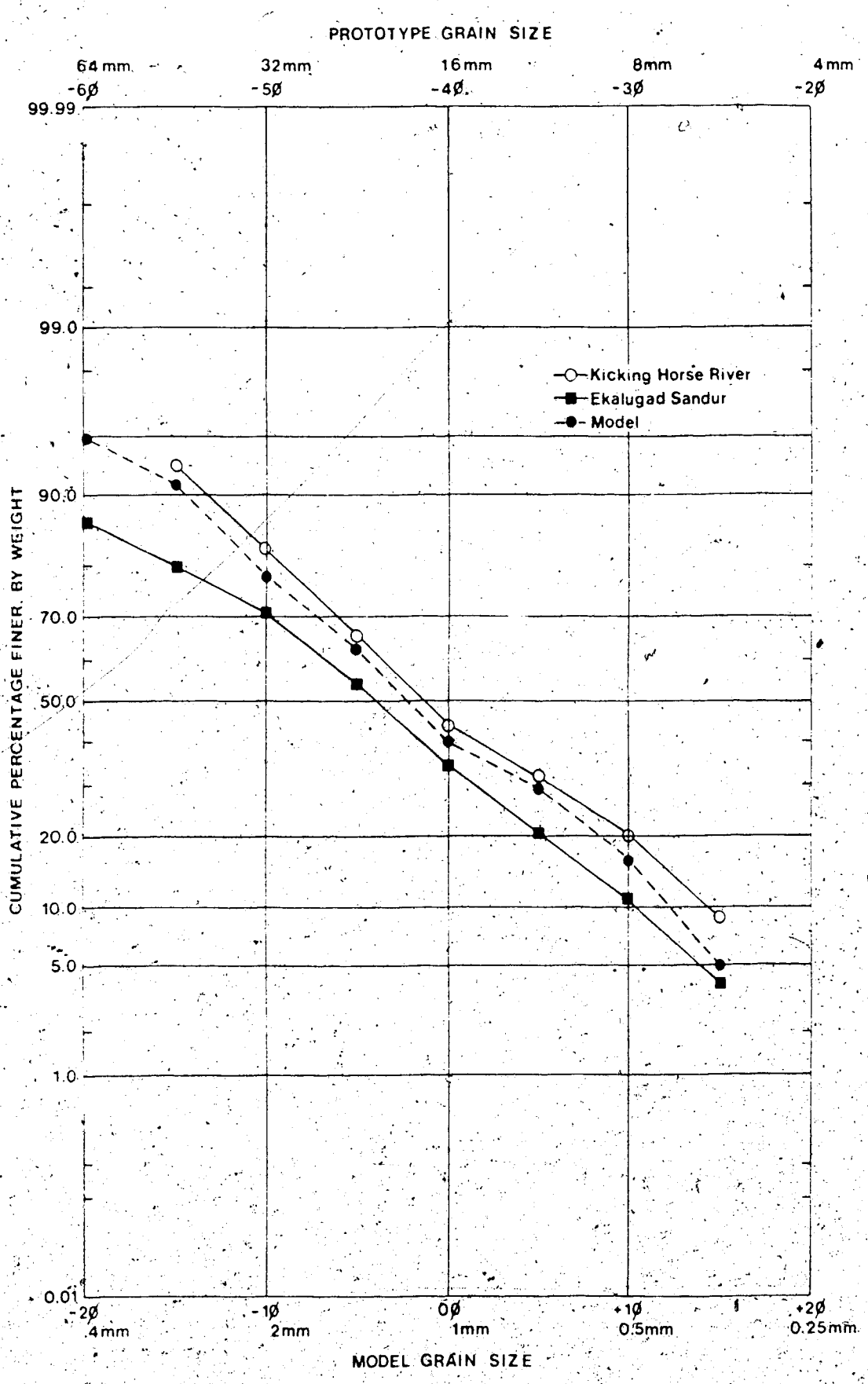

Figure 4-3 Comparison of model and prototype particle size distributions.

Eleven experimental runs were made. Each was begun by levelling the sand bed and cutting a straight trapezoidal channel down the centre of the bed using a metal template. The size of the channel for each run was calculated using a standard resistance equation for gravel bed channels (Parker and Peterson, 1980):

$$u = \left(\frac{g\,h\,S}{C}\right)^{0.5} \qquad 4\text{–}1$$

where;

$$\frac{1}{\sqrt{C}} = 2.5 \ln\left(11\,\frac{h}{D_{90}}\right) \qquad 4\text{–}2$$

C is a resistance coefficient, u the mean velocity, h the channel depth, and S the water surface slope. This was used to give channel dimensions that would just convey the intended discharge at the chosen slope. Figure 4-4 shows the channel at the start of a run.

Various combinations of slope and discharge were used in ten runs. These are listed in Table 4-1 along with the dimensions of the initial channel and the duration of the run. The run numbers in Table 4-1 will be used throughout the thesis when referring to a specific run. Each run was given 10 or 15 hours to establish a braided channel and was then run for another 50 hours. The flume was turned on and off daily because it could not be left unattended overnight.

In the majority of runs sediment was introduced to the head of the flume through four input nozzles (see Figure 4-2). This arrangement induced some aggradation at the head of the flume and in an attempt to reduce this, and to assess its potential effect on channel form, three runs (2,3 and 4) were carried out using only two nozzles on the sediment return line. These runs, 2,3 and 4, are

Figure 4-4 Upstream view of the flume prior to the commencement of a run showing the initial channel cut in the sand bed.

Table 4-1

Flow conditions for the experimental runs

Run	Discharge ($m^3 s^{-1}$)	Flume Slope	Duration (hours)	Initial Channel and Flow Characteristics				
				Width (m)	Depth (m)	Froude No.	Shields Stress	Particle Reynolds Number
1	0.00300	0.015	60	0.50	0.015	1.04	0.114	101.5
2	0.00300	0.015	60	0.50	0.015	1.04	0.114	101.5
3	0.00150	0.010	70	0.40	0.012	0.91	0.061	74.1
4	0.00150	0.015	60	0.35	0.011	1.19	0.083	86.9
6	0.00150	0.015	60	0.35	0.011	1.19	0.083	86.9
7	0.00150	0.010	65	0.40	0.012	0.91	0.061	74.1
8	0.00450	0.010	60	0.50	0.018	1.19	0.091	90.8
9	0.00450	0.015	60	0.50	0.017	1.30	0.129	108.0
10	0.00225	0.015	60	0.40	0.013	1.21	0.098	94.5
11	0.00120	0.015	67	0.30	0.010	1.28	0.076	82.9

replications of runs 1,7 and 6 respectively and differ from them only in the method of sediment introduction. The morphological consequences of this are discussed in Chapter 7. A variety of measurements were made in each run and these are explained in the following chapters along with the presentation of the results for each of the aspects of braided river form and process investigated. After completion of the ten runs listed in Table 4-1 insufficient data on scour at confluences had been collected. Therefore, at the end of run 11 discharge was increased to 0.0025 $m^3 s^{-1}$ for several hours during which time scour data only were collected. This supplementary run is referred to as run 12.

4-2 Field Observations

Field work concentrated on measurements of confluence scour holes and also observations of channel changes during July and August, 1981. The field site was located on the proglacial Sunwapta River in Jasper National Park, Alberta (Figure 4-5). The reach chosen is about 8km long and begins 10km downstream of the river's source at Athabasca Glacier. Although some of the small tributaries along this reach are predominantly fed by rainfall during the summer, the regime of the Sunwapta River is characteristic of proglacial streams, with peak discharges coinciding with spells of hot weather. During hot spells, river stage (recorded continuously at the downstream end of the reach) also fluctuates daily (Figure 4-6), with peak discharge at about 4p.m. at the upstream and 10p.m. at the downstream end of the reach.

The valley floor in the study reach is about 0.5km wide and occupied completely by outwash deposits. Average main channel slope declines from 0.01 at the upstream end, where median grain size is about 80mm, to 0.001 in the

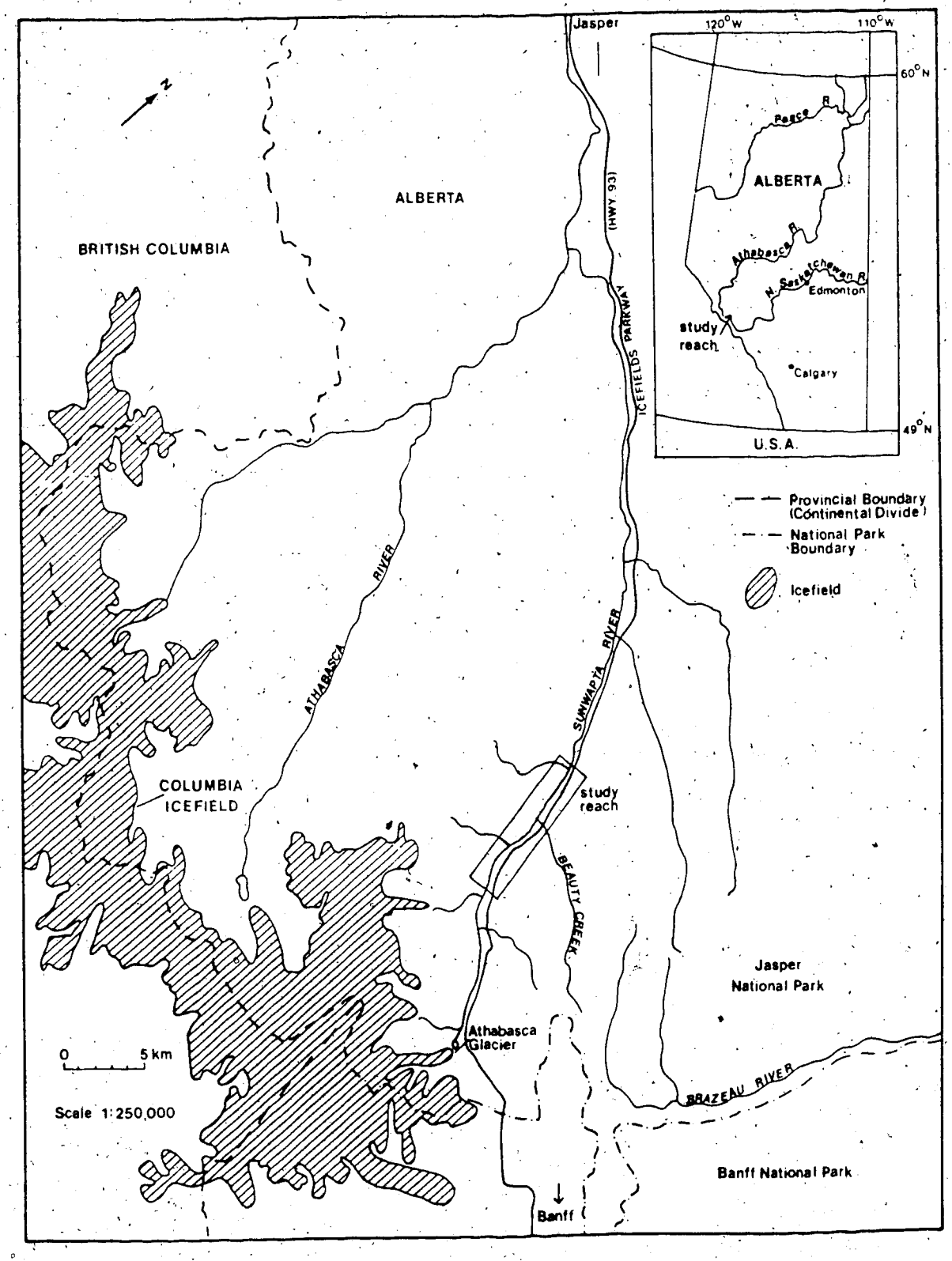

Figure 4-5 Location of the field site on Sunwapta River, Alberta.

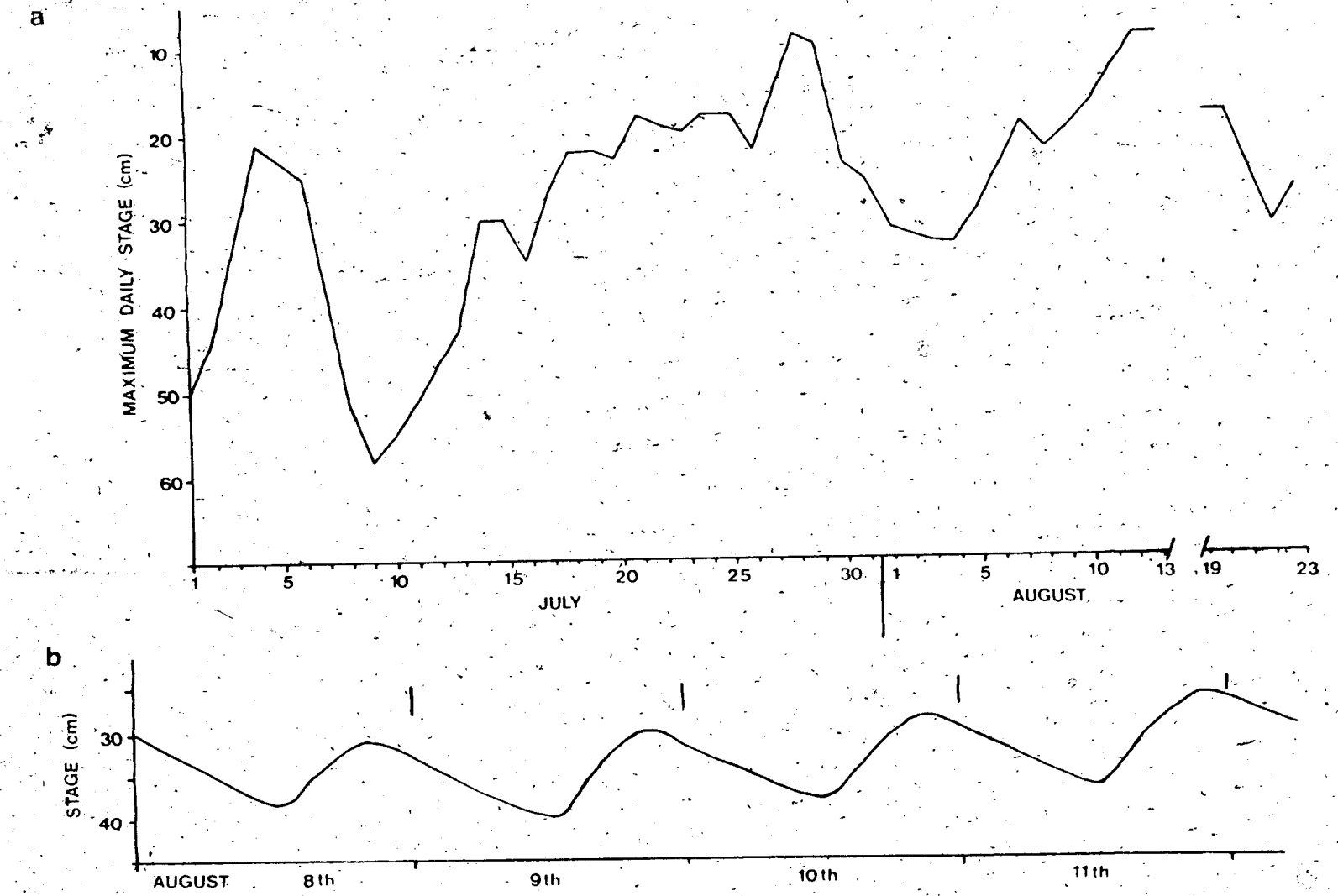

Figure 4-6 Flow regime of Sunwapta River at the downstream end of the study reach in July and August, 1981.

(a) Maximum daily stage.

(b) Diurnal fluctuations in stage during warm weather in August.

sandy downstream section where a local base-level is imposed by an alluvial fan deposited by a tributary (Diadem Creek). The reader is referred to Rice (1979) and Dawson (1982) for further details on the area. Figure 4-7 gives an idea of the general character of the study reach.

Photographic sites were chosen at several vantage points along the reach and during high flow periods photographs were taken every six or seven days to monitor channel changes. Data collection for the confluence scour study is described in Chapter 6.

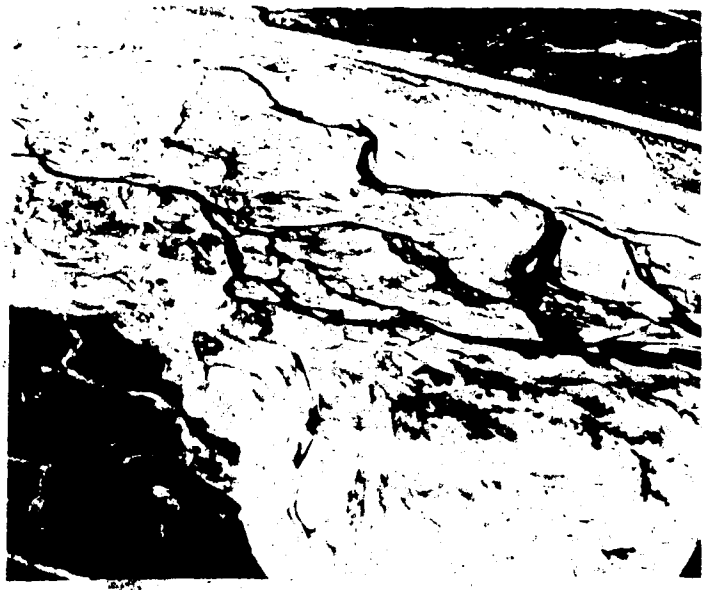

Figure 4-7 Oblique aerial view of Sunwapta River showing the general character of the river in the vicinity of Beauty Creek. Flow is from right to left. The two lane highway running along the top of the photograph gives an indication of scale.

Chapter 5 : Sediment Transport

5-1 Introduction

Bedload has been shown to comprise up to 50 per cent of the total load of some gravel braided streams (Church, 1972; Østrem, 1975; Kang, 1982; Hammer and Smith, 1983) and is thus an important component of their sediment load. From the point of view of calculating total stream load and denudation rates the large proportion of load carried as bedload is important in itself. From the point of view of stream morphology, however, the bedload is important because of its role in producing bedforms through its interaction with the flowing water. It is this aspect of sediment transport with which this thesis is primarily concerned; the spatial and temporal fluctuations in bedload transport rate that are responsible for scour and bar formation. In addition, it is concerned with the influence of slope and discharge on the stream morphology and process, and the mean sediment transport rate is an important aspect of this discussion. Finally, sediment transport measurements are a useful means of attempting to verify the validity of the model by comparing the data with other published sediment transport studies on gravel-bed streams.

This chapter is concerned with all three of these aspects of sediment transport : the relationship between mean transport rate and flow rate, the comparison of these rates with published data, and the temporal fluctuations about the mean transport rate.

5-2 Data Collection

Bedload sampling was carried out for the complete duration of each run by placing a fine-mesh 8"(0.23m) diameter sieve below each of the outlets of the

sediment return line at the head of the flume for one minute every fifteen minutes. There are two convenient points of access to the sediment recirculation system where sampling is possible; the downstream end of the flume as the sediment falls into the tail box, and the upstream end as it is introduced into the flow. Trial sampling at both points showed the upstream sample point to be more convenient because the downstream point required a rather cumbersome collecting tray extending across the entire width of the flume. The disadvantage of sampling at the upstream end is that occasionally the sediment transport rate exceeded the capacity of the sediment recirculation pump. This resulted in temporary accumulation of sediment in the tail box until the sediment transport rate declined again and the accumulated sediment was gradually removed. The consequence of this was to attenuate the sediment transport peaks delivered to the upstream end of the flume. In other words the delivery rate at the upstream end did not always correspond exactly with the sediment transport at the downstream end of the flume. This problem occurred only a few times and was most common in the runs with high sediment transport rates, particularly run 9. As far as long-term average sediment transport rate is concerned this problem is irrelevant provided that, at the end of the run, little or no sediment remains stored in the recirculation system itself.

The choice of sampling interval was a compromise between two requirements: the accuracy of the estimate of the population mean provided by a given sample size and the practical considerations of how frequently samples could be obtained. Initially guidance was provided by a statistical calculation of the sample size necessary to give an adequate estimate of the population mean. The

results from a pilot test indicated that a coefficient of variation of about 50% was to be expected and in that case sample size would need to be between 100 and 400 in order to estimate the mean to within 10 and 5 per cent respectively, with a confidence limit of 95 per cent. For a 60 hour run this requires a sample interval of between 10 and 30 minutes. The single-handed operation of the flume restricted the sample frequency because of the necessity to make other measurements apart from the sediment transport rate. Sampling at very short intervals may also affect the sediment transport delivery to the stream because in a recirculation system sediment delivery is interrupted during sampling. A 15-minute sampling interval was judged to be most convenient given these constraints. Subsequent calculations of the coefficient of variation (Table 5-1) for each run show the estimates at a 95 per cent confidence limit to be within 3 to 10 per cent of the population mean. Occasionally the 15-minute sampling was interrupted, and some samples missed, so that sample sizes are slightly smaller than the 240 that four samples per hour for 60 hours would provide (see Table 5-1). This sample interval also limited the periodicity of regular fluctuations in the sediment transport rate that could be identified. Ideally, one would like a continuous record of sediment load but the choice of a 15-minute sampling interval limited the subsequent analysis to fluctuations with a period of greater than one hour (see section 5-5).

For seven runs which covered the range of discharge and slopes used, three samples from each run, chosen arbitrarily but whose volume was about average for the run, were dried, sieved and weighed to obtain a conversion for wet volume to dry weight (Table 5-2) and to provide an impression of the range of grain sizes transported during each run.

Table 5-1

Average bedload transport rate for the laboratory experiments

Run	Discharge ($m^3 s^{-1}$)	Slope	Sediment transport rate				
			Arithmetic mean ($g s^{-1}$)	Standard deviation ($g s^{-1}$)	Coefficient of Variation	Geometric mean ($g s^{-1}$)	Sample Size
1	0.00300	0.015	9.92	4.20	42.3	9.08	221
2	0.00300	0.015	9.99	3.98	39.8	9.25	225
3	0.00150	0.010	1.69	1.09	64.5	1.38	256
4a	0.00150	0.015	3.63	1.77	48.7	3.28	111
4b	0.00150	0.015	5.71	1.54	27.0	5.47	108
6	0.00150	0.015	2.90	1.58	54.5	2.52	213
7	0.00150	0.010	1.06	0.62	58.5	0.90	242
8	0.00450	0.010	8.54	3.51	41.1	7.93	217
9	0.00450	0.015	22.71	7.23	31.8	21.00	225
10	0.00225	0.015	5.29	2.53	47.8	4.76	231
11	0.00120	0.015	1.51	1.26	83.4	1.13	225

5-3 Analysis of the Model Data on Sediment Transport Rate

The arithmetic mean, standard deviation and geometric mean of the measurements of bedload transport rate for each run are displayed in Table 5-1. The geometric mean is probably a better estimate of average transport rate than the arithmetic mean because the latter is biased by a few very high transport rates present in most of the runs. The coefficients of variation range from 27-83 per cent, dispersion about the mean being proportionally greater for runs with low mean transport rates. For analysis of run 4 the data were divided into two halves. The first half (run 4a) represents the braided channel present in the first thirty hours of the run, while the second half (run 4b) are data from the entrenched single channel that developed thirty hours into the run. Chapter 7 gives a more detailed description of these morphological aspects of the experiments.

A power relationship between sediment transport rate and total stream discharge is apparent from the data. Figure 5-1 shows a graph of this relationship and also illustrates that for a given discharge sediment transport rate is strongly affected by the flume slope. Thus, runs 3, 7, and 8, with slopes of 0.010, have markedly lower sediment transport rates than their counterparts at the same discharge but with slopes of 0.015 (runs 4, 6, and 9). This is not surprising given the dependence of sediment transport rate on the transporting capacity of the flow (measured by stream power or bed shear stress) and thus partially on water surface slope. In view of this dependence on slope as well as discharge there is little point in fitting a least-squares regression line to the complete data set. Instead the data have been separated into the two slope classes. Figure 5-1 shows

Table 5-2

Conversion of volume of sediment to dry weight

Run and Sample time (hours and minutes)	Wet Volume (cm^3)	Dry weight (g)	Dry weight : wet volume ($g\ cm^{-3}$)
Run 3			
25.00	70	116.4	1.66
35.00	60	95.3	1.59
45.00	112	171.9	1.53
Run 4			
55.00	200	304.8	1.52
57.30	275	351.5	1.28
56.00	220	343.7	1.56
Run 7			
57.00	28	45.9	1.64
61.00	16	26.0	1.62
41.00	40	52.6	1.31
Run 8			
58.00	180	264.0	1.47
48.00	250	401.5	1.61
54.00	308	586.8	1.91
Run 9			
39.15	490	786.1	1.60
52.45	950	1537.8	1.62
58.00	850	1377.2	1.62
Run 10			
59.00	134	230.0	1.72
58.00	230	356.3	1.55
51.15	250	406.0	1.63
Run 11			
53.30	56	94.1	1.68
57.45	48	80.3	1.67
62.30	74	120.5	1.63
		mean =	1.59
		standard deviation =	0.13

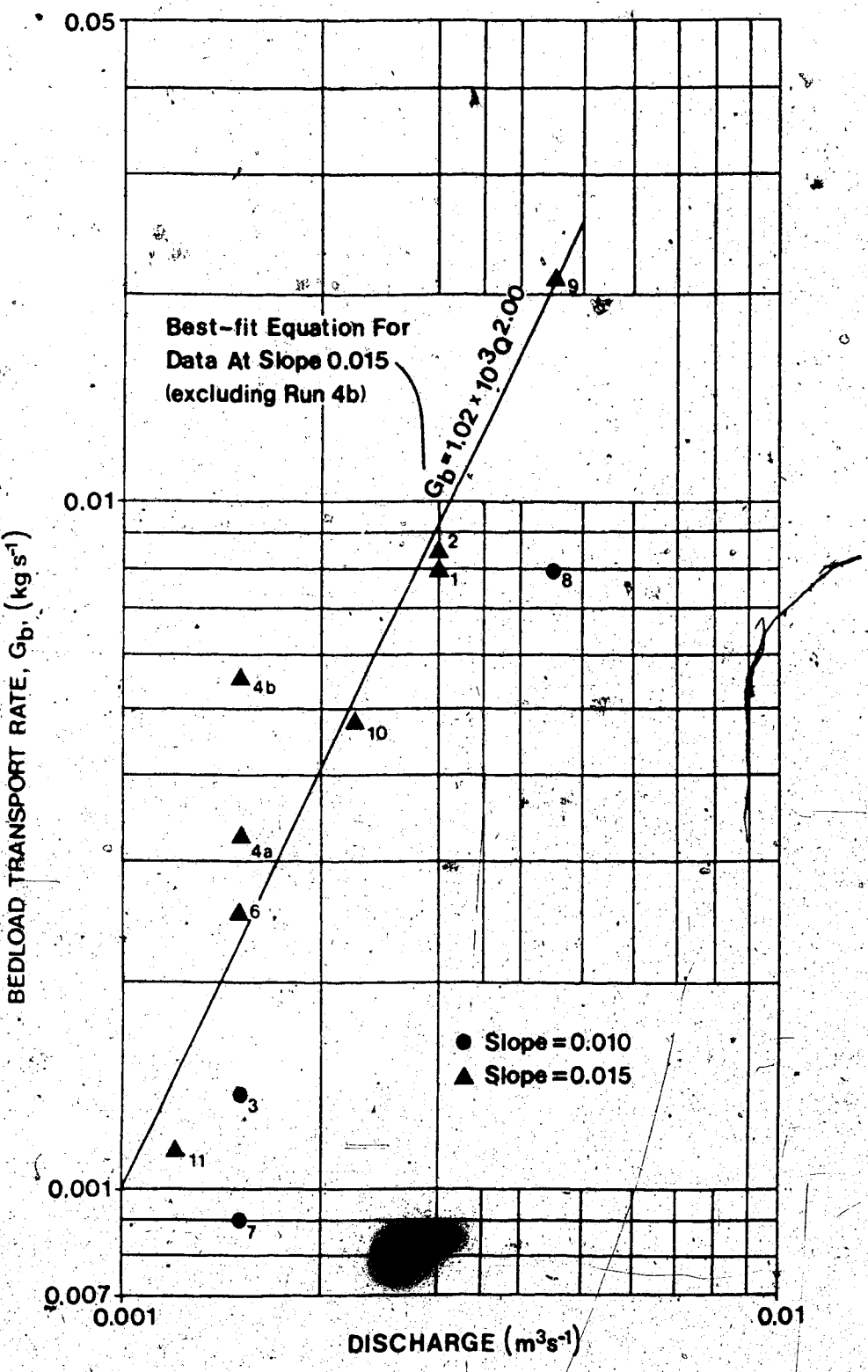

Figure 5-1 Relationship between bedload transport rate (G_b) and stream discharge (Q), stratified for slope.

the best-fit regression equation (by the method of least squares) for the runs at slope 0.015 :

$$G_b = 351\, Q^{1.81} \qquad 5\text{-}1$$

where G_b is the geometric mean dry weight rate of bedload transport (in kg s^{-1}) and Q is the total flume discharge in m^3s^{-1}. All the data fit this line very closely except for run 4b which has an anomalously high sediment transport rate. If this run is eliminated the best-fit equation becomes :

$$G_b = 1020Q^{2.00} \qquad 5\text{-}2$$

where G_b and Q are defined as for Equation 5-1. The incision of the channel in run 4b (see Chapter 7) may account for the exceptionally high transport rates in that case. The sample size for runs at the lower slope is too small to allow line fitting but there is an apparent trend approximately parallel to that at the higher slope.

At a given slope and discharge there is some difference in the sediment transport rate using different head arrangements (see Chapter 4 for a description of this and Chapter 7 for further discussion of its morphological effects). Runs 1 and 2 have almost identical sediment transport rates despite their different head arrangements, but runs 3 and 7, and 4 and 6, both show markedly higher sediment transport rates when there are two sediment input lines (runs 3 and 4) instead of four (runs 6 and 7). This is apparently related to the tendency for runs with two sediment input lines to be less braided than runs at the same slope and discharge with four input lines. Discussion of this point is presented in Chapter 7.

Figure 5-2 is a plot of the stream power index, Ω, versus bedload transport

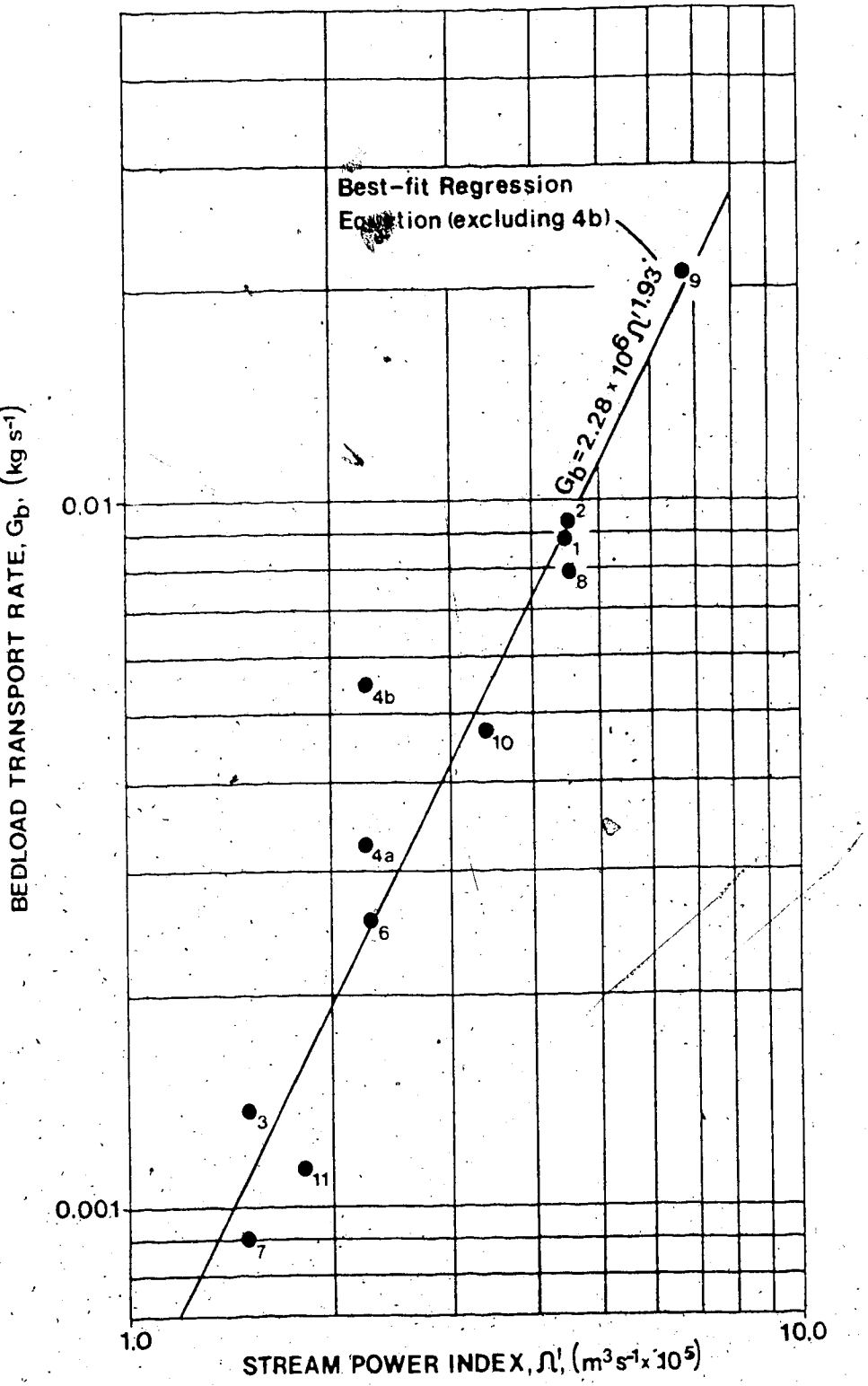

Figure 5-2 Bedload transport rate (G_b) versus stream power index (Ω').

rate. The stream power index is simply the product of slope and discharge and indicates the rate of energy expenditure along a unit reach of channel. (Stream power itself is the product of Ω' (the power index) and the specific weight of water (Richards, 1982)). The use of stream power has the effect of bringing the runs for the two different slopes onto a single graph. The best-fit straight line for this graph is :

$$G_b = 1.13 \times 10^6 \, \Omega'^{1.86} \qquad 5\text{-}3$$

Leaving out the apparently anomalous point for run 4b gives the best-fit equation:

$$G_b = 2.28 \times 10^6 \, \Omega'^{1.93} \qquad 5\text{-}4$$

This is confirmation of the influence of stream power on bedload transport rate as suggested by Bagnold (1973). This relationship is examined further in a later section.

Table 5-3 displays the mean size, sorting, ϕ_5 and ϕ_{95} of the three samples of bedload analysed for each of runs 3, 4, 7, 8, 9, 10 and 11. Variation within runs is likely to be large so that these samples are inadequate for drawing any major conclusions. However, they do give an indication of the trends and, despite the sparsity of the data, it is surprising to find apparently little consistent increase in the mean grain size with increasing slope and discharge. Parker, Klingeman and McLean (1982) report an increase in mean bedload size with increasing discharge (bed shear stress) in the gravel-bed Oak Creek, Oregon, and it seems reasonable to expect a similar result in the model experiments. While there is no increase in mean size with increasing discharge, ϕ_{95} does increase in size and thus the bedload is less well sorted at higher discharges. It is also apparent that several of the runs,

Table 5-3

Grain size and sorting data for seven experimental runs

Run	Discharge (l s^{-1})	Slope	ϕ mean	ϕ_{95}	ϕ_5	ϕ standard deviation
8	4.50	0.010	-0.257	-1.640	+0.990	0.834
3	1.50	0.010	-0.303	-1.470	+0.877	0.759
7	1.50	0.010	-0.227	-1.450	+1.050	0.789
9	4.50	0.015	-0.382	-1.940	+0.957	0.893
10	2.25	0.015	-0.276	-1.630	+0.967	0.822
4	1.50	0.015	-0.440	-1.700	+0.670	0.759
11	1.20	0.015	-0.309	-1.470	+0.733	0.715

particularly those with low slopes and discharges, were not transporting the coarsest sizes available.

5-4 Comparison of Model Data with Published Data and Theory.

5-4-1 Introduction

The sediment transport data illustrate the often observed dependence of sediment transport rate on discharge and slope (and hence stream power). It is possible to refine this limited, qualitative conclusion by attempting to establish whether there is a quantitative correspondence with other empirical data from gravel rivers and flume models, and with sediment transport theory.

Sediment transport rate is a function of two basic variables: the characteristics of the sediment and the ability of the flow to move it. The most important sediment characteristic (given the sediment density), and often the only one considered, is the size of the particles to be transported. When the sediment consists of a mixture of sizes, as do fluvial sediments, it is necessary to use a single particle size representative of the mixture as a whole or to analyse the problem by breaking the sediment down into a series of size ranges. This, together with the influence of particle shape, specific gravity and the structure of the sediment exposed to the flow (phenomena such as packing, imbrication, and hiding) render the problem rather complicated under field conditions. Add to this the difficulty of finding a suitable parameter to express the transporting capacity of the flow, and the value of this parameter at which transport commences, and one can appreciate why a single, generally applicable sediment transport relationship remains elusive. One is left, then, with numerous empirical and theoretical studies between which it is often difficult to find agreement. This is perhaps an

overly pessimistic view of the situation, but it is worthwhile bearing these comments in mind throughout the ensuing discussion.

Empirical studies of sediment transport rely mainly on one of two parameters for expressing the transporting ability of the fluid; average bed shear stress (τ_o) and stream power per stream length (Ω). In a steady, uniform flow the former is defined as :

$$\tau_o = \rho g h S \qquad 5\text{-}5$$

where ρ is water density, g the acceleration due to gravity, h is the mean flow depth, and S the water surface slope. Stream power per unit stream length Ω is also, by definition, the mean rate of kinetic energy supply and dissipation per unit length of channel (Bagnold, 1980, p.455) and can be shown to be equal to :

$$\Omega = \rho g Q S \qquad 5\text{-}6$$

where Q is the total stream discharge and the other variables are as for Equation 5-5. Dividing by stream width gives power per unit bed area (ω) and :

$$\omega = \tau_o u \qquad 5\text{-}7$$

where u is the mean velocity of the flow. Hence there is a direct relationship between ω and τ_o. Since there is a finite value of both stream power (ω) and bed shear stress (τ_o) below which sediment transport rate is effectively zero, and since these critical values (ω_c and τ_c) vary with sediment characteristics and flow conditions, it is normal to relate sediment transport rate to the difference between, or the ratio of, actual to critical stream power or bed shear stress (i.e. $\omega - \omega_c$, $\tau_o - \tau_c$, ω/ω_c or τ_o/τ_c).

Ideally one would like to compare the laboratory data reported herein with

other laboratory and field data for braided streams. Unfortunately the availability of such data is severely limited although this is perhaps not surprising given the complexity of such streams. To the author's knowledge there are two laboratory studies of braided streams (apart from this one) that report sediment transport measurements; Leopold and Wolman (1957) and Schumm and Khan (1972). The situation with respect to field data is no better and only Kang (1982) and Hammer and Smith (1983) provide data that are sufficiently detailed to give a bedload rating curve. Both sets of field data are from a small, (discharges are less than 0.5 m^3s^{-1}) steep, cobbly outwash stream, Hilda Creek, in the Canadian Rocky Mountains. Pickup and Higgins (1979) have attempted to analyse sediment transport in the braided Kawerong River, Papua-New Guinea (the braiding is the result of mine tailing disposal in the river) but unfortunately provide figures only for discharge and sediment load averaged over several months, so that no instantaneous rating curve can be derived. Because of the paucity of data for braided streams it becomes necessary to attempt a comparison with data from single channel gravel streams. In principle there is no reason why this should not be possible provided reasonable values for the average hydraulic parameters in a cross-section can be derived along with unit sediment transport rates (sediment transport rate per unit width). In single channel streams this presents little problem. Bed shear stress, for example, is known to vary across the channel and, at a given point, to fluctuate around an average value at a given discharge due to turbulence in the flow. Despite these variations it is possible to obtain strong correlations between, say, average bed shear stress in a cross-section of the channel and sediment transport rate, although considerable scatter may

exist in the relationship. Deriving cross-sectionally averaged values of, say, depth for a braided stream may be much more problematic than for single channel streams; the cross-section shapes are more complicated and at a given point the cross-sectional form undergoes constant change at discharges high enough for sediment transport to occur. The result is that, unlike single channel streams, braided stream cross-sections do not have a stable predictable form at a given discharge. Thus arriving at an average value of, for instance, bed shear stress, for sediment transport calculations, first involves obtaining knowledge of the average width, mean depth, and mean channel slope at a given discharge, and then calculating an average bed shear stress for that cross-section. In other words there are two parts to the problem of finding a suitable cross-sectionally averaged value for bed shear stress at a given discharge in a braided stream. The first is to define the typical form of the cross-section at that discharge and the second is to calculate average depth, slope and width for that cross-section. Pickup and Higgins (1979) discuss this second problem and suggest that one possible procedure is to average across the entire section, lumping all the separate channels together and in a sense treating the braided channel the same way one would a single channel. The drawback to this approach is that the hydraulic parameters derived by this method may give a different sediment transport rate from that obtained by treating separately each channel within the braided river section and summing the results. Pickup and Higgins (1979) imply that the latter method would provide more accurate results. They suggest instead a completely different procedure which involves obtaining the frequency distributions of the relevant hydraulic variables: the number of channels per cross-section, the

proportion of the total discharge in each channel, the channel shape, the channel slope and the flow resistance. Values of these parameters are calculated for each mean daily discharge using an algorithm based on random numbers to sample each frequency distribution, and so derive values of the hydraulic variables for each channel in the braided stream cross-section. These are then used, along with a sediment transport equation, to calculate the expected sediment transport rates. This is a satisfactory approach when one is attempting to compare a predicted value with the actual value of sediment transport rate in a braided stream, but if a direct comparison with data from single channel streams is required the averaging procedure, despite its potential inaccuracy, is probably the only possible solution. Assessing the accuracy, or otherwise, of the averaging procedure is rather difficult. Given that one carries out the prediction using some suitable published sediment transport formula, there are two sources of error in the prediction: the averaging procedure, and the sediment transport formula itself. If there is a discrepancy between the predicted rate and the actual rate of sediment transport it is impossible to determine to what extent the error can be ascribed to the sediment transport equation rather then the averaging procedure. Thus, while Pickup and Higgins (1979) claim that there is a small average discrepancy between their predicted and actual rates of sediment transport, there is no means of checking whether or not this is a fortuitous cancelling out of errors, nor whether the same fortuitous circumstances might not have given similar discrepancies for a simple averaging procedure which Pickup and Higgins (1979) reject. Clearly there is much potential for detailed research into these problems but only if the two sources of error can be separated.

5-4-2 Analysis and Results

The data sources for the analysis of sediment transport rate are displayed in Table 5-4. The only field data available for braided streams are from Hilda Creek, Alberta (Kang, 1982; Hammer and Smith, 1983). Unfortunately these data lack details on channel dimensions and flow properties, particularly channel width and depth, and it will become apparent that this limits their utility in the analysis. Therefore these data are not listed in Table 5-4. The laboratory channels are very similar in scale to those of the present study but only eight of a total of 68 data points are from braided channels. The field data are all from single channel gravel streams. Limiting the sample to gravel streams ensures bedform similarity with the laboratory streams so removing the influence of different bedform regimes on flow resistance and hence sediment transport rate. In addition the restriction to gravel bed streams reduces the influence of relative depth (h/D) on the transport rate. Bagnold (1977, 1980) has shown that at a given stream power the sediment transport rate is higher in streams with low relative depth. In the laboratory streams h/D_{90} is generally less than 10 whereas the field data range from about 12 for the Elbow River up to about 60 for the Tanana and Clearwater Rivers. These differences may influence the comparison between the field and laboratory data but it should be borne in mind that they are relatively small differences when one considers that in sand bed streams h/D_{90} would be of the order of 1000 or greater. The accuracy of the sampling procedures employed is bound to vary considering that some of the laboratory data were obtained by almost continuous sampling of sediment transport while many of the field data are instantaneous samples collected in only a few tens of

Table 5-4 Summary of Sources for Sediment Transport Data

Source	Location	Channel Pattern	Bedload Sampling Procedure	Sample Size	Particle size (mm) D_{50}	Particle size (mm) D_{90}	Discharge ($m^3 s^{-1}$)	Width (m)	Mean depth (m)	Slope (m/m)
Leopold and Wolman (1957)	Laboratory streams	Single channels plus 4 braided channels	Monitoring of sediment feed rate and bed elevation to maintain equilibrium	27	0.80	2.50	0.001-0.002	0.1-0.6	0.1-0.2	0.001-0.0015
Schumm and Khan (1972)	Laboratory streams	Single channels plus 4 braided channels	Monitoring of sediment feed rate and bed elevation to maintain equilibrium	19	0.70	1.50	0.0042	0.5-1.5	0.003-0.05	0.001-0.020
Wolman and Brush (1961)	Laboratory streams	Straight, single channels	Continuous weighing of sediment at downstream end of flume	27	0.67	0.88	0.00028-0.00240	0.1-0.4	0.01-0.02	0.002-0.007
Present Study	Laboratory streams	Braided channels plus one single channel	Regular samples, 4 per hour, from sediment recirculation system	11	1.20	2.60	0.0012-0.0045	0.3-1.0	0.007-0.012	0.010-0.015
Hollingshead (1971)	Elbow River, Alberta	Single channel	Basket sampler, VUV sampler and filling of bed excavation	24	25.00	95.00	35.0-110.0	10-25	0.5-1.0	0.00075
Burrows et al. (1979)	Tanana River, Alaska	Single channel	Regular samples, 20 per cross-section, using Helley-Smith sampler	7	15.00	50.00	750-1700	200-600	1.8-2.9	0.0005
Jones and Seitz (1980)	Snake River, Idaho	Single channel	Regular samples, 20 per cross-section, using Helley-Smith sampler	24	27.00	110.00	1100-3300	166-195	3.8-5.5	0.0007-0.0011
Jones and Seitz (1980)	Clearwater River, Idaho	Single channel	Regular samples, 20 per cross-section, using Helley-Smith sampler	10	18.00	90.00	1500-3100	142-149	4.9-5.5	0.00035-0.00062
Parker (pers. comm) and Parker, Klingeman and McLean (1982)	Oak Creek, Oregon	Single channel	Regular samples using vortex sampler	21	20.00	65.00	1.53-2.83	3.66	0.305-0.445	0.0097-0.0108

seconds. The large amount of scatter in the field data may well be explicable in these terms. The reliability of some of the laboratory data may also be questionable, however, particularly that of Leopold and Wolman (1957) and Schumm and Khan (1972) who relied on changes in bed elevation to determine whether the rate of sediment feed was the correct one for the imposed slope and discharge. The accuracy of this technique depends on the accuracy of the bed surveys and to some extent on the size of the channel since a large bed area requires a greater volume of sediment loss or gain before changes in elevation are detectable.

To avoid extrapolating graphs from very small-scale rivers to very large field rivers the comparison between laboratory and field requires the selection of dimensionless parameters for sediment transport rate and the transporting capacity of the flow. For the former the most widely used parameter is that originally proposed by Einstein (1950). This uses the sediment particle diameter as a scaling factor and can be written :

$$\phi = \frac{q_s \rho^{0.5}}{(\gamma_s D)^{1.5}} \qquad 5\text{-}8$$

where q_s is the weight rate of sediment transport per unit width, γ_s the submerged specific weight of the fluid, ρ is the fluid density and D the grain size of the sediment. When this expression is used in the sediment transport calculations for which it was derived, and where there is a mixture of grain sizes, the sediment is broken down into several size ranges and the calculations performed separately for each size range. If the analysis is simplified by using a single characteristic grain size to represent the entire grain size distribution, it is open to question

which percentile of the size distribution should be used. Add to this the fact that many gravel streams have a bed surface pavement whose size distribution differs from that of the underlying material and one is presented with a difficult choice. With little basis on which to make this choice any decision is arbitrary but both Parker et al. (1982) and Milhous (1973) (quoted in Klassen, 1982) suggest D_{50} of the sub-pavement since it is close to D_{50} of the sediment load, and this is the size adopted here. In the case of the laboratory channels this is actually D_{50} of the sediment mixture used in the experiments. When written in terms of volume rather than weight, Einstein's sediment load parameter (Equation 5-8) becomes :

$$q^*_b = q_b/(R\,g\,D_{50})^{0.5}D_{50} \qquad 5\text{-}9$$

where q_b is the bedload discharge per unit width of channel, R is the submerged specific gravity of sediment (1.65), and g the acceleration due to gravity. This is the version of Einstein's parameter used herein.

On the other side of the sediment transport equation is the transporting power of the flow. Again it is necessary to find a dimensionless form for this and two parameters are used herein. The first is the Shields stress, τ^*, which can be written :

$$\tau^* = \frac{h\,S}{R\,D} \qquad 5\text{-}10$$

where h is the water depth, S the water surface slope, R the submerged specific gravity of the sediment and D the particle size. When used to represent the average dimensionless shear stress across the channel, h is calculated as the cross-sectionally averaged depth.

The second parameter, the dimensionless unit stream power index, ω, is defined as :

$$\bar{\omega}' = q\,S/(R\,g\,D)^{0.5}D$$

5-11

where q is the water discharge per unit width and S, R, g and D are water surface slope, submerged specific gravity of sediment, acceleration due to gravity and particle size, respectively. It is important to note that as mentioned previously (section 5-3), stream power per unit bed area is defined as the discharge-slope product multiplied by the specific weight of water so that $\bar{\omega}'$ is only a dimensionless index of stream power, not dimensionless stream power itself.

Both the Shields stress and the stream power index require a suitable percentile of the grain size distribution to be chosen for defining the characteristic grain size (D). Milhous (1973) suggested the use of D_{35} of the pavement, rather than D_{50} of the subpavement used in calculating q^*_b. However, this is impossible to calculate for the laboratory channels because it is not clear that a pavement was present and in any case there are no size distributions available for the surface layer whether or not the channels were paved. Initially, therefore, the subpavement D_{50} is used herein for both τ^*, the average Shields stress, and $\bar{\omega}'$, the stream power index.

Arising at this point is the problem, discussed in the previous section, of averaging the flow parameters across the channel. The calculation of q^*_b and $\bar{\omega}'$ requires a value of channel width and the calculation of τ^* requires an average depth. In the single channel streams which comprise the majority of the data these are simply defined. In all cases total stream width is used for the sake of consistency despite the fact that the active width is available in some cases (for example, Hollingshead, 1971). In the case of the braided channels both Leopold

and Wolman (1957) and Schumm and Khan (1972) quote channel widths and depths but give no indication as to how they were measured. This lack of knowledge of the method used in each case limits the usefulness of these data. For the braided streams of the present study 80 detailed cross-sections are available for each run, measured in batches of 8 at five-hourly intervals. This allows the calculation of cross-sectional parameters that can be averaged to provide values typical of each combination of slope and discharge. In other words the temporal and spatial variability of cross-section form is accounted for. It is still necessary to derive widths and average depths from these cross-sections and the procedure adopted was as follows. Average width for each run was calculated by measuring from each cross-section the width of channel where water depth exceeded 2mm. This depth was taken to be an indication that water was flowing through that part of the cross-section and that the water present was not a thin film of 'groundwater' which immersed most of the sediment surface during each run. Taking the arithmetic mean of these widths (80 for each run) gave an average channel width for each run. Average depths were calculated in a similar manner. The cross-sections were measured by recording water surface and bed elevations at 0.05m intervals across the flume. Average depth for a cross-section was calculated as the arithmetic mean of the depths in excess of 2mm, and the mean of these 80 mean depths provided an average depth for each run. These techniques are simple, but they provide reasonable estimates of width and depth and an estimate of their likely variability. Given the concurrent variation in sediment transport rate one can think of the points that appear on subsequent diagrams as mean plotting positions for each run around which there is

considerable scatter in both the x and y directions. The difference in plotting position between runs 4a and 4b is an indication of the extremes possible for a given combination of bed slope and discharge.

Dimensionless bedload discharge, dimensionless stream power index and Shields stress were calculated for all data listed in Table 5-4 and these computations are tabulated in Appendix 2. The Tanana, Snake and Clearwater Rivers all transport a mixture of sand and gravel which at low discharges is predominantly sand. The size of the data sets for these streams was reduced by eliminating the points representing predominantly sandy bedload. The provision of grain size distributions for the bedload in each sample allowed the elimination of any data points which have D_{50} of the bedload less than 8mm, that is, those with bedload which was not predominantly gravel. Parker et al. (1982) found this procedure of benefit in finding orderly relationships within these data, although their criteria for selection of data points were slightly different from those adopted here.

The graphs of q^*_b (the dimensionless sediment transport rate) versus $\tilde{\omega}'$ (the dimensionless unit stream power index), and $1/\tau^*$(the reciprocal of the Shields stress) are shown in Figures 5-3 and 5-4 respectively. The scatter on both graphs is considerable although individual data sets show quite well defined trends. The trends for the data from the present study and of the field data from the Elbow River and Oak Creek are perhaps the best defined. In contrast, the laboratory data of Leopold and Wolman (1957) and the field data from the Snake and Clearwater Rivers show considerable internal scatter and a poorly defined trend. Figure 5-3 includes a curve showing the approximate relationship between q^*_b and

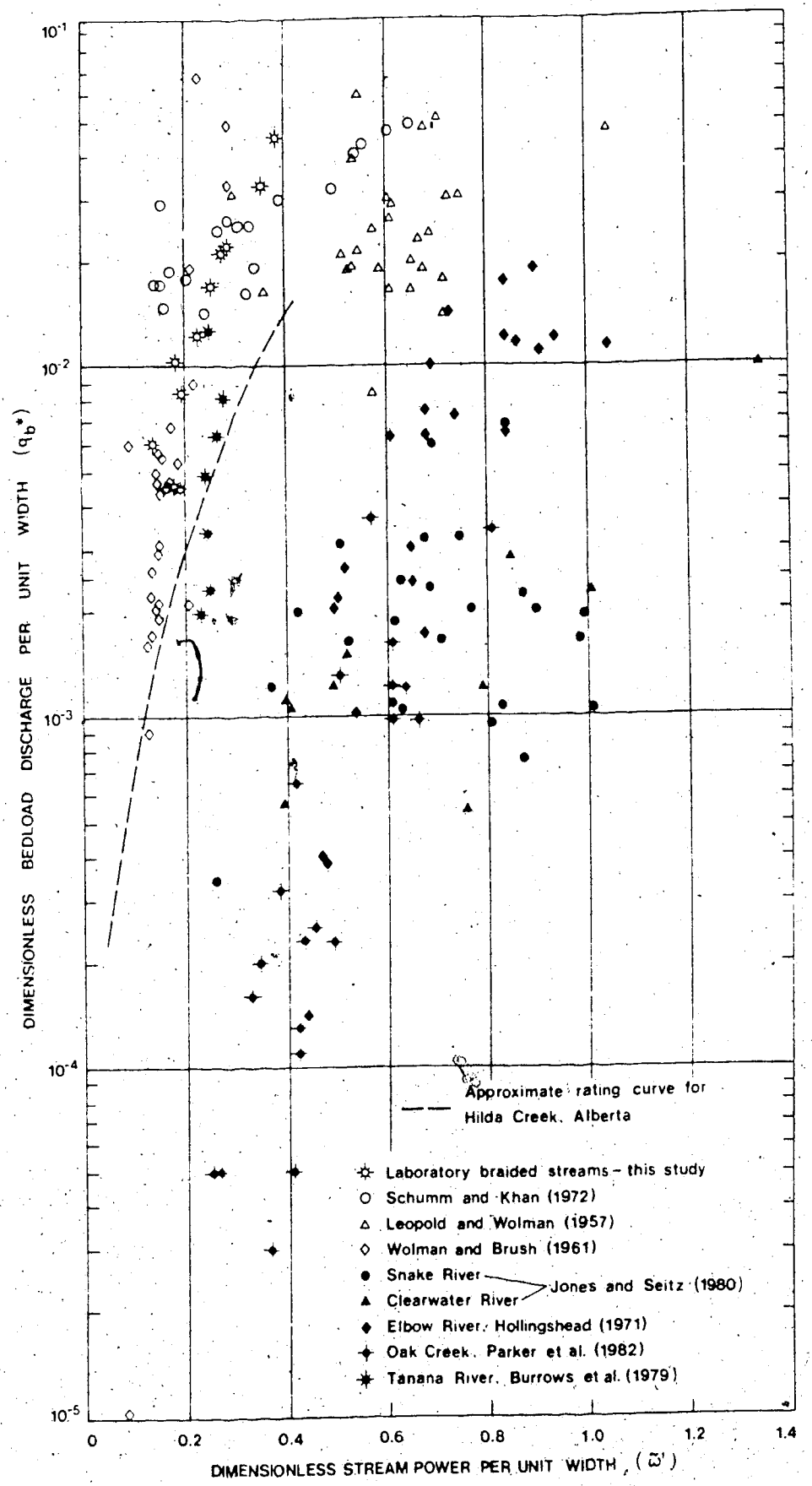

Figure 5-3. Dimensionless bedload discharge per unit width (q_b^*) versus dimensionless stream power per unit width ($\tilde{\omega}'$) for laboratory and field data.

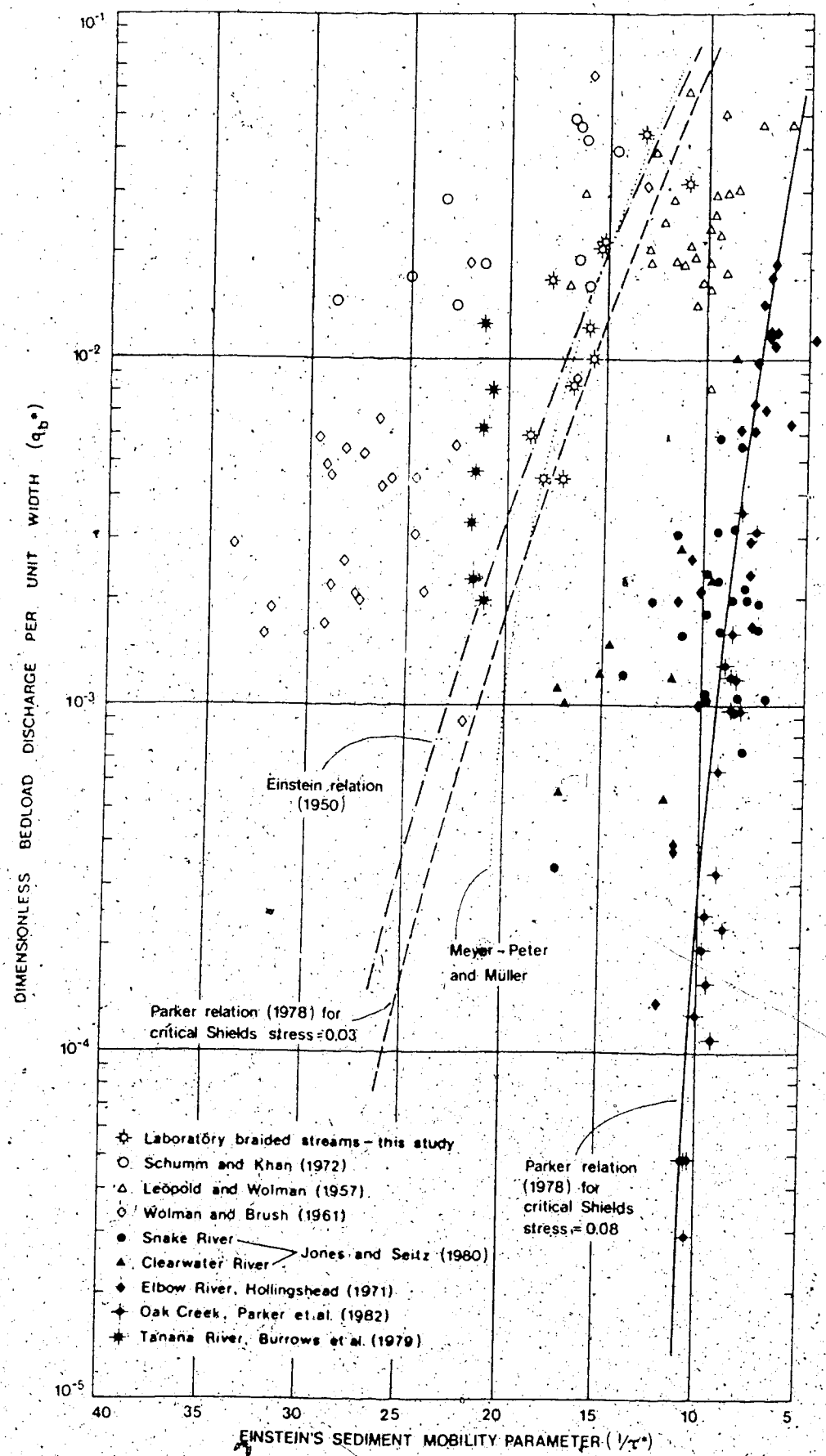

Figure 5-4 Dimensionless bedload discharge per unit width (q_b^*) versus Einstein's sediment mobility parameter ($1/\tau^*$) for laboratory and field data.

$\bar{\omega}'$ for the coarse-grained outwash of Hilda Creek. The curve was calculated from the rating curves (discharge versus sediment load) presented by Kang (1982), and Hammer and Smith (1983), assuming a channel width of 6m (a figure estimated from photographs of the site) and a slope of 0.05.

For all the data there is a very rapid increase in the bedload transport rate with increasing stream power and bed shear stress. One can discern two separate groups of data having roughly parallel trends in both Figure 5-3 and 5-4. The first group showing higher sediment transport rates for a given stream power or bed shear stress is predominantly composed of laboratory data, although the Tanana River and Hilda Creek data plot close to this group. The second group showing comparatively lower sediment transport rates for given flow conditions comprises solely field data. An exception to this generalisation is the data of Leopold and Wolman (1957) which appear to occupy a position between these two groups. This separation of field and laboratory data clearly indicates that the dimensional analysis is by itself inadequate to allow the comparison of data from these two sources; at least one additional factor needs to be accounted for and this problem will be discussed shortly. While no published relationships for q^*_b versus $\bar{\omega}'$ exist, the use of τ^* or its reciprocal is quite common and two such relationships are plotted in Figure 5-4. The Parker (1978) relation is an empirical one derived from 278 data points assembled from previously published laboratory experiments on gravel transport in flumes. The relation has the form :

$$q^*_b = 11.2(\tau^* - 0.03)^{4.5}/(\tau^{*3}) \qquad 5\text{-}12$$

Parker (1978) obtained this equation by fitting a line by eye to the data. The relationship is important because it incorporates a large number of data points in

addition to those plotted in Figure 5-4. It is therefore gratifying to find that Parker's (1978) equation fits the laboratory data from the present study very closely. Einstein's (1950) relation, one which is used widely in sediment transport calculations, compares closely with Parker's (1978) curve and is known to fit other data sets quite closely. For example Yalin (1971) shows that Gilbert's (1914) data for transport of coarse sand and gravel in a laboratory flume are described very well by Einstein's (1950) relation. This implies that Gilbert's (1914) data ought to compare closely with those from the present study as well. Also shown on Figure 5-4 is the Meyer-Peter and Muller equation (Yalin, 1971, p.114) which also fits the laboratory data very well. While the Parker (1978), Einstein (1950) and Meyer-Peter and Muller (Yalin, 1971, p.114) relations fit the data from this study quite adequately it is apparent that the fit with other data is considerably worse. Wolman and Brush's (1961) data plot above the three curves while most of the field data plot well below them. In fact the Wolman and Brush data (1961) are ambiguous, agreeing well with the laboratory data in Figure 5-3 (q^*_b versus τ') but deviating somewhat from the same data when plotted in Figure 5-4, the graph of q^*_b versus $1/\tau^*$.

The amount of scatter evident in Figures 5-3 and 5-4 is typical of sediment transport relations. The data from which Parker (1978) derived Equation 5-12 show an order of magnitude variation in τ^* for a given value of q^*_b and a variation over two orders of magnitude of q^*_b for a given value of τ^*.

The Parker (1978) relation is amenable to manipulation by altering the value chosen for the critical Shields stress. The original equation used a value of 0.03 and this is the relation which fits the laboratory data very well. Also shown

in Figure 5-4 is the Parker (1978) relation adjusted by using a critical Shields stress of 0.08 rather than 0.03. It is clear that this curve fits the field data very well, particularly the data for Oak Creek and the Elbow River, and herein lies a means of adjusting the field data so as to bring them into alignment with the laboratory data. The necessity for using different values of critical shear stress or stream power for the laboratory and field data amounts to a failure of the two data sets to model one another since an exact model would have the same critical Shields stress as the prototype. Lest this sound like a dismissal of the value of the model results it should be pointed out that it is common to find field streams failing to model one another in this fashion, as Klassen (1982) has pointed out with respect to the Snake and Clearwater Rivers. The cause of the discrepancy almost certainly relates to the sorting of the bed material and its structure (particularly the surface pavement), although the differences in Reynolds number between field and laboratory data may also be partially responsible. It was suggested by Rouse (1940) that the size distribution of the sediment would have a marked effect on its mobility. Rouse (1940) indicated that a poorly sorted sediment of a given mean size would be less mobile than a well sorted sediment of similar mean size. It is difficult to find any explicit experimental evidence to confirm this idea but Raudkivi and Ettema (1977) showed that for given flow conditions channel bed-scour was greater for well sorted than poorly sorted sediment. If this notion is widely applicable then the sorting of the sediment could have an important influence on the sediment transport rate. Using the ratio D_{90}/D_{50} as a crude index of the sediment sorting, the laboratory data plotted in Figures 5-3 and 5-4 have values of this ratio of between 1.31 and 3.12, with a

mean of 2.20. The field data range from 3.25 to 5.00, with a mean of 3.89. It is interesting that Leopold and Wolman's (1957) sediment has a ratio of D_{90}/D_{50} of 3.12 which is closer to that of the field data than the laboratory data and this may explain their plotting position in Figures 5-3 and 5-4. Similarly, the very low ratio of 1.31 for Wolman and Brush's (1961) data may help explain their position to the left of the majority of the data in Figure 5-4. If some means can be found of accounting for these differences in sorting it may be possible to remove the discrepancy between the field and laboratory data apparent in Figures 5-3 and 5-4. The differences in mobility caused by differences in sorting can be thought of as differences in the critical shear stress (τ^*_c) or stream power ($\bar{\omega}'_c$) necessary for motion to commence. Thus plotting q^*_b as a function of excess stream power ($\bar{\omega}'/\bar{\omega}'_c$) and excess Shields stress (τ^*/τ^*_c) should remove the discrepancy between the two data sets if one uses different values of $\bar{\omega}'_c$ and τ^*_c for each of them. Figures 5-5 and 5-6 are the result of carrying out this adjustment. The critical values of $\bar{\omega}'$ and τ^* were calculated by first accepting that the data can be divided into three groups :

1. All the laboratory data, excluding Leopold and Wolman's (1957) data, plus the Tanana River data.
2. All the field data excluding the Tanana River.
3. Leopold and Wolman's (1957) data.

Values of $\bar{\omega}'_c$ and τ^*_c were then sought for each of these three groups. The plotting of Parker's (1978) relation on Figure 5-4 made it apparent that τ^*_c for groups 1 and 2 should be 0.03 and 0.08 respectively and that for group 3 should

be in between these two. It was decided to use 0.04 as the value of τ^*_c for the third group because it corresponds to the average value for fully turbulent flow and there is no empirical reason for thinking that it is much higher than this. A similar inspection of the data resulted in values of $\bar{\omega}'_c$ of 0.1, 0.4 and 0.3 being chosen for groups one, two and three respectively. These values were actually arrived at by a combination of methods. First, Figure 5-3 showed approximately the minimum value of $\bar{\omega}'$ at which sediment transport was present for each data set. Second, Bagnold (1977) suggested choosing a value which brings the points at low $\bar{\omega}'$ into a straight line with the remainder of the graph and showed (Bagnold, 1980) that this corresponds with the value obtained by manipulating the equation for the velocity profile in a turbulent flow for a chosen critical Shields stress [see Bagnold(1980, p.457)]. Each of these methods was applied to the data and the chosen values are approximate averages of the results obtained in each case.

Both Figures 5-5 and 5-6 show that this adjustment of the data markedly reduces the scatter in the relationships, brings all the data (both field and laboratory) into close alignment and allows a single relationship to describe the trend of all the data. In the case of Figure 5-5, the plot of transport rate against excess stream power ($\bar{\omega}'/\bar{\omega}'_c$), it is possible to fit a linear regression line to the data with the equation:

$$q^*_b = 0.00072(\bar{\omega}'/\bar{\omega}'_c)^{3.02} \qquad 5\text{-}13$$

but the distribution of residuals about this line indicates that an equation of polynomial form might provide a better fit. Polynomial regression gave the following quadratic equation which fits the data slightly better ($R^2 = 0.56$ versus 0.51 for the linear equation):

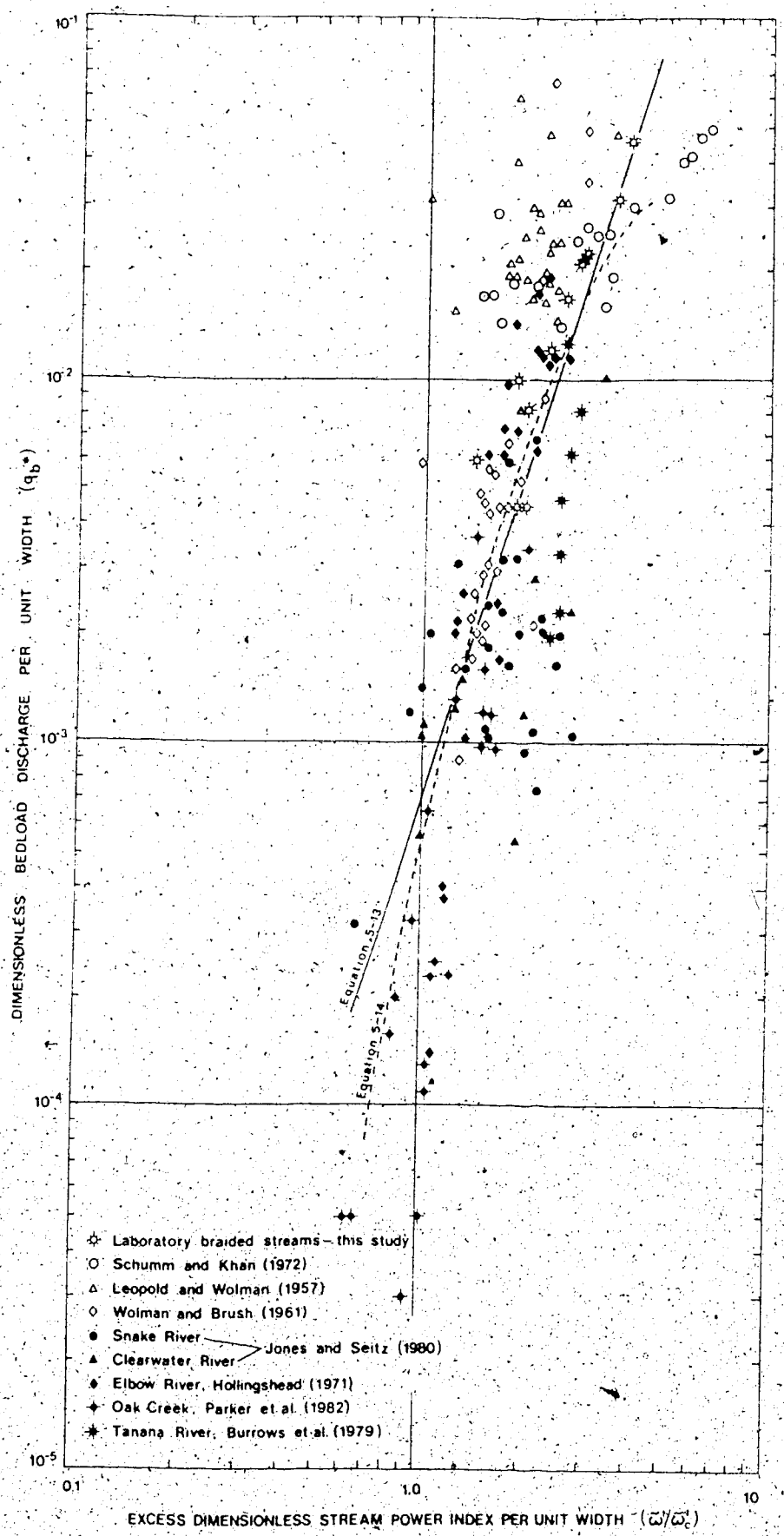

Figure 5-5 Dimensionless bedload discharge per unit width (q_b^*) versus excess dimensionless stream power index per unit width ($\bar{\omega}'/\bar{\omega}'_c$) for laboratory and field data.

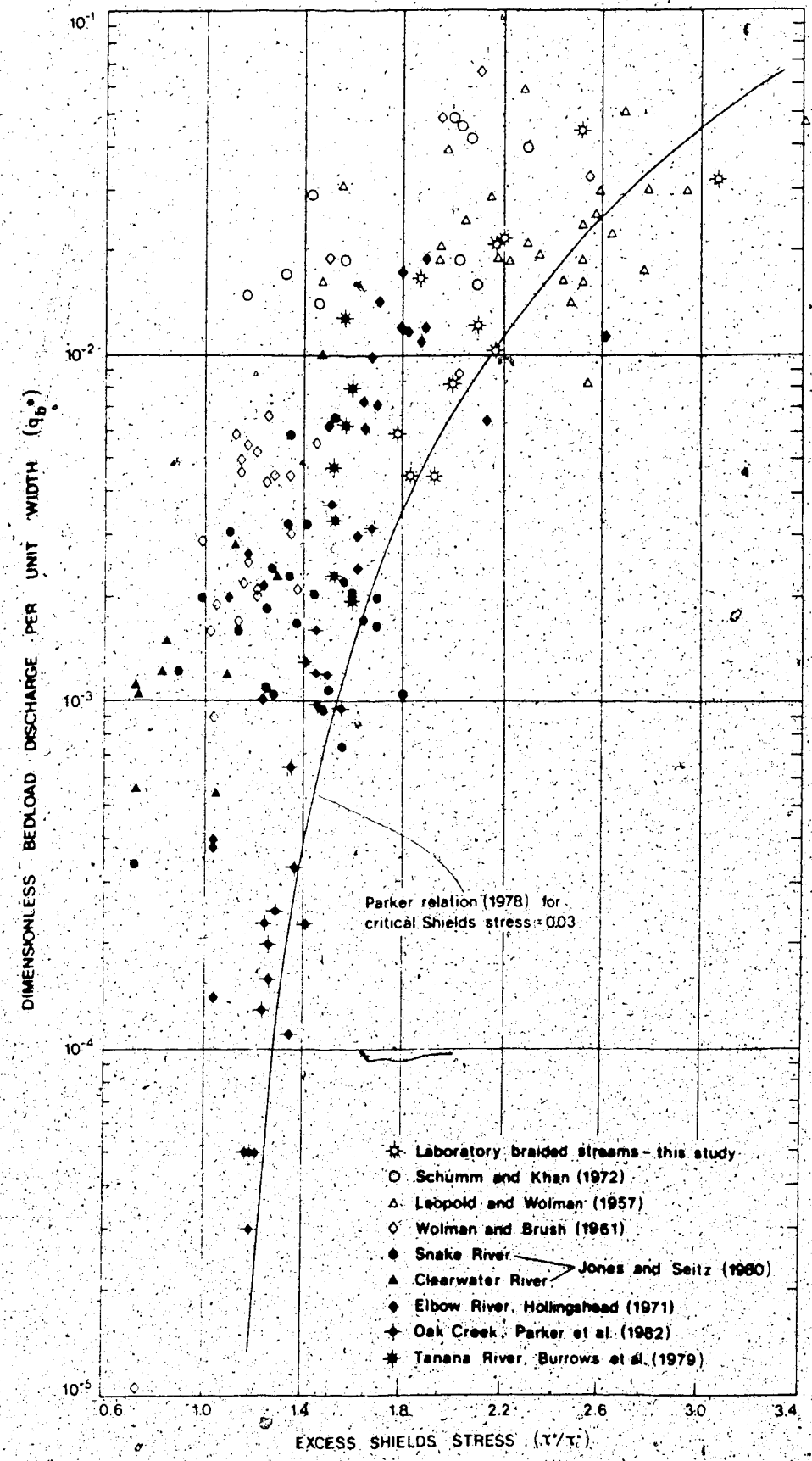

Figure 5-6 Dimensionless bedload discharge per unit width (q_b^*) versus excess Shields stress (τ^*/τ_c^*) for laboratory and field data.

$$\log (q^*_b) = -3.277 + 4.643(\log \bar{\omega}'/\bar{\omega}'_c) - 2.907(\log \bar{\omega}'/\bar{\omega}'_c)^2 \qquad 5-14$$

Figure 5-6 also demonstrates that the adjustment of the data, in this case using critical Shields stress τ^*_c, brings the laboratory and field data into close alignment, and again allows a single relation to be fitted to the entire data set. Scatter is again considerable in some cases because of internal scatter in individual data sets. The Parker (1978) relation was recalculated in terms of excess Shields stress and is plotted in Figure 5-6. The majority of the data plot to the left of this curve, but the Oak Creek data, Leopold and Wolman (1957) data and the data from the present study all lie close to the curve.

This exercise demonstrates that much of the discrepancy between the laboratory and field data apparent in the plots of sediment discharge versus stream power and Shields stress (Figures 5-3 and 5-4) can be accounted for by differences in the critical conditions for sediment motion. By removing this influence the laboratory data can be shown to correspond very closely with field data and in this respect model the field conditions quite reliably.

In the analysis so far the $q^*_b - \tau^*$ relationship has been compared with other similar equations from the literature but this has not been carried out for q^*_b versus $\bar{\omega}'$ because of the absence of a suitably generalised equation. Bagnold (1980) has proposed a general empirical relationship between stream power and sediment transport rate which appears to fit several data sets reasonably well, including the Elbow, Snake and Clearwater River data used here. The relationship has the following form (Bagnold, 1980, Equation 3) :

$$i_b = (i_b)_* \left(\frac{\omega - \omega_o}{(\omega - \omega_o)_*}\right)^{1.5} \left(\frac{h}{h_*}\right)^{-0.66} \left(\frac{D}{D_*}\right)^{-0.5}$$

5-15

where i_b is the submerged weight rate of bedload transport per unit width, ω is the stream power per unit bed area (which Bagnold defines in terms of mass i.e. $\omega = \rho qS$), ω_o the value of ω at the threshold of sediment movement, h is mean depth and D particle diameter. The asterisk denotes reference quantities for the respective variables for which Bagnold (1980) uses the following :

$(i_b)_* = 0.1\ kg\ m^{-1}s^{-1}$

$(\omega - \omega_o)_* = 0.5\ kg\ m^{-1}s^{-1}$

$h_* = 0.1m$

$D_* = 1.1 \times 10^{-3}m$

The results of performing this calculation for the braided river models are tabulated in Table 5-5 and plotted in Figure 5-7 along with the actual measurements for each run. It is apparent that the agreement between the two is quite good, the mean discrepancy ratio being 1.15, and that the data therefore agree with Bagnold's (1980) general empirical relation between stream power and bedload transport rate.

It was mentioned above that the Hilda Creek data of Kang (1982) and Hammer and Smith (1983) were unsuited to the dimensional analysis used for the rest of the data. This is because no data on stream dimensions are available apart from discharge and slope. However, by estimating the channel width from photographs, an approximate rating curve for the Hilda Creek data was plotted on Figure 5-3. Because the Hilda Creek data are the only ones available from a

Table 5-5 Calculation of Unit Bedload Transport Rate (i_b) Using Bagnold's (1980) Empirical Formula

Run	Unit Stream Power ($kg\ m^{-1}\ s^{-1}$)	Mean depth (m)	$\omega-\omega_0$	$\left(\frac{\omega-\omega_0}{0.5}\right)^{3/2}$	$\left(\frac{h}{0.1}\right)^{-2/3}$	$\left(\frac{D}{0.0011}\right)^{-1/2}$	Calculated i_b ($kg\ m^{-1}\ s^{-1}$)	Actual i_b ($kg\ m^{-1}\ s^{-1}$)	Calculated i_b / Actual i_b
1	0.0462	0.0086	0.0282	0.0134	5.17	0.96	0.0067	0.0058	1.155
2	0.0474	0.0087	0.0294	0.0143	5.13	0.96	0.0070	0.0060	1.167
3	0.0234	0.0106	0.0054	0.0011	4.50	0.96	0.0005	0.0014	0.357
4a	0.0309	0.0085	0.0129	0.0041	5.21	0.96	0.0021	0.0028	0.750
4b	0.0595	0.0121	0.0415	0.0239	4.12	0.96	0.0095	0.0090	1.056
6	0.0331	0.0079	0.0151	0.0052	5.48	0.96	0.0027	0.0023	1.174
7	0.0326	0.0109	0.0146	0.0050	4.41	0.96	0.0021	0.0012	1.750
8	0.0425	0.0110	0.0245	0.0108	4.39	0.96	0.0046	0.0047	0.979
9	0.0643	0.0100	0.0463	0.0282	4.68	0.96	0.0127	0.0125	1.016
10	0.0384	0.0083	0.0204	0.0082	5.30	0.96	0.0042	0.0034	1.235
11	0.0316	0.0077	0.0136	0.0045	5.57	0.96	0.0024	0.0012	2.000
								mean =	1.149

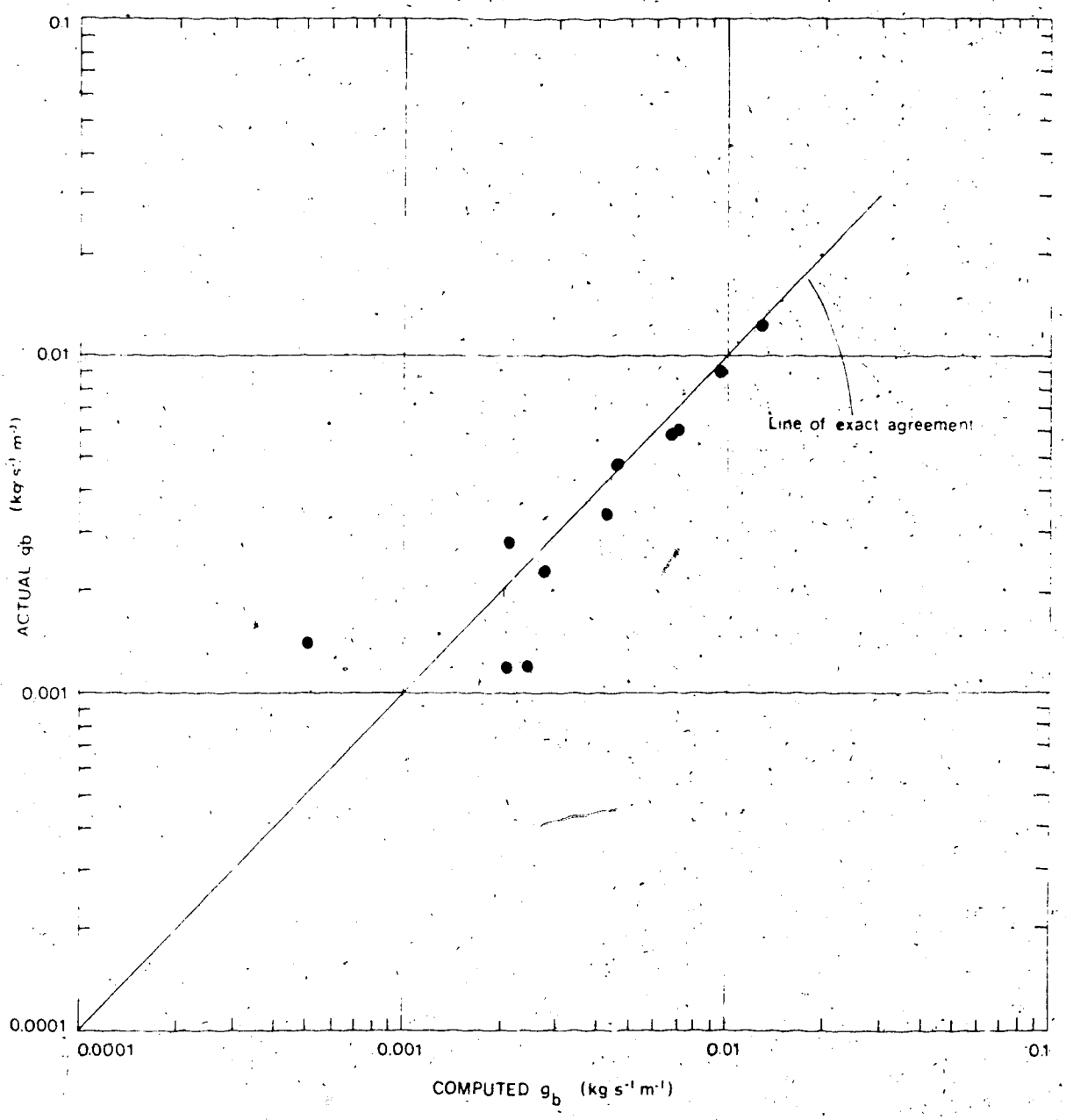

Figure 5-7 Comparison of observed bedload transport rate in laboratory braided channels with the rates predicted from Bagnold's (1980) general empirical relation.

field braided stream it is worthwhile looking more closely at their comparability with the laboratory data. This can be achieved in the absence of measurements of width and depth by using total stream power and sediment transport rate rather than their unit values. The dimensionless quantities used are therefore : dimensionless total sediment discharge,

$$Q^*_b = Q^b/((R\,g\,D_{50})^{0.5}D_{50}{}^2) \qquad 5\text{-}16$$

and dimensionless total power index,

$$\overline{\Omega}' = QS/((R\,g\,D_{50})^{0.5}D_{50}{}^2) \qquad 5\text{-}17$$

The rating curve for Hilda Creek and the laboratory data are displayed in Figure 5-8 as a plot of Q^*_b versus $\overline{\Omega}'$.

Figure 5-8 should be treated with some caution for two reasons. The first is that a reliable grain size distribution is not available for the Hilda Creek sediment but it is likely that the sediment is very poorly sorted and, therefore, D_{50} is inappropriate as the characteristic diameter in $\overline{\Omega}'$ (see previous discussion in this chapter). In view of the likelihood that D_{90}/D_{50} is much larger in Hilda Creek than in the model, recalculation of $\overline{\Omega}'$ using D_{90} might well produce a larger discrepancy between the two data sets than appears in Figure 5-8. Secondly, the channel width for Hilda Creek at various discharges is not known, but given the extremely steep slope of the stream (0.05) one might anticipate much higher width/depth ratios in Hilda Creek than in the model channels. That is to say they are not geometric models of one another and the use of unit transport rate and stream power index may again cause greater deviation than occurs in Figure 5-8. Nevertheless it is encouraging to find the general trend of the field and laboratory data to be so similar.

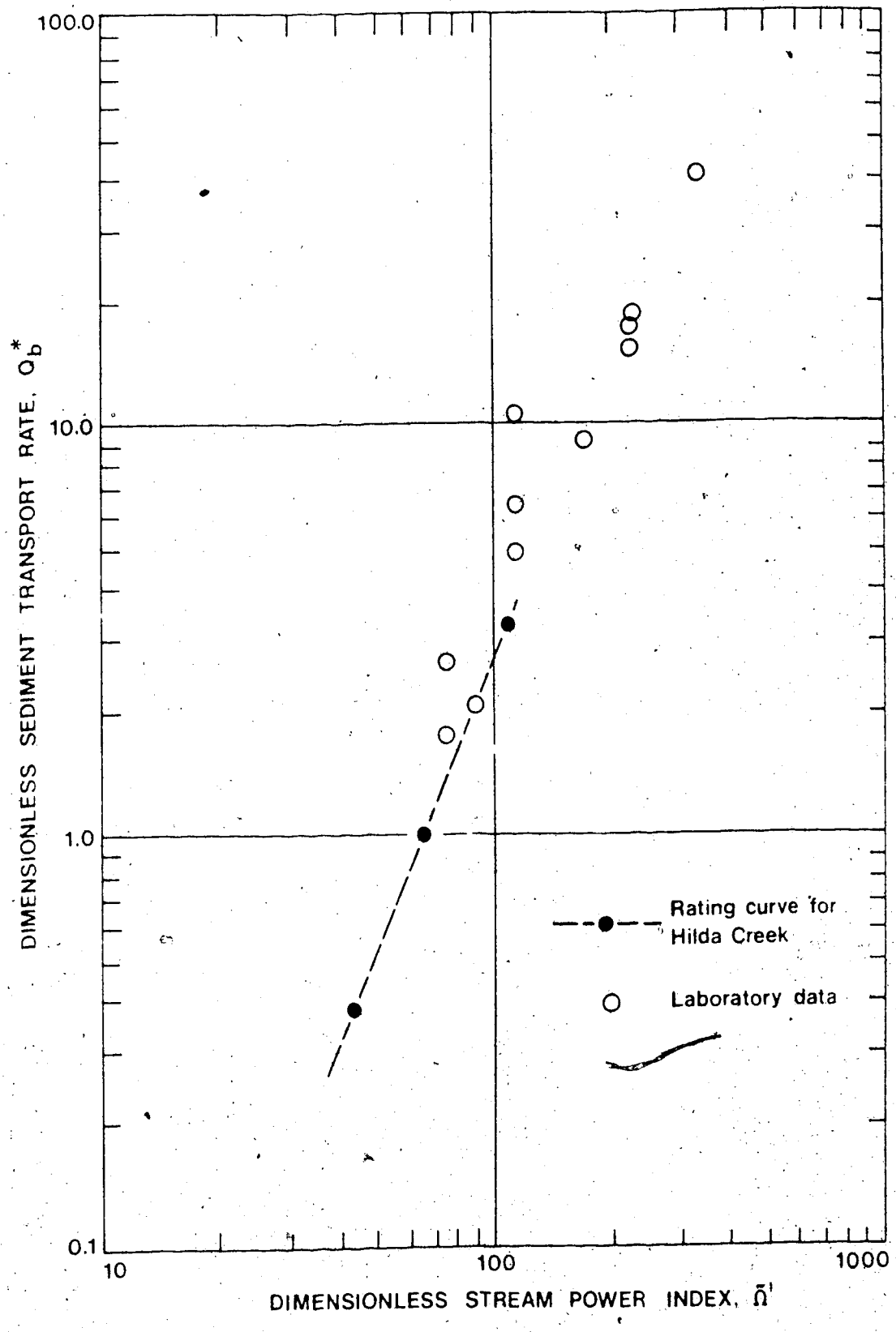

Figure 5-8 Comparison of the relationship between the dimensionless sediment transport rate (bedload discharge) and dimensionless stream power index for the laboratory braided channels and Hilda Creek, Alberta.

5-5 Temporal Fluctuation in Bedload

The analysis has so far dealt only with the mean bedload transport rates for each run, their relationship to stream power and shear stress, and the extent to which these data agree with other published data. It is clear from section 5-3 that considerable fluctuations about the mean bedload transport rate occurred in all the runs. Four-fold changes in sediment transport rate at the downstream end of the flume in the space of an hour were not unusual. Figure 5-9 shows the complete sediment transport series for each run, smoothed using a three-point, unweighted, moving average. Missing values were calculated by linear interpolation. The majority of runs show an initial period of high sediment load during the first one or two hours of the run. This is probably the result of water flowing over an initially unpaved, loosely compacted bed. After this initial period bedload fluctuates with a minimum frequency of about one or two hours. This high frequency fluctuation is present in all the runs but is most pronounced, and its absolute amplitude greatest, for the high discharge runs (8 and 9). Apart from these short-term fluctuations there is an impression that longer-term periodicities are present in many of the series. This is more apparent in some series than others but, for example, the series from run 11 shows some obvious large peaks spaced about 6 to 8 hours apart. Three questions immediately come to mind. Is it possible to show more convincingly that these long-term periodicities exist and, if so, what is their physical form and how do they arise ?

There are several possible methods of analysing time series to examine the possibility that there are regular fluctuations in sediment load. The simplest approach is to expand the moving average procedure using longer-term averages

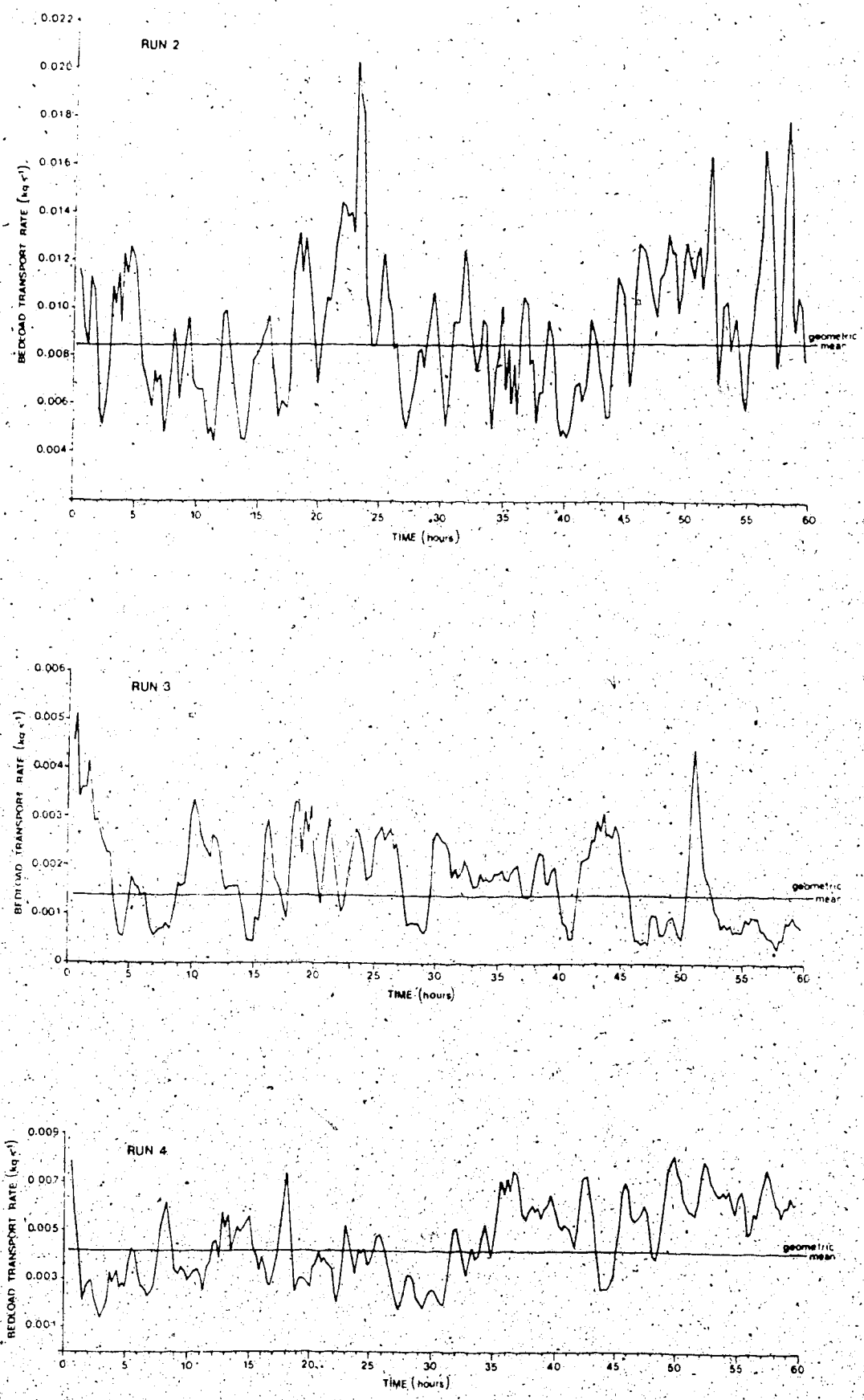

Figure 5-9 Three-term moving averages of the sediment transport rate measured at the head of the flume for the duration of each run.

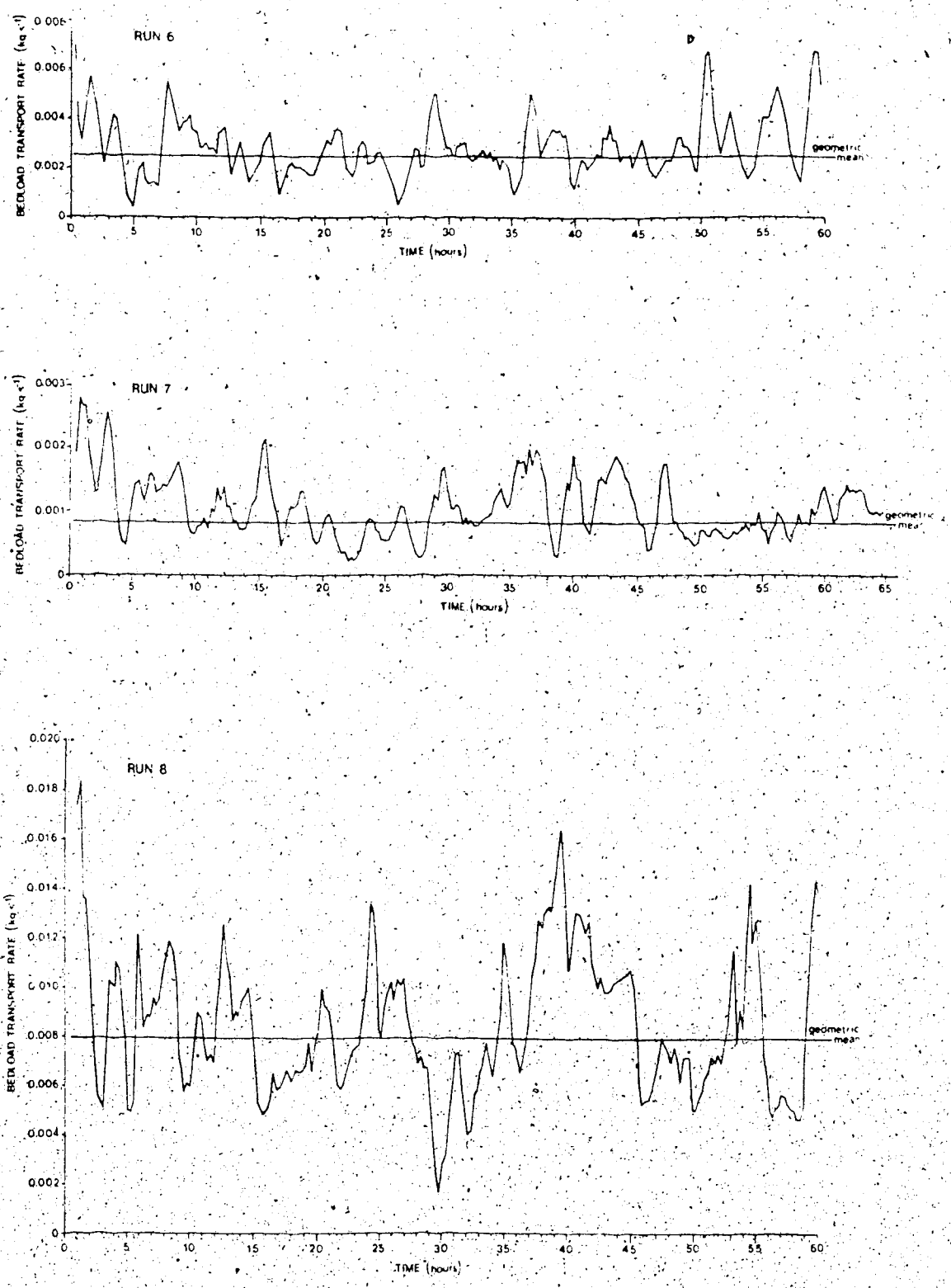

Figure 5-9 Continued.

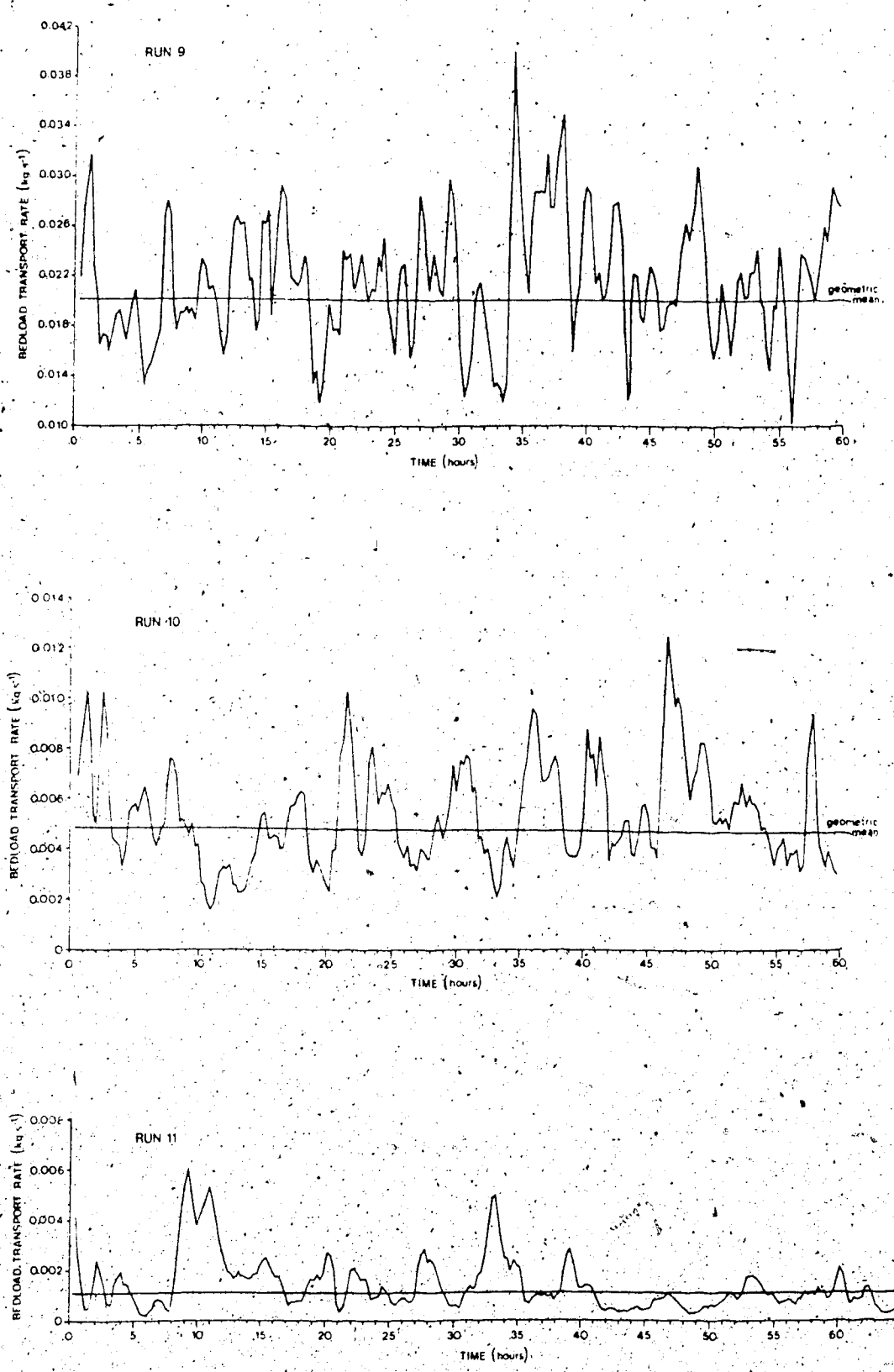

Figure 5-9 Continued.

and/or weighted averages. Figure 5-10 shows the effect of running unweighted 3 and 11-term moving averages through the run 1 data. The removal of the short-term irregularities is achieved quite effectively and the lower frequency fluctuations become more apparent. In particular a 6 to 8 hour periodicity appears in the 11-term average. This helps confirm the presence of these long-term regularities but the calculations are extremely time consuming and the unweighted longer-term averages often displace the position of the peaks and troughs in the series. Autocorrelation is a more convenient method for examining the periodicities in the series.

Autocorrelation is the first step in the commonly used technique of spectral analysis (Jenkins and Watts, 1968: Box and Jenkins, 1970; Bennett, 1979; Chatfield,1980). Spectral analysis is, in simple terms, the representation of the autocorrelation function by a series of sine and cosine terms. Whether one uses autocorrelation or spectral analysis depends on the aims of the study (Box and Jenkins, 1970, p.414). As an exploratory tool for visualising the relationship between points in the series at various spacing the autocorrelation function is very useful. However, Jenkins and Watts (1968, p.5-6) point out that interpretation of the autocorrelation coefficients may be difficult because of visual distortion resulting from highly correlated neighbouring values. They do not elaborate this point but there is at least one geomorphological study which compares the results of both spectral analysis and autocorrelation analysis on the same data. Ferguson (1975) estimated meander wavelength from change of direction series and found reasonable agreement between the wavelengths given by the two techniques, although differences were as great as 20% in some instances. Since the intention

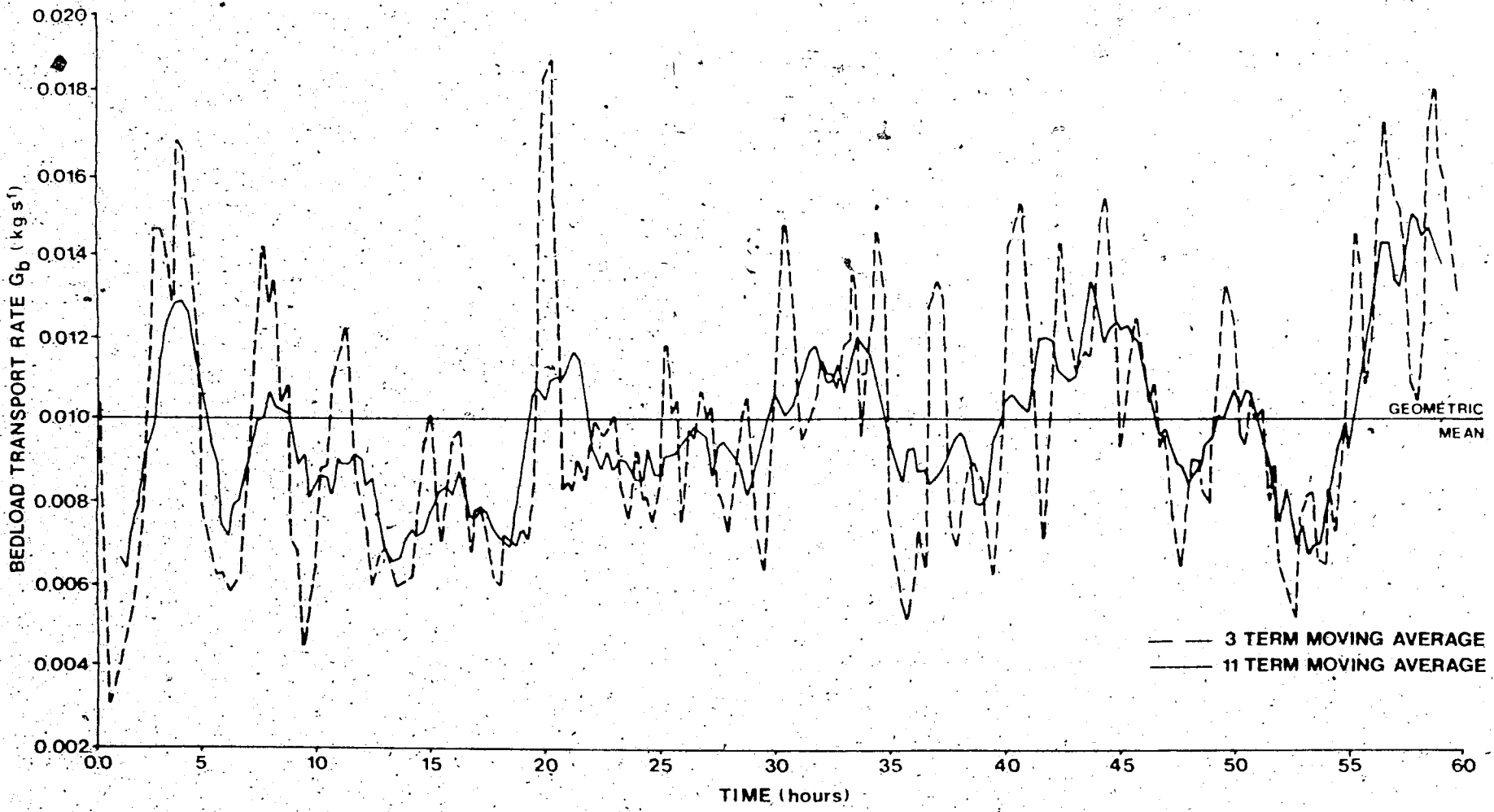

Figure 5-10 Three and eleven-term unweighted moving averages of the sediment transport rate measurements for run 1.

here is simply to establish the presence, or otherwise, of the longer-term periodicities in sediment transport rate, and to estimate their spacing, the autocorrelation function is adequate.

Given a series of data points $z_1, z_2 \ldots z_n$, the series may be correlated with itself using pairs of points (z_t, z_{t+k}) where k, the lag, is a constant interval. If $k = 0$ each point in the series is correlated with itself. If $k = 1$ each point is correlated with its neighbour, and so on. By calculating the correlation coefficient, r, at several values of k the variation in the correlation coefficient with k can be plotted. This function is called the autocorrelation function (ac.f.) and the plot of the correlation coefficients versus lag is the correlogram. The correlogram is then used to identify the lags at which the series correlates with itself, i.e. at which the fluctuations in the variable (in this case sediment input at the head of the flume) are in phase.

There are several methods of calculating the autocorrelation function (Cox, 1983) the simplest of which (and the one subject to the greatest bias) is :

$$r_k = \sum_{t=1}^{n-k} (z_t - \bar{z})(z_{t+k} - \bar{z}) / \left(\sum_{t=1}^{n} (z_t - \bar{z})^2 \right) \qquad 5-18$$

where r_k is the correlation coefficient at lag k, and $\bar{z} = \sum_{t=1}^{n} z_t/(n)$ and is the mean of the whole time series. The autocorrelation function is symmetrical about $k = 0$, so that $r_k = r_{-k}$ and only half the function needs to be calculated. Some general rules of thumb apply to the analysis. The sample size should be at least 50, in order to discern periodicities of a given frequency sample points must be spaced at least 1/4 or 1/5 of that frequency apart, and the autocorrelation coefficients are not valid for k greater than about n/4 (Bennett, 1979 p.32).

One further assumption, referred to as stationarity, is central to the analysis. A stationary time series is one whose statistical character is unchanged throughout. This means that the probability density function associated with any part of the series is identical to that for any other part of the series. Usually, for the purposes of analysis, a series must obey second-order stationarity. This requires that the mean and the variance of the series remain unchanged throughout the series. In other words if there is an obvious trend in the mean or variance of the series this must be removed (assuming one is interested in the underlying series, not the trend). This also applies to seasonal fluctuations (i.e. regular periodicities) in the series, but in this case it is these in which we are interested. Removal of the trend, once its presence has been recognised, can be achieved by one of three methods; curve fitting, filtering or differencing. The simplest of these is curve fitting in which a low order polynomial regression line is [redacted]data and the residuals from the regression used in the analysis in [redacted]original series. A trend in variance can be corrected to some extent by [redacted]ming the data to logarithms. This was done for all ten series before fur[redacted]nalysis was carried out. Of the ten series analysed, four (Runs 1, 8, 9 and [redacted]showed no significant trends (that is, the slopes of the fitted linear and seco[redacted]order polynomial regression lines were not significantly different from zero[redacted]three were fitted by linear regression (runs 2, 4 and 7) and three by second-order[redacted]olynomial equations (runs 3, 6 and 11). The stationarity of variance is much more difficult to establish but the crudest method, a visual inspection of the residuals, showed no obvious trends in most of the series. The exception to this is run 4 in which non-homogeneity of variance is obvious and may be amplified by

the log transform because the variance declines as the mean sediment load increases (contrary to normal expectation of an increase in variance with increasing mean). For this reason the run 4 data were detrended (using a second order polynomial regression) without using a log transform and this produced a more satisfactory result from the point of view of homogeneity of variance.

Significance testing of the autocorrelation function is often accomplished by assuming that mean r_k equals zero and it can be shown that the 95% confidence limits are at $\pm(2)/\sqrt{n}$ (Richards, 1979, p.24 and Chatfield, 1980, p.25) and Correlations outside these limits are significantly different from zero. Even if the series is completely random it should be expected that 19 of every 20 values of r_k will lie between these limits. Thus in this case where each ac.f. consists of 50 values of r_k we would expect two or three values to exceed the confidence limits even if the series were random. If r_1 is significant the estimate of the standard error given above is not valid and the significance of the subsequent r_k values should be tested by :

$$S.E. = \frac{1}{\sqrt{n}}[\,1 + 2(r_1^{\,2} + r_2^{\,2} + \cdots r_q^{\,2})]^{0.5}, \; for \; k > q \qquad 5\text{-}19$$

where S.E. is the standard error of r_k. For example, to test the significance of r_6, the standard error incorporates the values of r_k for k = 1 to q, where q in this case is 5 (Richards, 1979, p.24). Figure 5-11 shows the autocorrelograms for the 10 series with 95% confidence limits calculated from Equation 5-19 plotted on them. The sample size for each series is 240 so the maximum lag (k = 50) equals approximately n/5.

Interpretation of the autocorrelograms is complicated, first, by the fact that

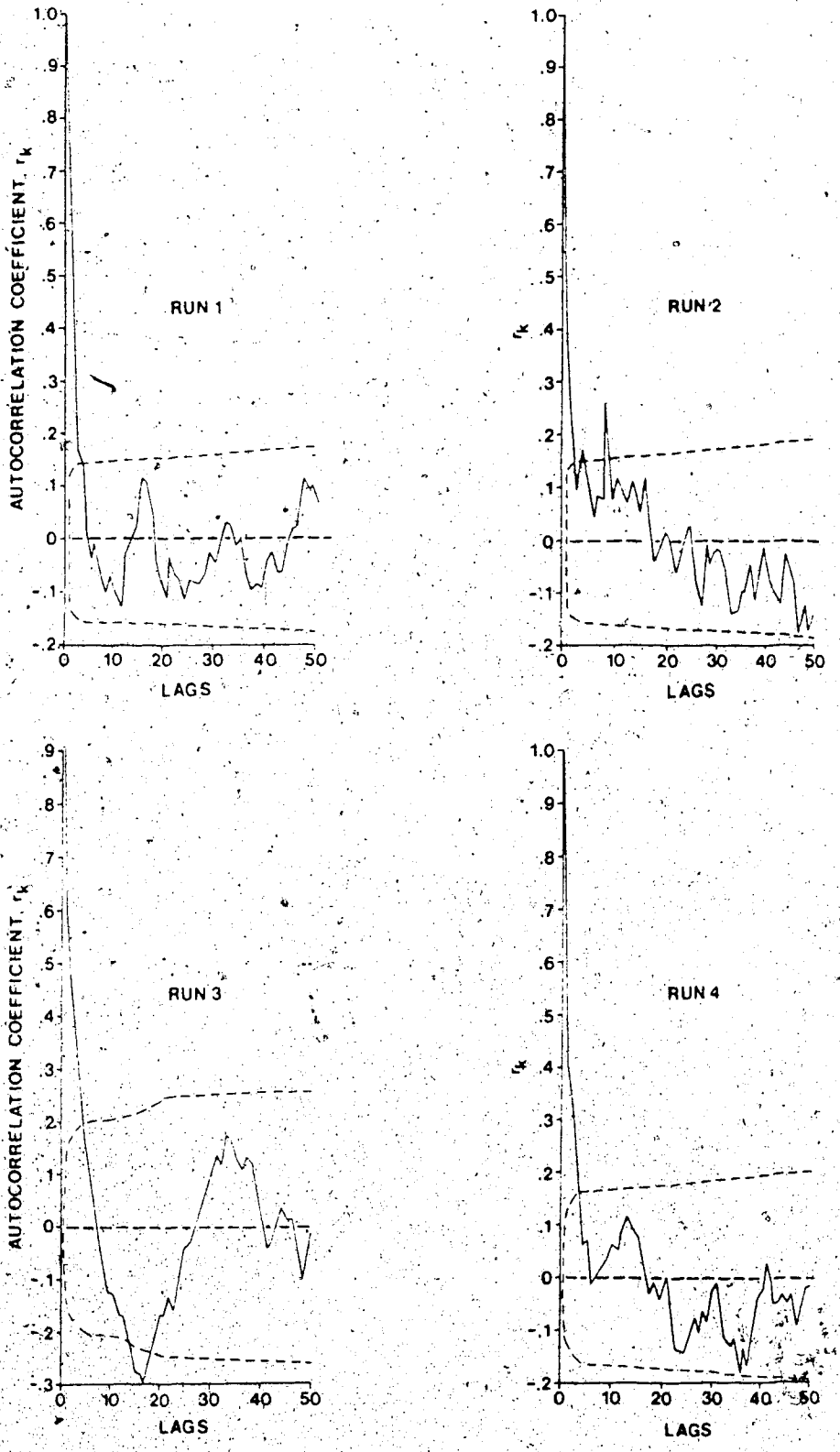

Figure 5-11. Autocorrelograms of the three-point moving averages of the sediment transport rate in each run. Dashed lines are the 95% confidence limits.

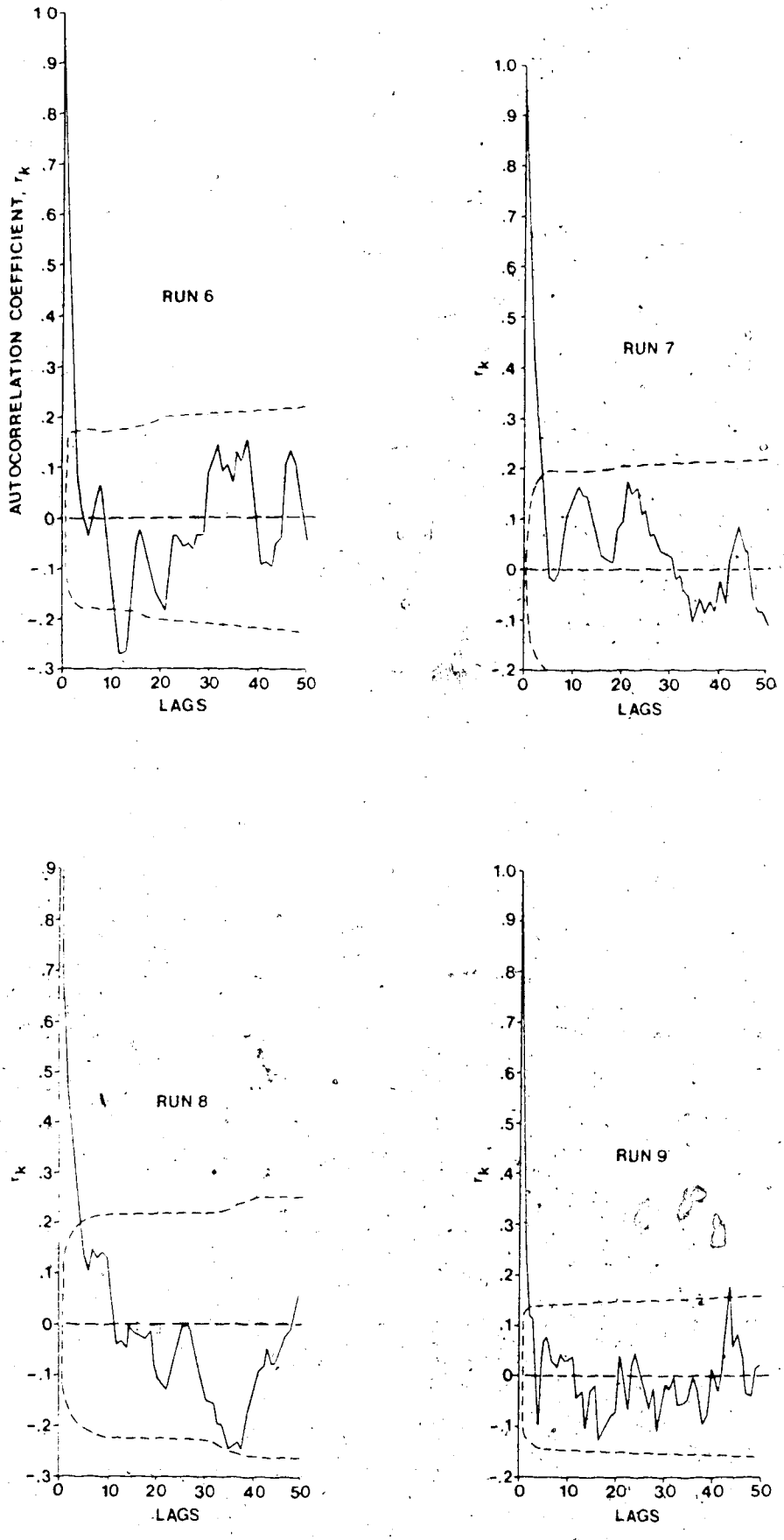

Figure 5-11 Continued.

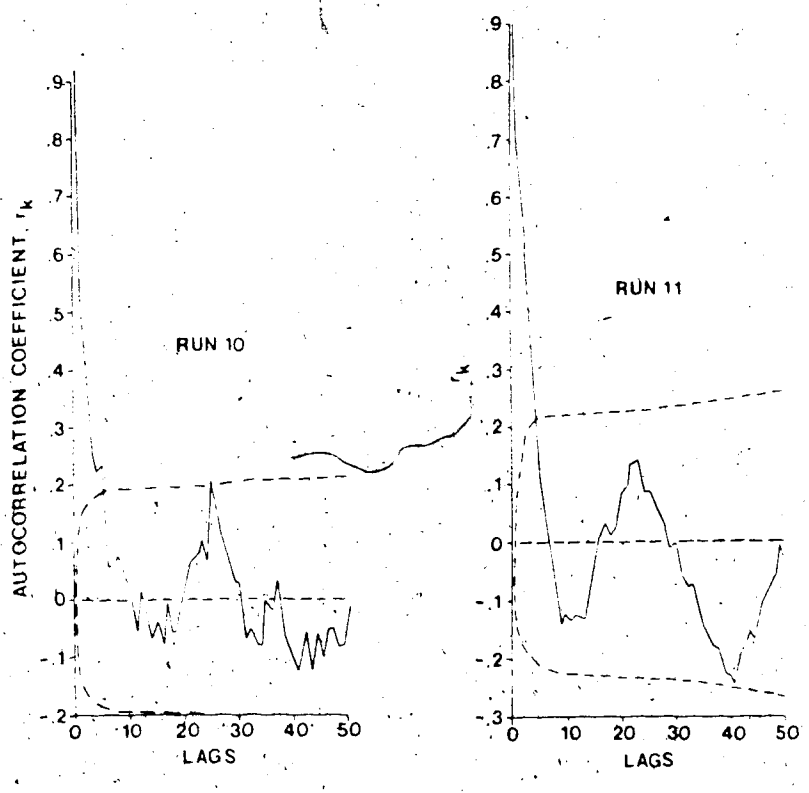

Figure 5-11 Continued.

extreme values of k for which interpretations are valid are in some doubt and, second, by the fact that different estimates of the ac.f. will produce different results. In relation to the first point Bennett (1979, p.32) notes that opinions on the maximum lag for which interpretations are valid range from about 1/10 to 3/10 of the data (in this case 6 hours to 18 hours). This indicates that any peaks in the correlogram beyond 21 lags (6 hours) should be treated with caution. On the second point Cox (1983) notes that the simplified estimate of the ac.f. used here (eqn. 5-18) tends to underestimate the strengths of the values of r_k so that the values shown may be marginally low compared with those from more accurate estimators. By how much is impossible to say without calculating the ac.f. by both methods. Cox (1983) found that the difference between the abbreviated estimator used here and the more accurate one varied with the degree of second-order non-stationarity of the series. Series with bursts of very high and/or very low values would be particularly susceptible to error from the simplified estimate. In these cases differences between the accurate and simplified estimate were as great as 0.243, but typical values were about 0.05. Many of the series analysed here are subject to these bursts of activity so there is some doubt about the actual ac.f. values and their significance. This should be borne in mind throughout the subsequent discussion.

All the series have a damped periodic form. In other words r_k declines rapidly at first and then oscillates at fairly low values with occasional larger peaks. The initial damping shows adjacent values to be significantly correlated up to about 4-6 lags (1 to 1.5 hours). Generally speaking the lower discharge runs show slower initial damping, suggesting less frequent fluctuations in sediment

load. The peaks at higher lags show no consistent pattern. Four of the low discharge runs (3, 6, 10 and 11) show peaks at 24-32 lags (6-8 hours) but runs 4 and 7 do not fit this pattern. Run 7, has two peaks at about 12 and 22 lags which is a very different pattern from that of run 3 which was run at the same slope and discharge. Thus, there is doubt about the reproducibility of the results at the same slope and discharge under different head conditions. The higher discharge runs show very few significant peaks as the more chaotic appearance of the original series for these runs suggests. Run 9 shows one significant peak at 43 lags but a long-period peak of this kind is not present in any of the other series. Both runs 2 and 8 have minor peaks at about 2 hours and other runs (1, 4 and 7) show short-period peaks of about 2-4 hours also. It is interesting to note that the correlogram for run 1 suggests the presence of weak periodicity at 4, 8 and 12 hours. These regularities are also visible in the moving average values for run 1 (Figure 5-10) which indicates that either of the two techniques would have given the required information.

Generally speaking, therefore, periodicities in the sediment yield series are not strongly developed but there is an indication that there are regular fluctuations on the order of 6-8 hours in several of the series, these being most obvious at low discharges. Some shorter (2-4 hours) and longer (10-12 hours) peaks are also present, particularly at higher discharges. Few of these peaks are statistically significant at the 95% level.

If these pulses of sediment are transferred downstream as a fairly coherent wave it might be anticipated that at high discharges (and therefore high sediment transport rates) these waves would migrate more rapidly. It is possible, therefore,

that the short term (2-4 hours) peak at high discharges represents the same feature which at lower discharges appears as a 6-8 hour periodicity. Assuming a model length scale of about 30, and given that the time scale is equal to the square root of the length scale, these peaks occurring several hours apart in the model would be separated in time by five or six times that amount in the field. This is a crude estimate not only because the model scale is approximate but also because it is not possible to predict accurately the time scale for sediment transport from modelling theory which is based on the water flow (Yalin, 1971). In addition, it should be remembered that the model discharge is high enough that sediment transport is always present, the fluctuating flows in the field would result in longer-period pulses than those given from a straightforward scaling up of the model values.

The long-term fluctuations present at high discharges would not appear at lower discharges because the time between successive pulses could be too great for a 60 hour sample length to pick up.

Although rather speculative, these conclusions are supported to some extent by other field and laboratory experiments. Kang (1982) observed 13- and 30-minute pulses in bedload on Hilda Creek, Alberta, that are too closely spaced to be equivalent to the pulses observed here, but Southard and Smith (1982) recorded pulses in sediment load at a variety of scales in a laboratory model of Hilda Creek. Some of these corresponded with those observed in the field but others were detected that were a few tens of hours apart when scaled to the prototype dimensions. Southard and Smith (1982) attributed the short-term pulses to in-channel processes such as the migration of gravel bedforms (unit bars)

and the long-term pulses to "aggradation/degradation cycles" affecting the entire system. Kang's (1982) field observations were not carried out over a long enough time to record these long-term pulses, but their spacing suggests that they are similar to those described here.

Griffiths (1979) speculated that the braided Waimakariri River, New Zealand, is characterized by waves of aggradation and degradation about 1km in length migrating downstream but he gave no estimate of the celerity of these waves. Griffiths (1979) further proposed that these waves would appear as groups of slip-face bars each moving downstream. The time-lapse films of the present experiments are used in Chapter 7 and 8 to trace the nature and movement of these longer-period sediment pulses. It is possible that the pulses are an artifact of the flume but their presence in other studies militates against this. Even so, because of the sediment recirculation system used, it is possible for an initial pulse to persist in the system for some time. In fact temporary storage in the tail box damped out fluctuations in load to some extent, particularly in the case of the larger pulses for which the input to the tail box was greater than the capacity of the recirculation pump.

5-6 Discussion

The analysis of the sediment transport data has shown that there is a power relationship between sediment transport rate and stream power and that when plotted in dimensionless form these data compare closely with other published data and sediment transport equations. In addition the fluctuations about the mean transport rate have been shown to contain some regularities (although most of the fluctuation is random), suggesting the presence of waves of sediment

moving downstream causing periodic aggradation and degradation. Some aspects of these general findings are worthy of further discussion.

The general trend of increasing sediment transport rate with increasing stream power is to be expected from numerous previous analyses of sediment transport, particularly those of Bagnold (1973, 1977, 1980) who is emphatic that stream power is the most suitable parameter to express the transporting capacity of the flow. It is interesting that when one examines Figures 5-3 and 5-4 the braided stream data show a more orderly trend of increasing sediment transport rate with the stream power index than with Shields stress and this is perhaps a confirmation of Bagnold's argument. On the other hand it may reflect the errors in calculating average Shields stress in the braided streams by simply averaging depth across the entire stream.

Runs 4a and 4b provide an interesting comparison of sediment transport rates in single and braided channels. Since the total discharge and average slope are the same in both runs the total stream power is also the same. Figure 5-2 clearly shows the single channel (run 4b) to have a much higher sediment transport capacity than the braided channel (run 4a). The conclusion to be drawn is that the single channel is much more efficient (expends less energy to achieve a given transport rate) than the braided channel. If the braided channel is to transport as much sediment as the single channel it would require a higher stream power. One possible means of achieving this is to increase the slope. Thus, to maintain sediment transport continuity along a reach of river in which the channel pattern changes from a single to a braided channel, may require that the channel slope in the braided reach be steeper than that of the single channel.

This is indeed a commonly observed adjustment (Rubey, 1952; Leopold and Wolman, 1957; Church, 1972; Nordseth, 1973). When the analysis is carried out in terms of unit stream power and unit transport rate the discrepancy between runs 4a and 4b disappears because run 4b has a smaller width and therefore a larger unit stream power and a correspondingly higher unit sediment transport rate. The fact that a braided channel and a single channel exist at the same slope and discharge clearly indicates that the channel pattern regimes overlap, as Richards (1982) has suggested.

It has been shown that by using an appropriate dimensional analysis sediment transport data from a variety of sizes of channel can be compared directly with one another. Unfortunately the various channels used are not exact models of one another since the degree of sorting of the sediments varies. This causes marked problems in the analysis; the poorly sorted sediment (from field streams) is less mobile than the well sorted laboratory sands. The explanation for this seems to be that either poorly sorted sediment is less mobile than well sorted sediment of the same mean size, or that poorly sorted sediment develops a coarse pavement on the bed surface that is absent in well sorted sediment, and by implication from the laboratory streams. The data analysed here indicate that for mixtures of grain sizes with different sorting characteristics, similarity in sediment transport is achieved by adjusting the data for variations in the critical conditions for motion. This variation occurs presumably because in poorly sorted sediment the removal of particles from the bed is controlled by larger particles which protect the smaller ones from the flow and therefore inhibit their movement. As the sediment becomes increasingly poorly sorted the size of these controlling

particles is likely to increase and, additionally, then would represent a higher percentile of the size distribution (White and Day, 1982). In the case of the field data used here, this percentile seems to be about D_{70} or D_{80}(about 3 times D_{50}), if D_{50} is used for the laboratory streams. This estimate is based on the empirical evidence that critical Shields stress for the laboratory data is 0.03 whereas for the field data it is about 0.08. Clearly an alternative to adjusting the field data using different critical shear stress or stream power as was done here, would be to calculate the dimensionless shear stress or stream power using a different 'effective' grain size for the laboratory and field data while calculating the dimensionless sediment transport rate in terms of D_{50}. In fact this solution has been adopted previously by Milhous (1973, quoted in Klassen, 1982) who used D_{35} of the surface pavement and Parker, Klingeman and McLean (1982) who used D_{50} of the pavement to bring the Oak Creek data into closer alignment with published equations such as Einstein's (1950). It is worthwhile noting that D_{50} of the pavement corresponds to about D_{90} of the subpavement in many gravel streams (Parker et al. 1982) and this agrees approximately with the suggestion made above that the laboratory and field data could be brought together by using D_{50} of the subpavement for the laboratory data and D_{80} for the field data. It is frustrating to find that the only field data available from gravel streams appear to be from streams with poorer sediment sorting than those used in Chapter 3 to design the bed material size distribution for the model. Complete verification of the laboratory data awaits the collection of field data from a stream with a similar bed material size distribution. It should also be pointed out that not all the descrepency between field and laboratory data is attributable to differences in

sediment sorting. The lower Reynolds numbers in the laboratory streams may contribute to the greater sediment mobility apparent in those data.

In view of the close correspondence between the laboratory data and equations such as Einstein (1950), Meyer-Peter and Muller (Yalin, 1977, p.114) and Parker (1978), the method of averaging the hydraulic parameters across a braided stream appears to be successful. If any errors arise in this technique their magnitude is likely to be small in comparison to the discrepancies evident between most of the data and so the prospects for detecting these errors seem slim. The best one could hope for is to demonstrate that a difference exists between two methods of averaging but it seems unlikely that one could show one of them to be more accurate than another. The use of stream power rather than shear stress seems preferable from this point of view since all that is required is a measure of the channel width. The implication is that many of the statements about the problems of finding suitable average hydraulic parameters for sediment transport relations for braided rivers (Pickup and Higgins, 1979; Kang, 1982) may be overstated, and that if a sufficiently large number of measured cross-sections are available, together with a long-term average sediment transport rate, sediment transport relations for braided streams can be as easily derived as for single channel streams. This is a surprising statement when one considers the complexities of non-uniform and unsteady flow in braided channels, but the analysis in sections 5-3 and 5-4 strongly supports this conclusion. The presence of large fluctuations in the sediment transport rate clearly emphasises the need for repeated measurements of sediment transport rate and channel dimensions in order to arrive at an orderly sediment transport relation. Recent observations of

fluctuations in sediment transport rate apparently unrelated to changes of discharge are several (Emmett, 1976; Reid, Layman and Frostick, 1980; Hudson, 1983; Lekatch and Schick, 1983) although most are over periods of a few minutes or hours in the field. These have implications for the way in which sediment transport is measured in the field but their morphological implications are also intriguing. The chaotic arrangement of erosional and depositional areas in braided streams is a manifestation of spatial variability in the transport rates, and the changing channel form a manifestation of temporal variability. Presumably, therefore, if one observed a given cross-section for long enough one would observe a number of changes in channel form which are both a result and a cause of fluctuations in the transport rate. The analysis in this chapter has shown that some of these fluctuations are quite large in scale and of long period but it is likely that smaller, more frequent fluctuations are superimposed on these large-scale ones and would only be revealed by more frequent sampling and removal of the large-scale periodicities. Later chapters explore some of the morphological characteristics of braided streams caused by these fluctuations in sediment transport rate.

5-7 Conclusions

Analysis of the mean rate of sediment transport for the model braided streams shows that a strong relationship exists between sediment transport rate and the stream power index (the product of discharge and slope). Deviation from this relationship occurs in one case because of the greater efficiency of sediment transport in single channels than in braided channels. Comparison with other sediment-transport data from laboratory and field streams can be accomplished

by using dimensionless forms of stream power, bed shear stress and sediment transport rate. Many of these data are necessarily taken from single channel streams because of the paucity of data from braided streams. Braided and single channel data compared by this method provided a suitable number of cross sections where braided streams are available to provide average values for width and depth. The trends in the various data sets are very similar and compare well with the relationships of Einstein (1950), Meyer-Peter and Muller (Yalin, 1977, p.114), Parker (1978) and Bagnold (1980) but some large discrepancies appear, particularly between the field and laboratory data. These can be removed by adjusting the data using suitable values for critical shear stress or stream power. Replacing D_{50} with a different percentile of the size distribution in the calculation of Shields stress and the dimensionless stream power would achieve a similar end. This points to the importance of modelling the grain size distribution if similarity in sediment transport rate is to be obtained.

Large fluctuations about the mean sediment transport rate occur and statistical analysis revealed that some of these can be resolved into regular periodicities. A period of 6 to 8 hours is most prevalent but at higher discharges periods of 2 to 4 hours and 10 to 12 hours are also detectable. No field measurements are available with which to compare these results apart from the speculative results of Griffiths (1979). However, Southard and Smith (1982) have identified similar periodicities in a model of Hilda Creek, Alberta, which they attribute to "aggradation/degradation cycles" in the river. Such long-period fluctuations would occur over several days or weeks in the field.

The implications of these conclusions, particularly the periodicities in sediment transport rate, are explored in subsequent chapters.

Chapter 6 : Confluence Scour

6-1 Introduction

Secondary currents and the associated scour in bends are a well known feature of meandering streams. In gravel braided streams, where channel sinuosity and relative depth are very low, such scour is poorly developed. Pronounced scour of the bed is, however, a feature of channel confluences in such rivers. The main factors influencing the depth of scour in these confluences are known from Mosley's (1976) laboratory experiments, in which discharge, sediment load, channel shape and curvature, and confluence angle were carefully controlled. Under field conditions the same basic controls on scour depth would operate but scatter may be introduced into the relationships because of a lack of control over such factors as sediment load, channel shape and channel curvature. This chapter reports an investigation of the nature of confluence scour in the field and in a laboratory model of a gravel braided stream to determine whether under natural conditions the principal controls identified by Mosley (1976) can be discerned and to examine the morphology of, and sediment sorting processes in, these features. The laboratory experiments were carried out in non-cohesive sand rather than the finer grained, cohesive sediment used by Mosley (1976). The data also provide a means of verifying quantitatively the adequacy of the model. The role of these confluences in braided stream sedimentation is discussed in Chapter 8.

6-2 Data Collection

6-2-1 Laboratory Data

Data were collected from several of the runs although the majority (22 confluences of a total of 38) came from run 12. This data collection scheme

assumes that scour hole form is controlled by local flow variables and is essentially independent of overall river characteristics such as slope and total discharge. Ashmore and Parker (1983) present data to support this assumption. Confluences have a wide variety of forms (Ashmore, 1979) but to simplify the analysis only those with two straight well-defined channels were measured (Figure 6-1). Scour holes were often short-lived, remaining unchanged in form for only five or ten minutes, so that measurements had to be taken quickly before major changes in form occurred. Data collection for each scour hole took about fifteen minutes and on several occasions measurement was abandoned because of obvious changes in form while data were being collected.

Confluence angle was measured using two straight metal blades about 15cm long bolted together at one end. One blade was aligned parallel with the flow in each of the two channels and a protractor was used to measure the angle between the two blades. Maximum scour depth (water surface to bed) and cross-sections of the confluent channels immediately upstream of the scour hole, were measured using the point gauge. Surface velocity in these channels was measured using small (25mm) plastic beads timed with a stop watch over a 0.3 or 0.5m length of channel (depending on the length of straight channel available) immediately upstream of the confluence. Five floats were timed in each of three positions; close to either bank and in the centre of the channel. These velocities were averaged and converted to mean channel velocity using a conversion factor of 0.72 (this value was empirically determined in the field and is discussed in section 6-2-2). In addition, sediment samples were taken to examine sediment sorting through each confluence. Bed material was sampled from the centre of the two

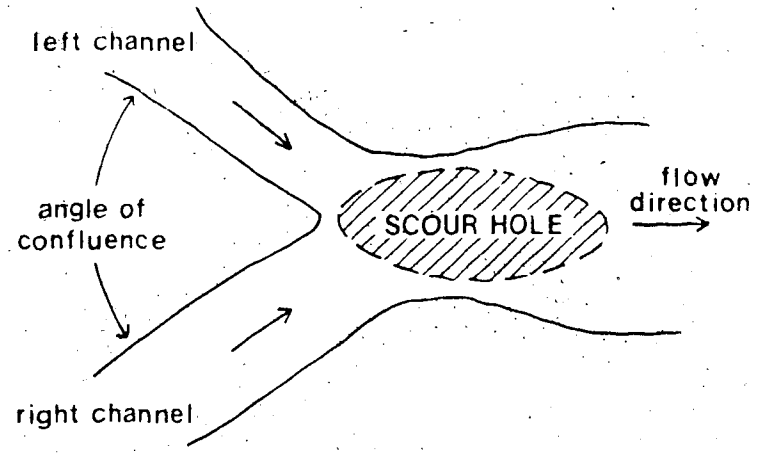

Figure 6-1 Plan form of a confluence scour hole of the type analysed showing the area of maximum scour depth.

confluent channels and from the deepest part of the scour hole, by lightly pressing on to the bed a 20mm square of thin metal sheet with its underside smeared with vaseline. The amount of vaseline was such that the largest particles (4-6mm) would adhere to it. This technique is commonly used in beach sand tracer studies (e.g. Ingle, 1966) and limits the sample to the surface layer of sediment. Bed material in motion was collected using a small metal trough (3 sizes were constructed for use in the appropriate size channel) which could be pressed into the bed so that the lip was flush with the bed and all material moving into it was trapped. The length of the trough was greater than the width of the bed over which sediment was moving. Samples were taken in the two confluent channels and at the downstream end of the scour holes. These bed material and bedload samples were collected for only 21 of the 38 scour holes measured (one from runs 2 and 6, two from run 7, three from run 8, five from run 10, four from run 11 and five from run 12).

The bedload samples were dried, and sieved at 0.5ϕ intervals to obtain grain-size data. The bed material sample sizes were too small (less than 10 grams) to be sieved so an alternate method was devised. After dissolving the vaseline using naphtha, the samples were spread out in petri dishes and a vertical photograph taken. The enlarged prints, with a scale of about 4:1, were used to measure the length of the apparent b-axis for all the grains in each sample. The accuracy of this estimate of the length of the b-axis depends on the orientation of the grains on the dish, in other words, on the deviation of the c-axis from vertical. For well-rounded grains (ellipsoids) this deviation is unlikely to be great, but for angular particles considerable error may be introduced. These angular particles

were numerically a very small proportion of each sample generally comprising the coarse tail of the distribution, derived from crushed gravel.

Grain size on the photographs was measured with an Apple II+ computer and digitizer. Each photograph was taped to the digitizer tablet and the stylus was placed at either end of the apparent b-axis of each grain. The computer was programmed to calculate the length of the axis from these coordinates and to perform some simple calculations on the data, including conversion to phi sizes, calculation of mean and standard deviation, and plotting of histograms. The digitizer stylus could be placed quite accurately for grains whose actual size was greater than about 0.4mm (tests showed the results to be consistent to within plus or minus 10 per cent). Any grains smaller than this were taken to have a b-axis of 0.2mm; an arbitrary value based on the known size distribution of the flume material.

The bed material sampling and analysis technique is equivalent to an area-by-number sample (Kellerhals and Bray, 1971b) while the bedload samples were analysed using a standard sieve-by-weight method. These two sampling procedures are not equivalent to one another so that in order to make direct comparisons it was necessary to convert the area-by-number samples to the equivalent of a sieve sample. Kellerhals and Bray (1971b) indicate that this is achieved from frequency curves by weighting the frequency in each size range by the square of the particle size at the mid-point of the size range. The median and mean particle size can then be calculated from the new cumulative frequency curve. In the case of the bed material samples analysed here in which individual particle diameters were measured the conversion was achieved by applying the

weighting to each particle. The mean grain diameter of the sample was then calculated as :

$$\sum_{i=1}^{n} D_i \times D_i^2 / \sum_{i=1}^{n} D_i^2 \qquad 6-1$$

where D_i is the intermediate diameter (b-axis length) of an individual particle and n is the sample size. This conversion was incorporated in the Apple II computer program. This conversion is only approximate because it is subject to error introduced by particle shape (Sahu, 1964). This relates to the fact that the conversion is, in part, a calculation of weight based on the cube of the intermediate diameter. Only if the particle is a sphere does this method give an exact conversion to particle weight. Variations in particle shape produce further error because sieve diameter and intermediate axis length are only exactly equivalent for spheres. Hence some error is inherent in the comparison of the bed material samples with the bedload samples. The same is true when one compares the laboratory bed material samples with those obtained in the field.

6-2-2 Field Data

Data were collected from a reach of the gravel, braided, Sunwapta River, Alberta, during July and August, 1981 (see Chapter 4). The summer regime of this proglacial river is governed largely by glacier melt conditions. Discharge is, therefore, highest during warm sunny weather and during these periods a pronounced diurnal fluctuation in stage occurs. The diurnal discharge cycle peaks in the late afternoon and early evening in the study reach. Scour holes were measured in a variety of places along the reach so as to cover a wide variety of confluence angles and bed material grain size. The choice of scour holes was

dictated mainly by size and accessibility; only relatively small channels could be sampled at high discharge because much of the measurement procedure required wading in the channels, and some areas of the river were inaccessible because they lay on the far side of impassable channels. Most of the data were collected during a prolonged hot spell in August although measurements were also made during rainstorm discharge events in July. As far as possible, the scour holes were surveyed at the highest daily stage, usually in the evening. This was complicated by the fact that in braided streams peak discharge in a particular channel does not necessarily coincide with peak discharge in the river as a whole because of channel switching during high flows. However, by restricting observations to portions of the river currently active, and to channels in which bed material was moving or close to being moved, the effect of this complication was minimised.

As in the laboratory, only simple confluences involving two channels were sampled. Confluence angle was measured using a compass to sight parallel to the main current in the confluent channels. Scour depth was measured by one of two methods. When depth was less than 0.8 meters it was possible to wade close to the centre of the scour hole and measure the depth with a stadia rod or range pole. Because of disturbance of the water surface it was only possible to measure depth to the nearest 0.05m. Where scour depth was greater than 0.8 meters, and therefore too deep to wade, a portable echo sounder was used. The echo sounder transducer was bolted through the centre of the wooden platform of a small raft which floated on two sealed 0.8m lengths of 0.05m diameter P.V.C. pipe. The transducer was immersed about 0.15m below the surface and the transducer cable was run to the recorder positioned on the bank between the confluent channels.

A rope attached to the raft allowed the transducer to be manoeuvred over the deepest part of the scour hole. The two opposing flows of the confluent channels helped keep the raft over the centre of the scour hole while the raft was moved up and down its long axis (see Figure 6-2). Surface waves and turbulence produced rolling and pitching of the raft, which made the sounder traces difficult to interpret, so it was often necessary to pass the raft over the length of the scour hole three or four times to ensure that a reliable depth measurement was obtained. Of the 23 scour holes sampled in the field, eight were measured using the echo sounder. The accuracy of the sounding technique was verified by measuring some of the shallower scour holes with both a stadia rod and the echo sounder.

Cross-sections of the two confluent channels were measured using a marked rope or metric tape, and a stadia rod. Depths were taken every meter for channels greater than 5m wide, and every half meter in narrower channels. Velocity was measured by surface floats timed over a 10 meter section upstream of the scour hole. Three floats were timed in each of three locations; close to each bank and in the centre of the channel. The Pygmy Price current meter, with which it had been intended to measure velocity, broke down early in the field season. When a replacement was obtained, twenty cross-sections of varying size were gauged by both the float and current meter methods. Current meter readings were taken at 0.6 of the depth from the surface and spaced at 0.5m intervals across the channel. These data yielded an empirical constant for converting the discharge measured by floats to that obtained from the current meter. The conversion factor data are displayed in Table 6-1.

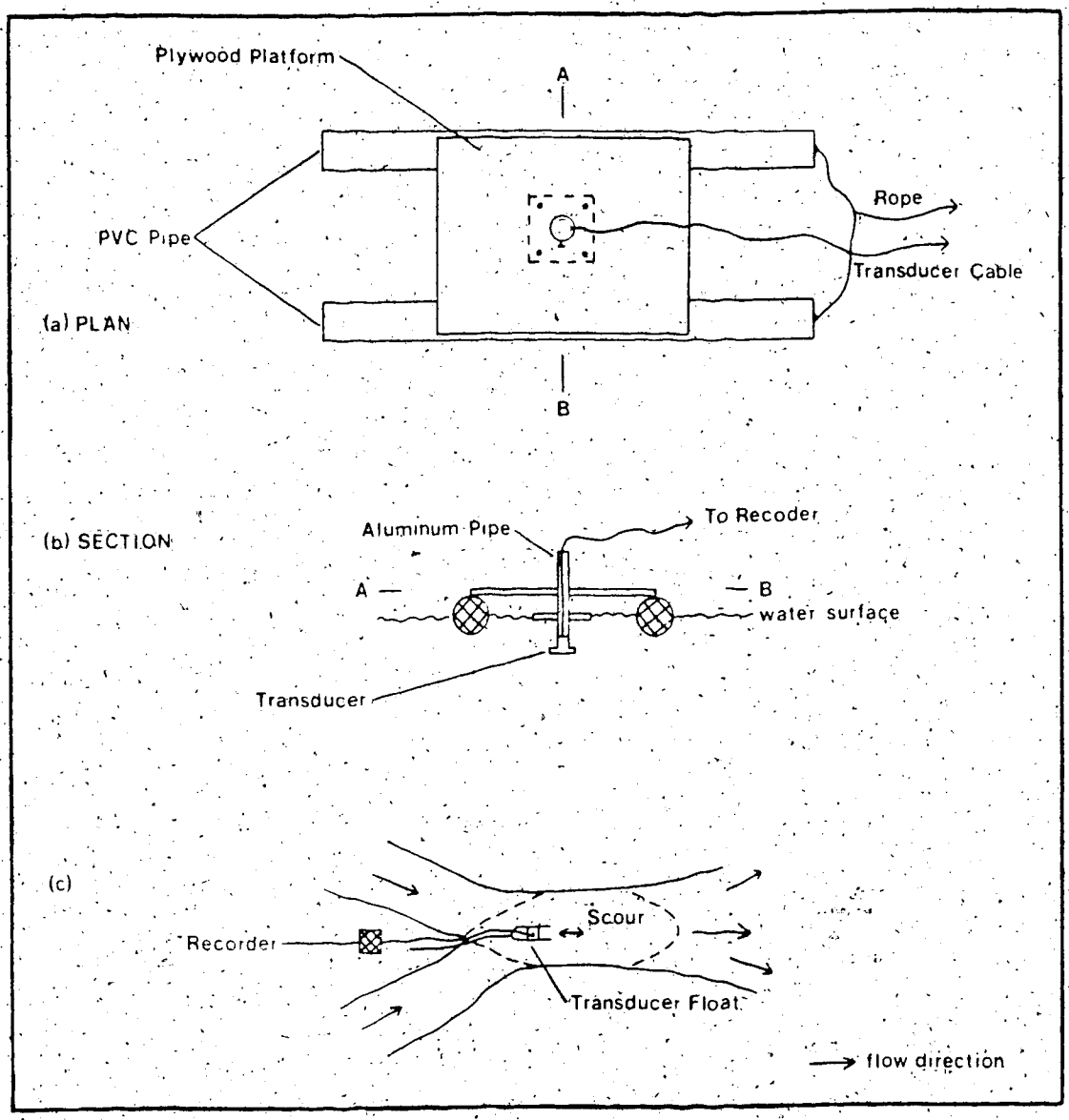

Figure 6-2 Field equipment and procedure for depth sounding of confluence scour holes.

(a) and (b) Plan and section of the floating platform carrying the depth sounder transducer.

(c) Plan of a confluence showing the arrangement of equipment used for depth sounding.

Table 6-1

Coefficients for converting surface float velocities to average velocities from 20 Sunwapta River cross-sections.

Channel number	Cross-section area (m^2)	V_F. Mean velocity ($m\ s^{-1}$) using floats	V_C. Mean velocity ($m\ s^{-1}$) using current meter	V_C / V_E
1	0.69	1.59	1.06	0.667
2	0.81	1.62	1.01	0.623
3	1.24	1.27	0.74	0.583
4	1.27	1.71	1.37	0.801
5	0.79	1.23	1.01	0.821
6	1.64	1.40	1.19	0.850
7	1.12	0.84	0.40	0.476
8	0.40	1.48	1.05	0.709
9	0.55	0.87	0.51	0.586
10	0.39	1.34	1.02	0.761
11	2.03	1.31	1.05	0.802
12	2.15	1.29	1.01	0.783
13	0.80	0.76	0.53	0.697
14	0.89	0.81	0.61	0.753
15	0.67	1.27	0.94	0.740
16	0.83	1.52	1.06	0.697
17	0.42	1.16	0.93	0.802
18	0.81	1.19	0.86	0.723
19	0.81	0.82	0.56	0.683
20	0.55	0.84	0.62	0.738
			mean =	0.715
			standard deviation =	0.093

Bed material size was obtained from Wolman samples (Wolman, 1954) taken immediately upstream of the confluence on a 0.3m grid. Fifty b-axes were measured for each sample. When flow was too deep and/or velocity too high to sample bed material during the evening peak flow, samples were taken at low flow the following morning. Kellerhals and Bray (1971b) demonstrated that this grid-by-number sampling technique is equivalent to a standard sieve-by-weight method. In order to make laboratory area-by-number bed material samples comparable with the field samples, the laboratory samples were converted to sieve samples by the method discussed in section 6-2-1.

Because the field samples excluded particles finer than about 8mm, all particles finer than 0.4mm (equivalent to 8mm in the field assuming a model scale of 1:20) were excluded from the laboratory samples for the calculation of mean grain size. The data from the field and laboratory are tabulated in Appendix 4.

6-3 Analysis

6-3-1 Scour Hole Form

The most obvious features of the flow in confluence scours are the super-elevation of the water surface over the centre of the scour and the presence of eddies. When confluence angles are high, super-elevation is as much as 50 to 100mm in the field. The super-elevated surface displays a series of waves and eddies in the centre of the confluence occupying perhaps 10 or 20 per cent of the surface width and extending the full length of the scour hole. On either side of the super-elevation is a zone of surface boils apparently produced by the surfacing of strong secondary currents set up by the super-elevation. There may also be separation eddies where the flow from each channel enters the confluence and

breaks away sharply from the downstream bank. Figure 6-3 shows these features developed in a small scour hole in the Sunwapta River and also illustrates that they are most pronounced at high stage.

Evidence of the nature of the circulation in these confluence scours was found in abandoned scour holes in the field. Occasionally these contained thin veneers of current-rippled sand revealing the local flow patterns at the bed. Figure 6-4 shows an example in which the ripples at the downstream end of the scour hole migrated obliquely, or in places directly, up the sides of the scour hole, indicating a strong secondary current in this direction. At the upstream end of the scour hole some ripples could be seen to have migrated upstream, presumably due to the presence of a separation eddy close to the bank.

The scour holes also show some pronounced sediment sorting produced by the secondary currents and by the divergent flow downstream of the scour hole. The most obvious example is the lateral fining outwards from the centre of the channel at the downstream end of the scour hole. This was observed in both the field and the laboratory and is illustrated in Figure 6-5. At five field sites, samples were collected from the downstream end of the scour hole and at the centre and margin of the channel. Fifty pebbles were collected on a 0.1m grid, 0.5m wide and 1.0m long. The mean phi sizes of the b-axes are displayed in Table 6-2 and test results show that in all five cases a significant lateral fining is present. No experiments were carried out to investigate the origins of this lateral fining but it is presumably largely due to the competence of the diverging secondary currents being insufficient to transport the coarsest particles of the bedload. Table 6-2 shows the bed material in the scour itself to be coarser than

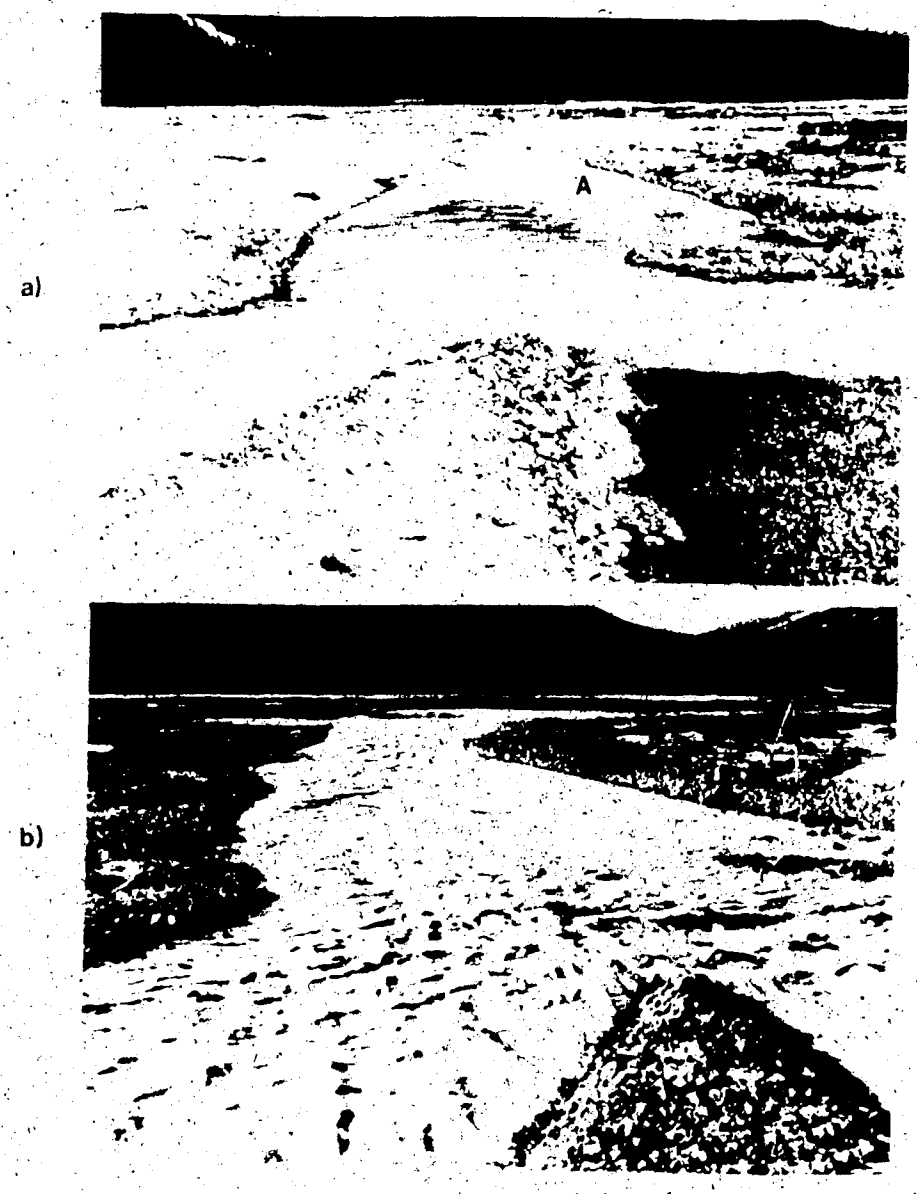

Figure 6-3 View in a downstream direction of a confluence scour on Sunwapta River, Alberta.

(a) At relatively low discharge. Note the flat water surface downstream of the centre of the confluence and the riffle and bar margin beyond (A).

(b) At high discharge. Note the pronounced turbulence and superelevation of the water surface in the confluence and the surface boils and eddies on either side of the intense turbulence.

The tripod in the upper right of (b) gives an indication of scale.

Figure 6-4 View of sand veneer in an abandoned scour hole. Flow was towards the top of the photograph. The standing water occupies the deeper part of the scour hole. Current ripples indicate flow obliquely away from the centre of the scour hole in the vicinity of the notebook and directly towards the camera (upstream) near the lens cap.

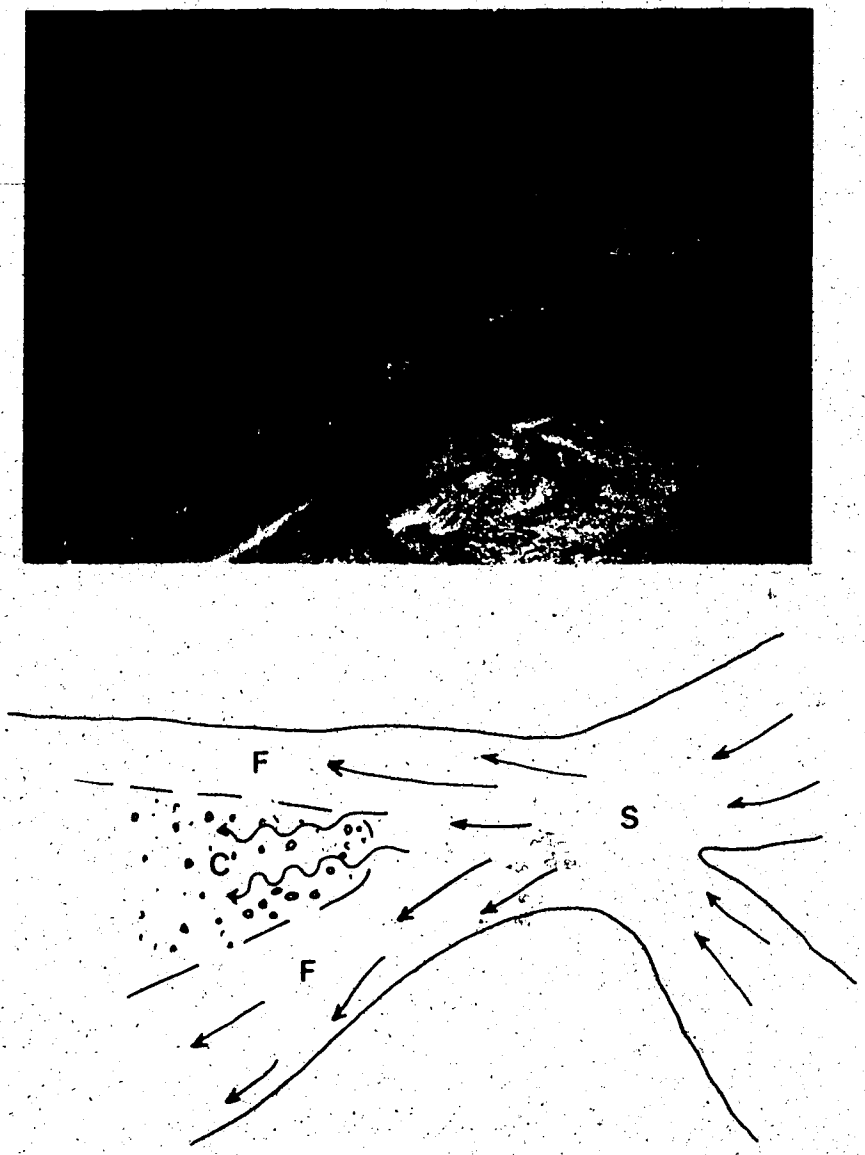

Figure 6-5 Sediment sorting downstream of a confluence scour. The secondary flow in the scour hole (S) and flow divergence downstream result in the deposition of fine material (F) at the margins of the channel and much coarser material (C) in the centre of the channel. Lighter grey tones indicate finer material. The length of channel portrayed is approximately 0.5m.

Table 6-2

Sorting of bed material in five abandoned confluence scour holes on Sunwapta River

	Mean b-axis (ϕ units)	Standard deviation (ϕ units)	t-test results
1. a)	-4.54	0.774	
b)	-3.90	0.524	a vs. b 4.83
c)	-5.15	0.657	c vs. a 1.32
2. a)	-4.25	0.527	
b)	-3.89	0.513	a vs. b 3.24
c)	-4.39	0.588	c vs. a 1.32
3. a)	-4.78	0.744	
b)	-3.89	0.486	a vs. b 7.13
c)	-5.00	0.773	c vs. a 1.42
4. a)	-4.28	0.760	
b)	-3.60	0.760	a vs. b 4.47
c)	-5.40	0.540	c vs. a 8.60
5. a)	-4.90	0.612	
b)	-4.14	0.617	a vs. b 4.47
c)	-5.17	0.650	c vs. a 2.05

t critical at $\alpha = 0.05$ and 98 degrees of freedom = 1.98
Significant t values are underlined.
a) = Centre of channel downstream of scour hole
b) = Margin of channel downstream of scour hole
c) = Scour hole

that immediately downstream. Sediment sorting in scour holes is discussed further in sections 6-3-3 and 6-4.

The scour hole shape is influenced greatly by the angle of confluence. As this angle increases the scour changes from an elongated trough to a bowl-shaped depression. Figure 6-6 illustrates this using bed profiles of high and low angle scours from both the field and laboratory.

6-3-2 Scour Depth

Previous studies (Mosley, 1976, 1977) showed that for a given total discharge the two principal controls of scour depth are the angle of confluence θ and the relative discharge of the two channels, ϵ. The relative discharge is defined as:

$$\epsilon = |Q_L - Q_R|/(Q_T/2) \qquad 6-2$$

where Q is discharge, the subscripts L and R denote the left and right confluent channels respectively, and $Q_L + Q_R = Q_T$. G. Parker (pers. comm., 1981) suggested that an expression of relative sediment mobility might be a further explanatory variable and proposed the use of a densimetric Froude number (equation 3-2). Statistical analysis showed this sediment mobility parameter to have no influence on scour depth in either the field or laboratory and was therefore eliminated as a factor contributing to the variations in scour depth.

Preliminary analysis of the correlation of the major variables (θ, ϵ, and Q_T) with scour depth (h_s) showed Q_T to be the dominant influence, with secondary control exerted by θ. This is true for both the field and laboratory data and confirms Mosley's (1981) conclusion about the importance of Q_T in predicting scour depth. The correlation coefficients are tabulated in Table 6-3. In order to

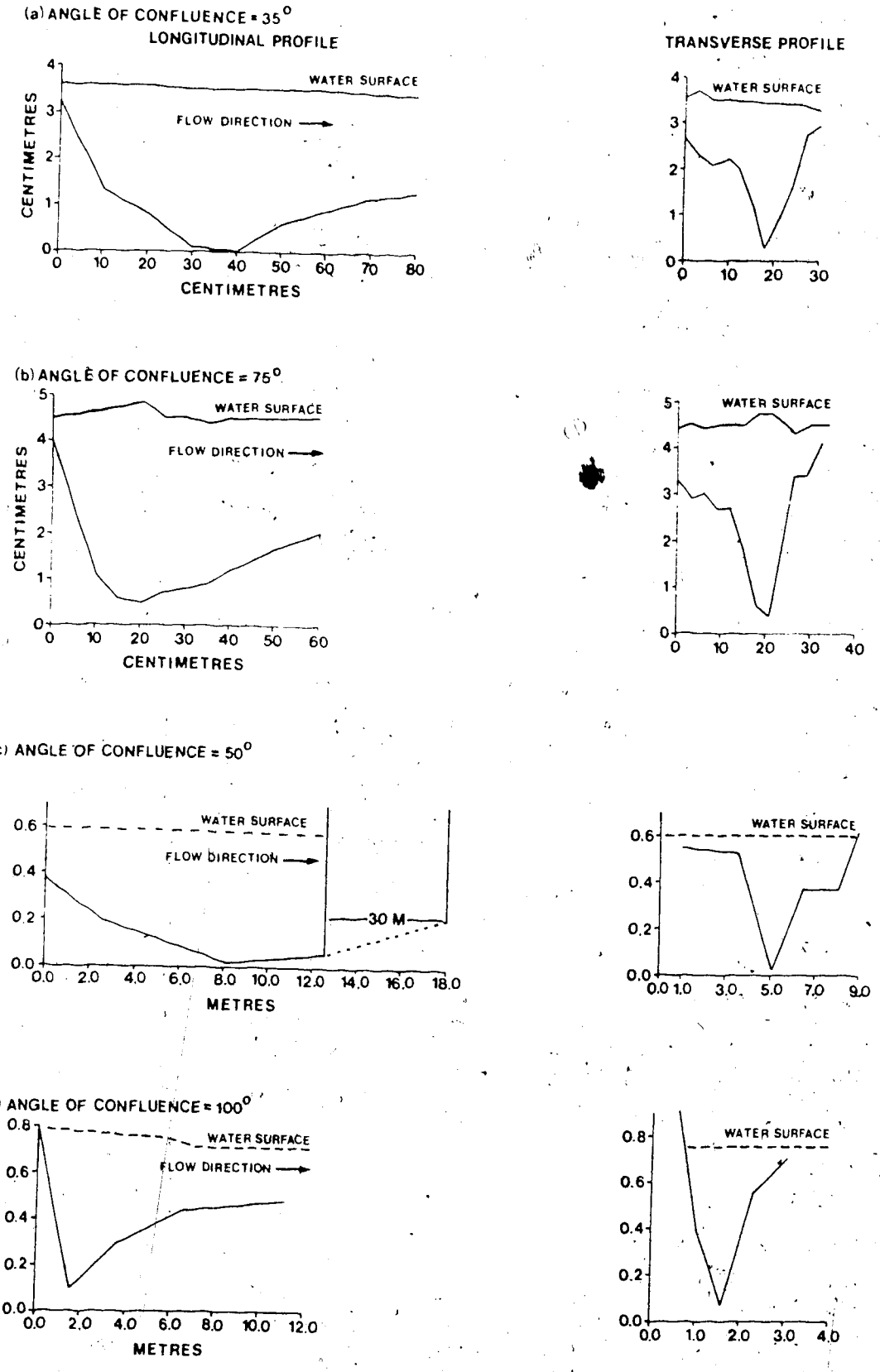

Figure 6-6 Longitudinal and transverse profiles of confluence scour holes in (a) and (b) the model and (c) and (d) the field to illustrate the effect of the confluence angle on the scour hole form and water surface profile.

eliminate the influence of Q_T and allow direct comparison between field and laboratory data, the rest of the analysis was carried out using relative scour depth, h_r, as the dependent variable :

$$h_r = h_s / \overline{h} \qquad 6\text{–}3$$

where $\overline{h} = (h_R + h_L^c) / 2$. The absolute scour depth, h_s, is defined as the water depth at the deepest part of the scour hole.

In both sets of data (field and laboratory) h_r ranges from about 2 to 6 except for four field data points where h_r reaches almost 8. These outliers may be the result of measurements being made at slightly lower than formative stage so that channel depth is underestimated by a disproportionate amount relative to scour depth. These scour holes were all measured early in the field season and it is possible that they are relict scours from the previous summer which, in the absence of high flows, had remained out of adjustment with the prevailing flow conditions. These complications that arise in the field can be eliminated under laboratory conditions where the development of a scour hole can be followed and one can be sure that it is a product of the prevailing flows, not inherited from earlier conditions.

Correlation analysis showed that for both data sets the only independent variable that correlates significantly with h_r is θ (see Table 6-3). This relationship between h_r and θ is graphed in Figure 6-7 along with the best-fit linear regression lines for each data set. Mosley (1976) suggested that this relationship was non-linear at very low ($<25^\circ$) and very high ($>90^\circ$) confluence angles but the data in Figure 6-7 do not show this effect. The best-fit least squares regression lines are :

Table 6-3

Correlation coefficients for the variables influencing scour depth.

	Field data	Laboratory data
θ versus h_s	0.442	0.551
θ versus h_r	0.415	0.695
Q_T versus h_s	0.528	0.598
Q_T versus h_r	0.229	-0.099
ε versus h_s	-0.203	-0.045
ε versus h_r	-0.184	-0.117

For the field data (at $\alpha = 0.05$) the correlation is significant when the coefficent exceeds 0.413.
For the laboratory data (at $\alpha = 0.05$) the correlation is significant when the coefficient exceeds 0.320.
The sample size is 23 and 38 for the field and laboratory data respectively.

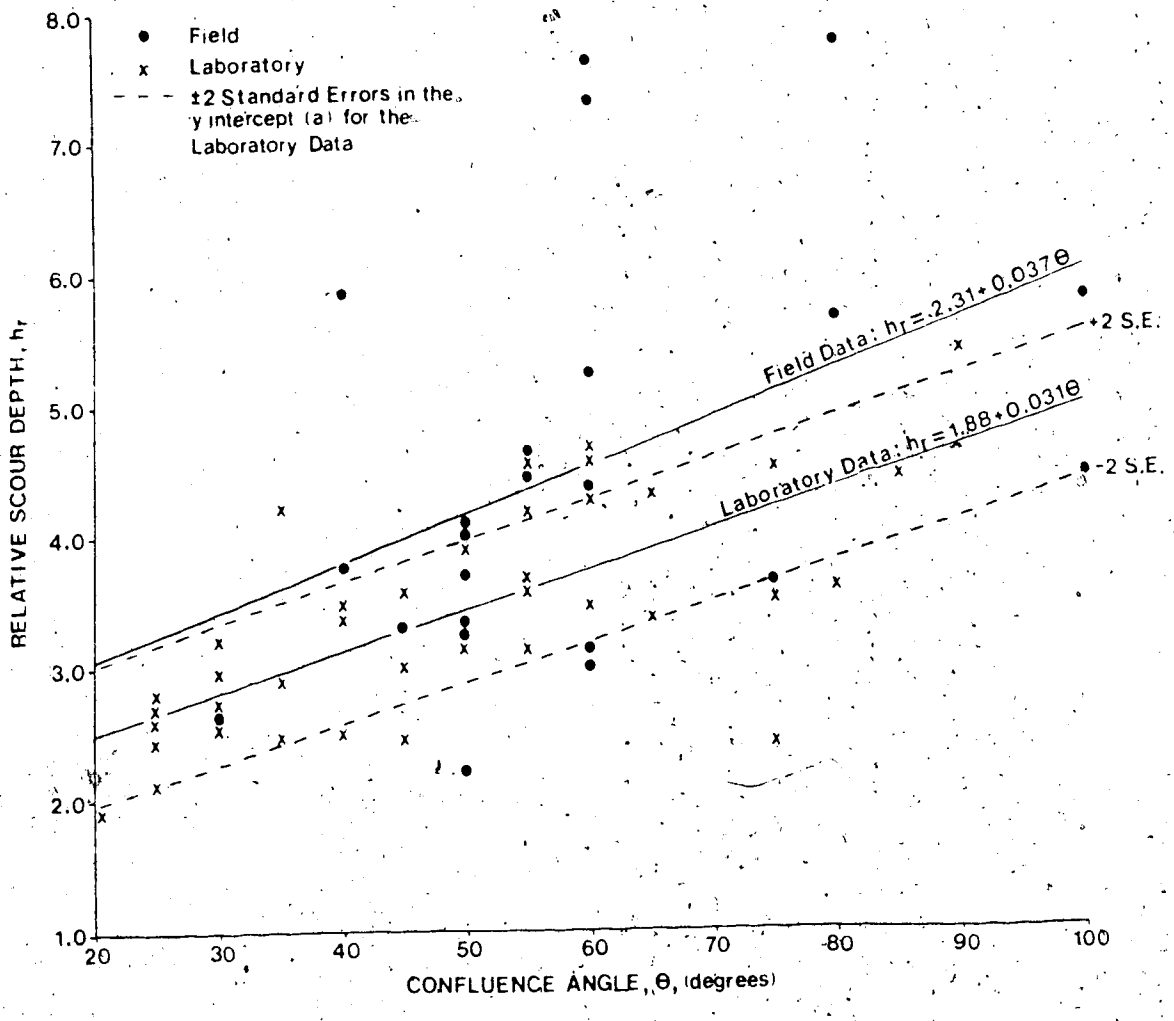

Figure 6-7 Relative scour depth (h_r) versus confluence angle (θ) for laboratory and field data.

Field data : $h_r = 2.31 + 0.037\theta$

Eqn. 1, Table 6-4

Laboratory data : $h_r = 1.88 + 0.031\theta$

Eqn. 2, Table 6-4

The intercepts of these two equations are within 2 standard errors of each other while the slopes are within one standard error. Thus, statistically, at $\alpha = 0.05$, there is no significant difference between the two regression lines (Ferguson, 1977; Kleinbaum and Kupper, 1978).

The relationship between h_r and θ may be modified when the influence of ϵ is taken into account. Since there is no significant difference in scour depth at a given confluence angle between the field and laboratory data, the two data sets were combined for this part of the analysis, to increase the sample size.

The data were split into three groups : $\epsilon < 0.25$, $0.25 < \epsilon < 0.75$ and $\epsilon > 0.75$ and the regression equations for the three groups for h_r versus θ are given in Table 6-4 (Equations 3, 4 and 5). While the slope of the linear regression increases with decreasing ϵ (that is with greater equality of the two discharges) the scatter about the relationships is so large relative to the sample size, that the statistical difference is negligible. The largest difference is between $\epsilon < 0.25$ and $\epsilon > 0.75$. The standard error of the slope for these two relationships is such that each line lies within two standard errors of the other. However, for $\epsilon > 0.75$ the slope is not significantly different from zero, whereas for $\epsilon < 0.25$ it is. Thus, scour is better developed where ϵ is small, and the relationship between relative depth and angle of confluence is also stronger in this case. At high ϵ there is little or no relationship between scour depth and angle of confluence because the

Table 6-4

Regression Equation Coefficients and Standard Errors.

	a	Standard Error of a	b	Standard Error of b	R^2	Sample size
1. h_r v θ (Lab.)	1.882	0.276	0.031	0.053	0.483	38
2. h_r v θ (Field)	2.307	1.085	0.037	0.018	0.172	23
3. h_r v θ (ε <0.25)	0.824	1.069	0.067	0.022	0.354	19
4. h_r v θ (0.25< ε <0.75)	1.670	0.448	0.038	0.007	0.473	31
5. h_r v θ (ε >0.75)	2.132	0.767	0.025	0.013	0.276	11
6. h_r v ε (Lab.)	3.521	0.245	-0.341	0.484	0.014	38
7. h_r v ε (Field)	4.826	0.518	-0.674	0.787	0.034	23
8. log h_s v log Q_T (Field)	-0.266	0.062	0.466	0.164	0.277	23

relative size of the contributing channels precludes the development of secondary flows, and hence scour holes, at any confluence angle.

Thus, ϵ has a minor influence on scour depth under naturally occurring conditions. Confirmation of this finding is provided by separate consideration of the laboratory and field data. Regressions of h_r against ϵ show slopes that are not significantly different from zero (Table 6-4, Equations 6 and 7). This weak influence of ϵ is shown graphically in Figure 6-8.

Having identified the influence of the two variables, θ and ϵ on the relative scour depth it should be pointed out that the combined level of statistical explanation for these two variables is quite low. Multiple regression analysis of combined laboratory and field data gave R^2 of 0.355 for these two variables. The lower scatter of the laboratory data, where data collection conditions are more favourable, results in a value of R^2 of 0.587 for the laboratory data alone while the field data give an R^2 value of 0.200. Reference to Table 6-4 shows that most of the explanation of variation in h_r lies with θ and only a negligible amount with ϵ.

6-3-3 Sediment Transport Through Confluence Scour Holes

Hein and Walker (1977, p.564) stated, in connection with pools developed at constrictions and confluences in braided streams, that "After a high discharge period, the only sediment remaining in a pool is a very coarse lag". The field observations reported earlier in this chapter (see Table 6-2) lend some support to their statement. However, when it is considered that at high discharges the pool is a site of convergent flow powerful enough to erode the bed to unusual depths, it is difficult to envisage even the coarsest components of the bed material being

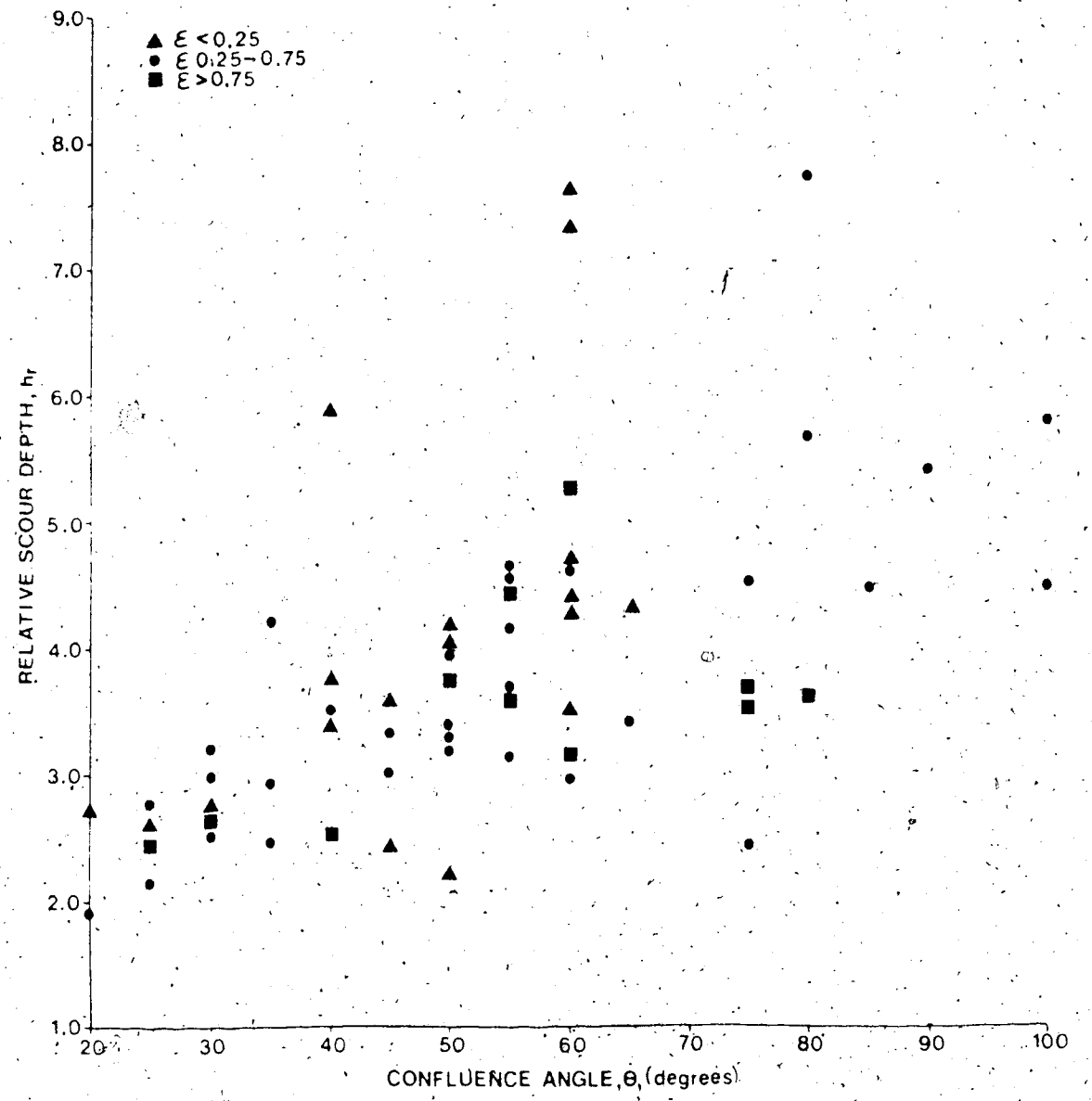

Figure 6-8 Relative scour depth (h_r) versus confluence angle (θ) stratified by the relative discharge of the confluent channels (ε).

deposited there. Intuitively one would expect higher competence in the pool than in the confluent channels immediately upstream, so that any particle delivered to the pool from upstream would be easily transferred through the pool. Indeed, this is the case for the pools in meander bends of single channel rivers (Keller, 1971; Lisle, 1979). Field measurements of sediment transport and bed material in confluence scours would be extremely difficult, but the laboratory model presents an opportunity to investigate the sediment transport through, and bed armouring of, confluence scour holes more thoroughly than has previously been attempted.

Twenty-two laboratory scour holes were sampled. Three bed material and three bedload samples were collected from each scour hole, one in each confluent channel and one in the scour hole. The scour hole bedload samples were collected at the downstream end of the scour hole, where the channel geometry was free of the influence of the turbulence in the confluence so that the bed was fairly flat and the bedload trap could be placed with its lip flush with the bed. The sampling methods are described in section 6-2-1. For sixteen of the scour holes both bed material and bedload samples were collected, in two others only bedload samples were taken, and in the remaining four only bed material samples were obtained. Sampling is incomplete in these six scour holes because rapid changes in channel form prevented all the samples from being collected. The samples from the two channels were combined to give an average value for comparison with the scour hole sample. The area-by-number bed material samples were converted to grid-by-number samples to facilitate comparison with the bedload samples. The data are summarised in Table 6-5.

Statistical comparison of the particle sizes in the channels and scour holes

Table 6-5

Comparison of the grain size characteristics of the bedload and bed material in the confluent channels and scour holes of twenty-two laboratory confluences.

	Bedload			Bedload			Bed material		
	D_A	D_S	D_A/D_S	D_{90A}	D_{90S}	D_{90A}/D_{90S}	D_A	D_S	D_A/D_S
1	1.41	1.36	1.04	2.91	3.46	0.84	1.61	1.35	1.19
2	1.31	1.65	0.79	3.16	3.63	0.87	1.83	2.83	0.65
3	1.33	1.63	0.82	2.89	2.91	0.99	1.51	2.00	0.75
4	1.25	1.12	1.12	2.31	2.64	0.87	1.85	1.27	1.46
5	1.10	1.37	0.80	2.25	2.53	0.89	1.64	1.80	0.91
6	1.47	1.42	1.03	3.55	2.73	1.30	1.37	1.49	0.92
7	1.08	1.40	0.77	2.19	3.64	0.83	1.67	1.36	1.23
8	1.17	1.49	0.78	2.58	3.03	0.85	2.54	1.65	1.54
9	1.29	1.22	1.06	3.07	3.20	0.96	2.03	1.40	1.45
10	1.33	1.22	1.09	2.75	2.36	1.16	1.56	1.64	0.95
11	1.09	1.29	0.84	2.43	2.73	0.89	1.14	1.05	1.09
12	1.19	1.43	0.83	2.62	2.81	0.93	2.21	1.16	1.90
13	1.30	1.12	1.16	2.81	2.55	1.10	1.35	1.50	0.90
14	1.47	1.04	1.41	2.75	2.41	1.14	1.51	0.76	1.99
15	1.03	1.13	0.91	2.28	2.50	0.91	1.22	0.97	1.26
16	1.16	1.34	0.87	2.44	2.64	0.92	--	--	--
17	1.14	1.38	0.83	2.31	2.53	0.91	--	--	--
18	1.30	1.29	1.01	2.33	2.48	0.94	1.50	1.24	1.21
19	--	--	--	--	--	--	2.10	2.56	0.82
20	--	--	--	--	--	--	1.76	1.72	1.02
21	--	--	--	--	--	--	1.72	2.03	0.85
22	--	--	--	--	--	--	1.55	1.65	0.94
$\bar{x}$ =	1.25	1.33	0.95	2.65	2.77	0.96	1.68	1.57	1.15

D_A = Mean grain size in confluent channels (mm)
D_S = Mean grain size in scour hole (mm)
D_{90A} = 90th percentile of the grain size distribution in the confluent channels
D_{90S} = 90th percentile of the grain size distribution in the scour hole

was carried out using a paired t-test (Hammond and McCullagh, 1974, p.164-166; Kennedy and Neville, 1976, p.210-211). In this test :

$$t = \frac{|\overline{d}|}{S.E_{\overline{d}}} \qquad 6-4$$

where $S.E_{\overline{d}} = \sigma_d / n^{0.5}$, $\sigma_d = [(\sum (d - \overline{d})^2)/(n-1)]^{0.5}$, d is the difference between x and y in each pair (in this case D_A and D_S (see Table 6-6)) and $\overline{d}$ is the mean value of d for the sample. The test results are summarised in Table 6-6. The test showed that neither mean bed material size nor mean particle size of the bedload was significantly larger in the scour hole compared to the confluent channels. The mean ratio of bed material size in the channels to bed material size in the scour hole is 1.15, with a range from 0.65 to 1.99. The mean ratio for bedload is 0.95, with a range from 0.77 to 1.41.

It could be argued that relative competence of the confluent channels and the scour hole is better assessed by considering the coarse tail of the particle size distribution than the mean size. The bedload data allow such an assessment to be made and the results are displayed in Table 6-5. Fourteen of the eighteen scour holes sampled show the ninetieth percentile of the grain size distribution of the bedload transported from the scour hole (D_{90S}) to be larger then that entering the scour hole from the confluent channels (D_{90A}). The ratio of D_{90A} to D_{90S} averages 0.96 with a range from 0.83 to 1.30. The paired t-test shows the difference between D_{90A} and D_{90S} to be statistically insignificant.

The results of this analysis clearly indicate that during formative flows there is no trapping in the scour holes of coarse material from upstream. If anything

Table 6-6

Summary of t-test for bedload and bed material samples in confluence scours.
See text for an explanation of the notation.

	$\lvert d \rvert$	σ_d	$SE_{\bar{d}}$	t	n	degrees of freedom
Bed material	0.119	0.357	0.084	1.42	20	19
Bed load D_{50}	0.159	0.561	0.125	1.27	18	17
Bed load D_{90}	0.082	0.231	0.054	1.52	18	17

For $\alpha = 0.05$ t must exceed 2.110 (for 17 degrees of freedom) and 2.093 (for 19 degrees of freedom) to be significant.

the scour holes are more competent than the confluent channels. It is interesting to note that D_{50} and D_{90} of the bedload samples average about 1.3mm and 2.7mm respectively. These are very similar to the values for the flume sand as a whole and indicate that not only are the scour holes as competent as the confluent channels but that both are capable of transporting the full range of particle sizes available. In fact many of the scour hole bedload samples contain particles greater than 5mm in diameter. D_{95} of the flume sand is 4mm so that even particles from the extreme coarse tail of the distribution were being transported through the scour holes.

Observation of the development of the scour holes revealed two further facets of sediment transport through these confluences. Firstly, it was common for scour depth to fluctuate by as much as 5mm over a period of several minutes during apparently stable flow conditions. The filling phase of such oscillations was characterised by the arrival of initially coarse particles followed by progressively finer material. Hence bed material and bedload particle size fluctuated, along with scour depth. Aggradation of the scour hole was preceded by aggradation in the confluent channels suggesting the passage of small pulses of sediment down the channel. Spatial sorting of grain size within the pulse would produce the temporal separation of coarse and fine material noted during aggradation in the scour holes. Perhaps these pulses are akin to Hein's (1974) diffuse gravel sheets, in which case they are clearly important to scour hole form as well as bar deposition.

6-4 Discussion

The dominant control of scour depth (h_s) is the total discharge (Q_T) entering the confluence. In both the laboratory and field scour holes the correlation of h_s with Q_T is stronger than with any of the other independent variables. Mosley (1981) suggested that absolute scour depth could be predicted quite reliably using the total discharge entering the scour hole in confluences with a confluence angle greater than 40°. Mosley's (1981) data are plotted in Figure 6-9 along with the field data from this study. The two data sets, while covering different ranges of total discharge, fit the same trend, although Mosley's (1981) data are less scattered. This confirms the general form of Mosley's (1981) relation which simply reflects a scaling effect of the same kind that causes single channels with larger discharges to have larger cross-sectional areas. The scatter evident on the graph suggests that other variables are also relevant. In the case of the geometry of single channels this is the character of the perimeter sediments (Richards, 1982, p.161-175) but for confluence scour the most important secondary variable is the angle of confluence. Figure 6-9 illustrates this for the Sunwapta River data since all but one of the scour holes with confluence angles less than 60° are negative residuals from the regression line. Statistical analysis shows that confluence angle correlates significantly with scour depth in both the field and laboratory scour holes.

In order to remove the scale effect of total discharge and allow direct comparison of the field and laboratory data, a dimensionless scour depth, h_r, the ratio of scour depth to the depth of the confluent channels, was used for the remainder of the analysis. Total discharge fails to correlate with relative scour

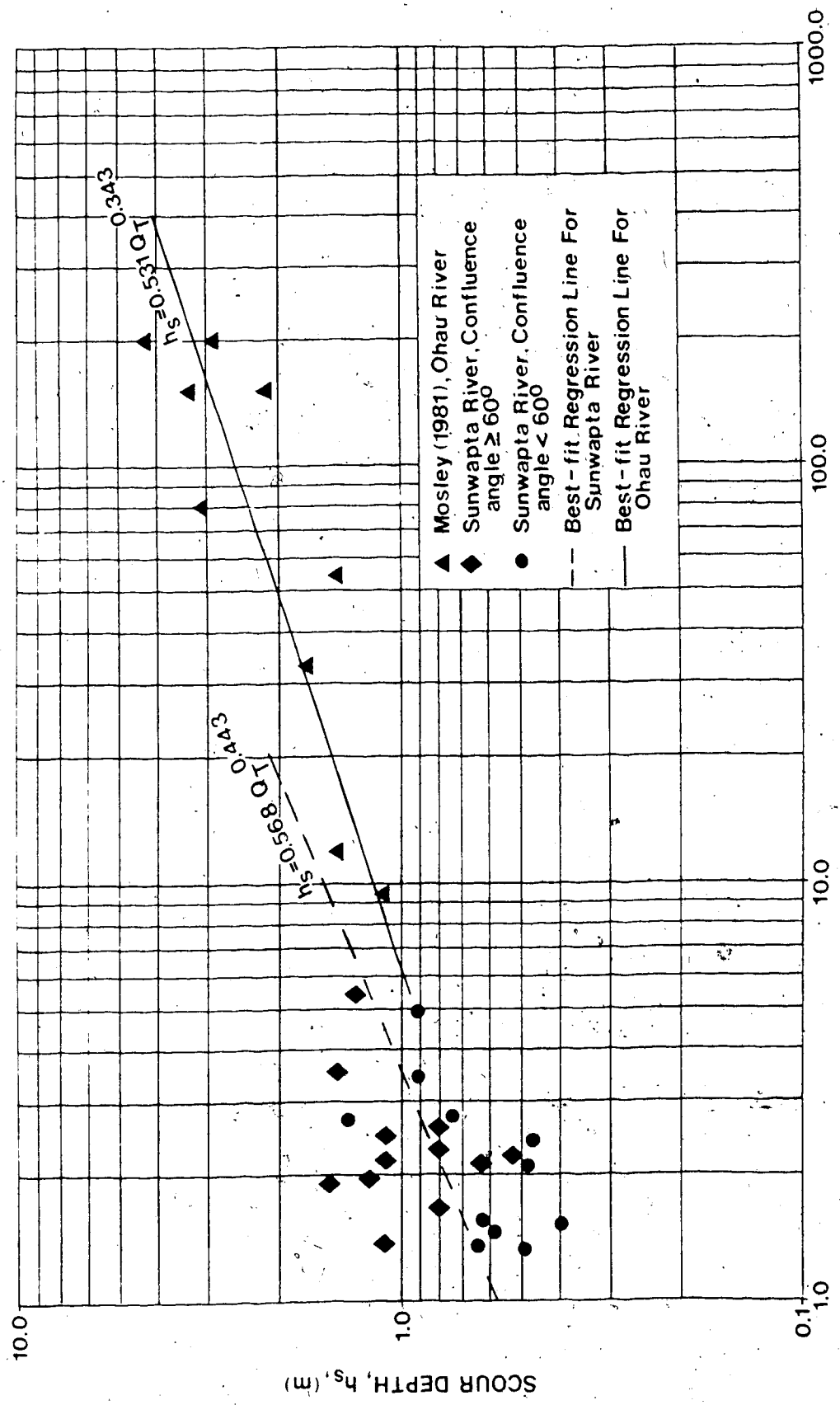

Figure 6-9 Comparison of the relationship between absolute scour depth (h_s) and total discharge (Q_T) for the Sunwapta River data (this study) and Mosley's (1981) Ohau River study.

depth, h_r, and instead the dominant variable is confluence angle (θ), confirming Mosley's (1976) conclusion. However, because of the absence of data from scour holes with confluence angles greater than 100° and less than 25° it is impossible to confirm the presence of the upper and lower asymptotes that Mosley (1976) reported. The correlation of scour depth with confluence angle is attributable to the increased relative strength of the secondary circulation and associated turbulence with increasing angle. Here an analogy may be drawn with secondary flows in meander bends which increase in relative strength as the angle of deviation of the curve increases (Chow, 1959, p.441). In the confluences the angle of confluence represents the combined angle of deviation of the two channels, and should therefore be directly related to the strength of the secondary currents and hence the scour depth.

The relative scour depths, for a given confluence angle, in the field and laboratory are statistically similar, indicating that this aspect of channel morphology is modelled reasonably well. Comparison with other laboratory data from experiments with different sediment types suggests that sediment characteristics are significant in scour hole geometry, as they are in channel geometry. Mosley's (1976) confluences were formed in cohesive sand, and Figure 6-10 shows that, while the rate of increase of relative scour depth with angle of confluence is similar in Mosley's experiments and those discussed herein, the actual depth at a given confluence angle is lower in the cohesive material than in the non-cohesive sand. Statistical analysis of the two regression lines (Table 6-7) shows the slopes to be statistically similar while the intercepts are statistically different. (The best-fit line for Mosley's (1976) data is beyond two standard errors

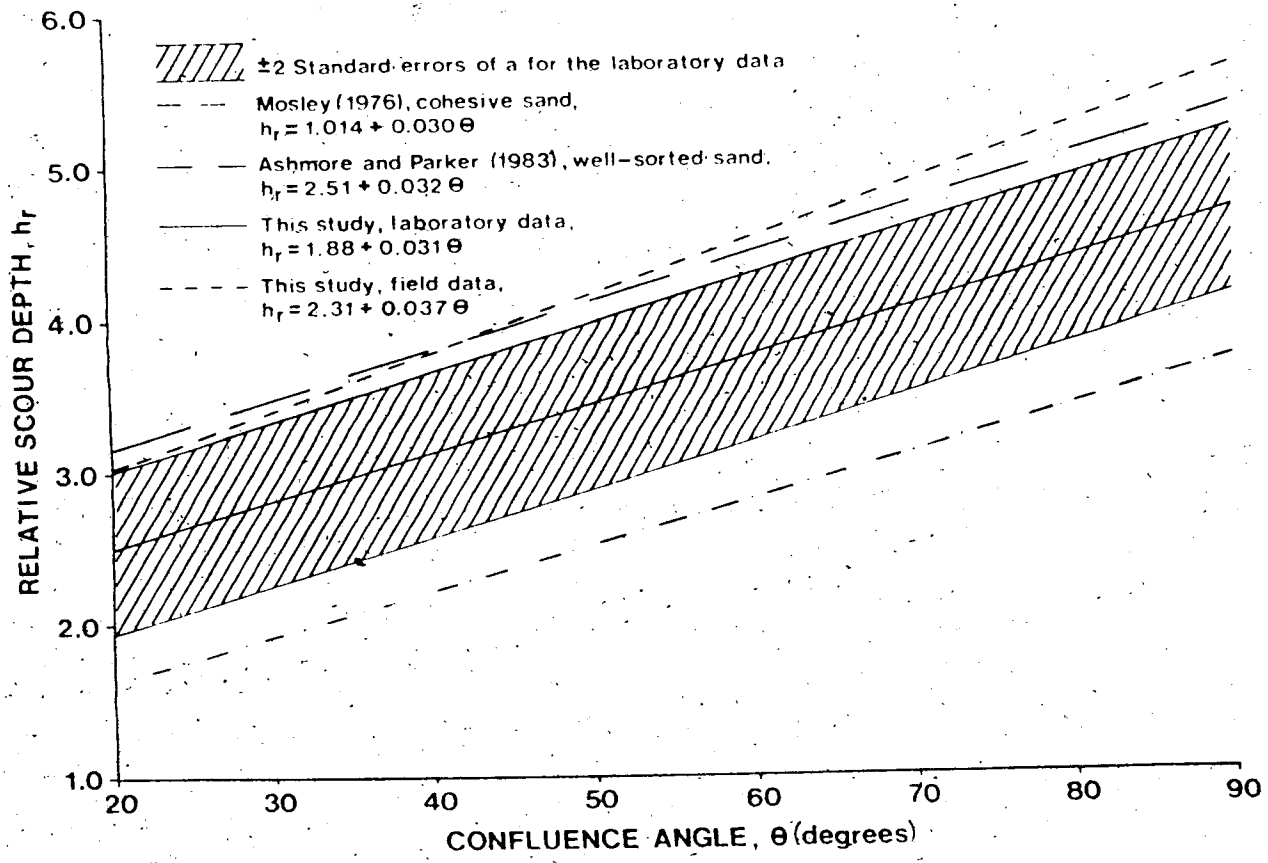

Figure 6-10 Comparison of the relationship between relative scour depth (h_r) and confluence angle (θ) for field gravel streams, poorly-sorted laboratory sand, well-sorted laboratory sand and cohesive laboratory sand.

Table 6-7

Regression summary for relative scour depth (h_r) versus confluence angle (θ)

$h_r = a + b\theta$

Data Set	a	b	Standard Error of a	Standard Error of b
Mosley (1976)	2.354	0.0311	0.889	0.0144
Well-sorted sand (Ashmore and Parker, 1983)	2.514	0.0316	0.517	0.0087
Poorly-sorted sand (this study)	1.880	0.0307	0.276	0.0053
Field data (this study)	2.354	0.0311	0.889	0.0144

of the intercept of the laboratory data regression line.) Comparison can also be made with Ashmore and Parker's (1983) data for scour in well-sorted sand of similar median size to the poorly sorted sand used in the present experiments. Again, the slopes of the best-fit lines for the two data sets are statistically similar (Table 6-7), but the best-fit line for the well-sorted sand, plots above that for the poorly-sorted sand (Figure 6-10). At a given confluence angle the scour depth in well-sorted sand is about 10 or 15 per cent greater than in the poorly-sorted sand. However, the confidence limits for the two regression lines overlap with one another (Figure 6-10, Table 6-7) indicating that statistically there is some doubt about the difference in scour depths between the two sets.

The influence of the relative discharge of the incident channels (ϵ), which Mosley (1976, 1977) found to be a significant factor controlling scour depth, was not particularly strong in this case. Only when ϵ exceeded a value of about 1 (one channel's discharge is more than twice that of the other) was there a notable reduction in relative scour depth at a given confluence angle. This is also borne out by Mosley's (1976, 1977) data which show scour depth to be unaffected by ϵ until it exceeds 0.7, and not strongly affected until ϵ exceeds 1 (Mosley, 1977, Figure 3). The data used here have only seven scour holes with ϵ greater than 1, thus it is not surprising that the influence of ϵ on scour depth is not strongly felt.

The effect of the relative sediment mobility, Fo, on scour depth is negligible. It was suspected that depth would increase with Fo as the relative mobility of the sediment increased but no such relationship is discernible from the data. However, Ashmore and Parker's (1983) data from laboratory experiments in well-sorted sand do show a weak positive correlation between relative scour depth and

Fo. It seems, therefore, that the role of Fo in controlling confluence scour depth is a minor one, although data with a wider range of values of Fo may show its influence more clearly.

The scatter in the laboratory data is rather less than in the field data but in both cases the level of explanation of the variation in relative scour depth (h_r) provided by the angle of confluence (θ), and relative discharge (ϵ) is fairly low. Multiple regression of these two variables against relative scour depth gave R^2 values of 0.587 and 0.200 for the laboratory and field data respectively. This low level of explanation, particularly for the field data, is also evident in the individual regression equations listed in the Table 6-4. It is possible that one or more variables that exert an influence on scour depth were omitted from the analysis. Examination of Mosley's (1976, 1977) data shows that the sediment load imposed on the two channels affects the scour depth; a four-fold increase in sediment load could produce a 25 per cent reduction in scour depth. The observation that scour depth appears to oscillate with the passage of sediment pulses supports this suggestion. Transport of a larger imposed load would result in a greater proportion of the stream power being expended in transporting the sediment, with a correspondingly smaller amount available for scour of the bed.

Other factors, apart from variation in sediment load, may also be responsible for the scatter observed in the relationship between scour depth and the controlling variables. Differences in channel shape and channel curvature, and the fact that perfect Y-shaped confluences with well defined channels are rare under natural conditions, all contribute to the scatter. A further factor contributing to scatter is that for given flow conditions it takes a finite time for

equiljbrium scour depth to be reached. It is assumed that all the scour holes measured were at equilibrium with the prevailing flows but given the rapidity with which discharge and channel alignment change in braided streams this is not necessarily the case. Scatter is greater for the field data because variations caused by antecedent conditions and disequilibrium with prevailing flows are much more difficult to eliminate here than in the laboratory where scour hole development can be monitored continuously.

The measurement of the particle size distributions of the bedload and bed material in the confluent channels and the associated scour hole demonstrated that, at formative discharge, the scour hole is no less competent than the confluent channels and that as a result no accumulation of a coarse lag occurred in the scour hole. Consequently the slightly lower relative scour depths for a given confluence angle, in poorly sorted rather than well-sorted sediment of similar mean size (see Figure 6-10), must be attributed to a cause other than armouring of the scour hole. The explanation may lie in the fact that the poorly sorted sediment is likely to be less mobile than its well-sorted counterpart (see Chapter 5, and Parker and Klingeman, 1982). This lower mobility might result in a relatively greater expenditure of energy to move the imposed sediment load through the scour hole, with a correspondingly smaller amount of energy available to scour the hole deeper. This is a similar argument to that proposed for the influence of imposed sediment load on scour depth.

The other consequence of the results of the laboratory measurements of sediment transport through scour holes is that the coarse lag reported from field scour holes (Hein and Walker, 1977) are not explicable in terms of differences in

competence between the confluent channels and scour holes. Two alternative causes are, first, that the coarse material accumulates as discharge declines, and second, that in the field the excavation of the scour hole may result in the exhumation of large particles deposited by previous, larger channel with much higher competence.

6-5 Conclusions

Measurements of a total of 61 confluences, 38 in the laboratory and 23 in the field, showed that the major control of relative scour depth is the angle of confluence of the two channels, the greater the angle, the greater the scour depth. There is a weak secondary influence exerted by the relative discharges of the two channels. For a given angle of confluence, relative depth is greater when the two channels have more nearly equal discharges. Absolute scour depth is controlled principally by the total discharge through the scour hole, with a secondary influence exerted by the angle of confluence. The model and field data compare very closely with one another, which is an important verification of the reliability of the model. The laboratory scours showed no accumulation of coarse material on the bed during formation and the scour holes are slightly more competent than the confluent channels immediately upstream.

Confluence scours are a manifestation of spatial variations in sediment transport rate and once formed they are affected by temporal variations in sediment transport. This is apparent from fluctuations in scour depth which are the result of migratory pulses of bedload passing along the channel. The role of these pulses in bar formation is described in Chapter 8.

Chapter 7 : Channel Pattern and Form

7-1 Introduction

Braided streams are known to vary considerably in the degree of braiding and in the types of bars prevalent in the channel, but there have been few attempts to analyse the circumstances causing such variation. Some attention has been paid to devising quantitative indexes of braiding intensity for descriptive purposes (Brice, 1964; Rust, 1978a; Hong and Davies, 1979), but to date only Howard et al. (1970) and Maizels (1979) have put such a braiding index to analytical use by demonstrating a positive correlation between the braiding index and the channel discharge and slope. This result of Howard et al. (1970) and Maizels (1979) is predictable when one considers the increasing tendency for braiding to occur as slope and discharge increase (Lane, 1957; Leopold and Wolman, 1957; Henderson, 1961; Schumm and Khan, 1972; Ferguson, 1981; Kellerhals, 1982) but no attempt has been made to confirm their conclusions under conditions that eliminate the error introduced by differences in river stage and map scale which are present in their field data (Howard et al., 1970).

The relative abundance of the various unit bar types identified by Smith (1974) is a characteristic of braided streams that is of both geomorphological and sedimentological importance. Several studies (Fahnestock, 1969; Smith, 1970; Hein, 1974; Boothroyd, 1975) have indicated that, particularly in proglacial streams, there is a downstream transition from channels with low sediment mobility in which bars predominantly resemble Smith's (1974) longitudinal unit bars, to channels in which sediment mobility is comparatively high and the most common bar types are linguoid or transverse unit bars, often with avalanche faces

at their downstream end. Accompanying this change in sedimentary characteristics is a difference in the channel topography. Both Smith's (1970) and Hein's (1974) observations suggest that average bed relief (the difference in elevation between the bar tops and the channel bed) decreases in the transition from coarse-grained channels upstream (proximal) to the fine-grained downstream channels (distal). However, it is apparent from their data that while absolute relief decreases in the proximal - distal transition, when scaled by the grain size there is actually an increase in relative relief downstream. Thus, there is a coincidence of increasing relative relief (or depth) and an increasing proportion of transverse rather than longitudinal bars. In addition to the role of relative depth, Hein and Walker (1977) noted that the most common locations for transverse bars, even in the distal reaches, were areas of width or depth increase such as scour pools. Thus, the availability of such sites may also prove to be an important control on the abundance of transverse bars.

Laboratory modelling provides an opportunity to study these aspects of braided river morphology more carefully under conditions of controlled slope and discharge and in which variations over the equivalent of several months or years in the field can be analysed in a few hours.

7-2 Data Collection

Data were collected from a total of ten runs at seven different combinations of slope and discharge (see Table 4-1). Run 1 was intended to be a pilot study for testing the proposed sampling procedures and assessing the likely variability over time of the variables to be sampled, so that suitable sample sizes could be estimated. Consequently the data from run 1 are incomplete.

Upon conclusion of run 1 it was decided that the head arrangement by which the sediment was delivered to the head of the flume through four nozzles resulted in too much aggradation at the head of the flume. The next three runs (numbers 2, 3 and 4) were carried out using only two sediment input nozzles. After run 4, in which the channel degraded and ceased braiding about 30 hours into the run, the four-nozzle arrangement was reinstated and aggradation was controlled by constricting the wooden head section into which the water and sediment discharged. To assess the influence of the head arrangement on channel form runs 3 and 4 were repeated using the four-nozzle arrangement, and these were denoted runs 7 and 6 respectively (run 5, at a discharge of 4.5 l s^{-1} and slope of 0.01, was abandoned after only a few hours because of obvious incision of the kind that occurred in the second half of run 4).

In each run the channel morphology was characterised by sampling three variables; the braiding intensity, the bed topography, and the number of transverse unit bars with avalanche faces. The measurement of bed topography also provided estimates of channel width and depth.

Braiding intensity was measured by two indexes; the average number of active channels per stream (flume) transect (N), and the total number of active channel segments within the flume (P). An active channel is defined as one in which there is visible sediment transport. This criterion removes from the sample any abandoned channels still occupied by water and the very small channels present on many large complex bar surfaces. In addition, it provides a simple distinction between what is, and what is not, a channel; a problem that plagues field investigations. These measures are very similar to those used by Howard et

al. (1970), Hong and Davies (1979) and Maizels (1979) to characterise braiding intensity. Because flume discharge is constant there is no problem of stage dependency of the kind encountered in the field (Brice, 1964; Rust, 1978a) but since the number of active channels per transect and the number of active channel segments per flume length are different estimates of braiding intensity it is possible that they will produce slightly different results.

The same data collection program was used in each run and consisted of the following :

1) eighty transects of bed and water surface elevation across the flume were measured, perpendicular to the walls, with measurements made every five centimetres along the transect. These were used to calculate average bed topography for each run. A pilot study of the variability of bed topography using 100 transects showed that the same result (plus or minus 5%) could be obtained 95% of the time using about 70 transects. Eighty transects turned out to be a convenient number for the flume length and the sampling method chosen. A random stratified sample was collected by dividing the flume into eight one metre long sections and choosing the location of a transect at random within each of these sections. The upstream and downstream extremities of the flume were eliminated from the sampling section to avoid the effects of the introduction of the flow to the flume at the upstream end, and drawdown at the downstream end. Transects were measured eight at a time every five hours, a new location for each transect being chosen each time. It took between one and two hours to measure a set of eight transects. The five-hour separation between samples was intended to ensure that the channel had undergone considerable modification between each set of measurements.

The standard deviation of bed elevation of each transect was calculated and the mean of these 80 standard deviations taken as the average bed relief (I) for that run. This is preferable to measures such as relief ratios (the difference between the maximum and minimum elevation) because it utilises information from the whole transect rather than selected points (Evans, 1972; Hughes, 1982).

The number of active channels in each transect was recorded at the same time as the topography was measured. This information was used to calculate N, the mean number of active channels per transect. The transects also provided data for calculating average width and depth of the laboratory channels, by the method described in Chapter 5.

2) Every hour the number of active channel segments in the braided network was counted by sketching of the stream network. The braiding intensity for each run was taken as the arithmetic mean of the number of active channel segments in this sample of 50 networks.

3) At the same time that the channel network was sketched the number of avalanche-face bars was counted. Avalanche faces were arbitrarily defined as those whose height exceeded approximately five millimeters (about twice D_{90}).

7-3 Results

The data for each run are displayed in Table 7-1 where the runs are arranged from left to right in order of increasing stream power index, Ω, (the product of slope and discharge).

7-3-1 Braiding Intensity

The two indexes of braiding intensity, the mean number of active channels per flume transect (N) and the mean number of active channel segments per

Table 7-1 Channel pattern and form characteristics of laboratory runs.

Figures in parentheses are standard deviations of the mean, in each case.

Run number	3	7	11	4	4a	4b	6	10	8	1	2	9
Slope	0.01	0.01	0.015	0.015	0.015	0.015	0.015	0.01	0.015	0.015	0.015	0.015
Discharge ($m^3 s^{-1}$)	0.0015	0.0015	0.0012	0.0015	0.0015	0.0015	0.0015	0.00225	0.0045	0.003	0.003	0.0045
Stream power index $\times 10^5$ (Ω')	1.50	1.50	1.80	2.25	2.25	2.25	2.25	3.38	4.50	4.50	4.50	6.75
Mean number of active channel segments (N).	6.2 (3.01)	6.7 (3.18)	6.5 (3.45)	7.2 (4.99)	13.4 (5.06)	2.61 (1.85)	10.5 (4.99)	13.9 (5.24)	10.7 (5.37)	-- --	13.4 (4.51)	14.3 (4.35)
Mean number of active channels per transect (P)	1.60 (0.61)	1.30 (0.56)	1.39 (0.54)	1.60 (0.87)	2.10 (0.95)	1.10 (0.30)	2.00 (0.91)	2.15 (0.90)	2.02 (0.90)	-- --	2.44 (0.97)	2.20 (0.80)
Mean bed topography index (I)	6.45 (1.44)	6.95 (1.51)	5.55 (1.43)	6.56 (1.71)	6.05 (1.53)	7.07 (1.77)	5.57 (1.28)	6.03 (1.67)	7.72 (2.08)	6.31 (1.49)	7.18 (1.79)	7.42 (1.61)
Mean number of avalanche-face bars (M)	0.46 (0.83)	0.71 (1.12)	0.63 (1.02)	0.82 (1.08)	1.81 (0.93)	0.13 (0.45)	1.17 (1.19)	1.16 (1.36)	1.44 (1.49)	-- --	1.02 (1.12)	1.47 (1.25)
Mean total width (B)	0.64	0.46	0.57	0.55	0.73	0.38	0.68	0.88	1.06	0.97	0.95	1.05
Mean depth (d)	0.0106	0.0109	0.0077	0.010	0.0085	0.0121	0.0079	0.0083	0.0110	0.0086	0.0087	0.0100
d/B	0.0166	0.0237	0.0135	--	0.0117	0.032	0.0116	0.0094	0.0104	0.0088	0.0092	0.0095
τ^*/τ_c^*	1.77	1.83	1.93	--	2.13	3.07	2.00	2.10	1.87	2.17	2.20	2.53
Head arrangement	B	A	A	B	B	B	A	A	A	A	B	A

Note: 1. Runs 4a and 4b are the first 30 hours and second 30 hours respectively of run 4.
2. Head arrangement A has 4 sediment input nozzles, and B has 2 input nozzles.

flume length (P), both show an obvious increase with increasing stream power index (Ω)' (Figures 7-1 and 7-2). In both cases, however, the rate of increase tends to decline at higher stream power.

The non-parametric correlation coefficient, Kendall's τ, was used to test the relationship between braiding intensity and stream power. This test relies on ranking the data and is particularly suited to small samples in which the normality of the data is questionable and there are a number of tied ranks (Hammond and McCullagh, 1974, p.201-205). The data are first arranged in pairs of x and y variables and the ranks for each variable calculated. The ranks for the x variable are then listed in their natural sequence (1 to n) and the paired rank for y placed next to the x variables. Beginning at the first y rank, the number of ranks below it that have a greater value are recorded and a score of +1 allotted to each one. This is repeated for the ranks smaller in value which are allotted a score of -1. When the scores for each rank have been calculated a final total is obtained. If the ranks of y correspond closely with the paired ranks of x the final total is a large positive number. The correlation coefficient, τ, is calculated by :

$$\tau = S / 0.5N(N-1) \qquad 7-1$$

where N is the sample size. The denominator of this equation is the maximum possible score so that τ is simply a ratio of the actual score (S) to this maximum possible score and therefore may range between 1 and -1. Significance testing is carried out by calculating a z value which is tested against the normal distribution. For a significance level of 95% the critical z value to be exceeded is 1.645 and z is calculated as :

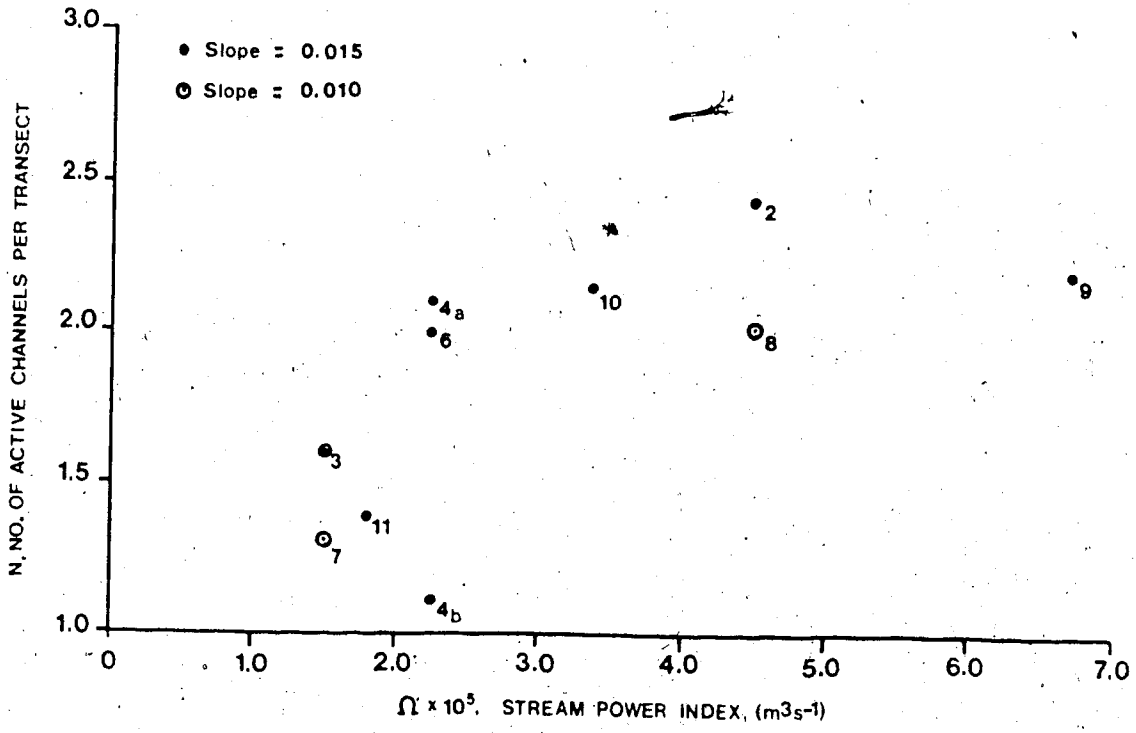

Figure 7-1 Mean number of active channels per flume transect (N) versus stream power index (Ω').

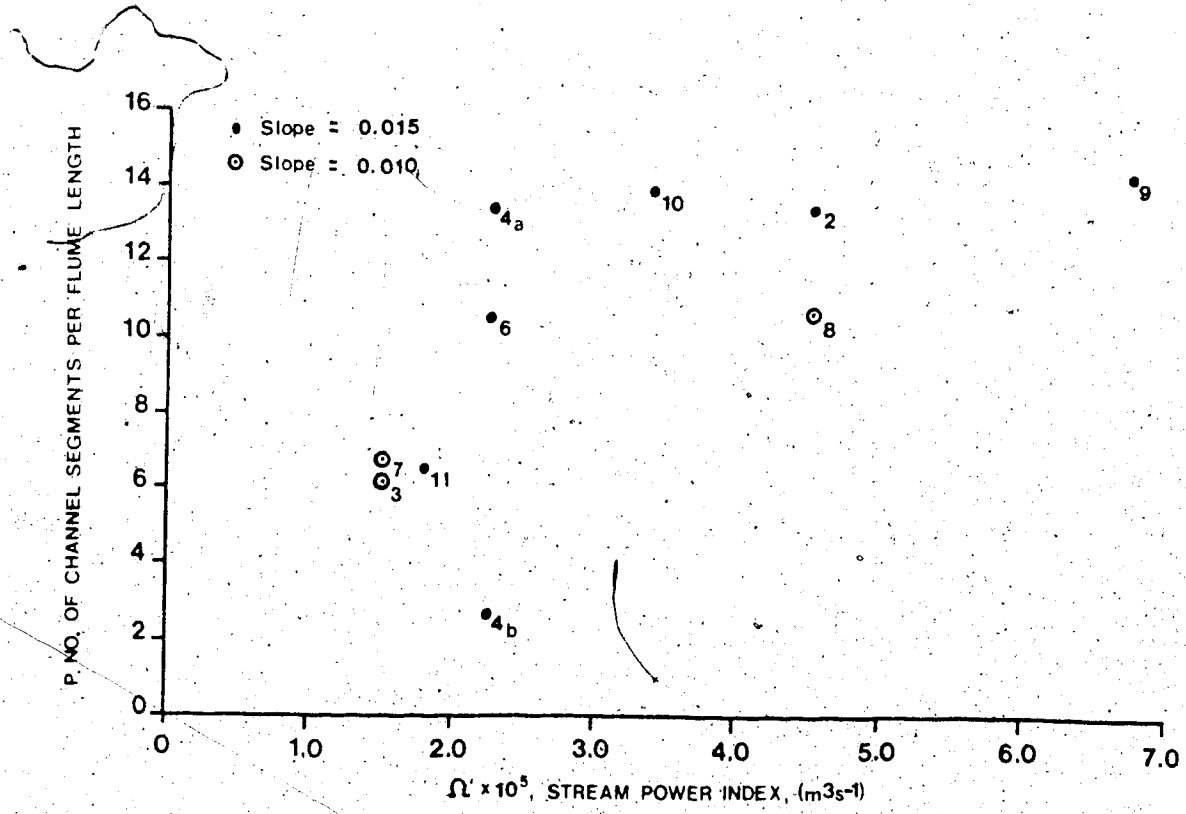

Figure 7-2 Mean number of active channel segments per flume length (P) versus stream power index (Ω').

$$z = \tau / \left(\frac{2(2N+5)}{9N(N-1)} \right)^{0.5}$$

The τ values for P versus Ω' and N versus Ω' are shown in Table 7-2 along with the results of subsequent tests. It is apparent that both positive correlations are significant.

The separate influence of slope and discharge can also be discerned from Figures 7-1 and 7-2. For example, runs 8 and 9 have the same discharge but different slopes (0.01 and 0.015 respectively) and it is apparent that the higher slope of run 9 produces a higher degree of braiding than in run 8. The same effect can be seen when runs 3 and 6 (both with a discharge of 0.0015 m^3s^{-1}) are compared with one another. Similarly, the effect of increasing discharge at a given slope can be easily discerned by comparing runs 11, 6, 10, 2 and 9 with one another. These runs represent a sequence of increasing discharge at a constant slope (run 11 is the lowest and run 9 the highest) and there is a corresponding increase in braiding intensity through this sequence of runs. However, this sequence is reversed in the case of runs 2 and 9 where the average number of channels per transect (N) is higher in run 2 than in run 9. The correlation coefficients for Q versus P and N show both relationships to be significant (Table 7-2).

The influence of the head arrangement (see Table 7-1) on the braiding intensity is not consistent. Runs 3 and 7 show very similar values for the mean number of active channel segments (P) but run 3 has a higher mean number of active channels per transect (N). In the case of runs 4 and 6 the two-nozzle arrangement (run 4) produced a lower degree of braiding for both indexes. It is

Table 7-2

Correlation coefficients (Kendall's τ) for braided stream morphology and flow characteristics

Independent variable	Dependent variable	τ	z
Ω'	P	0.65	2.80
Ω'	N	0.65	2.80
Ω'	I	0.46	1.99
Ω'	M	0.49	2.11
P	M	0.55	2.37
N	M	0.77	3.32
I	M	0.09	0.39
d	M	-0.11	0.47
τ^*/τ_c^*	M	0.35	1.43
Q	P	0.80	6.35
Q	N	0.93	7.41

τ is significant (at $\alpha = 0.05$) when z exceeds 1.645.

Correlation coefficients for the independent variable Q are calculated for runs 2,4,6,9,10 and 11 only.

P = Mean number of active channels per transect.
N = Mean number of active channels per flume length.
I = Bed relief index.
M = Mean number of avalanche-face bars per flume length.

noticeable that incision of the channel during run 4 produced a markedly lower degree of braiding in the second half of the run (4b) than in the first thirty hours (4a).

Statistical evaluation of the influence on braiding intensity of the channel slope and of the head arrangement requires testing of the difference in mean values for pairs of runs. This was accomplished using a normal distribution test (sometimes referred to as a z test). (The frequently used t-test is a version of the z test modified for sample sizes less than 30). In cases where the data characteristics violated the conditions for application of the z test (excessively large variance ratios were common) the non-parametric χ^2 test for two independent samples was used instead (Hammond and Mc Cullagh, 1974, 151-153). In this test, χ^2 is calculated by arranging the data in a matrix with two columns (one for each run) and a row for each frequency class. From this matrix:

$$\chi^2 = \sum^{r} \sum^{k} [(O - E)^2/(E)] \qquad 7-3$$

where $\sum^r \sum^k$ is the sum over all rows (r) and columns (k), O is the observed frequency for a given element of the matrix, and E is the expected frequency for the same element. E is calculated as the product of the sum of all values in the same row and the sum of all values in the same column as the observed frequency, divided by the sample size.

The results of the statistical analysis of the trends in the two braiding indexes with changing slope, discharge and head conditions are presented in Table 7-3. In general these tests confirm statistically the trends identified in the preceding analysis. Thus, braiding intensity is seen to increase with slope and to

Table 7-3

Statistical summary of tests of the effect of changing slope, discharge and head conditions on braiding intensity.

A. Effect of changing slope at a given discharge.

			No. of active channels per transect, N.		No. of active segments per flume length, P.	
			z	χ^2	z	χ^2
Run	9	versus run 8	-	N.S.	-	15.9
	6	7	4.32	28.4	4.32	13.9
	4	3	-	8.4	-	24.4

B Effect of changing discharge at a given slope.

			N		P	
			z	χ^2	z	χ^2
Run	8	versus run 7	6.29	31.60	4.19	14.63
	6	11	4.81	23.52	4.45	18.26
	10	6	N.S.	N.S.	3.27	17.67
	2	10	1.95	N.S.	N.S.	N.S.
	2	9	N.S.	N.S.	-	-
	9	2	-	-	-	N.S.

C. Effect of different head conditions for a given slope and discharge.

			N		P	
			z	χ^2	z	χ^2
Run	3	versus run 7	3,07	-	-	-
	7	3	-	-	N.S.	N.S.
	6	4	3.08	-	-	29.93

Note: 1) The run with the higher value of N or P is the first in each pair.

2) N.S. denotes a non-significant result; '-' no test carried out; and a number underlined, a significant result with the value of z or χ^2 given.

be lower with two sediment input nozzles than four. The flattening of the trend in braiding intensity at high stream power is shown by the statistically insignificant differences in both N and P between runs 10, 2 and 9. The results from P and N differ slightly in detail (for example, the difference between runs 8 and 9) but in general are much alike.

7-3-2 Bed Relief Index

Figure 7-3 illustrates that the bed relief index (I) tends to increase with increasing stream power but that there is considerable scatter in this trend. This is reflected in the comparatively low correlation coefficient (r) between these two variables (Table 7-2). In particular, there is a tendency for bed relief (I) to be higher at a given discharge in the lower slope runs (3, 7 and 8) than their higher slope counterparts (runs 4a, 6 and 9 respectively) although the difference between runs 8 and 9 is very small. The effect of increasing discharge on I, at a given slope, can be seen in the five runs at a slope of 0.015 (runs 11, 6, 10, 1 and 9). These runs show a steady increase in I with increasing discharge. The influence of the sediment input arrangement is not consistent. Runs 1 and 2, and 4 and 6 show that I is greater for the runs with two sediment input nozzles, while runs 3 and 7 show the reverse. It is also apparent that the incised channel of run 4b has a much higher I value than run 4a and thus there is an inverse correlation between I and braiding intensity (N and P) at a given slope and discharge in this case. Generally speaking, however, bed relief increases with increasing discharge at a given slope and decreases slightly with increasing slope at a given discharge and is, therefore, usually positively correlated with N and P.

As with the braiding indexes, a series of statistical tests (t and χ^2) was

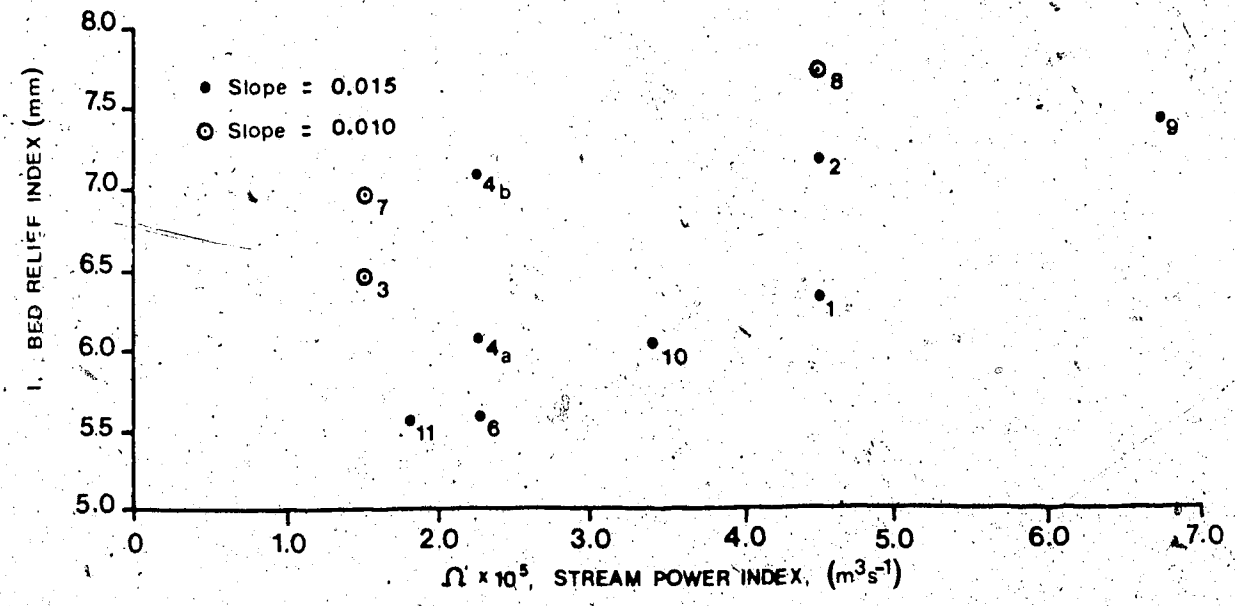

Figure 7-3 Mean bed relief index (I) versus stream power index (Ω').

carried out to confirm these generalisations. The results appear in Table 7-4. Some of the suggested trends are confirmed by these tests, notably the influence of the head arrangement on bed relief and the influence of discharge at a constant slope. However, the influence of changing slope at a given discharge yields only one statistically significant result (run 7 versus run 6) making this trend less certain than the others.

7-3-3 Frequency of Occurrence of Unit Bars with Avalanche Faces

The introduction to this chapter suggested that the abundance of avalanche-face bars may be a function of the relative depth of the flow in the channels and also the availability of unusually deep areas of the stream into which avalanche faces can prograde. On this basis one would expect a strong relationship between the abundance of avalanche-face bars and each of mean flow depth, bed relief index and braiding intensity. Braiding intensity would exert an influence by controlling the number of flow expansions and channel confluences in which competence declines rapidly downstream and depth is great enough for slip-face development. Figures 7-4 to 7-8 graph the relationship between M, the mean number of avalanche-face bars per flume length and stream power index (Ω'), bed relief index (I), braiding intensity (P and N) and mean depth (d).

In the absence of controlled experiments in which the independent variables are changed one at a time, it is difficult to attribute causality because of interrelationships between the variables. Figure 7-4 shows that increasing stream power produces an increase in M but there are some anomalies. In particular, runs 4a and 4b have identical values of Ω' but widely differing values of M. One possible explanation for this lies in the greater braiding intensity in run 4a (see below).

Table 7-4

Statistical summary of tests of the effect of changing slope, discharge and head conditions on the bed relief index (I).

A. The effect of changing slope at a given discharge.

				z
Run	8	versus	run 9	N.S.
	7		6	6.22
	4		3	N.S.

B. The effect of changing discharge at a given slope.

				z	χ^2
Run	8	versus	run 7	-	12.55
	6		11	N.S.	-
	10		6	1.95	-
	2		10	4.19	-
	1		10	N.S.	-
	2		1	3.34	-
	9		2	N.S.	-
	9		1	4.52	-

C. The effect of differing head conditions at a given slope and discharge.

				z
Run	7	versus	run 3	2.16
	4		6	4.13
	2		1	3.34

Note: 1) The run with the higher value of I is the first in each pair.
2) N.S. denotes a non-significant result '-' that no test was carried out; and a number underlined, a significant result with the value of z or χ^2 given.

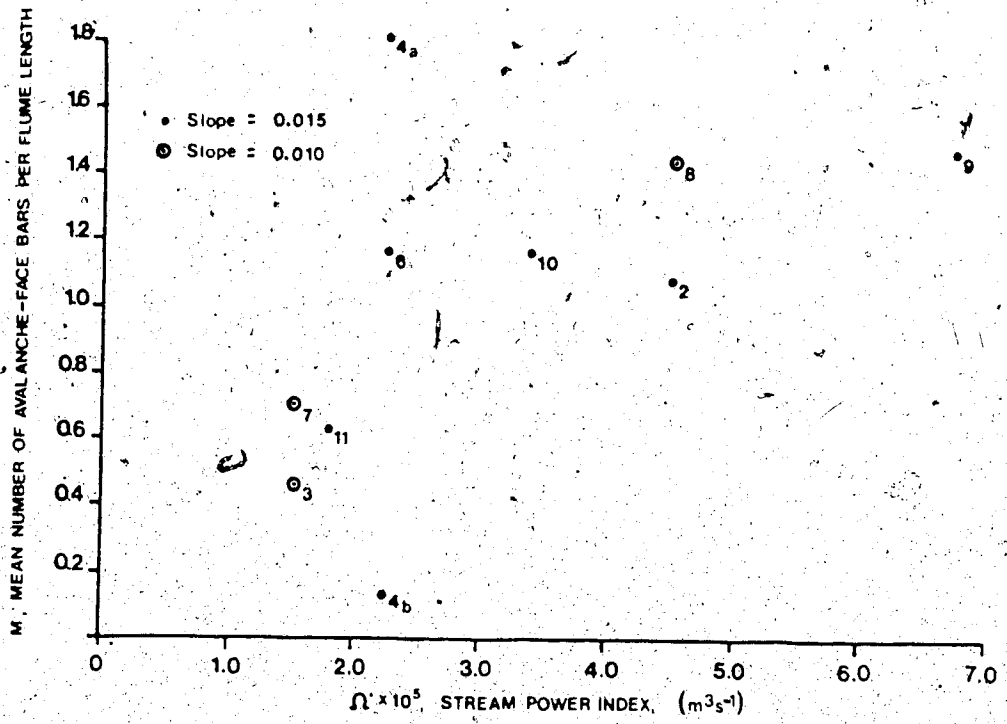

Figure 7-4 Mean number of avalanche-face bars per flume length (M) versus stream power index (Ω').

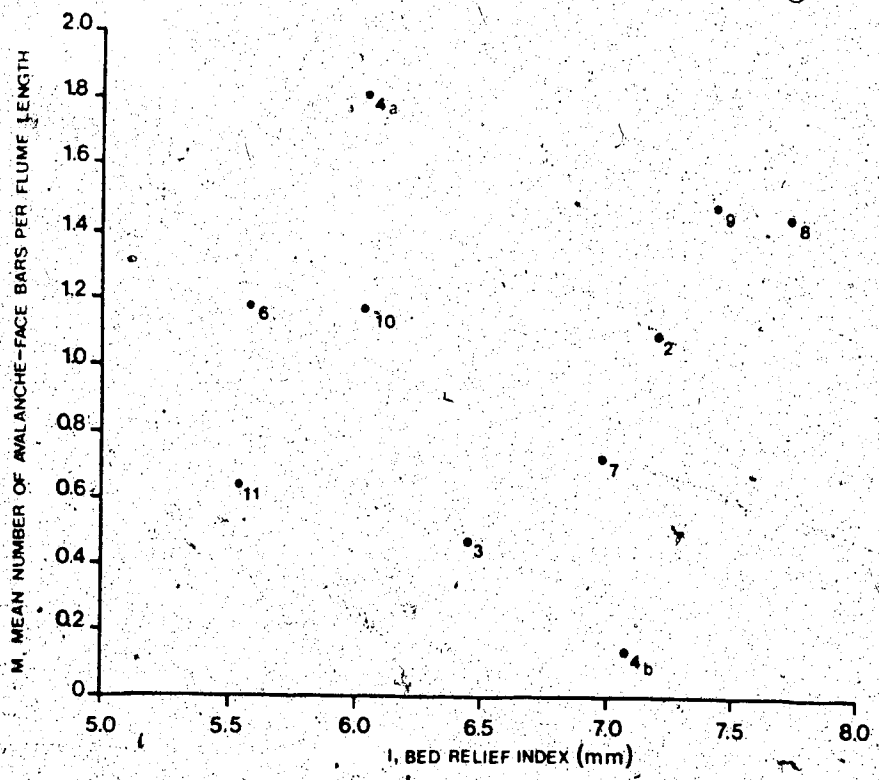

Figure 7-5 Mean number of avalanche-face bars per flume length (M) versus mean bed relief (I).

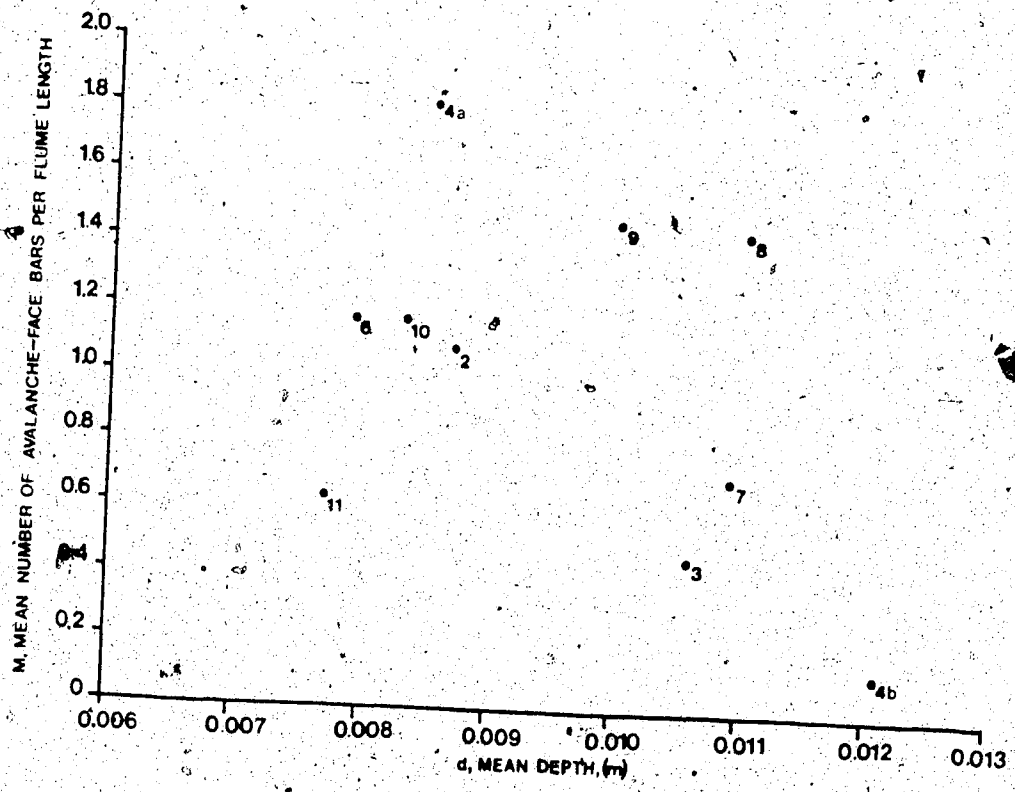

Figure 7-6 Mean number of avalanche-face bars per flume length (M) versus mean depth (d).

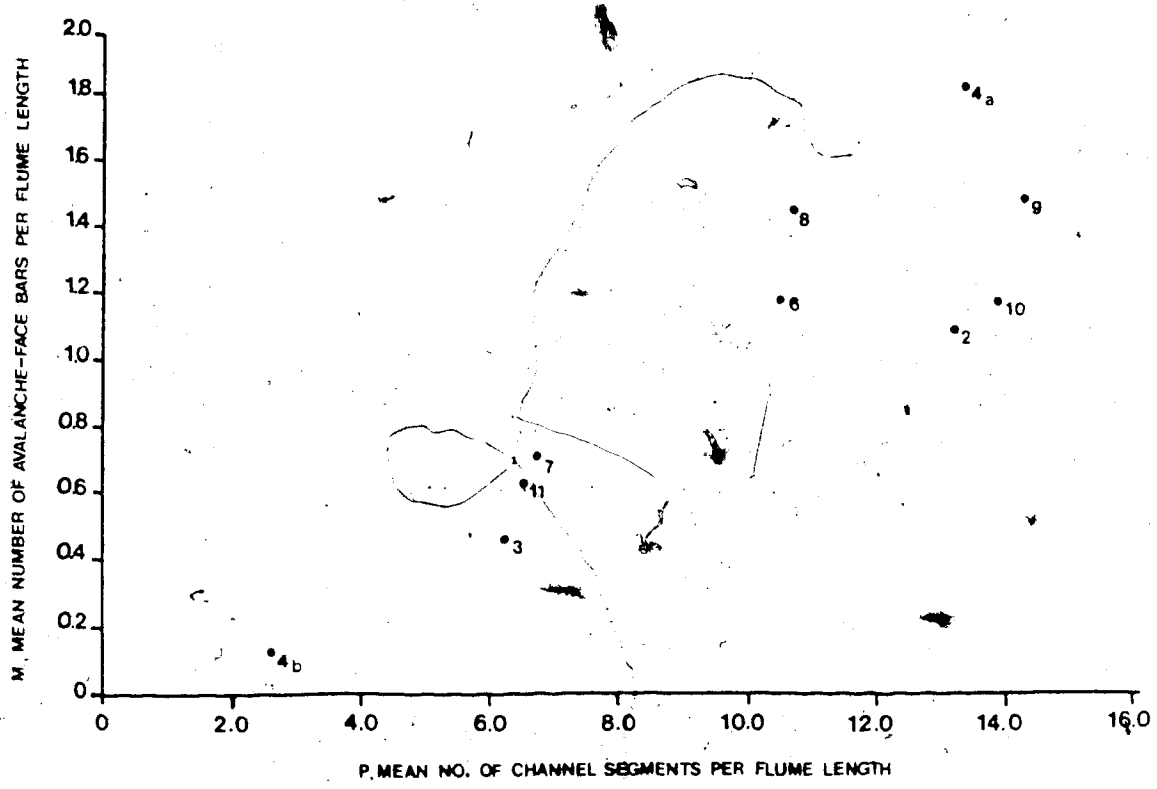

Figure 7-7 Mean number of avalanche-face bars per flume length (M) versus mean number of active channel segments per flume length (P).

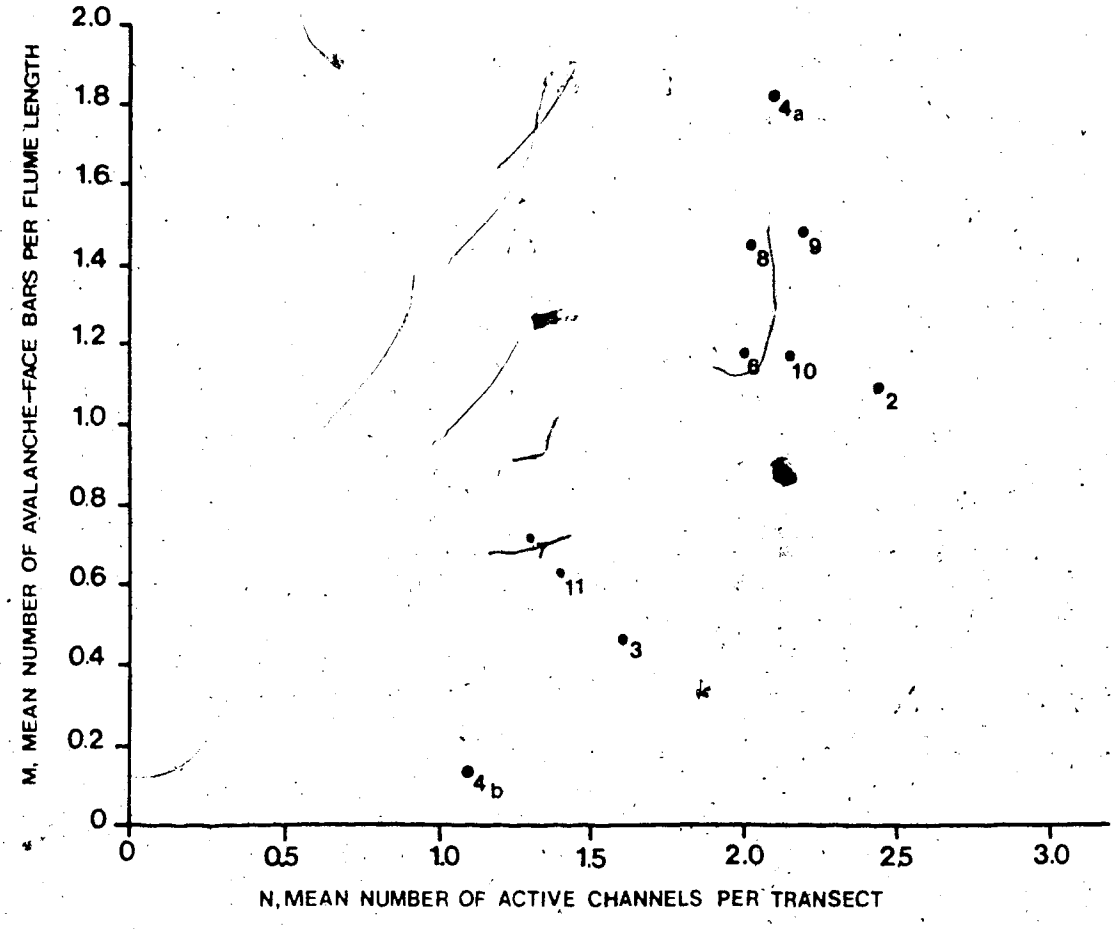

Figure 7-8 Mean number of avalanche-face bars per flume length (M) versus mean number of active channels per flume transect

The influence of bed relief index (I) (Figure 7-5) and mean depth (d) (Figure 7-6) on the abundance of avalanche-face bars is very poorly defined. No trends are present in either diagram and Table 7-2 shows that no statistical correlation exists in either case. If either of these variables have an influence on M it is being overridden by other variables, such as braiding intensity.

The influence of braiding intensity is seen in Figures 7-7 and 7-8. Here the frequency of occurrence of avalanche-face bars (M) is plotted against the mean number of active channels per flume length (P) and the mean number of active channels per transect (N). Of the variables considered so far, these two, P and N, produce the most consistent relationship with M and Table 7-2 shows the correlation coefficients to be significant. The two graphs showing a positive correlation between M and braiding intensity, are the only two so far discussed in which runs 4a and 4b fit the trend of the remaining runs.

Figure 7-9 illustrates the relationship between M and the excess Shields stress which the discussion in Chapter 2 indicated could influence bar height. Again there is some scatter in the relationship caused especially by run 4b but the general positive trend goes some way to confirming the suggestion made in Chapter 2.

The poor correlation of depth and bed relief with M may be the result of the fact that most of the runs with high bed relief and depth (for example 3, 7 and 4b) have low braiding intensity and that braiding intensity is the dominant control on the abundance of avalanche faces. Clearly, of the variables considered, P, N and Ω' have the most consistent effect on M. However, since P, N and Ω' are also correlated with each other as well as with M it is important to separate the

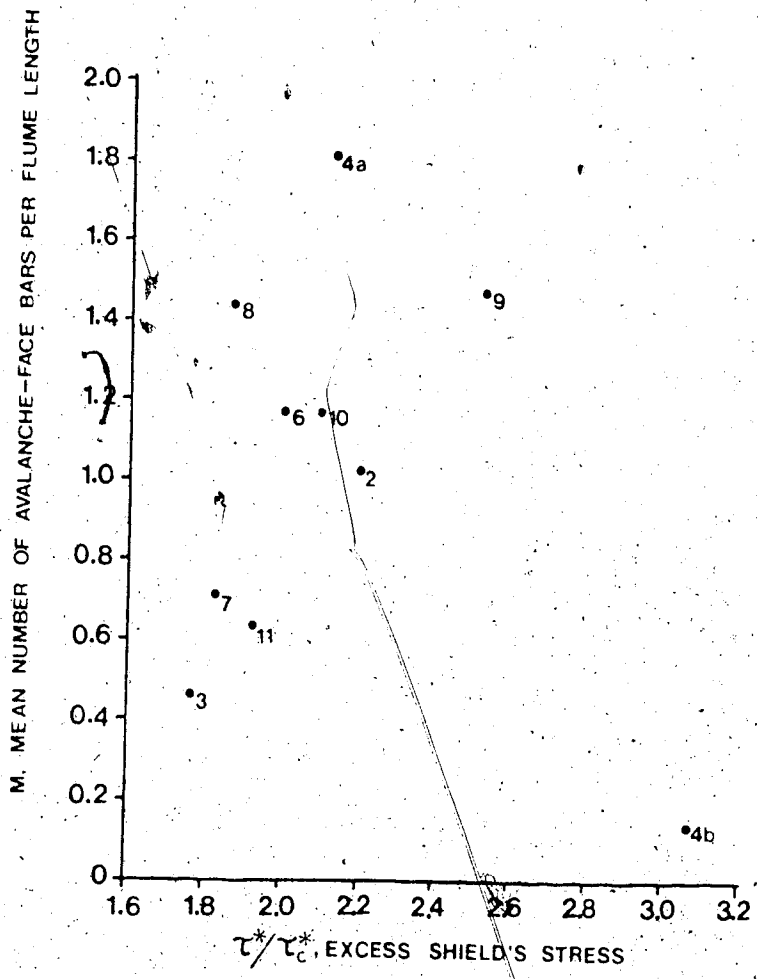

Figure 7-9 Mean number of avalanche-face bars per flume length (M) versus excess Shields stress (τ^*/τ^*_c).

effect of each variable on M. This can be accomplished using partial correlation, a simple version of which is available for use with Kendall's τ.

Kendall's partial correlation coefficient for the correlation between two variables x and y holding a third variable, z, constant is calculated as follows (Hammond and McCullagh, 1974, p.206-208) :

$$\tau_{xy,z} = \frac{\tau_{xy} - (\tau_{xz} \cdot \tau_{yz})}{[(1-\tau_{xz})^2(1-\tau_{yz})^2]^{0.5}} \qquad 7-1$$

Applying this to the channel data (Table 7-5) showed that while controlling the influence of Ω' reduced the correlation coefficient between M and P, and M and N, controlling the influence of P and N reduced the correlation between Ω' and M considerably. In other words, while there is a relationship between Ω' and M, there is a far stronger one between braiding intensity (P and N) and M. It is the correlation between P, N and Ω' which is responsible for the apparent correlation between Ω' and M. The reason for this will become clear later in this chapter.

A very similar result occurs when partial correlation analysis of the relationships between braiding intensity, excess Shields stress and abundance of avalanche-face bars is performed. None of these correlations is particularly strong (Table 7-6) but when the influence of Shields stress is controlled the correlation between M and both P and N increases. Conversely, holding P and N constant results in a decrease in the correlation coefficient between M and the excess Shields stress. Thus, as with Ω', it is P and N which directly influence M, the influence of excess Shields stress operates through its correlation with P and N.

The influence of the head conditions is evident in the frequency of occurrence of avalanche-face bars, as with other aspects of channel morphology.

Table 7-5

Partial correlation coefficients for analysing the influence of stream power index (Ω') and braiding intensity (N and P) on the abundance of avalanche-face bars (M).

1. M, N and Ω' (x = M, y = N, z = Ω')

τ_{xz} = 0.49 (z = 2.11)
τ_{yz} = 0.65 (z = 2.80)
τ_{xy} = 0.77 (z = 3.32)
$\tau_{xy,z}$ = 0.68 (z = 2.93)
$\tau_{xz,y}$ = -0.02 (z = 0.09)

2. M, P and Ω' (x = M, y = P, z = Ω')

τ_{xz} = 0.49 (z = 2.11)
τ_{yz} = 0.65 (z = 2.80)
τ_{xy} = 0.55 (z = 2.37)
$\tau_{xy,z}$ = 0.35 (z = 1.51)
$\tau_{xz,y}$ = 0.21 (z = 0.90)

τ is significant at 95% level when z exceeds 1.645.

Table 7-6

Partial correlation coefficients for the analysis of the influence of excess Shields stress (τ^*/τ_c^*) and braiding intensity (N and P) on the abundance of avalanche-face bars (M).

1. M, N and τ^*/τ_c^* (x = M, y = N, z = τ^*/τ_c^*)

r_{xz}	=	0.35 (z = 1.41)
r_{yz}	=	0.40 (z = 1.61)
r_{xy}	=	0.77 (z = 3.10)
$r_{xy,z}$	=	0.73 (z = 2.94)
$r_{xz,y}$	=	0.07 (z = 0.28)

2. M, P and τ^*/τ_c^* (x = M, y = P, z = τ^*/τ_c^*)

r_{xz}	=	0.35 (z = 1.41)
r_{yz}	=	0.35 (z = 1.41)
r_{xy}	=	0.55 (z = 2.22)
$r_{xy,z}$	=	0.49 (z = 1.98)
$r_{xz,y}$	=	0.20 (z = 0.81)

r is significant at the 95% level when z exceeds 1.645.

In this case the two-nozzle head arrangement tends to produce fewer avalanche-face bars than the four-nozzle arrangement. The difference is apparently due to decreasing braiding intensity rather than increasing bed relief since the two-nozzle runs (3 and 4) have higher bed relief lower braiding intensity, and fewer avalanche-face bars than their counterparts with four sediment input nozzles (runs 7 and 6 respectively). However, only the difference between runs 4 and 6 gave a statistically significant χ^2 value (10.33 with two degrees of freedom).

In general, therefore, the number of avalanche-face bars correlates positively with stream power and braiding intensity but not with bed relief index or mean depth. The most consistent relationship seems to be with braiding intensity, suggesting that the spatial changes in channel form associated with channel confluences are most important in determining the abundance of avalanche-face bars.

7-3-4 Channel Geometry

The mean channel width and depth for each run (see p.91) provide data that essentially constitute a downstream hydraulic geometry for braided streams. Such data exist for the geometry of individual channels in braided streams but to the author's knowledge no previous data exist for the geometry of the entire stream.

The trends in mean depth, d, and width B, with increasing discharge, slope and stream power index are graphed in Figures 7-10 and 7-11. The scatter in Figure 7-10 is quite marked but if runs 3, 4b, 7 and 8 are removed (4b has already been shown to be anomalous in several respects and the remaining runs all have slopes of 0.010) there is a consistent trend of increasing mean depth with

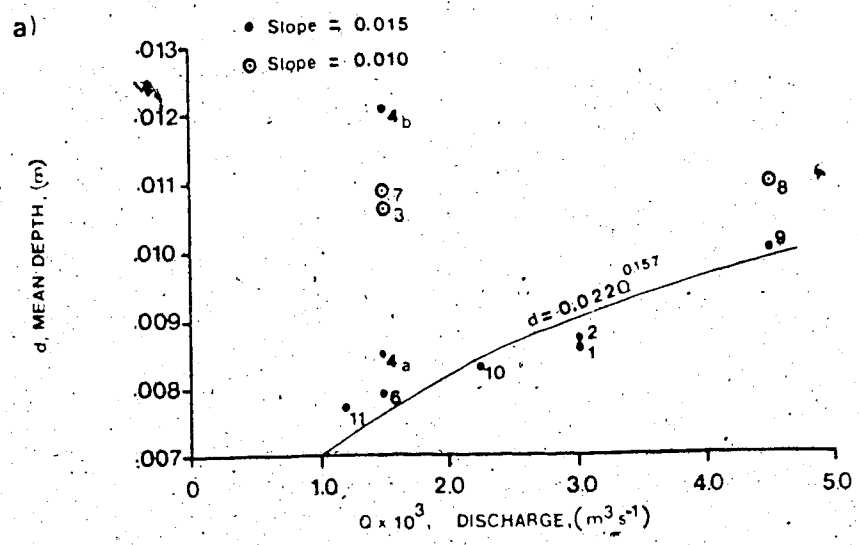

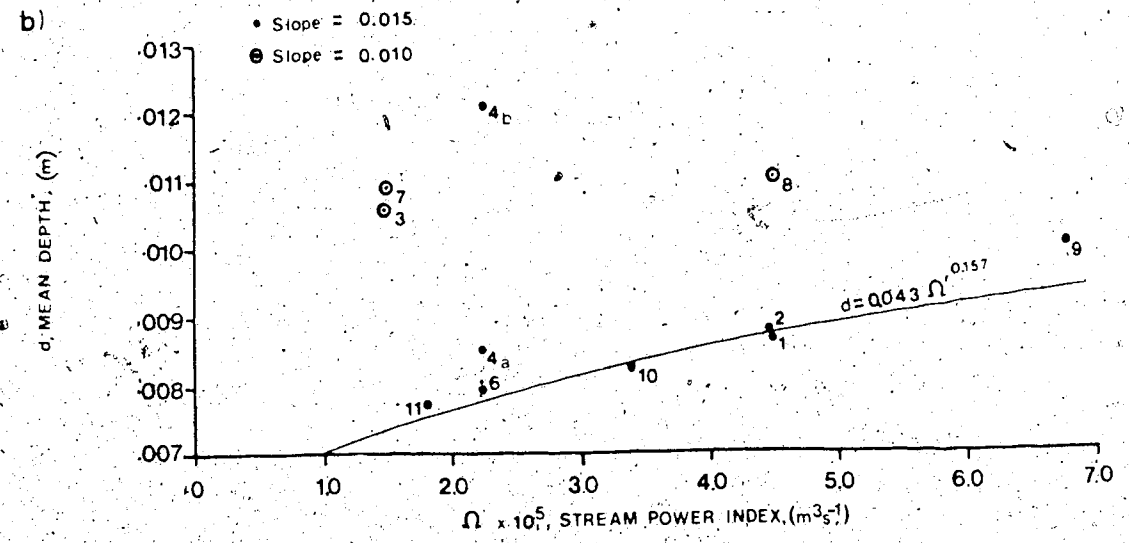

Figure 7-10 Mean depth (d) versus (a) total discharge, and (b) stream power index.

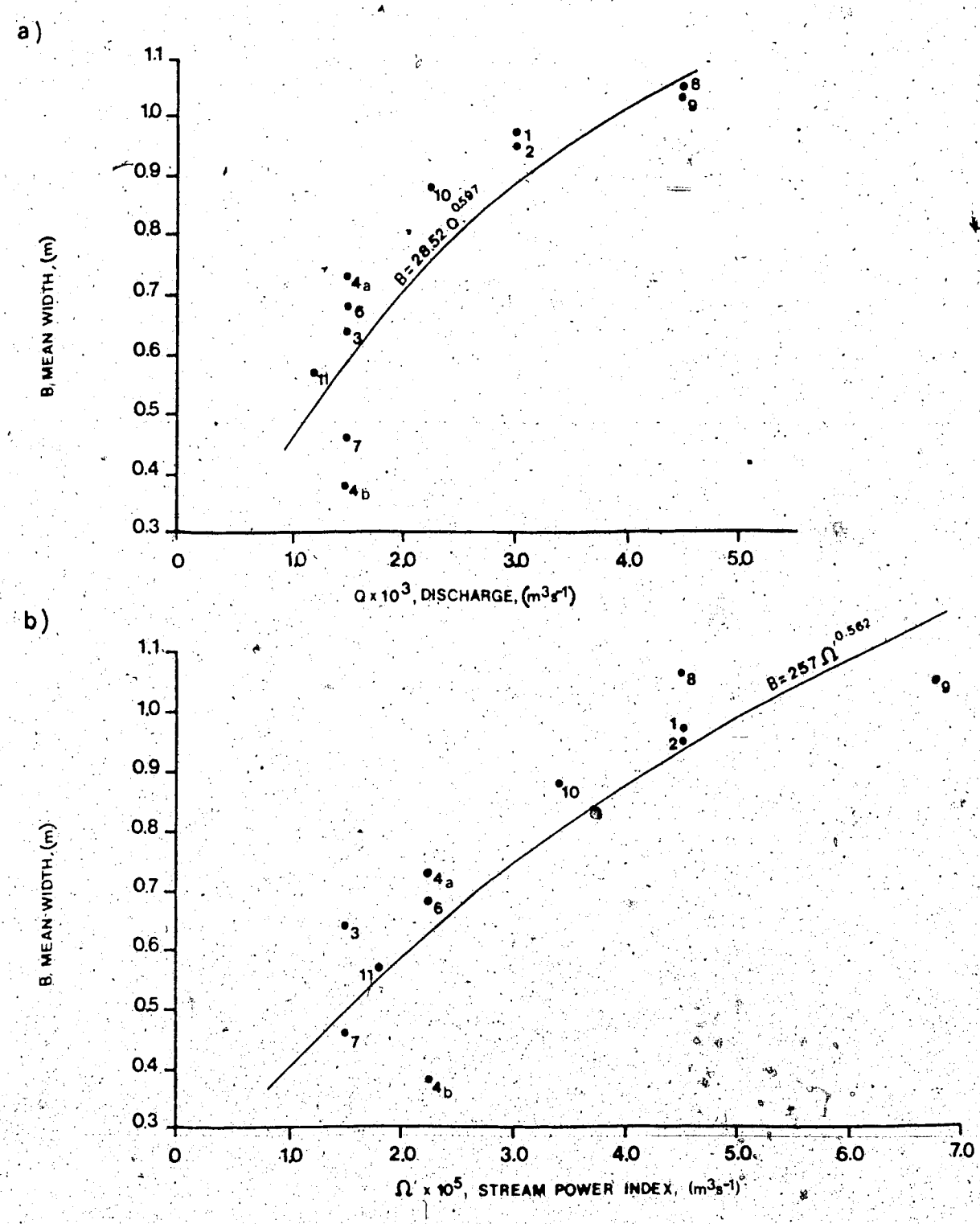

Figure 7-11 Mean width (B) versus (a) total discharge, and (b) stream power index.

increasing power index and discharge. Best-fit regression lines fitted to runs 1, 2, 4a, 6, 9, 10 and 11 have the following form :

$$d = 0.022\, Q^{0.157} \qquad 7-5$$

and

$$d = 0.043\, \Omega^{0.157} \qquad 7-6$$

The anomalous runs (3, 4, 4b, 7 and 8) all plot well above these regression lines and all, apart from run 8, are characterised by low degrees of braiding. Their anomalous behaviour may relate to their position at the transition from single channel to braiding (as indicated by their low braiding intensity). Interestingly no such anomalies appear in the width relationship (Figure 7-10). Thus, the morphological characteristic common to these anomalous channels is an unusually low width/depth ratio. The regression lines fitted to the relationship between width and discharge, and width and stream power index are :

$$B = 28.52\, Q^{0.597} \qquad 7-7$$

and

$$B = 257\Omega^{0.562} \qquad 7-8$$

All the regression lines are plotted on their respective graphs in Figures 7-10 and 7-11.

7-4 Temporal Variations in Channel Morphology

Differences in the average intensity of braiding, bed relief, and abundance of avalanche-face bars between runs have been shown to be related to differences in the discharge and slope of the stream. In addition there are inter-relationships

between these morphological variables related to their mutual variation with discharge and slope. For example, there is a strong correlation between braiding intensity and the abundance of avalanche-face bars, which may be a result of the greater availability of sudden flow expansions such as channel junctions which serve as sites for bar deposition. Variations in these morphological variables occur throughout each run independent of discharge and slope (which are presumed constant, although local slope may fluctuate around a mean value) and it is possible that these variations are the result of local aggradation and degradation caused partly by fluctuations in the sediment input rate to the head of the flume. It was demonstrated in Chapter 5 that sediment input to the flume fluctuated throughout each run, often in a regular manner. The possibility arises, therefore, that the fluctuations in channel properties are a direct result of fluctuations in the sediment transport rate causing local aggradation and degradation, and that the variations in channel pattern coincide with those in the sediment transport rate.

Unfortunately, the braiding intensity, bar forms and sediment transport rate are not necessarily related in a simple fashion. Firstly, variation in the sediment transport rate is not the only cause of variations in braiding and bar form. The occurrence of channel avulsion and migration may result in local changes in the braiding intensity and the availability of sites for bar deposition, independent of the sediment input to the flume. Secondly, a pulse of sediment delivered to the head of the flume may take several hours to migrate downstream. During this migration it may become attenuated and its effects felt less strongly the further downstream it migrates. Furthermore, while the stream is aggrading and braiding in one section of the flume in response to a sediment pulse, a section downstream

may be starved of sediment and undergoing incision. The available data are generalised for the whole flume so that the effect of differences in timing of the channel response between different sections of the flume may confuse the situation. Thirdly, the nature of the channel receiving the sediment pulse may be important. A channel that has been starved of sediment for several hours may show a much more obvious response to a given sediment pulse than a channel that has been aggrading for the previous few hours. Clearly, the fluctuations in channel morphology are unlikely to correspond with the arrival of a sediment pulse in a straightforward manner.

Two approaches were taken to the investigation of fluctuations through time in channel pattern and bar form. Firstly, a visual inspection of the time series for each variable, and of photographs of the channel taken at the time of sampling, was used to identify individual examples of channel response to sediment input. Secondly, a statistical analysis of these time series was carried out to attempt to show cross-correlations between the variables and to discern the amount of lag between the sediment input and the channel response. Run 10 is used as the primary example throughout the following account but very similar patterns can be identified in the other runs.

7-4-1 Observations of Channel Response to Sediment Input

Figure 7-12 shows the time series from run 10 for each of the three variables considered; sediment load (Q_b), braiding intensity (P), and the abundance of avalanche-face bars (M). The sediment load series is a simplified version of that analysed in Chapter 5. Each hourly observation in the time series is the mean of three samples taken on the hour and 15 minutes before and after. This

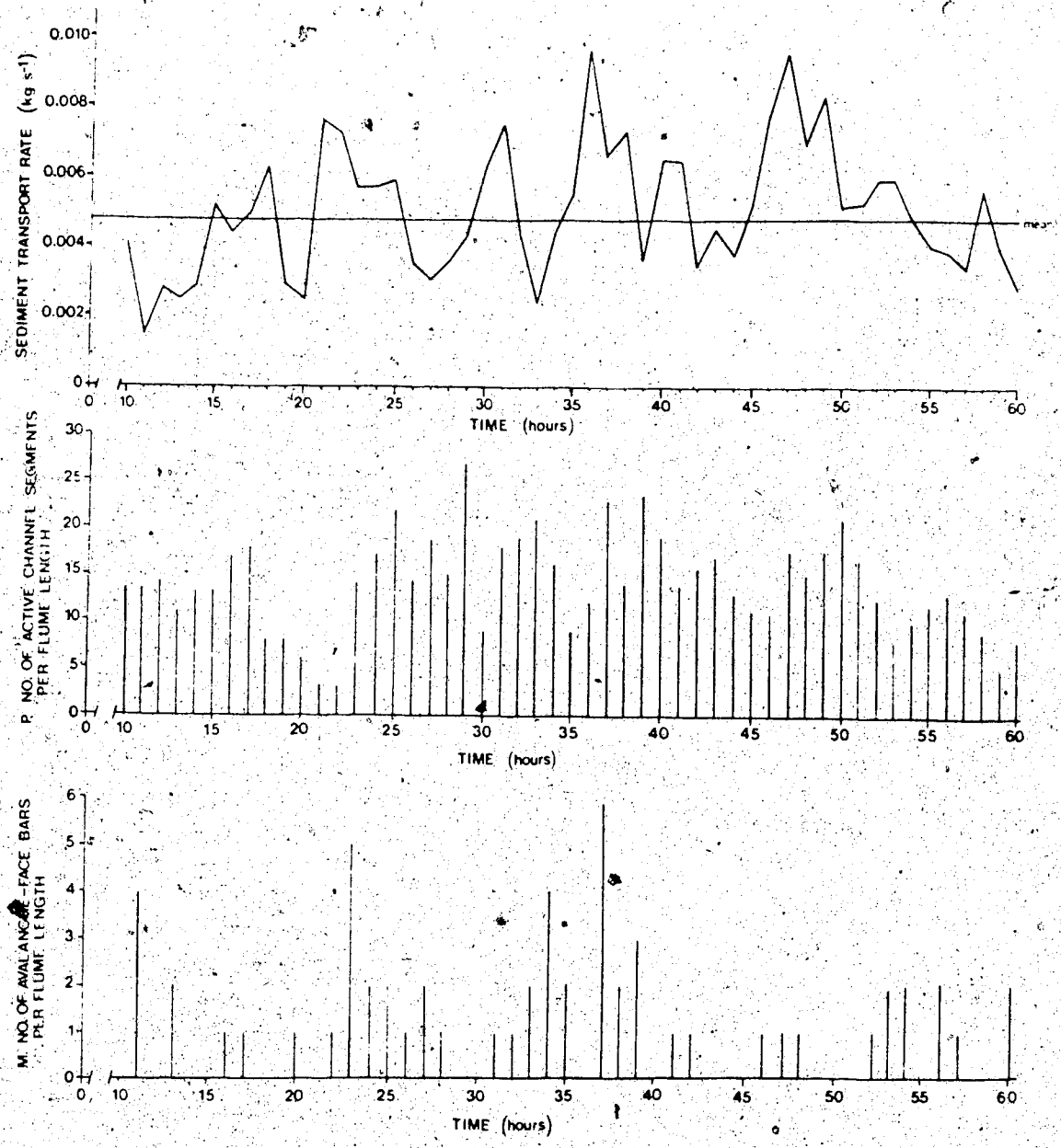

Figure 7-12 Time series of hourly samples of sediment load (hourly three-point average), braiding intensity and the number of avalanche-face bars, to illustrate their mutual variation over time. The data are from run 10.

simplification was carried out to reduce the sample size to 50 and allow statistical comparison of the sediment load data with P and M.

The other channel morphology variables (bed relief, width and depth and number of active channels per transect) were sampled only every five hours and are therefore impossible to analyse in this way. It is apparent from Figure 7-12 that, as expected, there is not a simple relationship between Q_b, and P and M. In some cases there are increases in P and M that are related to peaks in Q_b (for example, 21-25 hours) but in addition there are examples where changes in sediment load have little effect on channel form (for example, 47 - 48 hours) and also examples of changes in channel form unrelated to sediment load fluctuations (28 - 29 hours and 33 - 34 hours). Nor is the inter-relation between P and M direct; a change in P is not always accompanied by a change in M (for example, 28 - 29 hours). Some of these anomalies may be the result of an inappropriate sampling interval. Sediment pulses that influence channel form may occur between sampling periods and not appear in the sediment load time series but their effects may be visible in the P and M time series. Similarly, the avalanche-face bars resulting from large sediment pulses may be fairly short-lived and therefore not appear in the hourly samples. Bearing in mind these possible sources of error it is instructive to look at some of these examples in more detail.

Figure 7-13 shows vertical photographs of the channel taken hourly between 21 and 24 hours of the beginning of the run. Prior to the arrival of the sediment pulse that peaks at 21 hours (see Figure 7-12) the channel was incised into its deposit and the individual channels were devoid of large migratory unit bars. Shortly after the beginning of the increase in sediment transport rate the channels

Figure 7-13

The influence of a large pulse in the sediment transport rate at the head of the flume on the channel form downstream. The hourly vertical photographs were taken at 21,22,23 and 24 hours from the beginning of run 10. See text for explanation. Flow is from right to left.

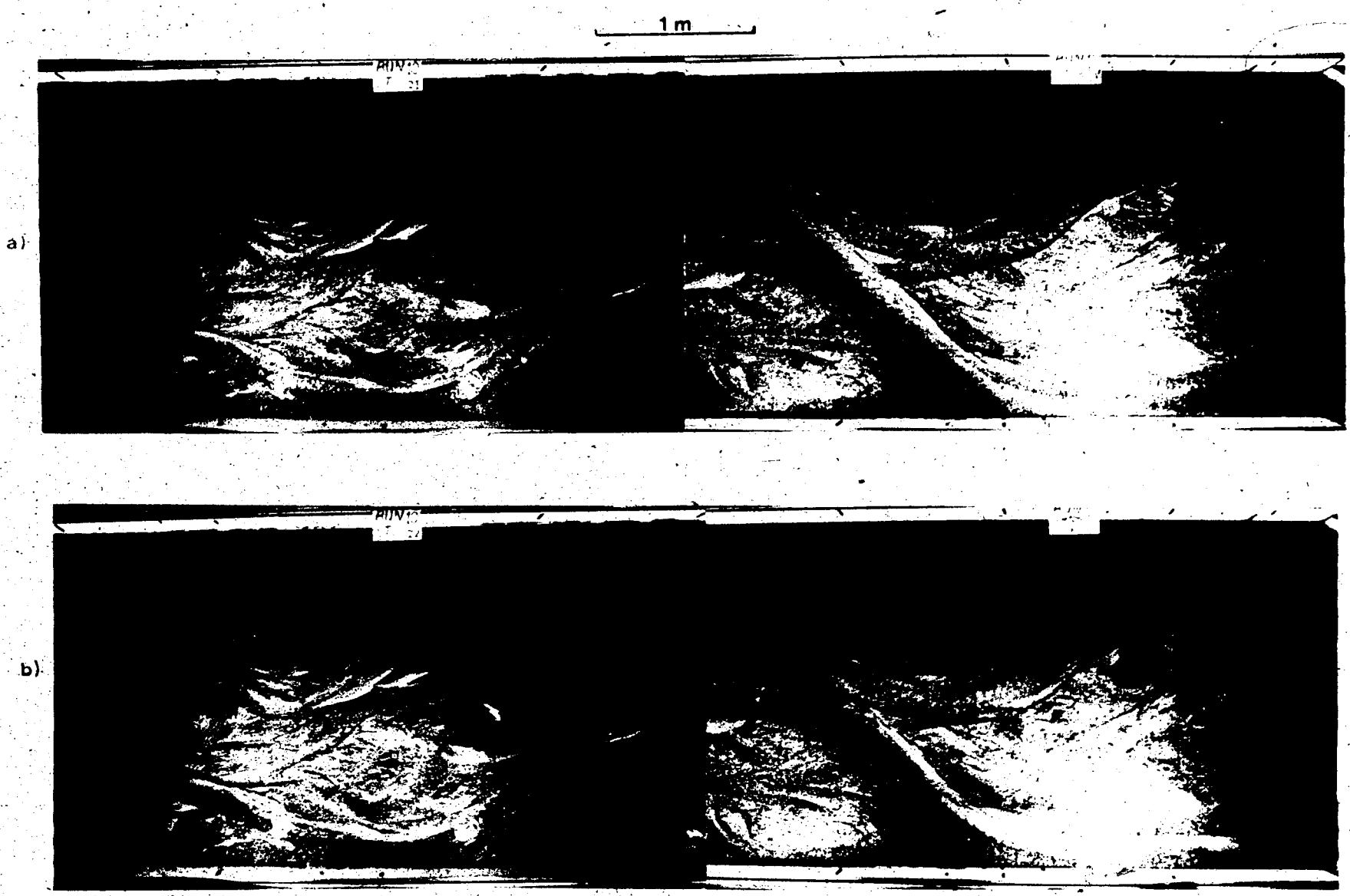
1 m
a)
b)

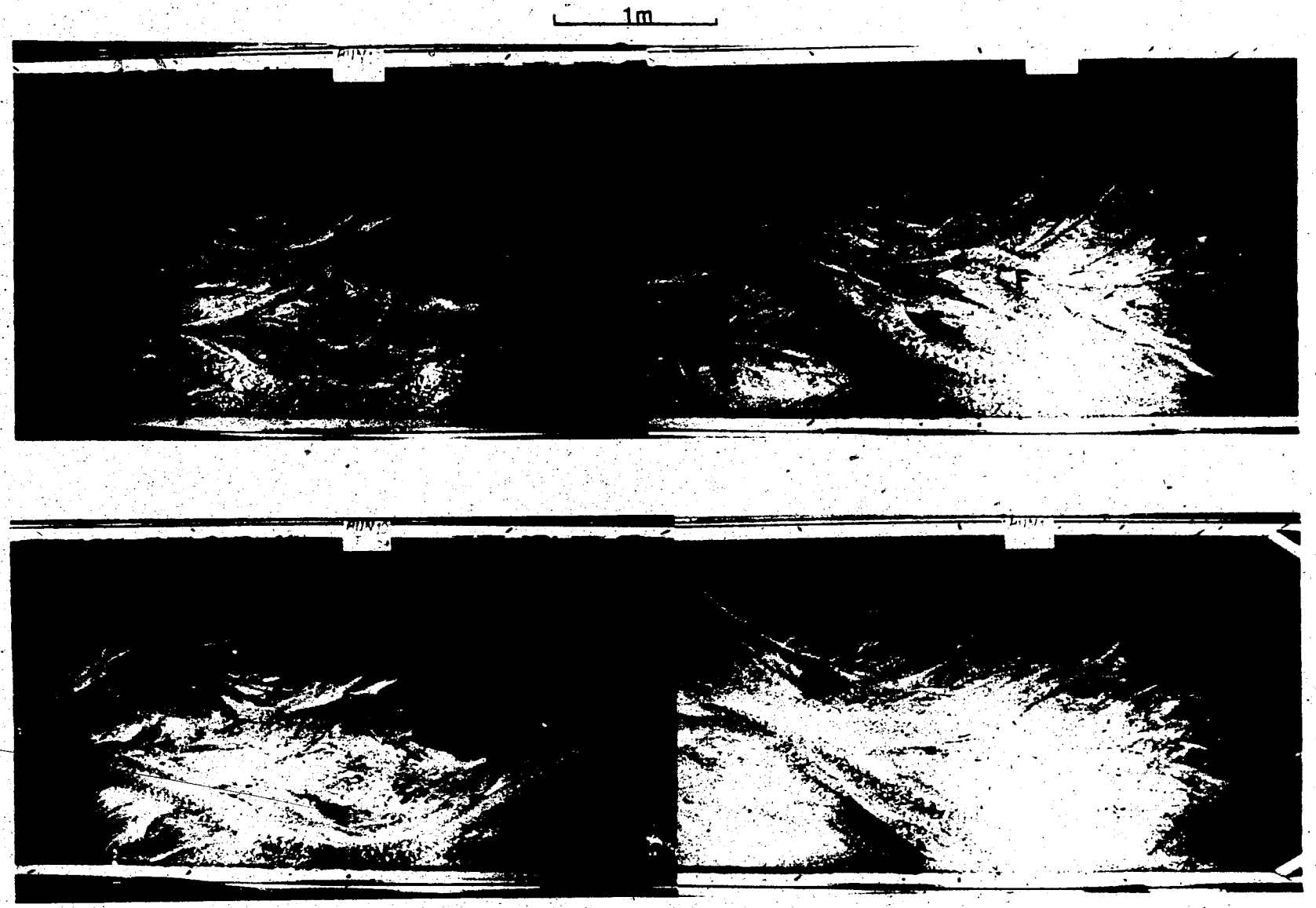
1m
c)
d)

at the upstream end of the flume became occupied by migratory lobes of sediment. These accumulations began to cause channel division, first close to the head of the flume (A, 22 hours) and later further downstream (B, 23 hours). The result was general aggradation in the first few meters of the flume and re-occupation of areas of the channel abandoned during earlier incision. This is most apparent about half-way down the flume where aggradation resulted in re-occupation of a large abandoned channel (C, 23 hours). By 24 hours the effect of the sediment pulse had penetrated to the downstream half of the flume where an initially entrenched single channel (D, 22 hours) was converted to a braided channel with a complex mid-channel bar (D, 24 hours). Avalanche-face bars formed most commonly where the sediment pulses migrated into deep and/or slack water. Thus, large bars were present in the large confluence about 2.5 meters from the head of the flume (E, 23 hours), in the large reoccupied channel (C), and at other minor confluences and channel bends (for example, F, 23 hours). This confirms the suggestion made earlier in this chapter that the availability of suitable sites is important in explaining the abundance of avalanche-face bars. Hence, there is a correlation between braiding intensity and the occurrence of avalanche-face bars. However, it also becomes apparent that in some cases the precursor of a flow division is often the deposition of a large avalanche-face bar (or a series of such bars) around which the flow divides (Ashmore, 1982). Such a bar is visible at 23 hours (D) and forms part of the complex bar which had developed at that location by 24 hours (D). Clearly then, P and M are closely related because each favours the presence of the other.

This sequence demonstrates the direct correspondence between sediment

pulses and channel pattern and form. In addition the inter-relationship between braiding and large avalanche-face bars is brought out, as is the migration of sediment pulses downstream causing channel response initially only at the head of the flume but, one or two hours later, several meters downstream. It is also noticeable from Figure 7-12 that the response of P, the braid index, is slower and longer lasting than that of M, which peaked suddenly at 23 hours and then returned to low values an hour later. The channels formed during aggradation remained active for two or three hours, while the avalanche-face bars were destroyed soon after aggradation ceased.

The correlation of Q_b, M and P described above is not always present. Figure 7-14 shows the channel changes related to the large sediment pulse which was delivered to the head of the flume at 47 hours. It was pointed out in the discussion of Figure 7-12 that this pulse was accompanied by some increase in braiding intensity but no large increase in the number of avalanche-face bars. Prior to the arrival of the sediment pulse (Figure 7-14, 46 hours) the channel was moderately braided ($\overline{P} = 11$) with most of the braiding occurring in the upstream half of the flume. The arrival of the sediment pulse was accompanied by some aggradation and the reoccupation of one abandoned channel (A, 47 hours). In addition one or two avalanche-face bars formed and are visible at 47 hours (B and C). Some further aggradation and division occurred near the head of the flume (48 hours) but throughout this time the entrenched channel downstream remained unaltered in form. It was not until four or five hours after the input of the sediment pulse that the downstream channel experienced some bar deposition and eventually channel migration and avulsion.

Figure 7-14. Subdued response to the input of a large pulse of sediment to the head of the flume. The hourly vertical photographs were taken at 46,47 and 48 hours from the beginning of run 10. See text for explanation. Flow is from right to left.

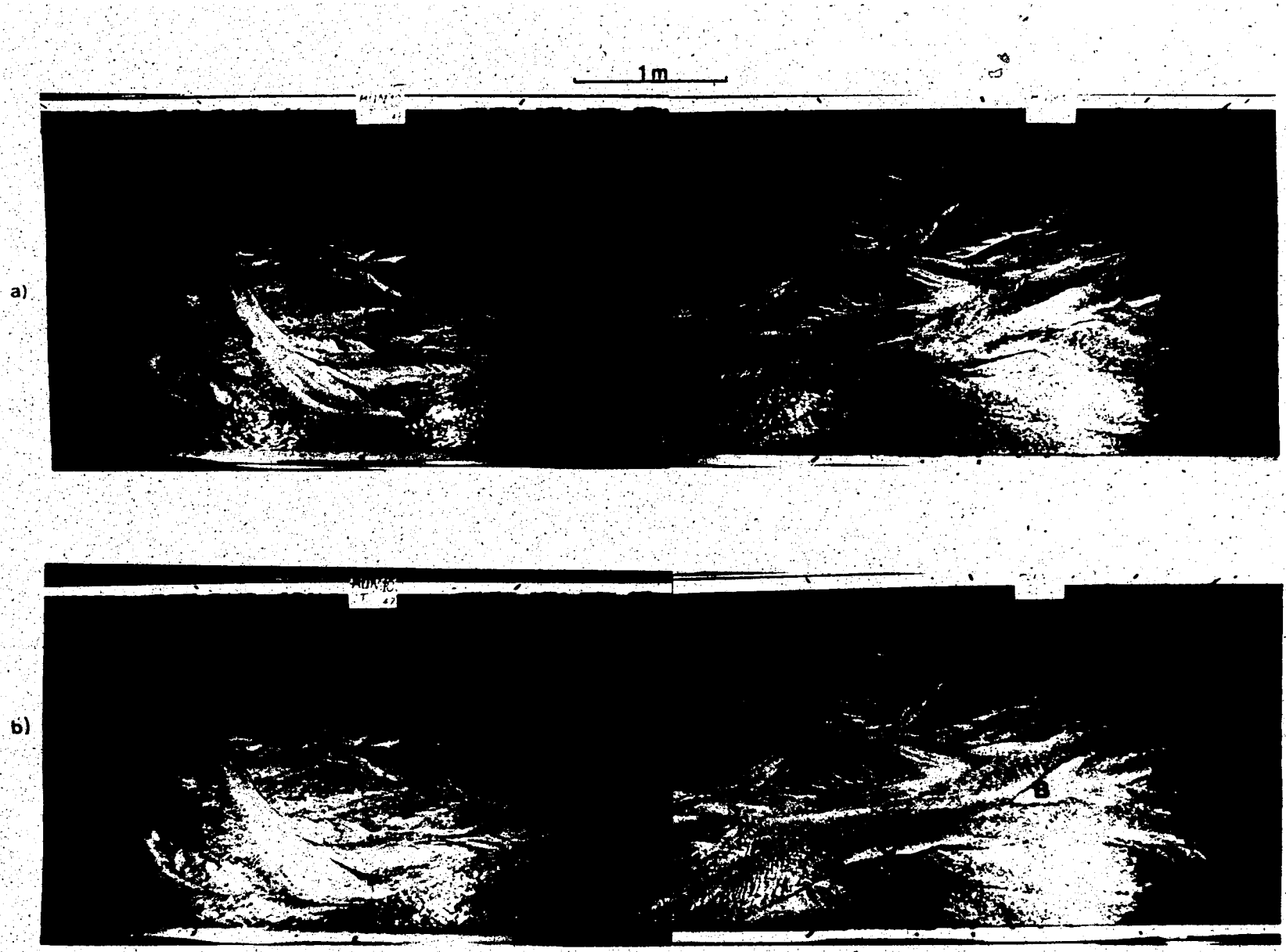
1m
a)
b)

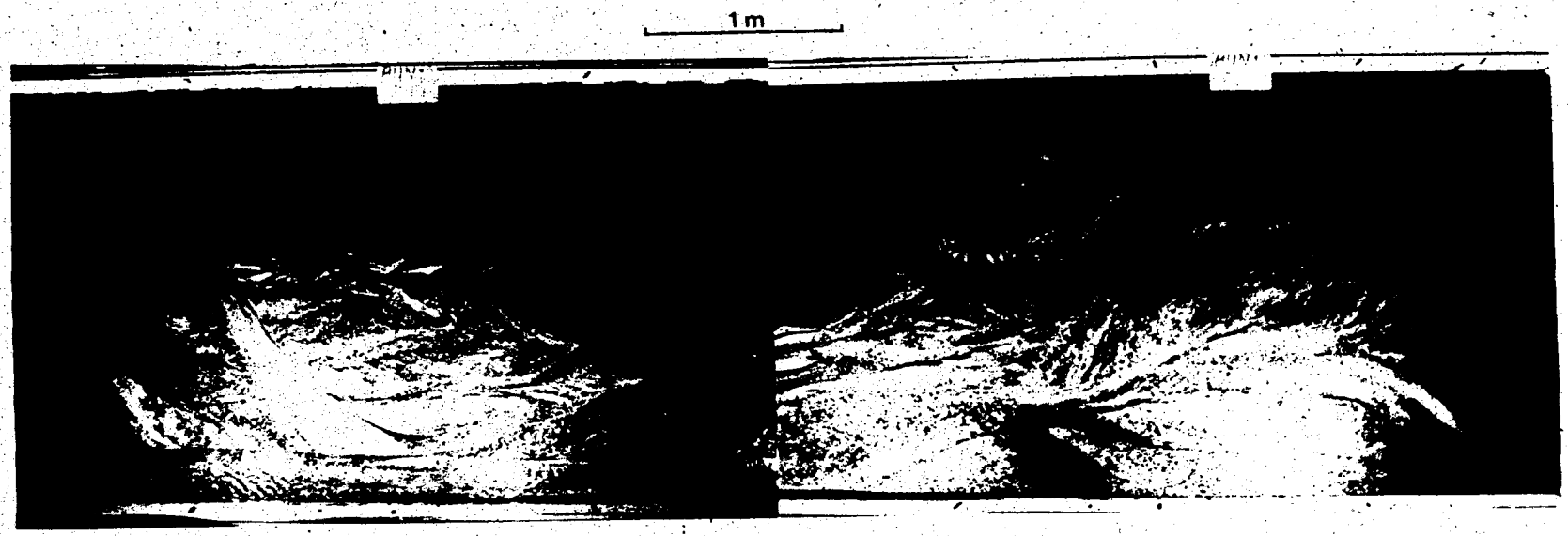

c)

The influence of this pulse at 47 hours was not as pronounced as that of the pulse at 21 hours. Few avalanche-face bars developed and the already moderately braided channel underwent only two or three further divisions. The effect of the pulse on channel form several meters downstream was not apparent for three or four hours after the arrival of the pulse at the head of the flume. The result of this was a very subdued response to the increase in sediment load, suggesting that the effect of the sediment pulse is to some extent a function of the pre-existing channel pattern. If the channel is already intensely braided, further increases in sediment load may have little effect on the channel pattern.

While Figure 7-14 illustrates a subdued response to a large sediment pulse, Figure 7-15 shows the reverse; a marked change in channel pattern following the arrival of a minor sediment pulse. In addition, it illustrates that events within the flume can cause changes in channel pattern independent of the sediment input to the head of the flume. At 27 hours the channel was moderately braided and contained several migratory bars, some with avalanche faces. At the downstream end of the flume the channel divided around a large complex bar (A; 27 hours). Upstream of this complex a large confluence scour was beginning to form (B, 27 hours) from which large bedload pulses began to issue. These pulses may have originated at the head of the flume between samples of the sediment transport rate, but some of the sediment was apparently supplied from a degrading channel immediately upstream of the confluence (C, 27 hours). Aggradation and channel division ensued in the downstream half of the flume (eg. D, 28 hours). By 29 hours, slight aggradation and further flow division (E, 29 hours), apparently the result of a minor sediment pulse, added to the braiding intensity of the channel as

Figure 7-15

Modifications in the channel morphology caused by channel switching within the braided river in the absence of a large sediment pulse at the head of the flume. The hourly vertical photographs were taken at 27,28 and 29 hours from the beginning of run 10. See text for explanation. Flow is from right to left.

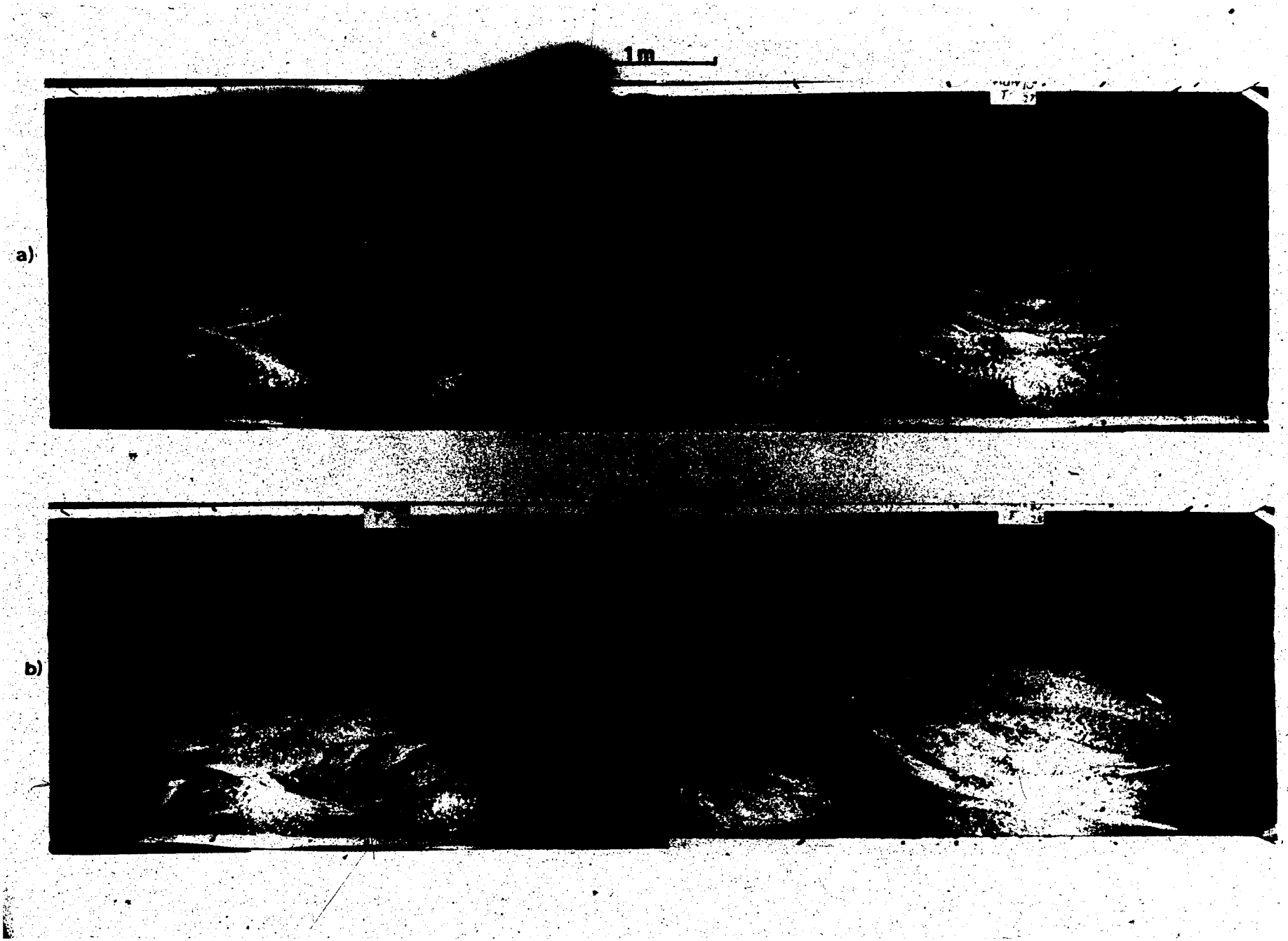
1m
a)
b)

c)

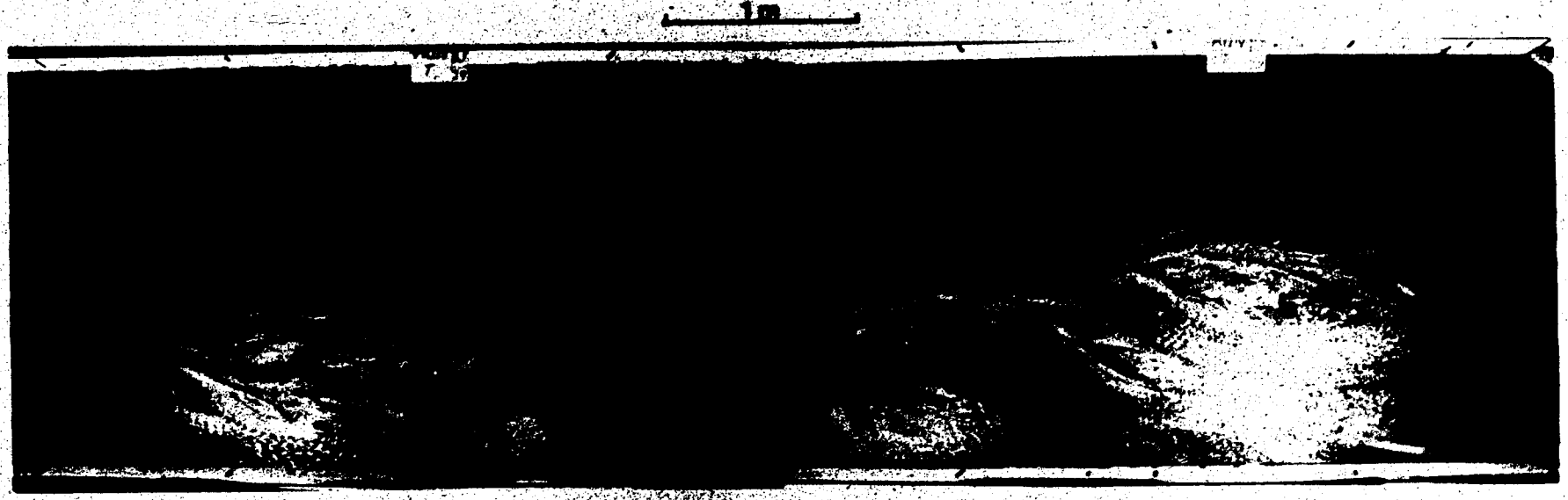

a whole. Throughout this period, any avalanche-face bars that appeared were apparently short-lived since they are not visible in the photographs.

Thus, some of the increases in braiding intensity in the flume as a whole may be a response to internally generated sediment pulses and aggradation, and hence do not appear in the graphs correlating Q_b, P and M. They do, nevertheless, confirm the basic notion of local aggradation causing fluctuations in the channel pattern index and bar form. It should be pointed out that the converse is also true; periods of low sediment input, such as the period from 17 to 21 hours in run 10, show a decrease in braiding intensity and decline in the number, or complete absence, of avalanche-face bars.

7-4-2 Statistical Analysis

In section 7-4-1 observations of channel changes related to individual pulses in sediment load are used to demonstrate the interdependence of sediment input, braiding intensity and bar morphology. However, it also showed that this correlation is not always apparent because of infrequent sampling failing to record all the responses (particularly of bar morphology), and also because of the occurrence of channel changes independent of the sediment input to the head of the flume. In addition, it was apparent that the response of braiding intensity lagged behind the sediment input pulse because of the time required for the sediment to migrate downstream. Despite these complications it may still be possible to demonstrate the interdependence of Q_b, P and M statistically and so confirm the conclusions reached in section 7-4-1 and extend the analysis to the other runs.

If there is a lag in the response of channel pattern to sediment input, a

standard statistical correlation is inadequate to show the existence or otherwise of a numerical relationship between the variables. However, it is possible to calculate correlation coefficients by shifting one series relative to the other and comparing the coefficients for each successive shift, to discern the lag at which the correlation between the input (Q_b) and the response (P and M) is a maximum. This technique is referred to as cross-correlation and is, in principle, the same as autocorrelation, except that the correlation coefficient is calculated for time series of two separate variables, rather than duplicates of the same time series.

The same rules apply to cross-correlation as to auto-correlation (see Chapter 5). The series must be stationary in their mean and variance, the maximum number of lags used should not exceed n/4 (where n is the sample size) and the sample size should be at least 50 (Chatfield, 1980). In this case the sample size is right at this lower limit.

The trends in the series were removed by fitting second order polynomial regression lines to each log-transformed series and analysing the residuals from the regressions. The log transformation reduces the magnitude of the differences in variance along each series. The cross-covariance function (C_k), for two variables x and y, is calculated as follows (Chatfield, 1980) :

$$C_k = \begin{cases} \sum_{t=1}^{n-k} (x_t - \bar{x})(y_{t+k} - \bar{y})/(n) & [k = 0,1,2, \ldots,(n-1)] \\ \sum_{t=1-k}^{n} (x_t - \bar{x})(y_{t+k} - \bar{y})/(n) & [k = -1,-2, \ldots,-(n-1)] \end{cases}$$

and the cross-correlation function ($C_{xy}(k)$) is then :

$$C_{xy}(k) = C_k/(C_{xx}(o) \cdot C_{yy}(o))^{0.5} \qquad 7-9$$

where $C_{xx}(o)$ and $C_{yy}(o)$ are the sample variances of x_t and y_t, the values of x and y at time t, n is the sample size and k is the number of lags.

Unlike the auto-correlation function, the cross-correlation function is asymmetric about k = o and it is therefore necessary to calculate the function for both positive and negative k. Confidence limits can be approximated in the same manner as those for the auto-correlation function (Chatfield, 1980, p.173), that is, the 95% confidence limit lies at $\pm(2/\sqrt{n})$. For n = 50 the confidence limit is 0.283, and for n = 40, 0.316.

Figure 7-16 shows the auto-correlograms for Q_b, P and M in run 10 along with cross-correlograms for Q_b versus P, Q_b versus M, and P versus M. While the sediment load is quite strongly positively auto-correlated at 6 to 7 hours the time series for P and M show no strong autocorrelation. The cross-correlograms reveal fairly strong correlations between all three variables. Sediment load and braiding intensity (P) are strongly positively correlated at -7 hours and +2 hours, and sediment load and abundance of avalanche faces (M) correlate at k = 1. Not all these peak correlations are significant at the 95% level but the pattern is, nevertheless, similar to that predicted from the observations in the section 7-4-1. Both P and M lag slightly behind the peaks in the sediment load curve, and the lag is greater for P than M. In addition the channel form variables are strongly positively correlated at zero lags; in other words, changes in braiding intensity and the abundance of avalanche-face bars are closely related.

This exercise was repeated for all the remaining runs and the results are summarised in Table 7-7 which records the lag at which the highest positive correlation occurs in each case. The data used in this analysis are tabulated in Appendix 5. In some runs no single dominant peak occurred and in these cases all the lags showing high positive correlations have been recorded and appear in

Figure 7-16 Auto-and cross-correlograms for sediment load (Q_b), braiding intensity (P) and number of avalanche-face bars (M) for the time series displayed in Figure 7-12.

(a) Autocorrelograms for Q_b, P and M. 1 lag = 1 hour.

(b) Cross-correlogram of sediment load and braiding intensity.

(c) Cross-correlogram of sediment load and the number of avalanche-face bars.

(d) Cross-correlogram of braiding intensity and the number of avalanche-face bars.

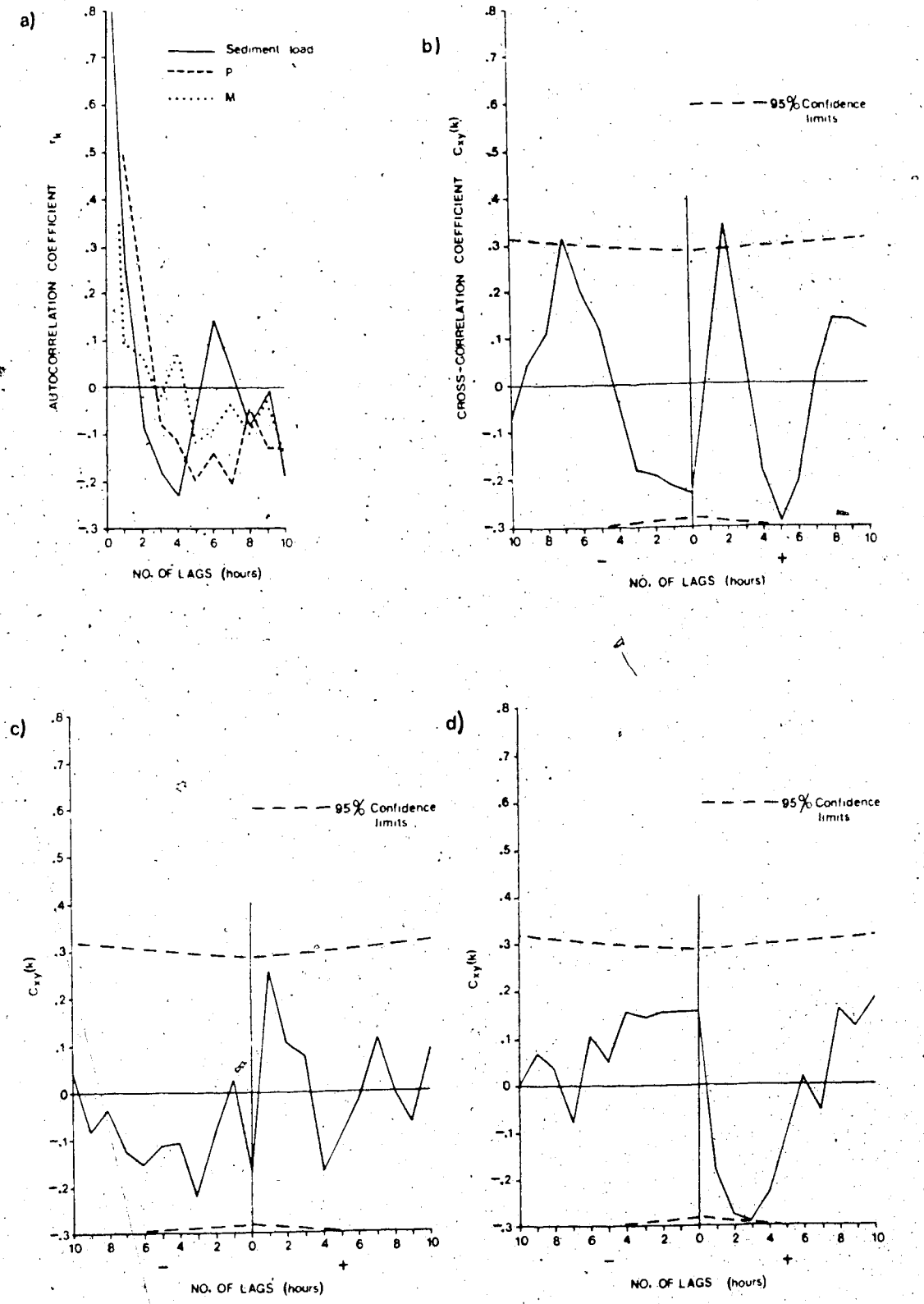
a)
Sediment load
P
M
AUTOCORRELATION COEFFICIENT r_k
NO. OF LAGS (hours)
b)
95% Confidence limits
CROSS-CORRELATION COEFFICIENT $C_{xy}(k)$
NO. OF LAGS (hours)
c)
95% Confidence limits
$C_{xy}(k)$
NO. OF LAGS (hours)
d)
95% Confidence limits
$C_{xy}(k)$
NO. OF LAGS (hours)

Table 7-7

Cross-correlation of sediment load (Q_b), number of active channels per flume length (P), and number of avalanche-face bars

	Q_b versus P		Q_b versus M		P versus M	
Run	Lag of peak C_k	Value of peak C_k	Lag of peak C_k	Value of peak C_k	Lag of peak C_k	Value of peak C_k
2	+3	0.311	+1	0.315	0	0.307
3	+5	0.309	+3	0.376	0	0.313
4	+1	0.185	+6	0.360	0	0.431
	(+1)	(0.122)				
6	+3	0.327	-4	0.391	0	0.393
7	+7	0.206	+8	0.228	-1	0.199
	(-4)	(0.175)	(+4)	0.173		
	(+1)	(0.156)				
8	+9	0.493	-5	0.518	0	0.504
	-5	(0.381)				
9	+4	0.181	-8	0.265	0	0.473
	(-1)	(0.118)	(-2)	(0.182)		
	(+1)	(0.091)	(+4)	(0.114)		
10	+2	0.340	+1	0.261	0	0.155
11	+1	0.316	-5	0.386	+2	0.218
			(+1)	(0.266)	(0)	(0.211)

Significant correlation coefficients (at 95% level) are underlined.

parentheses below the highest value. The most striking features of these results are the consistency with which P and M correlate at k = o and the fact that some of these correlation coefficients are surprisingly high (eg. runs 8 and 9). The results of the correlation of P and M with the sediment load are not nearly as consistent. The number of lags at which the highest positive correlations occur varies from +1 to +9 in the case of P, and from -8 to +8 for M. It is nevertheless true that the increase in P lags behind that for sediment load (Q_b) by, on average, 2 to 3 hours. It is much more difficult to make such a generalisation for the co-variation of M and Q_b.

To summarise : at constant discharge and mean slope, within-run variations in channel pattern and form, specifically braiding intensity and abundance of avalanche faces, are the direct result of local aggradation and degradation often attributable to fluctuations in the sediment load delivered to the head of the flume. This has been demonstrated from specific examples and, more generally, by cross-correlation of the time series for sediment load, braiding intensity and abundance of avalanche-face bars. There is often a lag between the increase in sediment load and the response of the channel pattern due to the fact that the sediment pulse must migrate a few meters downstream from the head of the flume before its effect is noticeable. From the cross-correlation analysis, this lag averages about 2 to 3 hours in the case of braiding intensity but only 1 or 2 hours for avalanche-face bar development.

Because both braiding intensity and abundance of avalanche faces are closely related to the sediment input at the head of the flume, they are also correlated with one another. The occurrence of more flow divisions provides more

sites at which flow competence changes abruptly (for example, channel confluences and the upstream ends of abandoned channels) and encourages bar growth. It is not true that all the avalanche-face bars occur under such circumstances, but it is rare to find migratory unit bars with avalanche faces within a single channel. At the same time the occurrence of rapid aggradation in the form of migratory bars encourages channel division at the downstream ends of these bars in the manner described by Ashmore (1982) for gravel rivers, and Cant and Walker (1978) for sandy rivers.

It should be emphasised that the pulses responsible for these morphological changes are themselves generated by the braided channel and hence are manifestations of earlier channel changes causing variations in the rate of sediment delivery to the downstream end of the flume.

7-5 Discussion

Investigation of the changes in channel pattern and form of braided streams with changing slope and discharge demonstrates that the intensity of braiding, the bed relief index and the frequency of occurrence of avalanche-face bars, all correlate positively with the product of slope and discharge. There is a tendency, however, for bed relief to decrease with increasing slope at a given discharge, but aside from this, increases in slope and discharge have essentially similar effects on channel form. Complications are introduced by the influence of the head arrangement for the introduction of sediment. One arrangement caused aggradation near the head of the flume, and hence increased braiding intensity, while the other tended to reduce braiding intensity. Temporal trends in channel pattern within a run can be traced to fluctuations in the sediment transport rate

at the head of the flume that cause alternating aggradation and degradation. During aggradation braiding intensity and the abundance of avalanche-face bars increase, while the reverse is true for periods of degradation.

The finding that braiding intensity increases with increasing stream power index concurs with previous work on channel pattern. Howard et al. (1970) found such a relationship between their 'excess segment index' and both slope and discharge of braided streams measured from maps and air photographs, and Maizels (1979) found an increase in the mean number of channel segments, nodes and bifurcations in a braided outwash stream undergoing aggradation (and hence an increase in slope). The fact that the trend of increasing braiding intensity with increasing stream power agrees with previous work confirms that the model predicts such behaviour well. Further verification of the model results can be obtained by checking their agreement with theoretical and empirical predictions of the expected braiding intensity. Figure 7-17 shows Parker's (1976) channel pattern threshold diagram with the data from the present experiments plotted on it. All the runs plot quite close to the braiding threshold and some (3, 4b, 7 and 8) are in the single channel regime. Runs 3, 4b and 7 all have very low degrees of braiding (N is 1.6, 1.1 and 1.3 respectively) and are characterised by dominantly single channels with only one or two divided reaches, so that their position in relation to the braiding threshold is not surprising, but run 8, with N greater than 2, does not comply with Parker's (1976) criterion. Otherwise the prediction that runs 1, 2, 4a, 6 and 10 are the most braided fits well the observations made during the runs. Clearly none of the runs is intensely braided (the maximum value of N recorded is 2.4) and this is also apparent in Figure 7-17. It should be

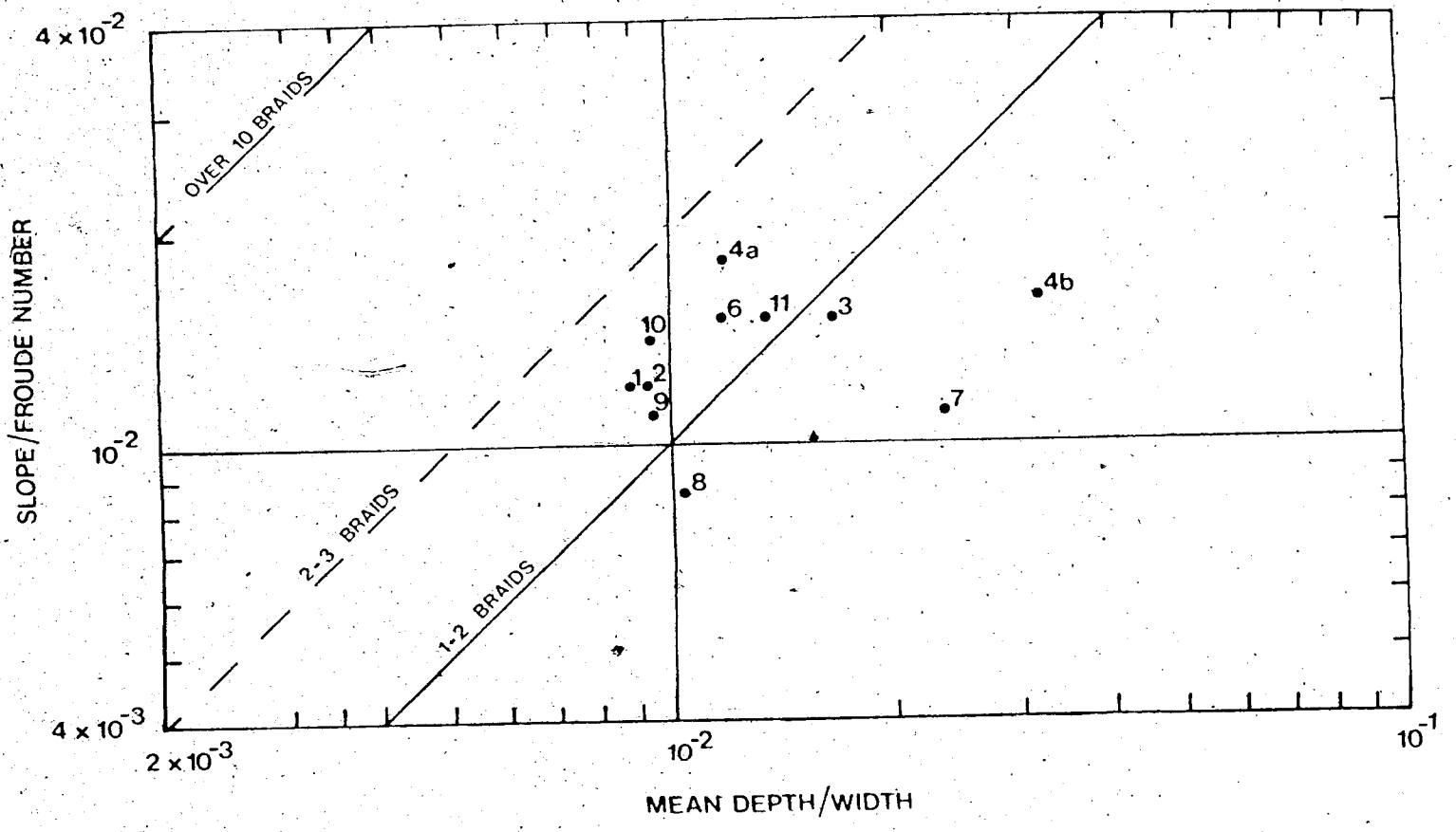

Figure 7-17 Comparison of the laboratory braided channels with Parker's (1976) channel pattern threshold criterion.

borne in mind that Parker (1976) is not explicit about the way in which depth and width should be measured in braided streams. If the widths used by Parker are total channel widths then the total active channel widths calculated for the laboratory channels may be underestimates of total width, and therefore the data plot further towards the single channel regime on Parker's (1976) diagram than they otherwise might.

Comparison with other channel pattern thresholds is more difficult. The standard slope-discharge curves (eg. Leopold and Wolman, 1957) do not include discharges as small as those used in the present experiments, and Richards' [1982, Figure 7-12(d)] stream power threshold predicts that a stream power index of 10^{-2} is required to produce braiding in 1mm sand; a value at least two orders of magnitude larger than the stream power indexes for the laboratory channels. It seems that Richards' (1982) criterion is not applicable to very small-scale streams but it is not obvious why this is so or how the criterion could be adjusted to fit such data. One possibility is that many of the streams used by Richards (1982) have resistant banks; a factor that Carson (1984b) suggests is important in determining whether meanders bends cut off to form braids. In such a case much greater power would be required to erode the banks sufficiently to allow braiding.

The two indexes of braid intensity, the number of active channels per transect (N), and the number of active segments per flume length (P), produce very similar results and thus both are presumably reasonable indexes of braiding intensity. However, there are some runs which plot in different positions relative to one another on the two graphs of the braiding indexes versus stream power (for example, run 7 has lower N but higher P than run 3) but these differences have no effect on the overall trend.

The events of run 4 are significant. It is apparent that runs 4a and 4b have very different channel patterns but the same slope and total discharge. It is conceivable that the channel in run 4b degraded to a lower slope than that in 4a and in the process crossed a channel pattern threshold, but it is unclear why it did so. The three or four hours prior to the entrenchment are characterised by lower than average sediment input to the head of the flume which may explain the degradation and confinement to a single channel, but when sediment input returned to normal the channel did not aggrade and return to a braided state. The explanation may be that the single channel has a much higher sediment load capacity than a braided channel with the same slope and discharge. Any sediment delivered to the head of the flume from the braided, aggrading channel downstream could easily be carried by the single channel without aggradation, bar deposition and braiding. When similar periods of degradation occurred in other runs the channel always reverted to braiding when sediment input increased again; run 4 is the one exception.

The frequency of occurrence of unit bars with avalanche faces (M) is a function of stream power (Ω), bed relief index (I), mean depth (d), braiding intensity (P and N) and excess Shields stress. Since the latter four variables are also positively correlated with stream power, their correlation with the abundance of avalanche-face bars is not surprising. However, this makes it difficult to isolate the separate effects of each variable. Partial correlation analysis shows that braiding intensity is the dominant variable and that the apparent influence of stream power and Shields stress is merely a result of their correlation with braiding intensity. The role of flow depth and bed relief index is similarly

obscured, particularly because of the presence of some runs with relatively high depths bu[redacted]iding intensity. However, for some of the runs there is a positive c[redacted]tween depth and the abundance of avalanche-face bars.

Furt[redacted]s of the controls on bar form is undertaken in Chapter 8 but at [redacted]stag[redacted]worth comparing the laboratory results with field observations. For[redacted] Kic[redacted]g Horse River Hein (1974) observed that the upstream sections of the r[redacted] steep, shallow channels, coarse-grained bed material and low braidi[redacted]ensity, had very few transverse bars and almost no avalanche margins. Relativ[redacted]pths in this reach seem to be about 10, although this is difficult to estimate[redacted]en the limited number of cross-sections surveyed by Hein (1974). By contrast, [redacted] downstream reach with finer sediment and relative depths approaching 30 has a much higher incidence of avalanche-face transverse bars. However, He[redacted] and Walker (1977) note that, even in this downstream reach, the avalanche-[redacted]s are largely restricted to the deeper channels and pools. The Sunwapta River shows a similar pattern of occurrence of avalanche-face bars and in this case relative depth ranges from about 6 upstream to about 20 at the downstream end of the outwash (Rice, 1979, and field observations by the author). This suggests a limiting depth for avalanche face development of about 10. This is difficult to compare with the laboratory results but relative depths in the laboratory channels are in the range 8 to 12 which might explain the comparative infrequency of avalanche-face transverse bars.

The field observations by Hein (1974) and Hein and Walker (1977) also confirm the role of increasing braiding intensity in avalanche face development. Many of the avalanche-face bar margins they observed occurred in areas of

unusually high channel depth. These include features such as channel confluences, slough channels adjacent to the banks, and channel bends. Similar observations from the laboratory channels were described in section 7-4-1. The availability of such sites at which depth and flow competence change abruptly is likely to be closely related to braiding intensity, particularly since channel confluences seem to be so important as sites for avalanche face development. It may seem paradoxical, in the light of the substance of Chapter 6, that channel confluences are the preferred sites for pronounced depositional features, but this can be reconciled by pointing out that the bar development occurs at the upstream and downstream ends of the scour holes, away from the strong secondary currents causing the depth increase. It is possible to observe the development and destruction of avalanche-face bars migrating through scour holes as depth first increases and then decreases again. The routing of sediment pulses through scour holes is described in more detail in Chapter 8, but at this point it is sufficient to note, first, the association between channel confluences and avalanche face development, and second, the obvious influence of depth on bar form as each bar migrates downstream from the scour hole.

While differences in channel form and bar development between runs can be explained by differences in stream power and depth and braiding intensity, changes in these variables within a run are closely related to fluctuations in sediment input to the head of the flume. Aggradation follows periods of relatively high rates of sediment input and is associated with increasing braiding intensity and abundance of avalanche-face bars. Degradation, accompanied by a decline in braiding intensity and frequency of occurrence of avalanche-face bars, occurs during periods of below average sediment input.

The apparent dominance of braiding intensity as a control on the occurrence of avalanche-face bars becomes more understandable as a result of this finding. While the mean values of braiding intensity and avalanche-face bar occurrence used in the analysis (section 7-3) reflect the influence of variations in the sediment load delivered to the stream, the values of stream power and excess Shields stress are for the most part calculated in such a way that they are not influenced by the sediment load variations. Thus, changes in slope and depth which may occur, along with variations in braiding intensity and avalanche-face bar development, and thus influence stream power and bed shear stress, are not accounted for in the analysis. At least some of the dominance of braiding intensity in explaining differences between runs in the abundance of avalanche-face bars must be accounted for by this fact and is therefore an artifact of the data collection scheme used. However, the observations reported in section 7-4 clearly document the association between braiding intensity and avalanche-face bar development so that what is in doubt is not the strength of this relationship but the apparent weakness of the influence of stream power and bed shear stress.

This conclusion is understandable when one remembers that stream braiding is commonly associated with long-term aggradation. Indeed Lane (1957) identified aggradation as one of the primary causes of braiding. Where more sediment is being delivered from upstream than the channel is capable of carrying, deposition occurs in the centre of the channel and flow division follows (see Henderson, 1966, p.448-450 for a detailed exposition of this idea). Fahnestock (1963) noticed a connection between the intensity of braiding and local aggradation of the kind observed here. Fahnestock (1963) observed that deposition in a given reach of

bedload,supplied from upstream, deprived the channel further downstream of sediment and lessened the likelihood of braiding in the downstream section. Recently Smith and Southard (1982) have noted the presence of waves of sediment moving downstream in both a prototype and model gravel braided stream. However, they were unable to find any significant changes in channel form resulting from the passage of such waves although they did note a tendency for more rapid channel changes in the aggradational sections. It is likely that these rapid changes are attributable to channel avulsion and division due to aggradation and bar deposition within the channels. Griffiths (1979) speculated that waves of this kind exist in the Waimakariri River, New Zealand, and that the areas of the channel showing increased braiding intensity, and more numerous mobile unit bars, are zones of local aggradation corresponding to the peak of the wave. As the wave migrates downstream each section of the river undergoes a phase of aggradation followed by one of degradation as the peak of the wave passes. It remains to be seen whether these sediment waves are transferred smoothly downstream or in a step-like progression from one aggradation zone to another through a node which remains fixed in place. Such a step-like progression is implicit in Church and Jones' (1982) and Church's (1983) description of the progression of a pulse of sediment down the Bella Coola River, British Columbia through a series of "sedimentation zones".

Insufficient data are available from Griffiths' (1979) paper to establish the time scale involved in the migration of the sedimentation waves. In the laboratory, aggradation and degradation occur over several hours and coincide with the periodicities in the sediment transport rate discussed in Chapter 5.

Several hours in the model is equivalent to a few tens of hours in the field (at a geometric scale of the order of 20). Since significant sediment movement would only occur during flood flows, an equivalent sequence of aggradation and degradation may take several weeks or months in the field.

7-6 Conclusions

The pattern and morphology of braided river channels varies under the influence of slope and discharge. Increases in these independent variables produce increased braiding intensity, greater average bed relief, an increase in sediment mobility, a tendency for larger numbers of avalanche-face bars to occur and an increase in mean width and depth. This result accords with previous observations of the role of slope and discharge in controlling channel pattern (Howard et al., 1970 and Maizels, 1979). The formation of avalanche-face bars is related to the independent variables (slope and discharge) but also correlates with other morphological variables, particularly braiding intensity. Indeed, braiding intensity appears to be the dominant influence on the abundance of avalanche-face bars although this may partly be an artifact of the data collection scheme employed. The relative depths in the laboratory rivers are too low to allow avalanche face development except in local flow expansions such as the upstream margins of the pools formed at channel junctions. As braiding intensity increases, the number of local changes in competence associated with divisions and confluences also increases, and likewise the number of sites for avalanche face development. Hein and Walker (1977) observed in the field that avalanche margins were rare except in such locations. Both the laboratory data and Hein and Walker's (1977) field data indicate that in braided streams, where relative

depths are of the order of 10 or 20, avalanche face development is rare. However, even within this range of relative depth there is a trend towards increasing numbers of avalanche-face bars as relative depth increases in braided streams. Total width and mean depth of braided channels increase with increasing stream power at rates comparable with the downstream hydraulic geometry exponents for single channel streams (Richards, 1982, p.157).

While differences in channel pattern and geometry between runs can be attributed to differences in slope and discharge, within a given run fluctuations in braiding intensity and the abundance of avalanche-face bars coincide with fluctuations in the sediment input rate which are themselves a product of channel geometry changes. For individual sediment pulses the peak rate of sediment input is followed shortly afterward by an increase in the intensity of braiding near the head of the flume, accompanied by an increase in the number of avalanche-face bars. This effect is transferred downstream over the following few hours. Statistical analysis revealed that in most runs, peaks in the sediment transport rate were followed by increased braiding and avalanche face development about 1 to 3 hours later. The increase in the number of avalanche faces was much shorter-lived than the associated channel pattern changes. Local aggradation and degradation is therefore very important in controlling channel pattern morphology in a given place at a given time. The possibility that the regular fluctuations in sediment transport rate discussed in Chapter 5 manifest themselves physically as migratory zones of aggradation and degradation is intriguing and provides a link between the discussion of sediment transport rate and channel morphology.

Some of these conclusions should be tempered by the finding that the two

different head arrangements used to introduce sediment to the flume produced different channel patterns and forms at the same discharge and slope. In general, the two-nozzle arrangement tended to favour channel incision, a lower degree of braiding, a greater abundance of avalanche-face bars and greater bed relief than the four-nozzle arrangement which favoured aggradation at the head of the flume.

Chapter 8 : Laboratory and Field Observations of Channel Division and Bar Formation

8-1 Introduction

In the previous three chapters selected aspects of the geomorphology of braided streams have been examined in a largely quantitative manner. The change in sediment transport rate with increasing stream power, the causes of variation in the form of confluence scour holes, and the role of discharge and slope in determining the intensity of braiding and the predominant unit bar types present were investigated. At the same time some themes have arisen which relate to the nature of braided stream sedimentation in general. Regular fluctuations in the sediment transport rate occur at a variety of scales from a few minutes to several hours. These influence channel form locally by, for instance, causing fluctuations in scour depth at confluences, and more widely by alternating aggradation and degradation causing bar deposition and changes in braiding intensity. In addition, the dependence of bar height on flow depth and braiding intensity is important for the character of bar deposition. In this chapter some of the features and processes of sedimentation in braided streams are described and the role of some of the forms and processes discussed in previous chapters pointed out.

8-2 Data Collection

Descriptions of braided river sedimentary processes were assembled from both laboratory and field observations. Laboratory observations were aided by time-lapse films of each experiment together with hourly, vertical, still photographs (see Chapter 4). Repeated field photography during July and

August, 1981, on Sunwapta River, Alberta, provided examples of forms and processes for comparison with laboratory observations. Photographic sites were chosen at several vantage points along the braided section of the Sunwapta River. Photographs were taken at irregular intervals depending on the river discharge. During most of July, few photographs were taken because of the absence of any prolonged high discharges and therefore channel changes. During August, photographs were taken once every few days usually in the morning when daily stage was at its lowest. Over the course of seven weeks of field work most of the sites were photographed seven or eight times. Not all the sites showed channel changes during this time and several, while showing changes, were difficult to interpret because of the low elevation of the photographic site and/or because changes were too great between successive photographs. The most useful site proved to be one on a road-cut about half way along the reach that provided a panorama of the central portion of the reach. Examples from the field are interspersed throughout the following discussion and include features observed at the photographic sites and also during day-to-day crossing of the river and aerial reconnaissance flown in early October, 1981.

8-3 Channel Division

A complete description of the process of channel division is clearly fundamental if braided stream morphology is to be understood. It is the process by which an initially single channel braids in the first place, and it is a process which occurs time and again in active braided streams where channel form changes continually. It is likely that the processes responsible for the initial flow division are also those by which division occurs within a braided stream

(Ashmore, 1982), but, initially, this description concentrates on the former situation.

Earlier discussion (see Chapter 2) indicated that three main mechanisms by which channels divide can be identified from previous work. In the first of these mechanisms, exemplified by the work of Leopold and Wolman (1957) and Ore (1964) and occurring in conditions of shallow flow and poorly sorted bed material, local channel widening and shallowing result in the accumulation of coarse bedload particles in the centre of the channel which divert the flow and encourage further deposition in the same location. Later experiments and field observations (Wolman and Brush, 1961; Hickin, 1969; Hong and Davies, 1979; Ashmore, 1982; Ferguson and Werritty, 1983) have shown that braiding follows the development of alternating, lobate, slip-face bars around which flow divides. The cause of this difference in division mechanism remains in doubt but it was suggested earlier (see Chapter 2) that the second mechanism occurs at higher relative depths than the first one. A more complete explanation may lie in the conditions under which alternating bars develop. This possibility is discussed later in the chapter. The third mechanism, observed by Moss et al. (1980, 1982) occurs when extremely shallow sheet flow selectively erodes the bed into "proto-channels" which then combine into an integrated network. This "proto-channel" network is subsequently simplified by combining adjacent channels and abandoning others until a braided stream results. Since this process appears to be limited to shallow flow (a few millimetres deep), relative depth again exerts a control on the division mechanism.

Each laboratory run was begun from a straight channel with a width/depth

ratio of about 30, and a trapezoidal cross-section (see Table 4-1). During the first few minutes of each run the channel bed was occupied by a series of migratory sheets of sediment no more than one or two grains thick [Figure 8-1 (a)(i) and (b)(i)]. A variety of sizes of such sheets were present, some thicker than others and initially it was difficult to discern any regularity to the pattern. The thinner sheets appeared to migrate faster than the thicker ones and could be seen migrating across the surface of the thicker ones towards their downstream margins. After a few minutes the pattern resolved itself into a series of obvious lobate bars on alternating sides of the channel. Flow direction was diagonally across each bar surface towards the bank, where some bed scour occurred, and then diagonally back to the opposite bank. Near each bank the bar margins developed avalanche faces which prograded into the scour hole [Figure 8-1 (a)(ii) and (b)(ii)]. It is apparent in Figure 8-1 that the bars in run 8 have a larger wavelength than those in run 11. Measurement of this wavelength (λ_1) for each of the runs yielded the data displayed in Table 8-1. Note that the wavelength is measured as the distance between the downstream ends of two bars across which flow is towards the same bank, in other words it covers the length of two alternating bars. Because there are no more than two or three bar wavelengths within the flume in each run, wavelength estimation is problematic. This is due to the influence of the head and tail conditions on the bars (wavelength tends to be greater near the upstream than the downstream end of the flume), the fact that measurements can only be made once for each run, and the fact that bars form at a time when the channel has obviously not reached its equilibrium pattern. A measurement could not be obtained from run 7 because of the absence

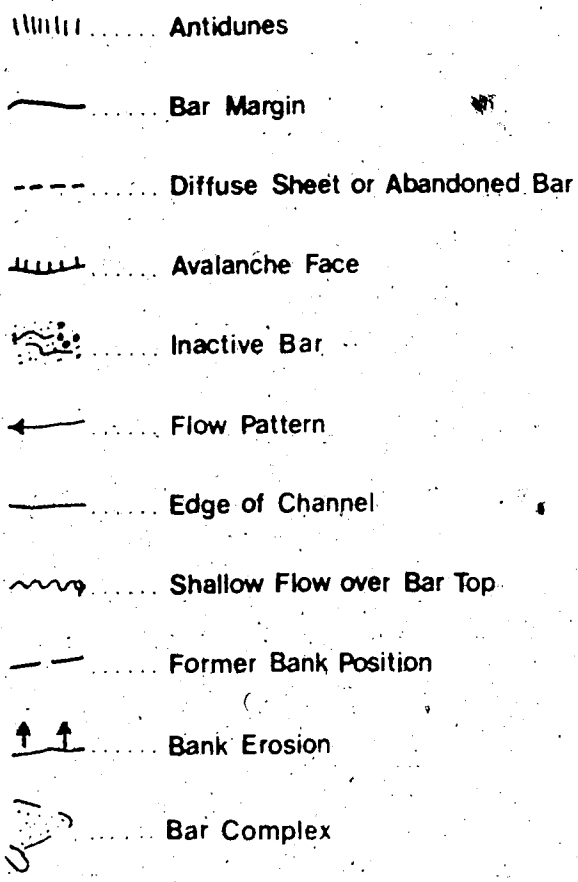

Legend for Figures 8-1, 8-2, 8-3, 8-4, 8-5, 8-7, 8-9, 8-12, 8-16 and 8-26.

Figure 8-1

Development of alternating bars and sinuous channel from an initial pattern of diffuse sheets in (a) run 11 (discharge = 0.0012 $m^3 s^{-1}$) and (b) run 8 (discharge = 0.0045 $m^3 s^{-1}$).

(i) 5 minutes from the beginning of the run.

(ii) 10 minutes from the beginning of the run.

(iii) 20 minutes from the beginning of the run.

The accompanying sketches illustrate the main features seen in the photographs.

a) Run 11

= 1 metre

i)

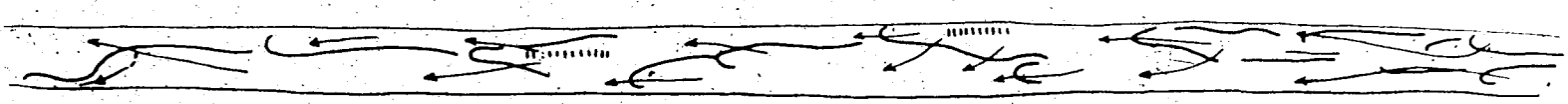

ii)

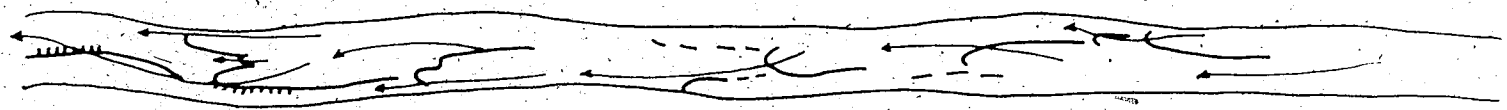

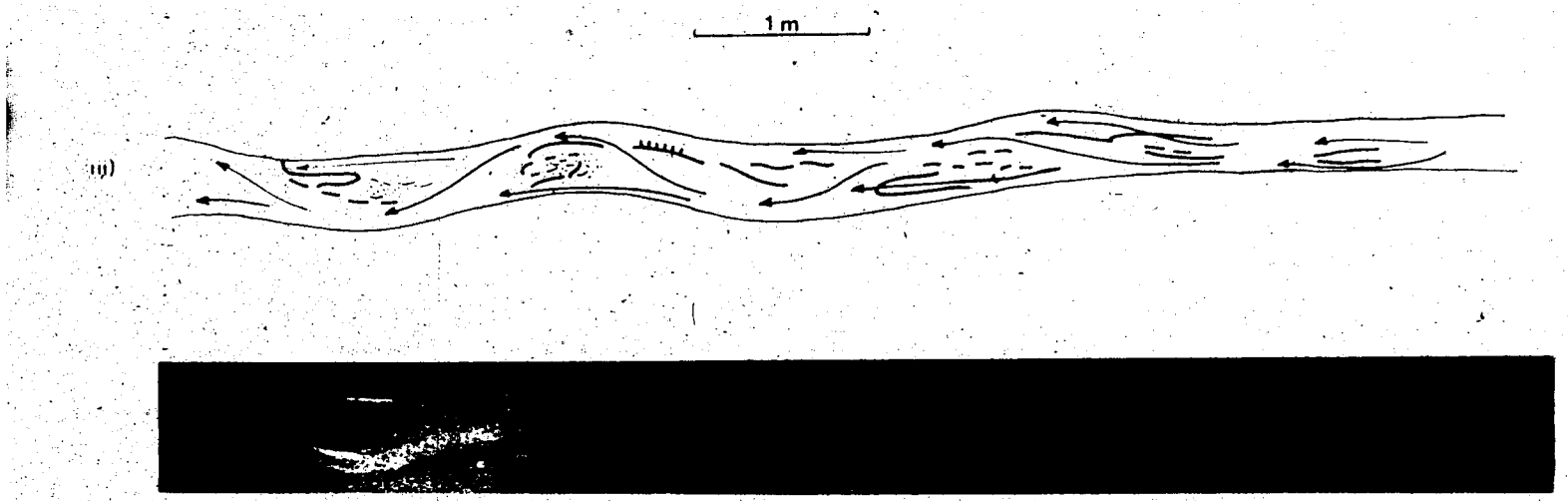

b) Run 8

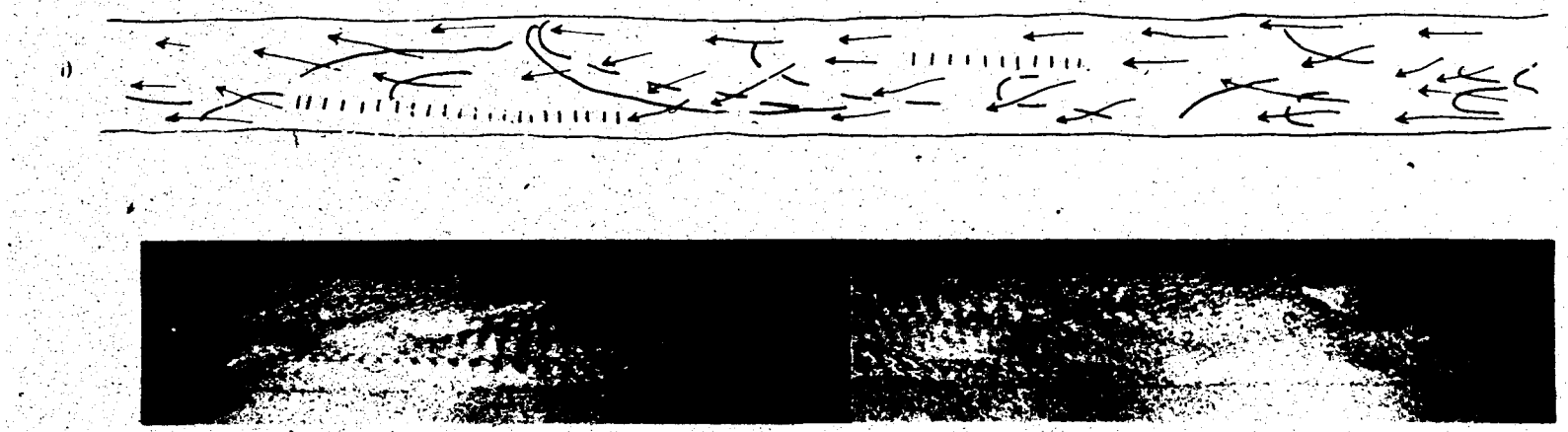

ii)

iii)

Table 8-1

Alternating bar, meander and braid wavelengths for the laboratory experiments.

Run	Initial channel width, B (metres)	Alternating bar wavelength (λ_1) (metres)	λ_1/B	Meander wavelength (λ_2) (metres)	λ_2/B	Braid wavelength (λ_3) (metres)
2	0.50	3.0	6.0	3.5	7.0	3.2
3	0.40	2.6	6.6	-	-	3.1
4	0.35	2.5	7.1	3.0	8.6	2.8
6	0.35	2.9	8.3	3.4	9.7	2.8
8	0.50	4.0	8.0	5.0	10.0	5.0
9	0.50	3.5	7.0	5.0	10.0	5.1
10	0.40	3.1	7.8	3.6	9.0	3.4
11	0.30	2.6	8.7	2.8	9.2	2.8

of a clear alternating bar pattern. Table 8-1 shows that there is a positive correlation between bar wavelength and channel width such that the wavelength/width ratio is between 7 and 9 for the majority of runs. The existence of this fairly constant wavelength/width ratio brings to mind the measurements made on river meanders and riffles (Richards, 1982, pp.185, 195 and Figure 1.1) and which show riffle-riffle spacing to be about 5 to 7 times the channel width, and meander wavelength about 10 to 14 times the channel width. The measurements from the alternating bars in the present experiments yield wavelength/width ratios rather smaller than average but certainly within the range of previous field observations and experiments.

Alternate bars have been reported in laboratory and field studies too numerous to mention individually. Kinoshita (1980) provided the first detailed observations of their formation and made the first attempt to suggest criteria for establishing the conditions under which they form. He noticed that when the width/depth ratio exceeded 20 (and in some experiments when it was as low as 5) the alternating bars were replaced by a more complex bed formation having more than one bar per cross-section (Figure 8-2). The present experiments showed a tendency towards this more complex pattern initially but usually resolved themselves into a simple alternating bar pattern of the type already discussed. Others have attempted to refine the criteria for alternating bar formation (Chang et al., 1971; Ikeda, 1973; Sukegawa, 1973; Jaeggi, 1984). Most of these criteria have a form incorporating the width/depth ratio, slope and excess shear stress. Jaeggi (1984) examined many of these criteria, found them to be in approximate agreement and then developed a criterion of his own based on the same variables; alternating bars develop in poorly-sorted bed material when :

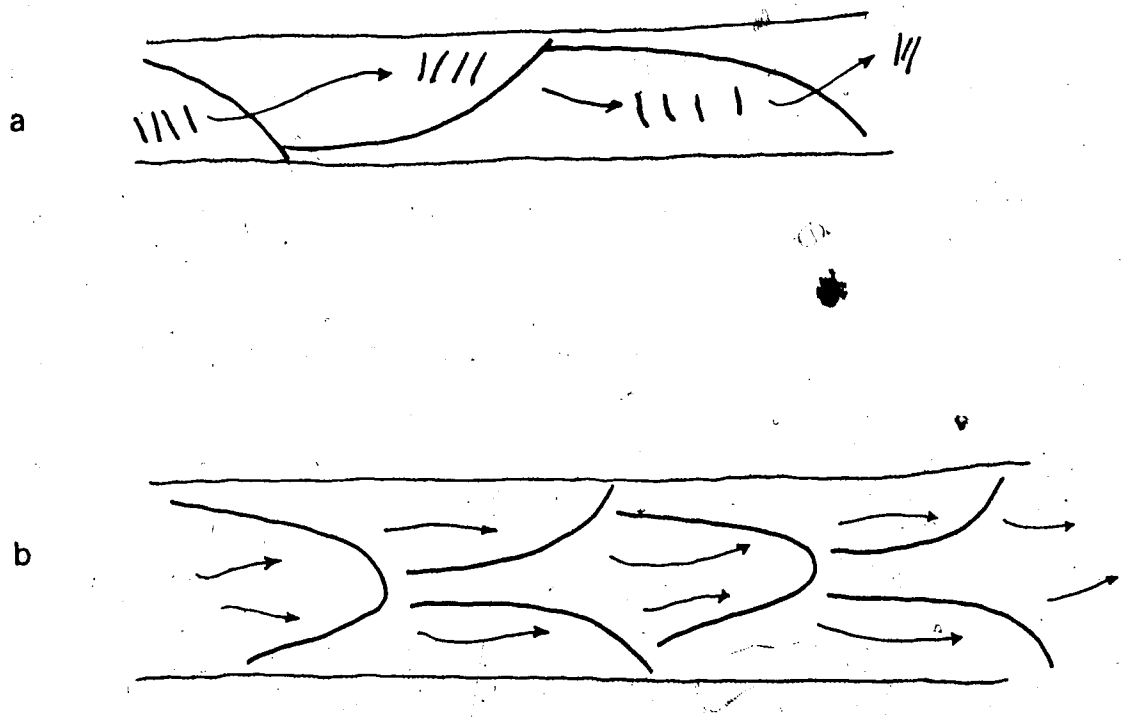

Figure 8-2

(After Kinoshita, 1980) Alternating "dunes" in flume experiments with steep slope, coarse sand and shallow flows.

(a) Width = 0.45m
Slope = 0.02
Depth = 0.02m
D_{50} = 0.023m
Q = 4.5 l s^{-1}
Froude no. = 1.15

(b) as for (a)
except
Width = 0.9m
Q = 8.9 l s^{-1}

$$\tau^*/\tau^*_c > (D_{90}/D_{50})^{0.67} \qquad 8-1$$

and

$$\tau^*/\tau^*_c > 2.93 \ln (\tau^*/\tau^*_c)_B - 3.13 (B/D)^{0.15} \qquad 8-2$$

where τ^* is Shields stress, τ^*_c the value of Shields stress above which sediment transport commences, D is mean particle size, B is channel width and $(\tau^*/\tau^*_c)_B$ is the ratio of Shields stress to critical Shields stress in which depth is replaced by width. For the bed material used in the present experiments, the right-hand side of inequality (8-1) has a value of 1.7. When these criteria are applied to the initial channels of each of the experiments discussed here all the runs except 3 and 7 fall between the upper and lower criteria. Runs 3 and 7 fail to satisfy criterion (8-1), indicating that they should have a plane bed. This is not strictly true but certainly the alternate bars in those two runs were very subdued and ill-defined. It is interesting that the initial channel in Leopold and Wolman's (1957) experiment fails to satisfy criterion 8-2 and hence lies outside the alternating bar regime.

The alternating bars show some internal sorting of sediment sizes, as did the initial migratory sheets. Particularly noticeable is a tendency for the largest particles to accumulate along the margins of the bars, especially at the downstream end, and for the centre of the bar to be dominated by finer material.

Within ten or fifteen minutes the alternating bars had begun to cause erosion where flow was directed against the banks; very low sinuosity meanders developed as a result. The early stages of this process are visible in Figure 8-1 (a)(iii) and (b)(iii). Figure 8-3 shows a similar stage in run 10 and follows the

Figure 8-3

Initiation of braiding from alternating bars in run 10.

The photographs and accompanying sketches illustrate the principal features of the process at :

(a) 5 minutes

(b) 20 minutes

(c) 35 minutes

(d) 55 minutes

(e) 1 hour and thirty-five minutes

from the beginning of the run. See text for a description of the events illustrated.

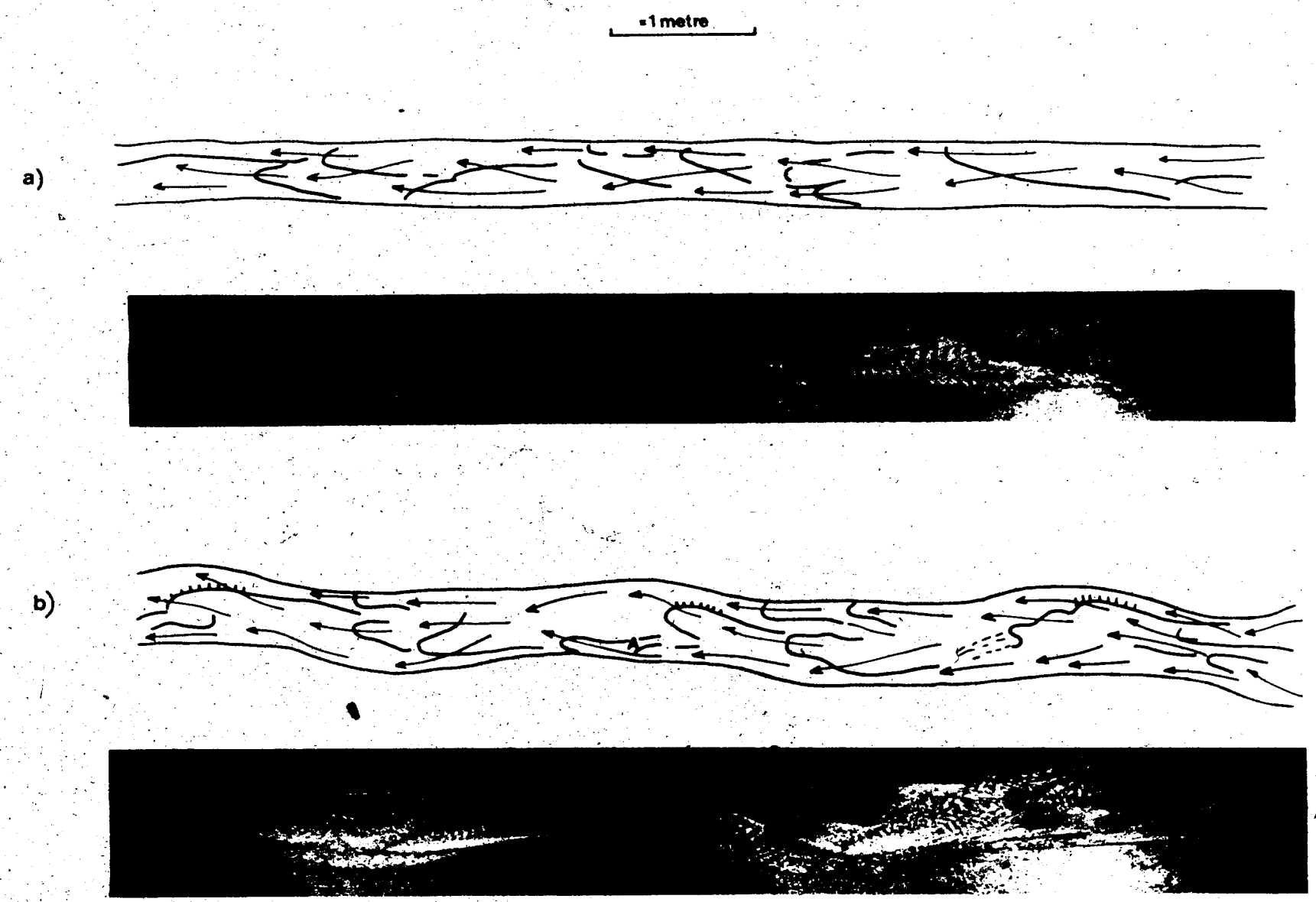
= 1 metre
a)
b)

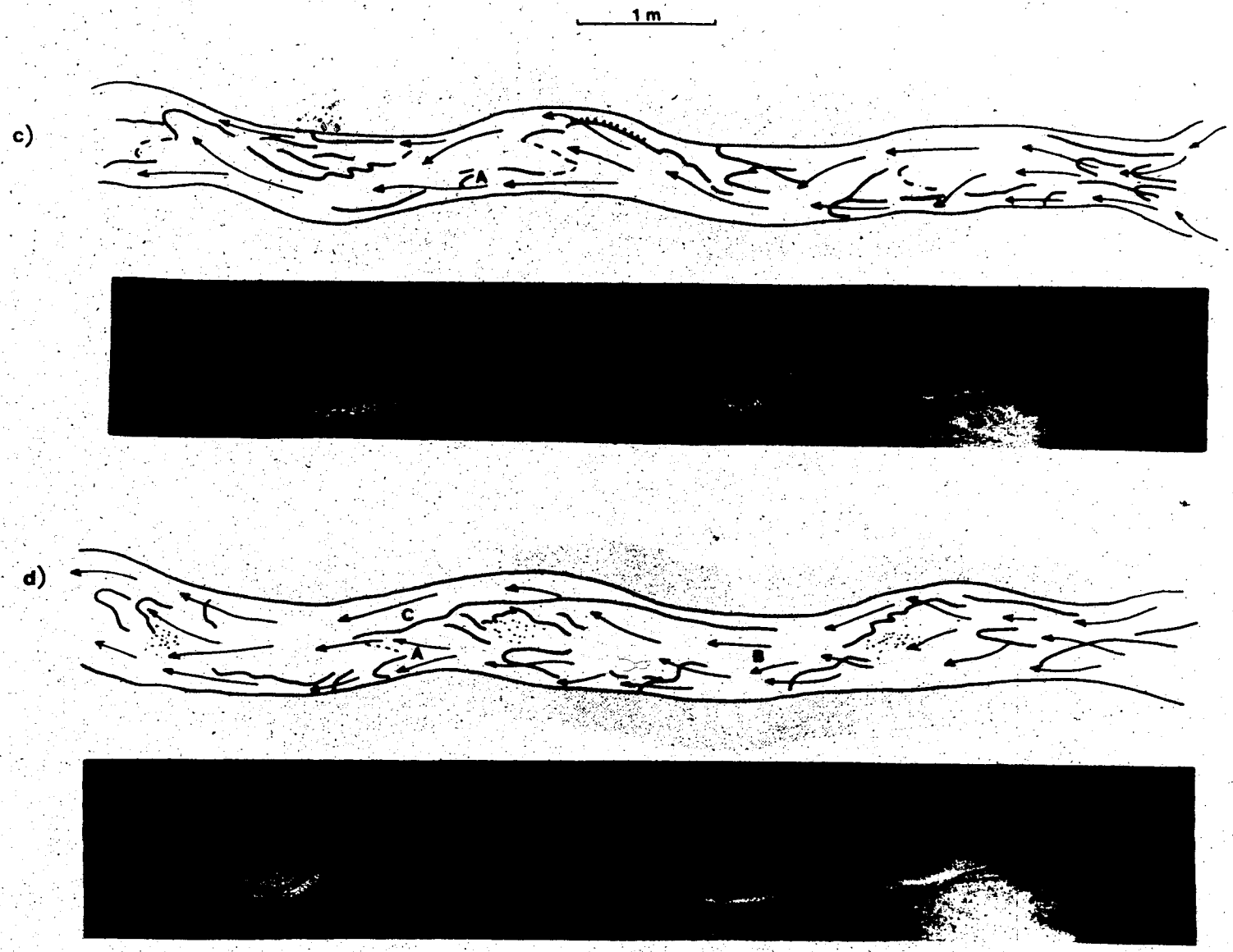
1 m
c)
A
d)
C
A
B

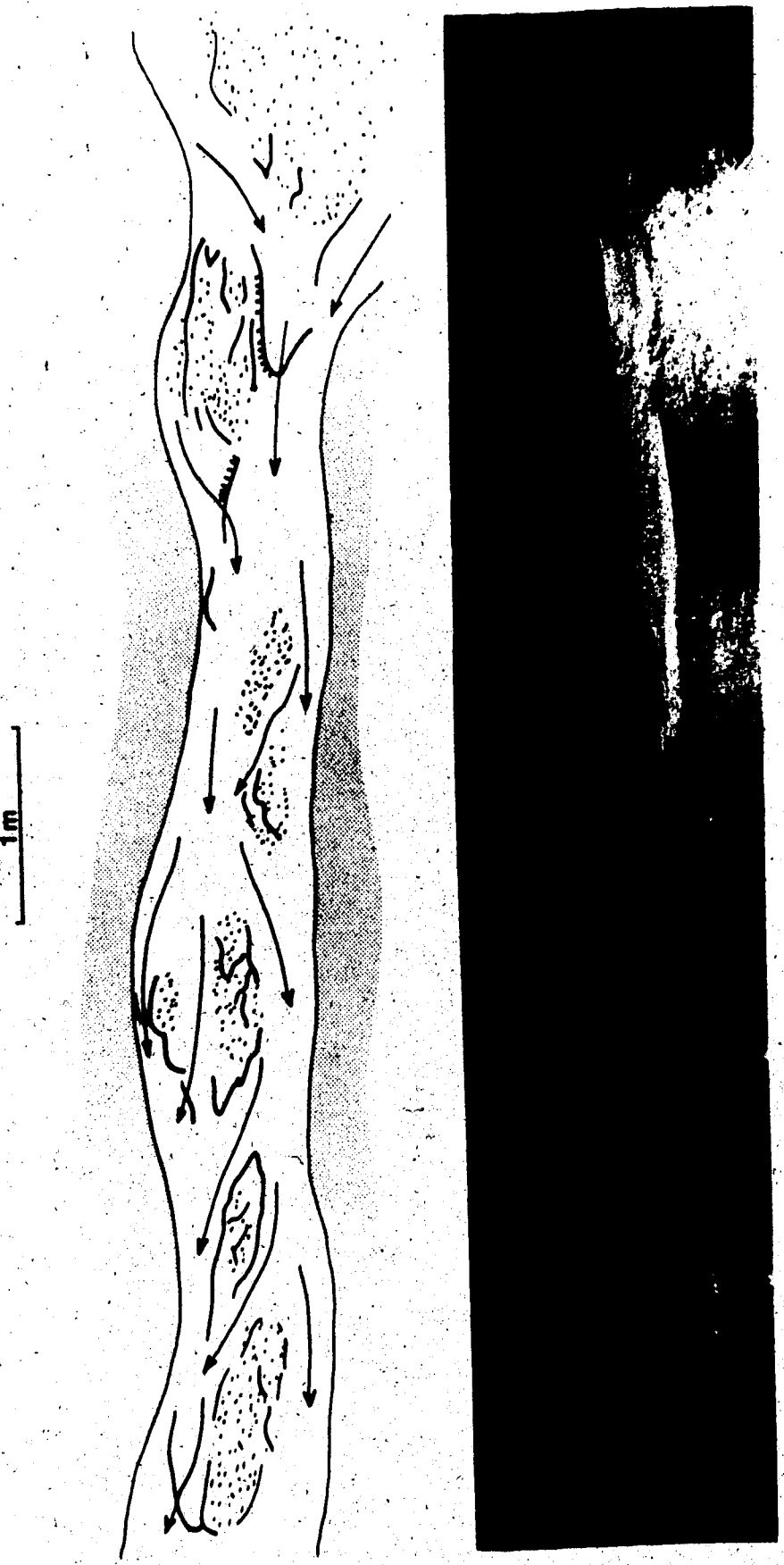
1m

subsequent events through to the development of a braided channel. The low sinuosity meanders that developed following the growth of alternating bars also, not surprisingly, show a correlation between wavelength and width. It is noticeable that this meander wavelength (λ_2) is slightly longer than the alternating bar wavelength (λ_1) (Table 8-1). There is no apparent increase in channel width during this transition so the result is slightly larger wavelength/width ratios for λ_2 than λ_1. The reason for this can only be guessed, but it is possible that the alternating bars represent a growth stage at which complete adjustment between the various channel dimensions (in this case wavelength and width) has not yet been achieved. The sinuous channel is closer to these equilibrium dimensions.

In each of the runs the sinuosity (thalweg length / flume length) of the meanders was not very high before braiding began to occur by chute cutoffs. In the case of run 10 this limiting sinuosity was about 1.1. The sequence of events leading to flow division by this process is documented in Figure 8-3 and illustrated diagrammatically in Figure 8-4. As the meanders increased in amplitude point bars developed on the inside of each bend. The structure of these point bars is illustrated in Figure 8-4 (a) and very similar forms have been described in low sinuosity gravel streams in the field (Bluck, 1976; Lewin, 1976). They are composed of individual unit bars which accrete to the head of the point bar and to the inside of the bend downstream of the bend apex [A in Figure 8-4 (a)]. Against the original bank (B) on the inside of the point bar very little sedimentation occurs, so that as the point bar grows by accretion to the inside of the bend downstream of the apex an elongated trough develops, free of coarse

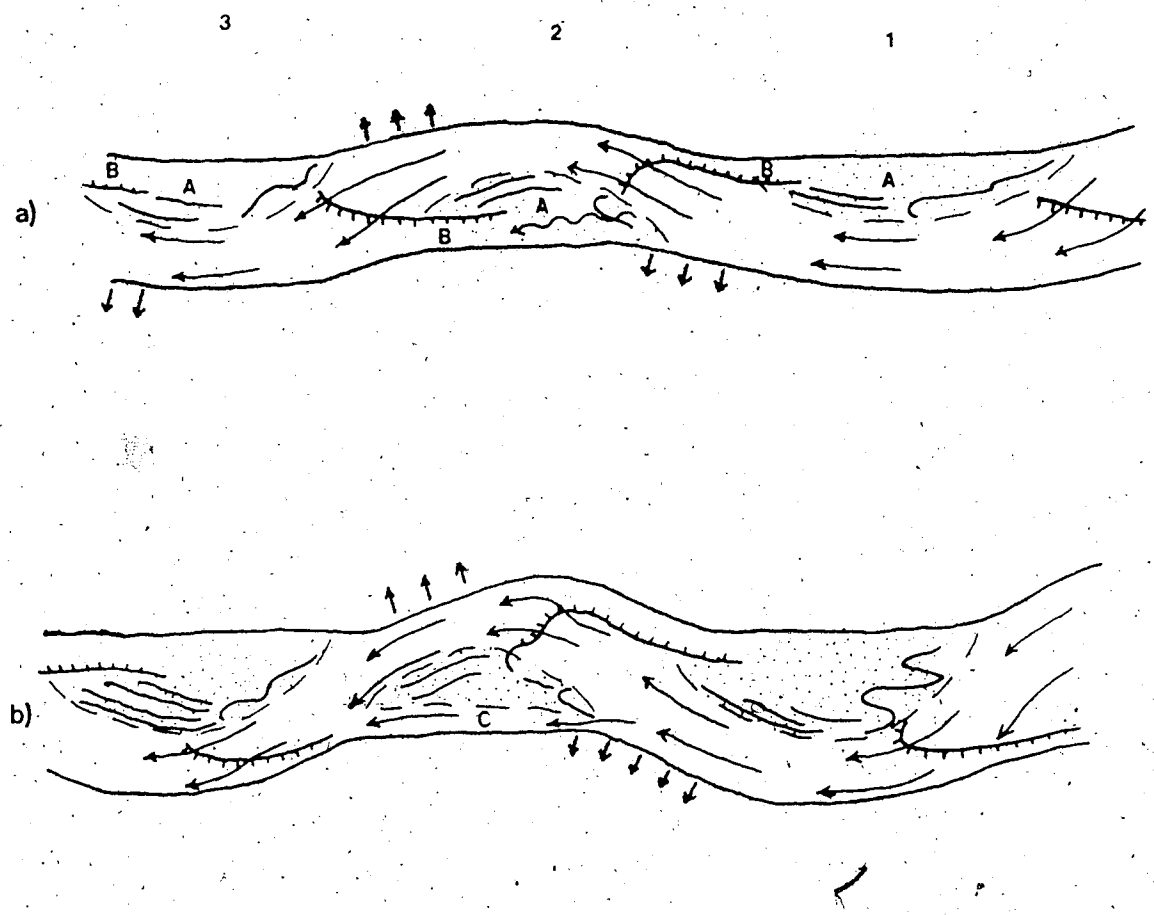

Figure 8-4

Point bar morphology and the cut-off process. These sketches are based on Figure 8-3 to illustrate the cut-off stage in more detail.

(a) The initial meandering pattern showing three bends (1,2 and 3), the point bars (A) composed of sedimentary sheets and the slough channels (B). Note the position of the main avalanche-face bars, one at the upstream end of each bend.

(b) Early stage in the cut-off of bend 2. Note:

(i) the increase in amplitude of the bends and the lateral and downstream growth of the point bars and avalanche-face bars.

(ii) erosion of the upstream margins of the point bars.

(iii) flow across the point bar in bend 2 at C leaving a medial complex.

sediment. In part this trough is the remnant of scour of the bed adjacent to the bank on the outside of the bend. The point bars grow outward as the bends increase in amplitude but they also grow downstream by greater accretion downstream of the bend apex than upstream. At the same time the head of each point bar is eroded because of the downstream growth of the next point bar upstream [Figure 8-4 (b)]. The effect of this erosion is to allow flow across the head of the point bar into the slough channel [Figure 8-4 (b)]. This is occurring in Figure 8-3 (b)(A). Initially this flow into the slough channel is incapable of eroding sediment but as the bar is overtopped by an increasing volume of water a channel is excavated along the bankward margin of the point bar. This process is aided by the comparatively steep slope from the head of the point bar into the slough channel. Once this channel begins to be excavated a positive feedback comes into effect whereby the channel begins to collect more flow, increase in size and divert further quantities of water from the main channel into the slough channel [Figure 8-3 (c)]. At this stage the sediment eroded from the surface of the point bar can be seen deposited as small lobate unit bars at the downstream end of the slough channel [A in Figure 8-3 (c)]. Shortly thereafter the flow division is completed when discharge in the original channel and the slough channel are approximately equal. A mid-channel bar is the end product of the cut-off of the point bar. In Figure 8-3 (d) it is apparent that a pattern of alternating bars has begun to develop in the original slough channel and the cut-off process has begun to operate on one of these bars (A) resulting in further subdivision of the channel.

Thus, at the upstream end of each point bar a divergence and division of flow occurs and at the downstream end the flow converges. In a simple braided

pattern like that in Figure 8-3 (d) and (e), in which the channel alternates between divided and undivided reaches, the divergences and convergences are fairly evenly spaced. One might expect the spacing to bear some relation to the wavelength of the bends from which the braided pattern developed, with perhaps two medial bars per meander wavelength of the originally undivided channel. In fact the 'braid wavelength' [the distance between adjacent convergences B-C in Figure 8-3 (d)] is similar to the meander wavelength rather than half the meander wavelength. Figure 8-5 attempts to show why this is true. The convergences occur in the same approximate locations as the scour holes in the bends of the meandering channel. However, only every second bend scour is converted to a confluence scour, the remainder stay to form bends on one side of a medial bar [Figure 8-5 (a)]. At the same time it follows that only every other point bar is converted to a medial bar, the others are eroded away as the confluence scour migrates toward the centre of the channel under the influence of increasing discharge through the cut-off channel [Figure 8-5 (b)]. However, in order for this to occur the bends must cut off sequentially up or downstream from the first cut-off. If the braided channel subdivides further this simplified situation breaks down because a variety of channels at different discharge each form their own flow divisions with different spacings. Even so, the dominant wavelength is likely to be equivalent to that formed by a simple division of the single channel. The approximate braid wavelength (λ_3) for the initial divisions of each run are assembled in Table 8-1 where it can be seen that λ_3 is very similar to λ_2, the meander wavelength.

In the field, it is impossible to observe the processes of flow division taking

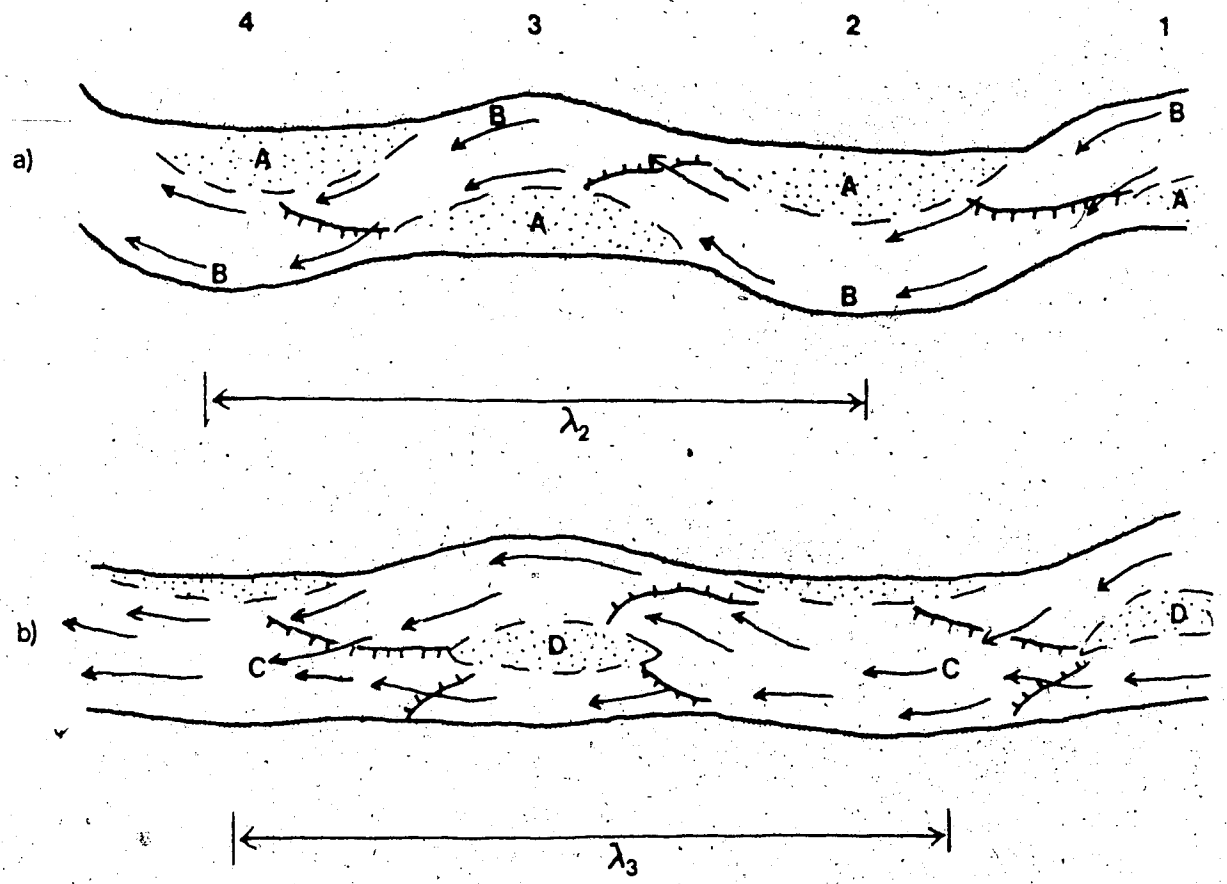

Figure 8-5

Schematic illustration of the relationship between meander wavelength (λ_2) and braid wavelength (λ_3) as a result of the cut-off process.

(a) Initial sinuous channel showing point bars (A) and bend scour (B) in 4 bends (1,2,3 and 4).

(b) Single braid formed as the result of the cut-off of bends 1 and 3 producing confluence scours (C) which migrate laterally under the increasing influence of the flow in the cut-off channel. The result is the erosion of a large portion of the point bars in bends 2 and 4. The point bars in bends 1 and 3 are converted to medial bars by the cut-off process.

place but it is possible to see the initial conditions and the final result. Figure 8-6 (a) shows an oblique view of part of Sunwapta River after a period of high discharge. The accompanying sketch points out the positions of avalanche-face bars and of the cut-off which is much like that seen in Figure 8-1. Figure 8-6 (b) shows a section of Sunwapta River on August 23, 1981, and on July 5, 1982. The low sinuosity channel in the earlier picture has been converted to a sinuous channel with point bars, one of which has been cut-off in the same manner as that in Figure 8-6 (a). [It is assumed that these two photographs represent a sequence of development despite the fact that they were taken ten months apart. This is reasonable because the first was taken at the end of the high discharge period in the summer of 1981 and the second at the beginning of the summer the following year. In addition, adjacent parts of the river could be seen to have undergone little or no change during the ten months].

The mechanism of flow division described here is obviously quite different from that of Leopold and Wolman (1957), in particular because it does not, apparently, involve any loss of flow competence causing deposition in the centre of the channel. However, the cut-off mechanism was not the only channel division mechanism observed during these experiments.

It was noted in connection with the criteria for alternating bar development that runs 3 and 7 failed to satisfy these criteria. Figure 8-7 shows the sequence of events leading up to flow division in run 7. At about 7:30 hours from the beginning of the run [Figure 8-7 (a)] a single diffuse sheet of sediment migrated down the upper two metres of the flume [A in Figure 8-7 (a)]. This was followed by a second sheet at about 8:30 hours, the central part of which stalled at position

Figure 8-6 (a)

Bend cut-off on Sunwapta River.

A = Scour and avalanche-face bar in the original bend.

B = Cut-off channel with a lobate bar prograding into the slough channel

C = Cut-off channel in the next bend downstream.

Note the similarity between this channel configuration and that illustrated in the downstream half of Figures 8-3(d) and 8-4(b).

i)

ii)

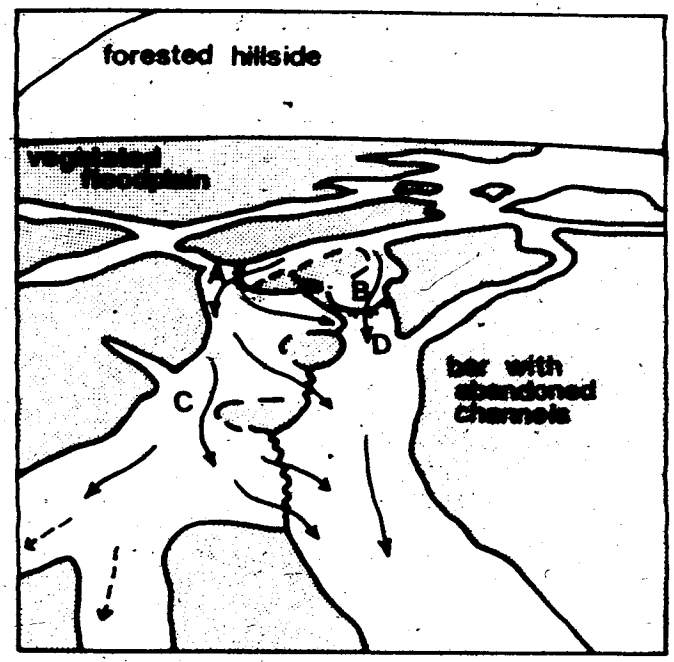

A–original 'meander'

B–cut–off channel

C– cut–off

D–meander bend converted to confluence by cut–off

Figure 8-6 (b)

Development of a sinuous channel and cut-off on a bend in Sunwapta River.

(a) August 23, 1981. Most of the discharge is carried in a low sinuosity channel with a confluence at A and a submerged bar at B.

(b) July 5, 1982. The channel has increased in sinuosity both upstream (C) and downstream (D) of the confluence. A small medial bar formed at E apparently as the result of flow through the chute channel at F. A similar process is also occurring in the foreground (G).

a)

b)

Figure 8-7

Channel division (a) and (b) downstream of a confluence in run 7 and subsequent construction of a medial bar (c) and (d) :

(a) 8 hours,

(b) 9 hours,

(c) 10 hours,

(d) 11 hours

from the beginning of the run. Comparison with Leopold and Wolman's (1957) photographs and sketches (Figures 34 and 35) shows some striking similarities, particularly the downstream fining along the medial bar (C) (as shown by the change from dark grey to light grey in the photographs) and the lack of any pronounced scour at the confluence downstream because of the low angle of confluence.

= 1 metre

)

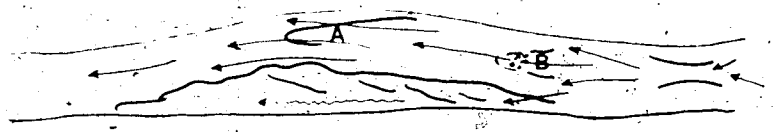

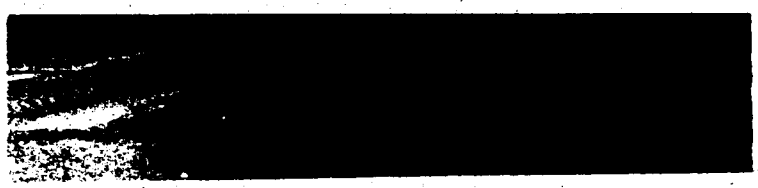

b)

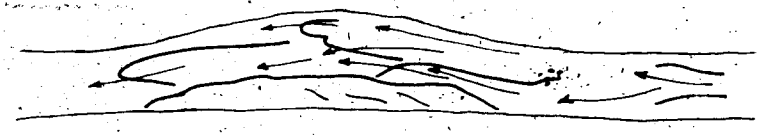

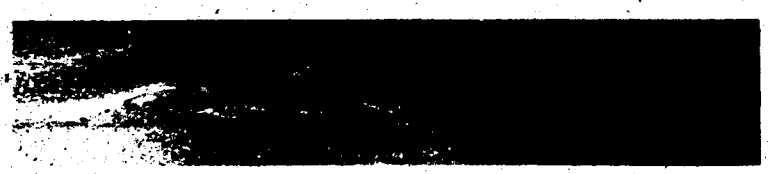

c)

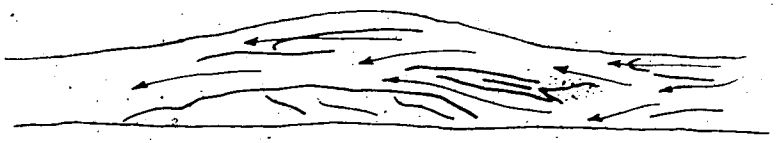

d)

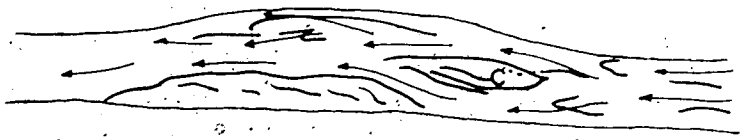

B [Figure 8-7 (a)]. Two further sheets migrated through the reach before 9 hours, both leaving a veneer of coarse material in the centre of the channel at B. In the next hour three or four more sheets added material to the bar. The sheets arrived at least 10 minutes apart. The resulting central bar was very similar to that described by Leopold and Wolman (1957), although they did not mention the accretion in steps as a result of the passage of bedload pulses. It should be noted that the described events occurred downstream from a confluence scour hole and this has some influence on the division mechanism, as will be discussed shortly.

Extremely high width/depth ratios also preclude the development of alternating bars. Under these circumstances, when relative depth is also extremely low (2-3), the mechanism of braiding is quite different from those described thus far. Two experiments (referred to here as A and B) were run in which slope and discharge were the same (0.013 and 0.003m^3s^{-1} respectively) but width/depth ratio was different. The initial channel in run A had a width/depth ratio of about 40 and braiding initiation followed the cut-off mechanism described previously. Run B had a width/depth ratio of 120, with an initial relative depth of about 3. Figure 8-8 illustrates the origin of the braided pattern in run B. Initially no channelized flow capable of transporting sediment was present in the flume. Re-working of material at the head of the flume concentrated flow into two faint channels after a few minutes, and shortly afterward other zones of transport, often marked by the presence of trains of standing waves, became visible. Antidunes developed beneath these standing waves. After about 30 minutes these zones had eroded faint channels in the sediment and had accumulated a few thin sheets of sediment at points where competence was

Figure 8-8

Initiation of braiding from an initial channel with high width/depth ratio and low relative depth :

(a) 2 minutes,

(b) 30 minutes,

(c) 1 hour, 25 minutes,

(d) 2 hours,

from the beginning of the run. Note the faint channels and sheets developed after 30 minutes (for example, A and B) and the medial bars formed after 1.5 hours (C and D) whose margins show many of the features of bars from other runs but whose nucleus is formed of unworked sediment from the bed of the initial channel. Flow is from right to left.

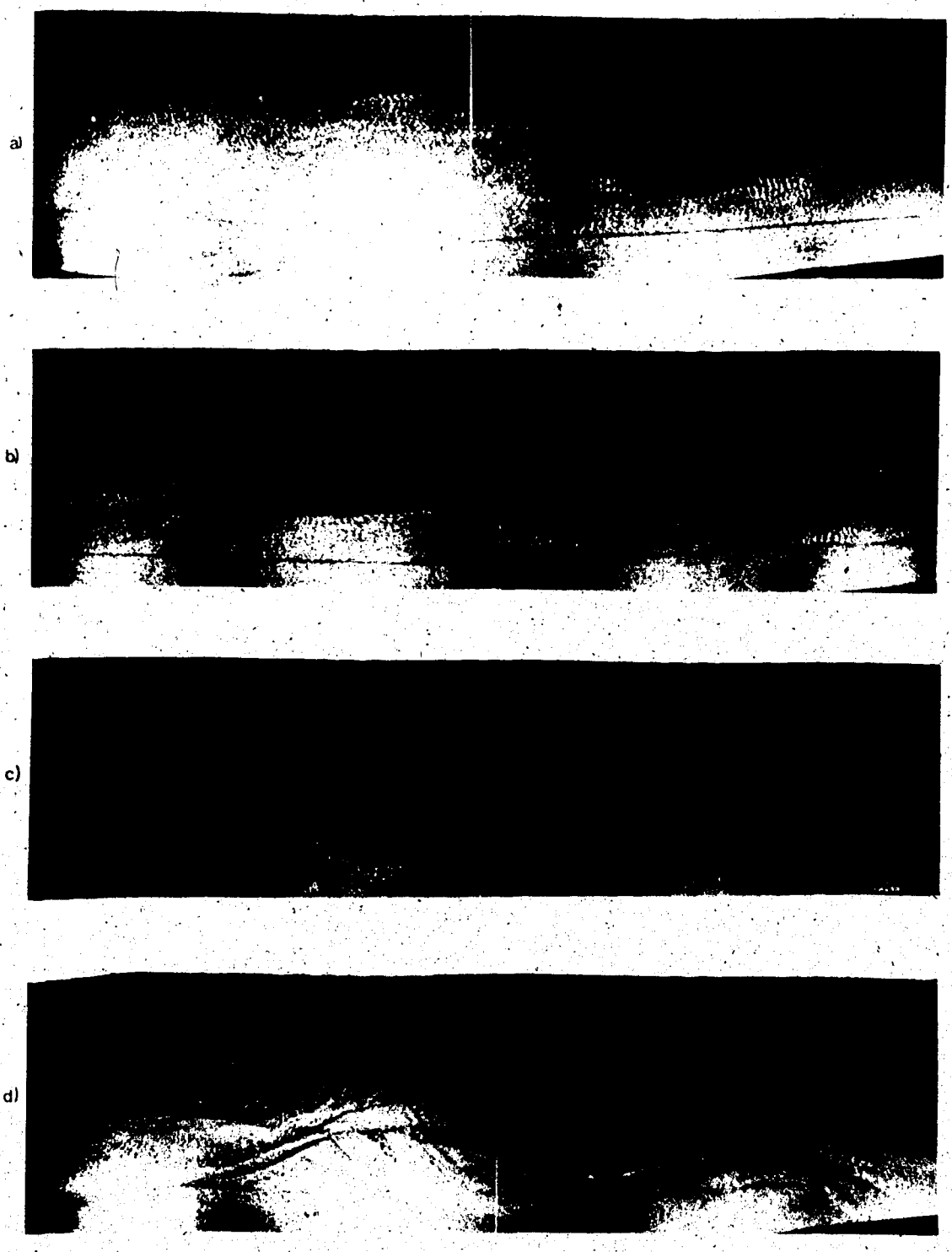
a)
b)
c)
d)
metres

reduced Figure 8-8 (b). After 1.5 hours [Figure 8-8 (c)] had elapsed a well-developed braided channel had developed consisting of two large medial bars around which flow divided. After two hours [Figure 8-8 (d)] the channel configuration in run B was indistinguishable from that in run A. Moss et al. (1980, 1982) observed very similar events in shallow, steep flows in coarse sand and, in addition, noted that the initial faint channels often extended upstream by the development of a headward-cutting notch. They referred to the antidunes as "supercritical ripples" but in view of their formation in phase with the water surface the term ripple seems inappropriate and although they were seen to migrate downstream or upstream there was no avalanche face present.

Thus, at high width/depth ratios alternating bars are completely absent and, rather than division from a single channel, the braiding seemed to develop by simplification of an initially complex network of faint minor channels. However, the final result was indistinguishable from the braided pattern formed at the same discharge and slope from a narrower, deeper channel. This is important from the point of view of modelling as it illustrates that initial channel form is irrelevant to the final form and the arbitrary choice of initial width/depth ratio is justified.

8-4 Confluence Scour and Associated Sedimentary Processes

Confluence scours represent channel convergences and an area of deposition usually occurs immediately downstream of confluences. The form that this depositional area takes, and its location, are to some extent governed by the flow through the scour hole upstream. In this sense the scour holes act as controls on the sedimentary processes but it should be remembered that the orientation and form of the scour holes are controlled by the confluent channels responsible for

their formation. Nevertheless, if one considers one confluence in isolation it is possible to see how it governs events occurring immediately downstream.

Consider a confluence in which the channels have approximately equal discharges and the angle of confluence is large enough for scour to occur. Such a confluence at the beginning of run 8 appears in Figure 8-9. Instead of an alternating bar pattern forming downstream of the scour hole at C, a single symmetrical transverse bar developed at A [Figure 8-9 (a)]. The downstream end of this bar formed an obstruction to the flow which therefore diverged around it. This divergence may have been due partially to the steeper water surface gradient obliquely across the bar than along its longitudinal axis. Because the bar had a fairly symmetrical form the resultant medial bar was also roughly symmetrical, as was the distribution of the discharge on either side of it. The final form of the bar was little different from that formed by cut-off of low amplitude meanders but the initial stages were somewhat different. The channel division sequence described from run 7 (Figure 8-7) is very similar to that just described. The difference is that in run 7 the bar has a much more subdued form.

A very similar sequence occurred at about 30 hours in run 10 (Figure 8-10). In this case, the deposition downstream of the scour hole at B can be traced to a pulse of sediment migrating down the left confluent channel [A in Figure 8-10 (a)]. An avalanche-face bar developed at the upstream end of the scour hole [B in Figure 8-10 (a)] and the sediment from this pulse was reorganised into a symmetrical transverse bar [C in Figure 8-10 (a)]. The channel downstream of the scour hole was deep enough for an avalanche face to develop at the margin of this transverse bar. Flow division then occurred in the manner described in the

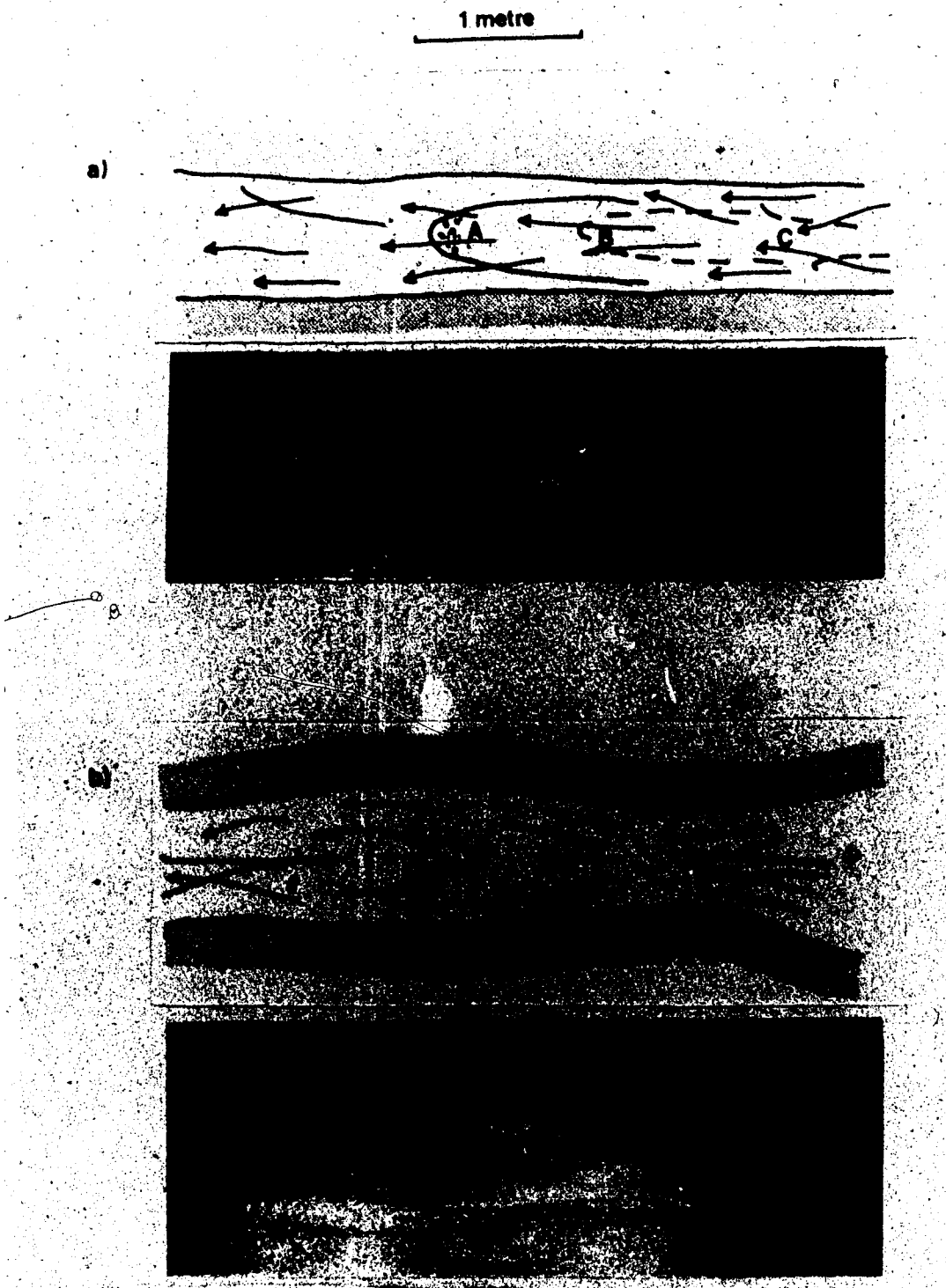

Figure 8-9 Flow division around a transverse bar formed downstream of a confluence.

(a) A large transverse bar, with relatively coarse material (A) at its downstream margin and diffuse migratory sheets (B) on its surface, has been deposited downstream of a confluence (C).

(b) The centre of the bar margin (A in Figure 8-9(a)) serves as the nucleus for the flow division (D).

Figure 8-10

Transverse bar deposition, channel division and medial bar construction downstream of a confluence in run 10. Flow is from right to left. See text for explanation. The black markings on the flume wall are one metre apart.

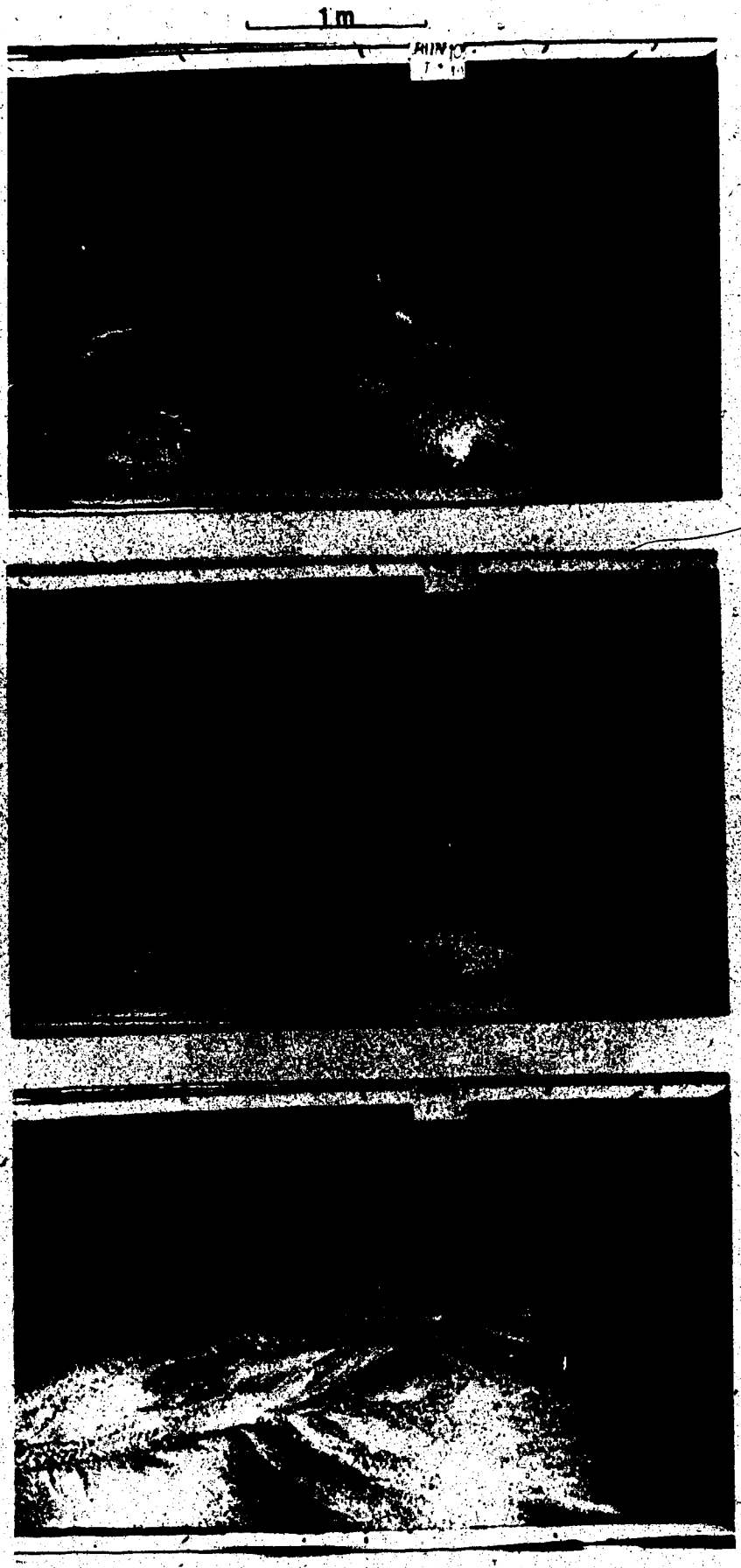
1m
a)
b)
c)

previous example and a medial bar accreted in the centre of the channel. By 31 hours [Figure 8-10 (b)] the medial bar was quite extensive (D) and continued to increase in size until about 33 hours. At this point sediment load to the flume declined and the confluence re-formed downstream a short distance under the influence of the changing location, number, and discharge of the confluent channels. The result was avulsion across the surface of the medial bar and eventual destruction of a large part of it as the originally aggradational area became one of degradation [Figure 8-10 (c)].

The production and migration of a transverse bar downstream of a confluence is also shown in Figure 8-11. This sequence is taken from run 9 and shows the initial pulse of sediment forming a large avalanche-face bar (A) downstream from the confluence (B). An hour later [Figure 8-11 (b)] this initial bar had increased considerably in area and flow division had begun at its downstream margin (C). Where the bar migrated into deeper water its avalanche face was maintained but elsewhere (D) this was destroyed as the margin prograded into shallower water. Numerous diffuse gravel sheets (for example, E) migrated across the bar surface as it migrated downstream.

In the example described from run 2 it was possible to trace the division process in detail and to observe the role played by sediment sheets accreting vertically to the transverse bar surface (Figure 8-1[redacted]er about four or five sheets had accreted the subsequent sheets could be seen to change in form as they approached the downstream end of the bar. Here the central portion of the margin was retarded (Figure 8-12, 12 minutes) relative to the rest of the sheet, and this portion of the sheet was left behind while the flow swept sediment round


1 m
a)
b)

Figure 8-11

Transverse bar development and migration, and flow division downstream of a confluence in run 9. Flow is from right to left and the markings on the side of the flume are 1 metre apart. The dashed line in Figure 8-11 (b) marks the edge of the diffuse gravel sheet (E). See text for explanation.

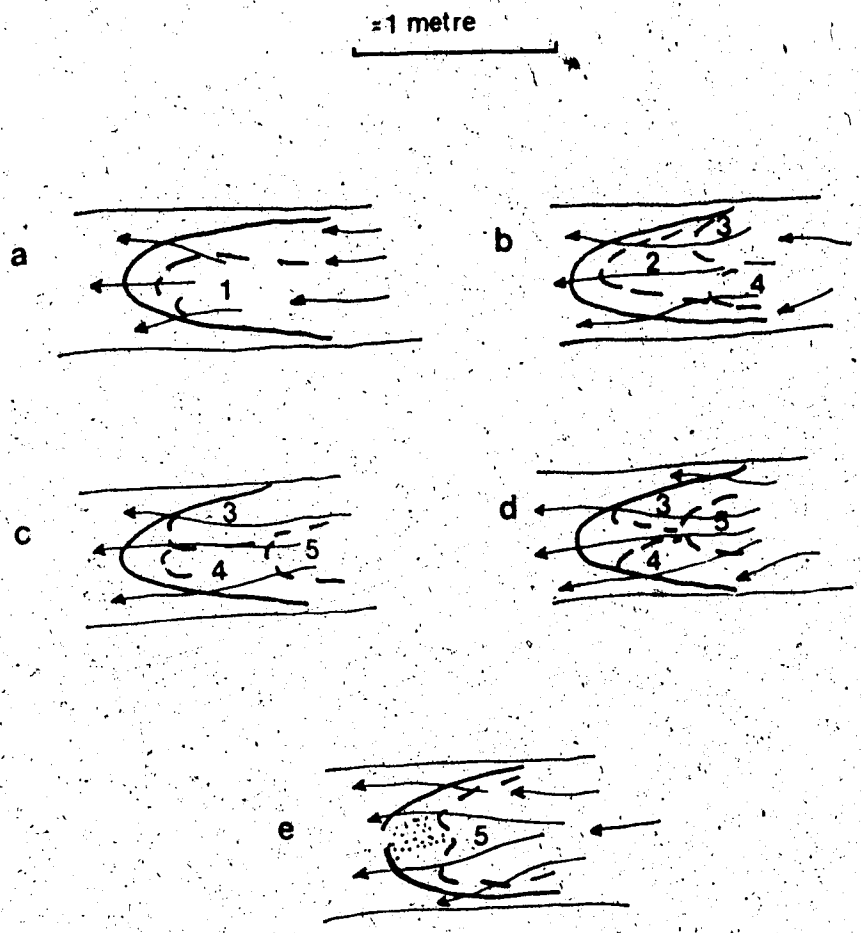

Figure 8-12

Flow division atop an avalanche-face bar by accretion of sediment sheets: an example from run 2.

The five sketches, drawn at about 2-minute intervals, illustrate the modification of the flow pattern over the bar as a result of the migration across the bar surface of a series of thin sheets of bedload. The margins of each of the sheets 1 to 5 are shown by dashed lines in the sketches which are drawn from the time-lapse film of run 2. Note the deformation of the margin of sheet 5 (e) as it approaches the bar margin, indicating the diversion of the flow around the central portion of the bar margin.

either side of it. This appears to be the beginning of the flow division and because accretion to the bar surface occurs in distinct phases the moment of division can be pin-pointed to the arrival of a particular sediment sheet.

The presence of thin sheets moving across large bars has been reported from sand bed streams (Smith, 1971b) and their form is reminiscent of the rheologic fronts described by Jopling (1964) from laboratory experiments in which flow depth was increased in small steps. These rheologic fronts are a result of the bed aggrading to a new equilibrium level. The sheets visible in the model may be a result of the same process but it seems more likely that they are the result of small magnitude, high frequency fluctuations in the bedload transport rate and are therefore equivalent to Jopling's (1964) saltation fronts. Figure 8-12 shows the sheets to be about 0.5m apart and to be separated in time by about two minutes. This spacing varies with the flow conditions; in run 7 the spacing was closer to ten minutes. Hein (1974) reported the presence of "diffuse gravel sheets" migrating along the bed of the Kicking Horse River and being modified to form transverse bars. Bluck (1979) has described very similar features from several braided streams. This accretion of thin sheets of gravel could account for the crude horizontal stratification which dominates most coarse braided river deposits. Whether or not such sheets develop into transverse bars by a process of stalling of coarse material and winnowing out finer material, as suggested by Hein (1974), is unclear from the present experiments. The diffuse sheets could be seen adding to existing bars and sometimes grew into slip-face bars themselves if they migrated into deeper water.

Where the confluent channels are uneven in discharge the bars developed

downstream of the scour hole are asymmetrical and the result is a deposit resembling a point bar rather than a medial bar. Figure 8-13 shows an example of this situation.

The discussion thus far has illustrated the influence of the confluence on the type of bars developed, and the flow division mechanism that occurs, downstream of confluences. The role of the relative discharge of the confluent channels is particularly important here and this can be seen most clearly when a confluence remains in approximately the same location for a number of hours, during which the relative discharges of the two channels fluctuate. An example of this, from run 8, appears in Figure 8-14. At 18 hours [Figure 8-14.(a)] a large confluence (A) about 3m from the head of the flume dominated the channel pattern. Immediately downstream of the confluence flow divided around a medial bar that had originated about 4 hours earlier from rapid sedimentation of the channel downstream from the confluence in the manner illustrated in Figure 8-13. Discharges in the confluent channels were approximately equal and the scour was oriented almost parallel to the long axis of the flume. By 19 hours [Figure 8-14 (b)] the discharge of the right-hand channel (A) entering the confluence had begun to increase at the expense of that of the left-hand confluent channel. The result was to reorient the scour hole obliquely to the long axis of the flume so that it was more nearly parallel to the flow direction in the right-hand confluent channel. The consequence of this was that the channel at the left-hand side of the medial bar downstream of the confluence gained discharge (B) and the right-hand one experienced a reduction in discharge and began to choke with sediment at its upstream end (C). An hour later [Figure 8-14 (c)] the right-hand channel round

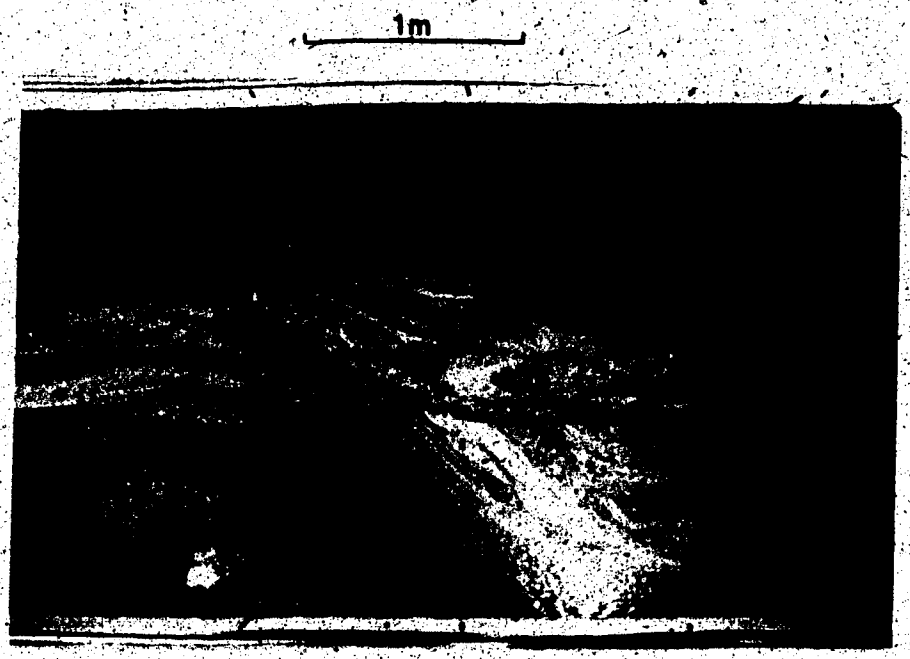

Figure 8-13

Asymmetrical avalanche-face bar formed downstream of a confluence. Flow is from right to left and the markings on the wall of the flume are one metre apart.

The two channels (A and B) forming the confluence (C) have slightly different discharges (A is larger than B) and as a result the large bar (D) is asymmetrical with most of the flow being directed over its left-hand margin. The result is lateral migration of the channel and erosion of the bank at E. Note also the beginnings of a cut-off at F and a diffuse sheet at G, the margin of which is marked by a dashed line.

Figure 8-14

Reorientation of a confluence scour and its influence on the sedimentation pattern downstream. See text for explanation. Flow is from right to left and the markings on the flume wall are one metre apart.

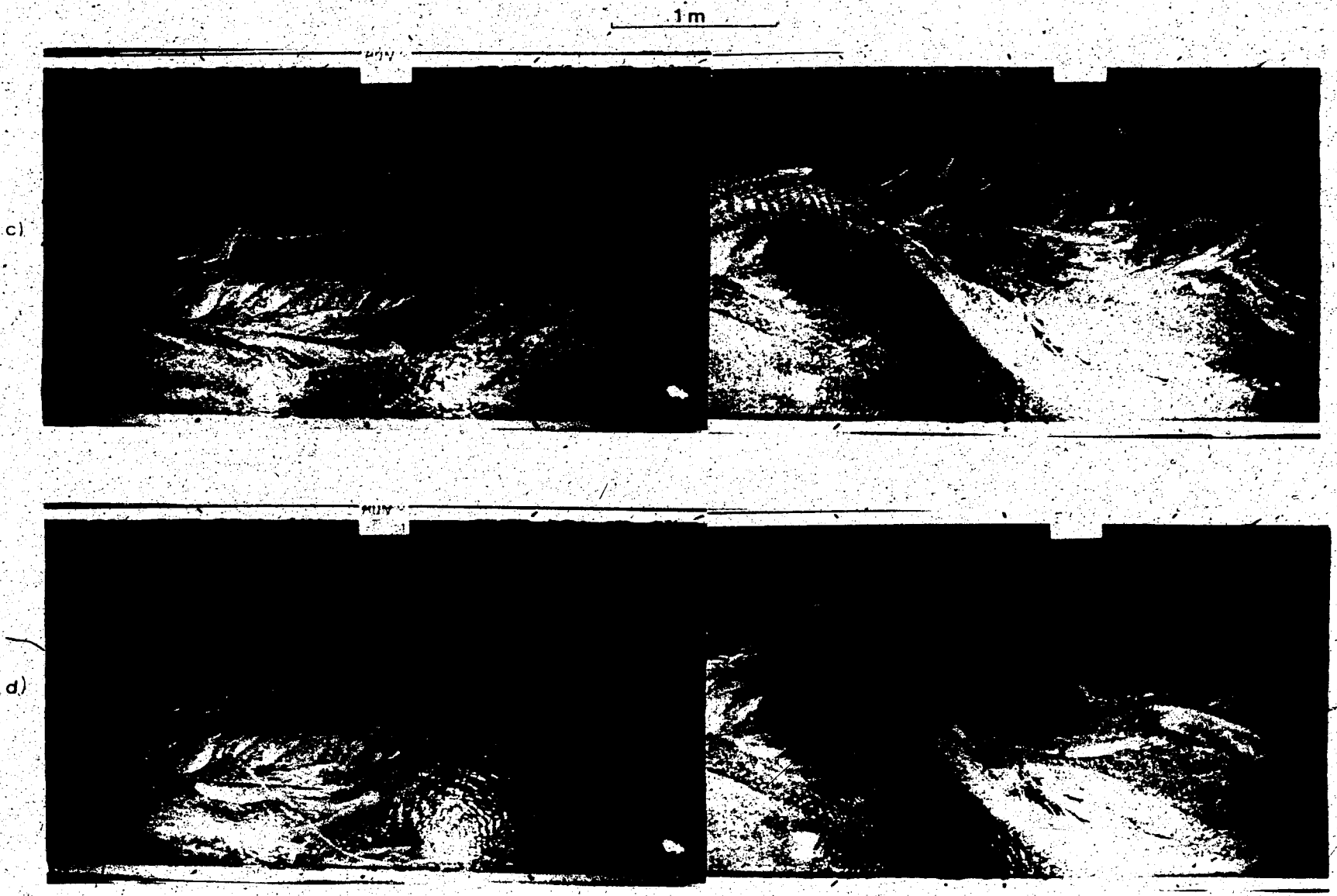
1 m
c)
d)

the medial bar had become almost completely abandoned with only a small discharge dissecting and reworking small areas of the bars deposited by the previous high discharge. Shortly afterwards a pulse of sediment from upstream passed through the scour hole and a large transverse bar developed downstream of the confluence [A in Figure 8-14 (d)]; the beginning of a new phase of sedimentation in the channel which reworked the left-hand side of the original medial bar.

A remarkably similar sequence of reorientation occurred on the Sunwapta River in August, 1981. Unfortunately, high discharge for several days made observation of the complete sequence of events very difficult but Figure 8-15 shows photographs taken 8 days apart in which dramatic changes in the channel pattern are apparent. On August 15 [Figure 8-15 (a)] a large confluence (A) was present downstream of which flow divided to run down both sides of the outwash (the left-hand route had been the dominant one for the previous several weeks, and possibly for several years, based on the author's occasional visits to the area). Within a week, however, the confluence changed its form completely; the right-hand confluent channel was almost completely abandoned and as a result [A in Figure 8-15 (a)] the left-hand confluent channel became dominant and directed the flow down the right-hand side of the outwash (B) [Figure 8-15 (b)]. The route down the left-hand side was almost completely abandoned (C) and shows a series of sediment sheets at its upstream end very similar to that described in connection with Figure 8-14. Figures 8-15 (d) and (e) show detail from Figure 8-15 (a) and (b), and Figure 8-15 (f) shows the same site viewed from the air in October, 1981, after peak summer flows had subsided. The following summer [Figure 8-15 (c)]

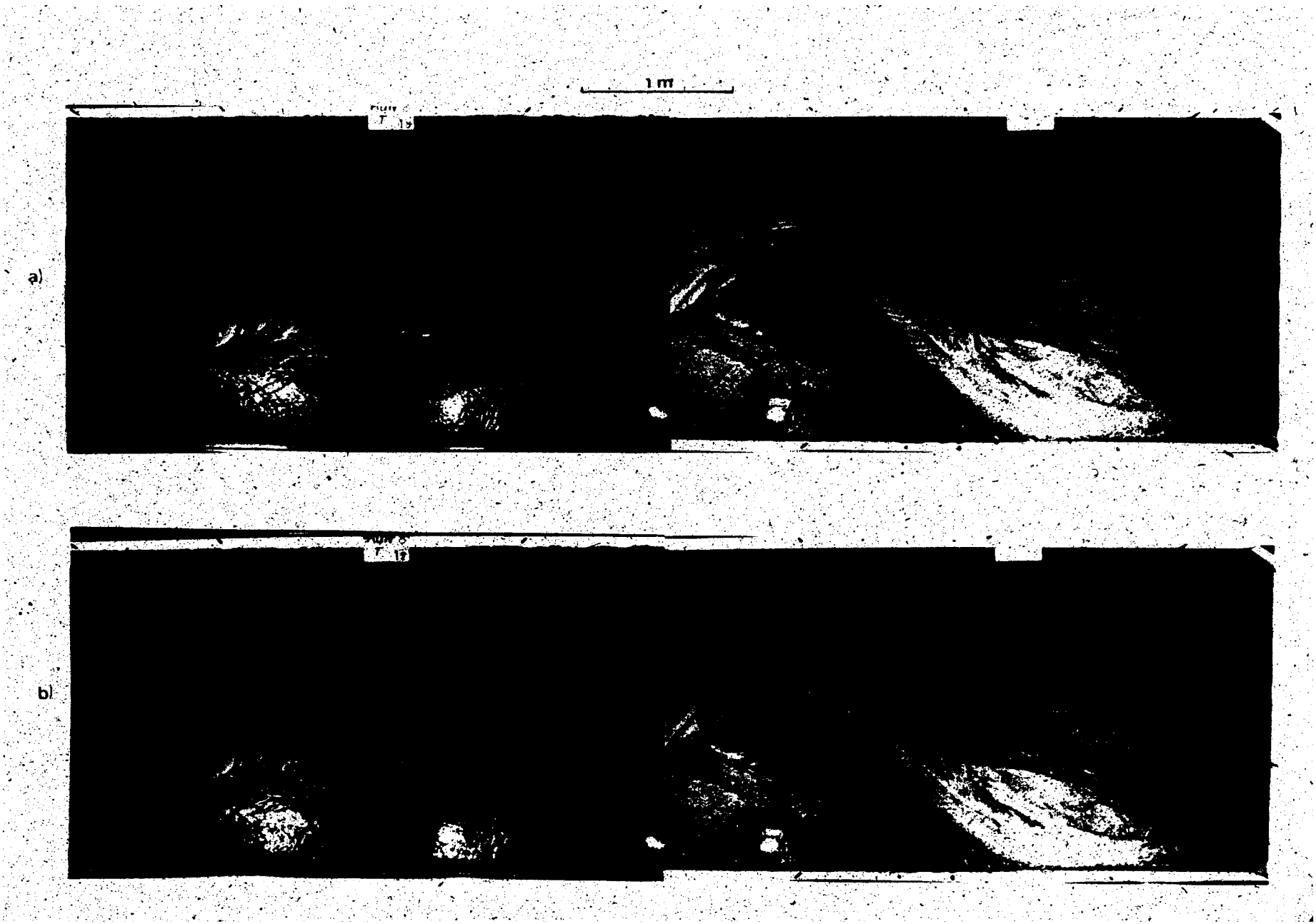
1 m
a)
b)

Figure 8-15

Channel switching downstream of a confluence on Sunwapta River. Photographs (a), (b) and (c) were taken on August 15 and August 23, 1981, and July 5, 1982, respectively, while (d) and (e) are enlargements of parts of (a) and (b). C in (b) and (f) marks the same location in both photographs. Photograph (f) was taken in October, 1981. Flow is from left to right and the highway gives an indication of scale.


a)
C
b)
c)
D

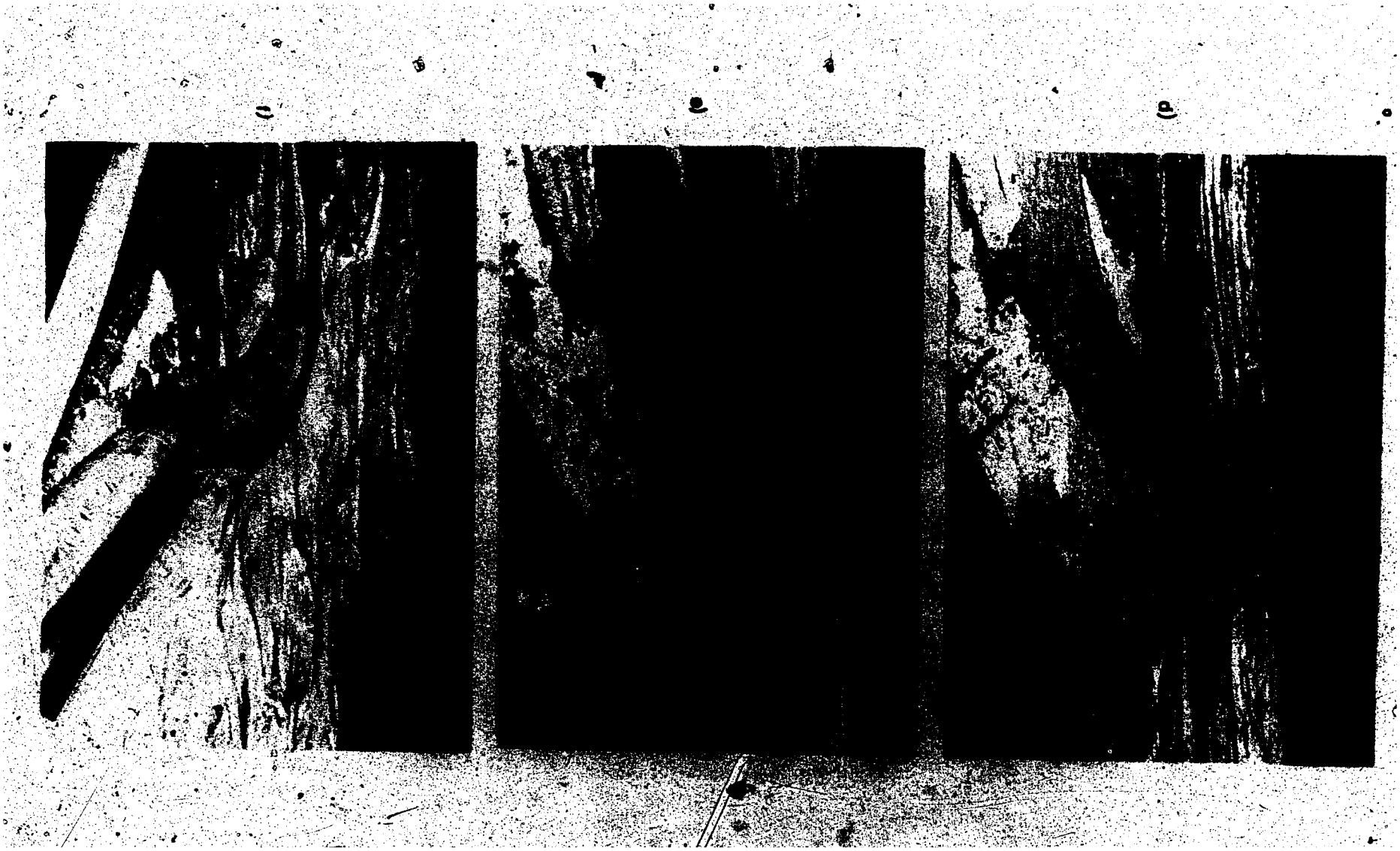

the new channel had become well established and the channel further downstream had undergone considerable modification [D in Figure 8-15 (c)].

Figure 8-16 shows a portion of an air photograph of the Sunwapta River in the field area taken in 1958. In the centre of the photograph is a complex bar (A) emplaced immediately downstream of a large, asymmetric confluence (B). A large slip-face bar (C) can be seen building into the scour hole from the right-hand confluent channel and a large asymmetric sediment lobe (D) is being deposited downstream of the scour hole, around which the flow is beginning to divide. The result has been to accrete a sheet of material (E) onto the head of the complex bar. There is a clear resemblance between these features and those from the laboratory discussed earlier in this section.

It is apparent from these descriptions that changes in the discharge, orientation or positions of the confluent channels can have a marked influence on the sedimentation further downstream. The confluences, as nodes in the system through which all the water and bedload must pass, are important in determining the location and nature of the sedimentary patterns in the river. This is particularly obvious when one views time-lapse films of the laboratory experiments and observes the repeated reorientation and relocation of scour holes and the resultant reworking of the bars downstream.

8-5 Bar Accretion

It has long been realised that the large inter-channel bars present in braided streams are the result of a long sequence of erosion and deposition (Krigström, 1962; Smith, 1974; Bluck, 1979, Ashmore, 1982). In some cases it is possible to identify from the complex bar the depositional stages responsible for the complex

a)

b)

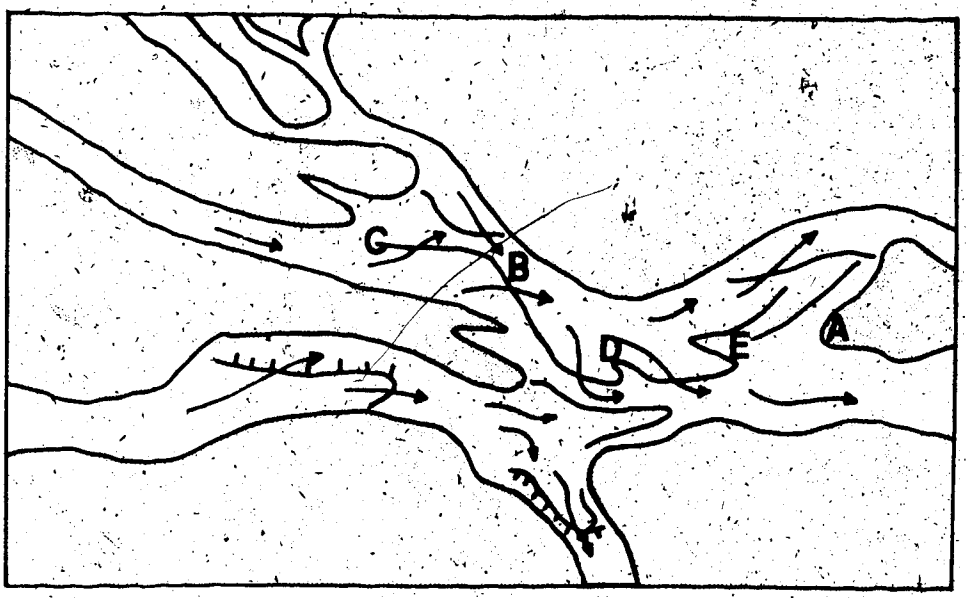

Figure 8-16

Sedimentation downstream of a confluence on Sunwapta River. Flow is from left to right. The accompanying sketch (b) and the text provide an explanation of the features labelled. This is an enlargement from airphoto A16084-99 supplied by the National Air Photo Library, Ottawa. The length of river portrayed is about 0.5km.

form and this is particularly true in braided streams. Bluck (1979) and Church and Jones (1982) suggest that the rapidity of channel migration is largely responsible for this. In more stable single channel streams there are many more opportunities for the river to rework the unit bars added to each point bar and for them to "anneal into their (the point bars') fabric in such a way that they are no longer recognisable" (Bluck, 1982, p.342). Thus, in braided streams, the evidence of the accretion of smaller units onto larger ones is present in the channel and floodplain sediments. Physical modelling allows observation of the processes by which this accretion takes place.

Observations in the model revealed that accretion occurred by both large unit bars and by thin diffuse sheets. Whether these two bedforms are end points of a continuum or separate forms is unclear. Their difference in scale is apparent when diffuse sheets are seen migrating across existing large bars, but in practice low transverse bars are little different in form from gravel sheets. As discussed previously, pronounced transverse bars with avalanche faces are particularly prone to develop in areas where depth increases rapidly or where there are obvious changes in flow competence. In this sense, therefore, the larger unit bars are much more a product of the changes in channel form encountered by a sediment pulse as it migrates downstream. The diffuse sheets, on the other hand, occur throughout the channel system, although their form must also be altered when they encounter features such as channel confluences. Regardless of this, the unit bars are more noticeable both before and after their accretion to complex bars, simply because of their greater size.

The observations of channel division described previously showed that bed

aggradation was accomplished by the deposition of discrete sedimentary sheets migrating downstream. It is apparent from the time-lapse films that this is also true of accretion to the margins of the channel. Figure 8-17 illustrates how accretion takes place at the head of a medial bar. Observation of the events producing this accretion showed that the major shifts in channel position were the direct result of individual sediment pulses in sheet or bar form. For example, the sheets whose margins appear at A in Figures 8-17 (a) and (b) were each deposited from single pulses in the space of only 2 or 3 minutes. These headward accretions commonly contain the coarser part of the load, particularly at the sheet margins. In the field the margins sometimes have finer material (granules and sand) covering them but these sizes were not represented in the model. The net result of this accretion is an upstream building of the bar head which may or may not preserve the individual sheets in the bar structure.

Lateral accretion to either medial or lateral complexes can also be traced to the passage of individual bedforms. In this sense the accretion is in some ways similar to the formation of scroll bars on the River Klarälven, described by Sundborg (1956), in which each scroll bar is formed by the deposition of an individual transverse bar swept onto the inside of the bend by secondary currents. In the case of the braided stream the individual bedforms vary in thickness but are either diffuse sheets or unit bars. Figure 8-18 illustrates how this kind of accretion may occur. In this case at least three distinct sheets of material passed through this section of channel over a period of one hour. The spacing of the sheets suggests that they should probably be referred to as unit bars. The deposition was accompanied by erosion of the far bank but it is not known

Figure 8-17

Accretion at the head and margins of a medial bar by successive pulses of sediment. See text for explanation. Flow is from right to left and the black marks on the inside wall of the flume are one metre apart.

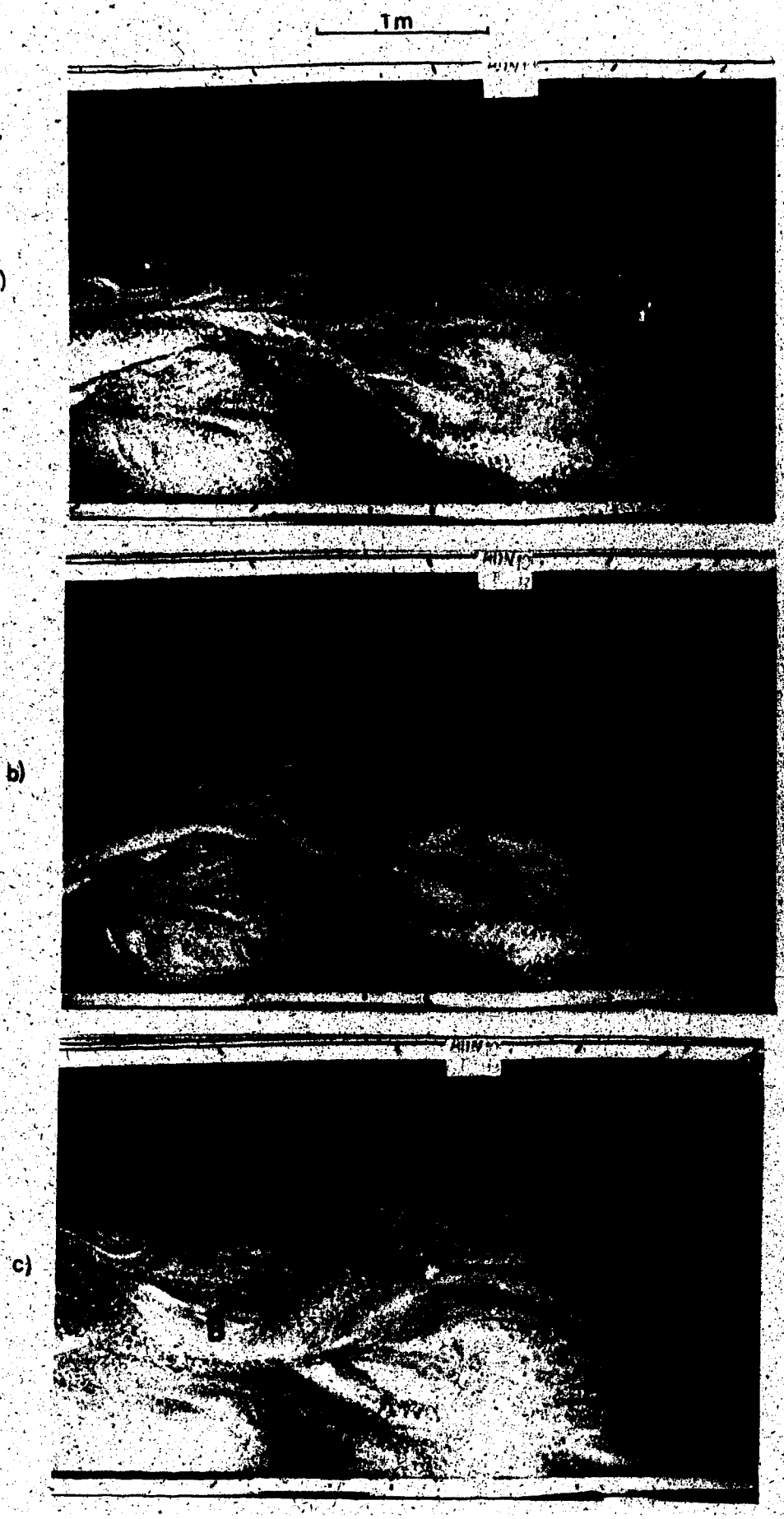
1m
a)
b)
c)

Figure 8-18

Lateral accretion by a series of sediment pulses.

Flow is from right to left and the black marks on the inside wall of the flume are one metre apart. Lateral migration of the channel at A is accompanied by accretion of sheets at B.

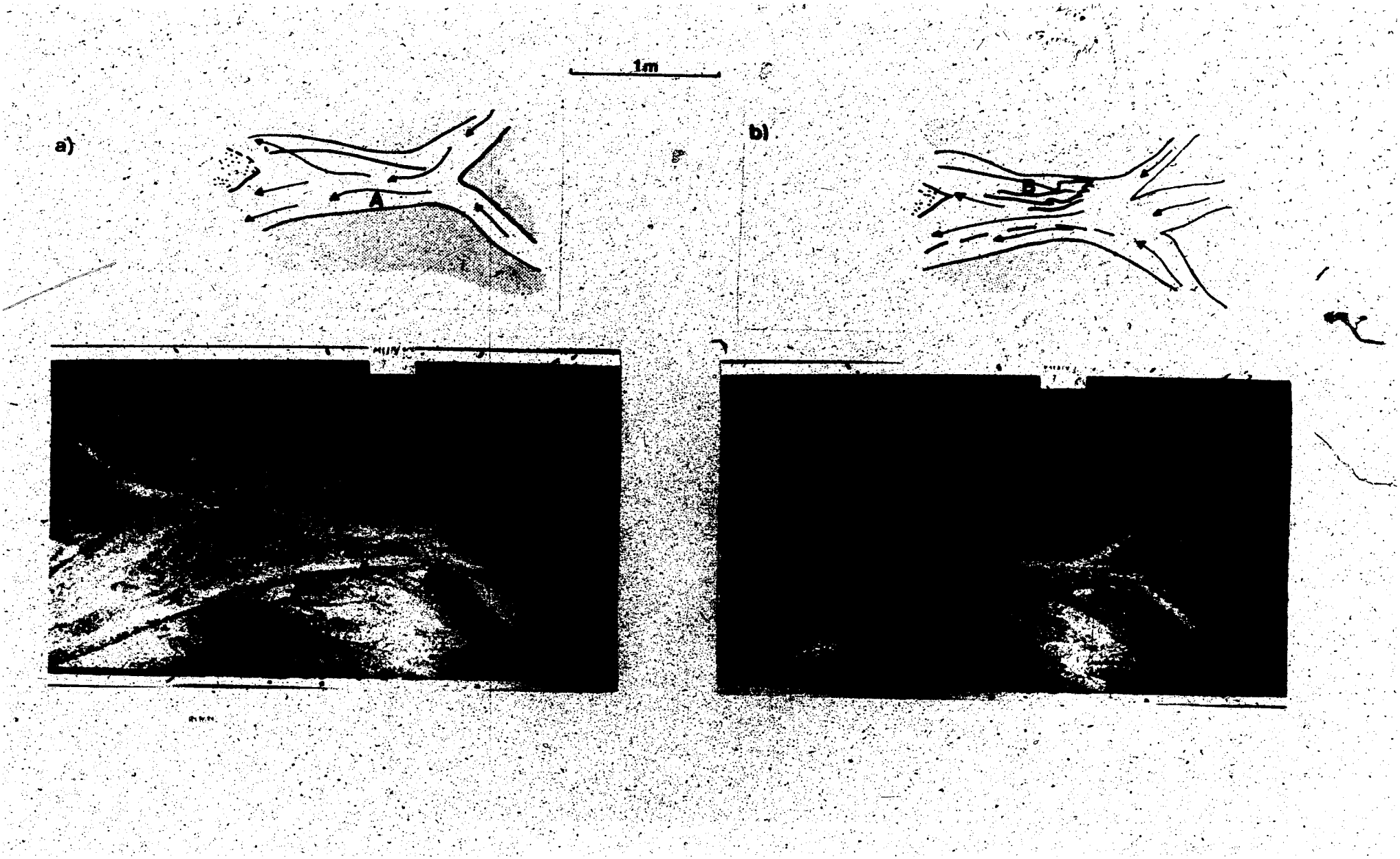
1m
a)
A
b)
B

whether the bank erosion occurred in stages associated with the passage of each sheet. Figure 8-17 shows a similar sequence of lateral accretion, particularly to the left-hand side of the medial bar [B in Figure 8-17 (c)]. The point bars illustrated in Figure 8-3 also show clear examples of accretion from individual sheets, some of which undergo further sorting and dissection after being deposited (Bluck, 1979). Ashmore (1982) described the accretion of these "overlapping sheets" but did not ascribe them to individual sheets of material passing along the channel.

The photographs in Figure 8-18 illustrate that the continued lateral migration of the channel resulted in the whole area being abandoned by avulsion and accreted to the pre-existing exposed bar complex. It also illustrates the important point that many medial bar complexes are the result of channel avulsion or cut-off of a lateral bar.

Figure 8-19 presents some examples of sheet deposition in the field. In Figure 8-19 (a) the medial bar (A) has at least two sheets accreted to its upstream margin. This kind of accretion is also visible splaying diagonally out from the bar head in Figure 8-19 (b), while in 8-19 (c) the sheet on the far side of the bar head is connected to a tongue of bed material in the adjacent channel. Figures 8-19 (d), (e) and (f) illustrate the deposition of similar features during the summer of 1981. Figure 8-19 (d) shows the accretion of a simple sheet to the inside of a bend. In Figure 8-19 (e) the downstream migration of a single sheet and its eventual division around a pre-existing bar is illustrated and Figure 8-19 (f) shows the development of sheets as part of a sequence of flow division and channel migration. Channel changes of a similar kind have been documented by Hein (1974) on the Kicking Horse River, British Columbia.

Figure 8-19

Examples of bar accretion from Sunwapta River.

(a) The medial bar, A, has two or three sheets accreted to its upstream margin. The edges of these sheets run in a V pattern from above and below the letter A meeting about 0.5cm to the left of the letter. Flow is from left to right, the highway in the foreground indicates scale.

(b) Sheet margins are visible on this medial bar near the upstream end of the study reach. The most obvious sheet (A) occurs on the right-hand side of the bar and its margin runs out into the adjacent channel just to the left of the letter A. Flow is from right to left.

(c) Several sheets are visible in the vicinity of this medial bar. The most obvious lies just above the two letter A's and runs diagonally outward down both sides of the bar from the upstream end of the bar. Flow is from bottom to top.

Figure 8-19 contd.

(d) Bar accretion in a bend.

(i) July 21, 1981. The flow is directed towards a confluence in the vicinity of A.

(ii) July 31, 1981. Bar deposition and channel migration upstream resulted in the deposition of a large sheet (B) on the inside of the bend downstream of the original confluence (A).

(iii) August 23, 1981. Further modification of flow in the confluence (A), in particular the dominance of the left-hand channel (C), has resulted in the accretion of a second sheet (D) to the inside of the bend.

d)

i)

ii)

iii)

Figure 8-19 contd.

(e) Migration of a single sheet. Flow is from bottom to top of each photograph.

(i) July 15, 1981. The margin of a sheet of gravel is apparent in the channel at A, just downstream of a flow division.

(ii) July 31, 1981. The sheet margin has migrated a few meters downstream.

(iii) August 23, 1981. Following a period of high flow the sheet has advanced several metres further downstream where flow division round a developing medial bar (B) has resulted in the formation of two separate avalanche faces (A and C).

e)

i)

ii)

iii)

Figure 8-19 contd.

(f) Development and migration of unit bars and their accretion into a medial bar. Flow is from top to bottom of each photograph.

(i) July 1, 1981. A small bar is apparent at A where flow is beginning to divide. This is causing bank erosion at B and deposition of sheet at C.

(ii) July 9, 1981. Following a heavy rainstorm bank retreat has occurred at B, accompanied by pronounced avalanche-face bar development at A (apparently an enlargement of A in (f)(i) and D. The sheet at C is exposed at this discharge.

(iii) August 7, 1981. Bank retreat at B has proceeded further and the original bars (A and D) have been partly abandoned and new sheets E and F have formed. The sheet C is still visible and has a log stranded on it.

Further examination of this site was unfortunately impossible because of its inaccessibility during high flows in August. When examined in late August the major channel switching upstream (Figure 8-15) and modification by high discharges made the features impossible to relate to those photographed on August 7.

f)

8-6 Channel Avulsion

Channel migration in braided rivers occurs either by progressive lateral movement associated with bank erosion and lateral accretion, or by sudden jumps in channel position caused by overtopping of banks, and often involving reoccupation of previously abandoned channels (Church, 1972; Ashmore, 1982). The latter is referred to as avulsion. In fact avulsion is most commonly a simple cut-off of the kind described in the earlier section on flow division. The alignment of the new channel is often almost parallel to the avulsing channel.

More radical channel shifting may also be the result of avulsion and an example of this is illustrated in Figure 8-20. A large transverse bar was deposited on the inside of a bend near the upstream end of the flume at 35 hours of run 11 [A, Figure 8-20 (a)]. Accretion of the downstream margin of this bar and cut-off of the bend caused erosion of the bank on the opposite side of the channel and, together with further aggradation downstream of the bend, eventually resulted in overtopping of the bank [B, Figure 8-20 (b)]. This overbank flow reoccupied an abandoned channel and began to enlarge the channel, transporting the eroded sediment downstream until it emerged into a deeper abandoned channel into which a delta-like avalanche-face bar then prograded [C, Figure 8-20 (b)]. The avulsion channel remained occupied for about one or two hours but, as is the case in many of the avulsions observed, it was eventually abandoned again. This was apparently the result of incision [D, Figure 8-20 (d)] of the larger channel into the deposit which had originally aided the avulsion.

It is interesting to note the role of local aggradation in response to the arrival of a sediment pulse in this process. Avulsion occurred during the

Figure 8-20

Avulsion following local aggradation. See text for explanation. Flow is from right to left and the markings on the inside wall of the flume are one metre apart.

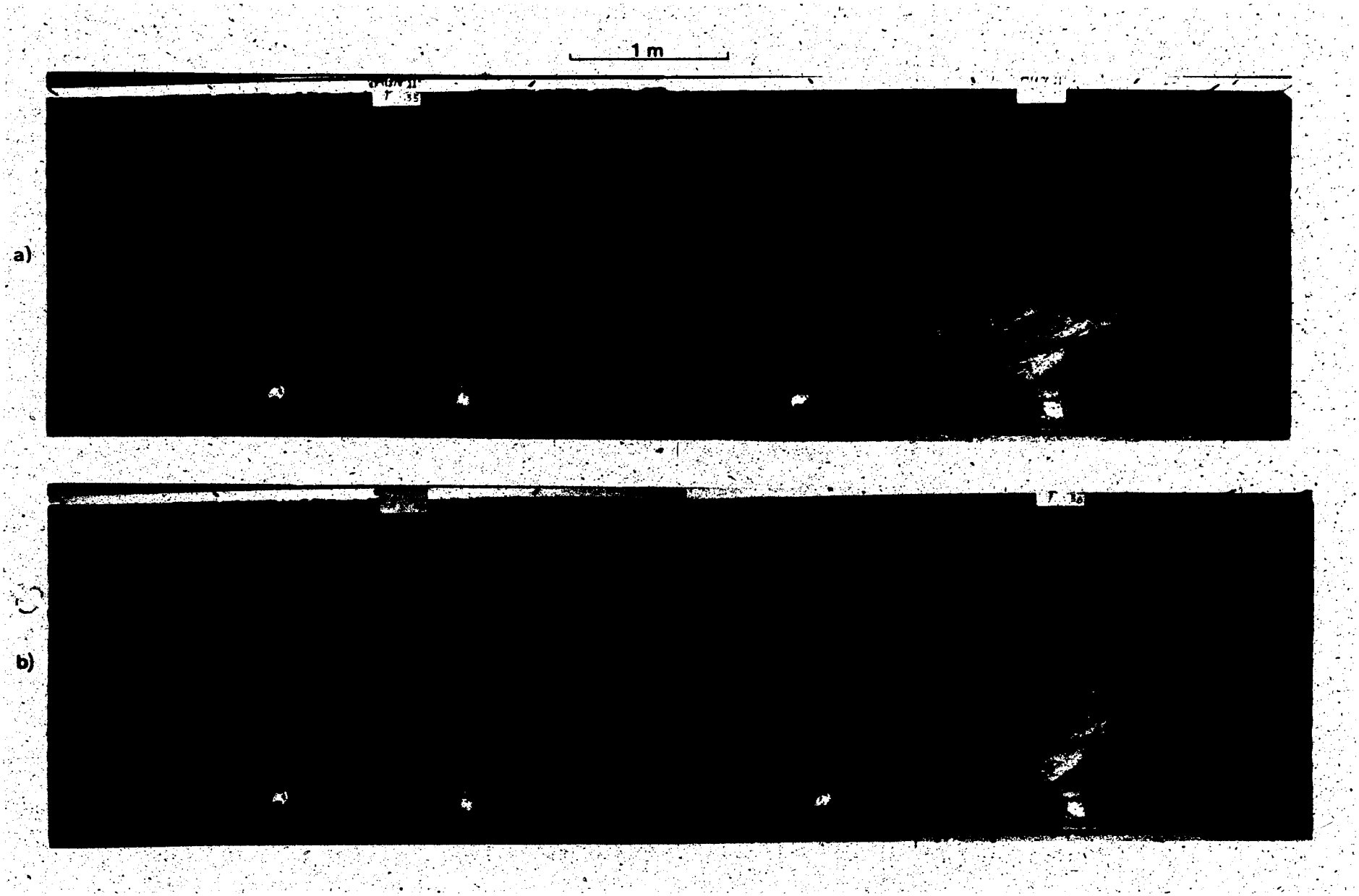
1 m
a)
b)

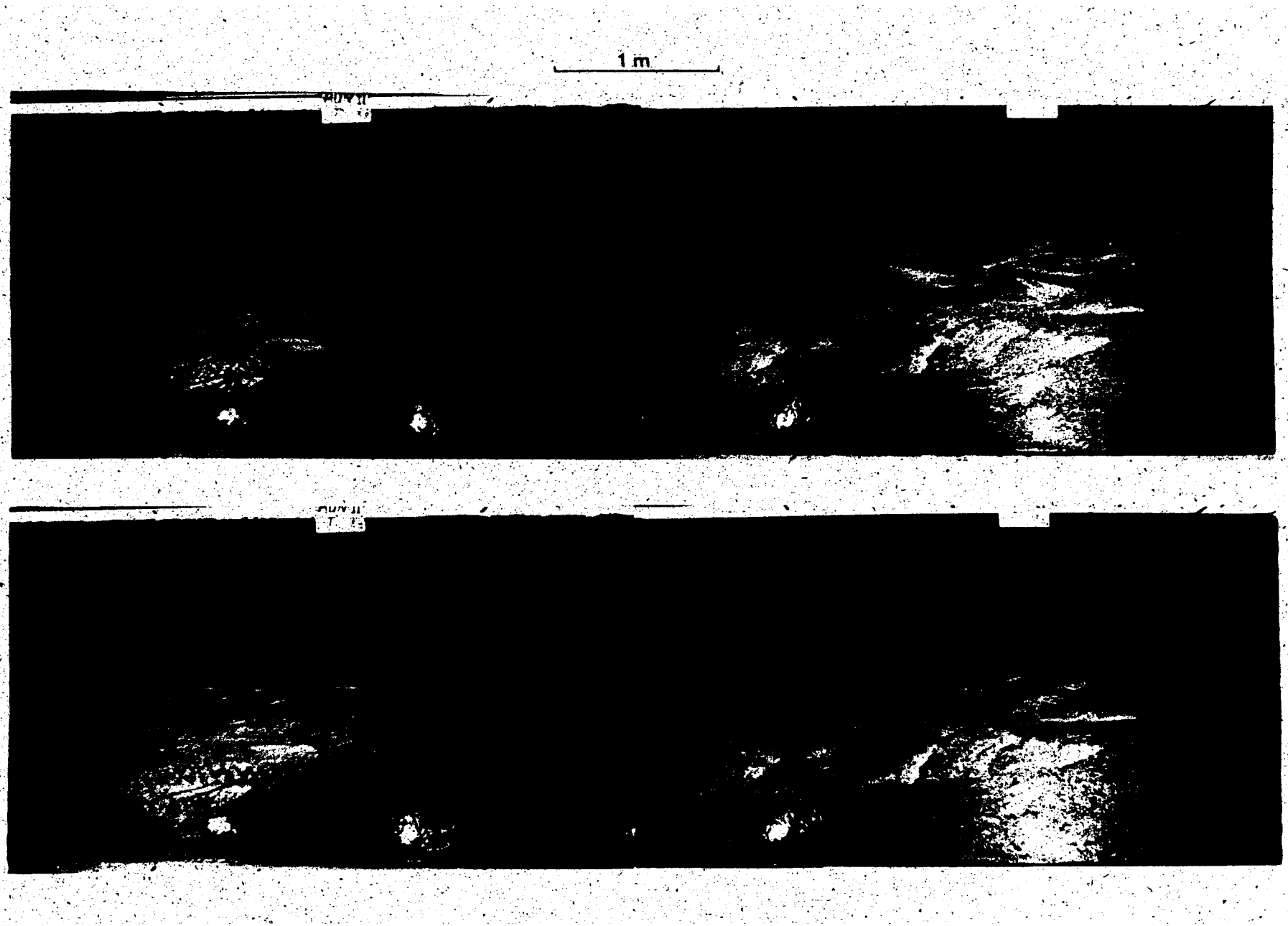
1 m

aggradation phase but soon afterwards the sediment transport rate declined and incision caused the abandonment of the avulsion channel. Inspection of the sediment input graph for run 11 reveals that a major sediment pulse arrived at the head of the flume between 33 and 34 hours. It was this sediment pulse that caused the avulsion illustrated in Figure 8-20. Indeed, Figure 8-20 illustrates a number of other features and processes previously discussed, such as alternating bar formation and point bar cut-off [E, Figure 8-20 (b)], and the general principles of increased braiding intensity and avalanche face development during local aggradation (see Chapter 7).

The idea that avulsion is most common during periods of local aggradation is an interesting adjunct to the discussion in Chapter 7. Demonstration of a general correspondence between the time of arrival of sediment pulses at the upstream end of the flume and the occurrence of channel avulsions is complicated for the reasons outlined in Chapter 7. Most notably there is a lag between the arrival of the sediment pulse and aggradation in the flume which increases with distance from the head of the flume. Thus, avulsion several meters downstream may be difficult to relate to a specific pulse in the sediment delivery at the head of the flume. Choosing between what is or is not an avulsion and deciding the exact time at which the avulsion occurs also make quantitative analysis difficult. Figure 8-21 shows the sediment delivery graph for run 11 together with the time of occurrence of obvious avulsions. Some of these clearly coincide with, or occur soon after, peaks in the sediment input (for example, 10, 22, 28, 35, 40, 61 hours) but others (18, 26, 56 hours) do not coincide with such pronounced peaks. Clearly not all avulsions result from the arrival of sediment pulses and nor do all sediment pulses produce avulsions, but there is often a coincidence of the two.

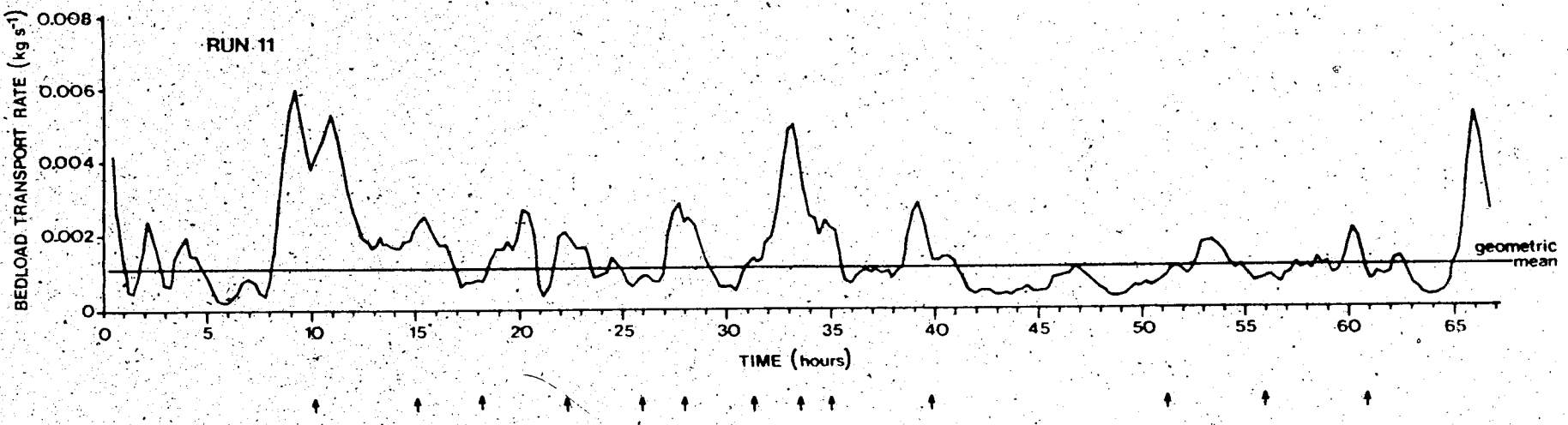

Figure 8-21 The relationship between the arrival of sediment pulses at the head of the flume and the occurrence of channel avulsions in the braided channel downstream in run 11. The arrows indicate the occurrence of avulsions identified from time-lapse film.

Avulsions are also common downstream of scour holes and are a common feature of the scour hole reorientation discussed in the previous section. Figure 8-22 shows an example of this from run 10. At 36 hours [Figure 8-22 (a)] no obvious scour hole was present near the head of the flume apart from a low angle confluence at A [Figure 8-22 (a)]. During the next hour a pulse of sediment was delivered to the head of the flume one of the results of which was to alter the channel configuration on the left-hand side of the flume [B, Figure 8-22 (b)]. The enlargement and rightward migration of a channel in this area resulted in the formation of an obvious scour hole at C [Figure 8-22 (c)] at 38 hours. The left-hand confluent channel (D) appeared to have a larger discharge and to be carrying a larger sediment load than the right-hand channel, so that the confluence that began oriented obliquely to the left, swung round roughly parallel with the long axis of the flume. A large diagonal bar with an avalanche face prograded into the scour hole (E) causing the flow to erode the bank on the right-hand side of the channel downstream of the scour hole. This, together with the aggradation, resulted in an avulsion into abandoned channels on the right-hand side of the channel [F, Figure 8-22 (d)] at 39 hours. By 41 hours [Figure 8-22 (e)] this avulsion had established itself as a major channel. Shortly afterwards, however, the balance of flow in the confluent channels changed again and the scour hole began to orient itself obliquely to the left again, and to migrate in that direction in response to lateral accretion at G [Figure 8-22 (f) and (g)]. This reorientation reduced flow through the avulsion to a comparative trickle [H, Figure 8-22 (h)] by 44 hours.

Figure 8-22

Channel avulsion in association with reorientation of a confluence scour hole. See text for explanation. Flow is from right to left and the markings on the inside wall of the flume are one metre apart.


1m
a)
c)

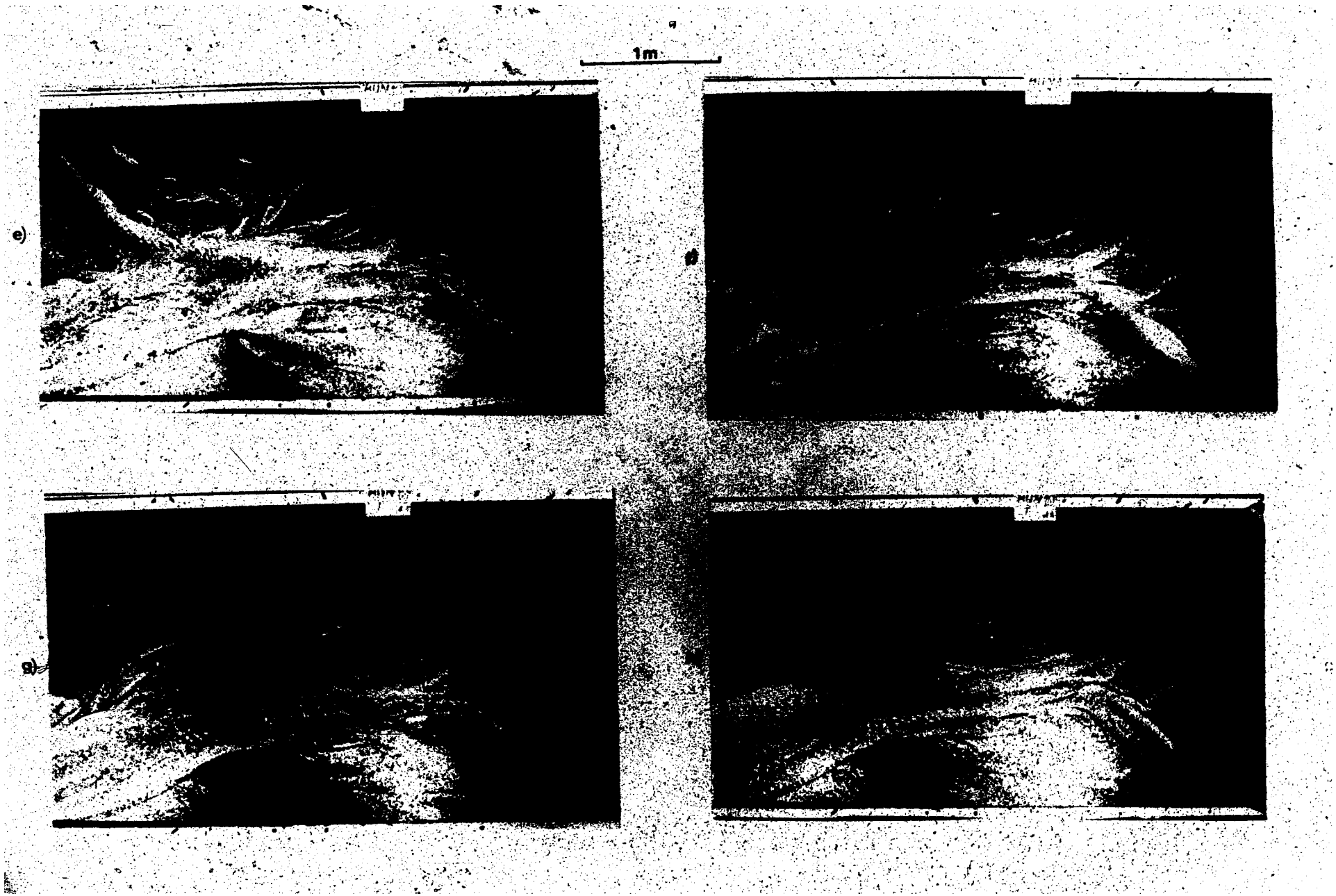
1m
e)
g)

8-7 Downstream Movement of Sediment Pulses

The morphological effects of the arrival of large sediment pulses at the head of the flume have been described in Chapter 7 and also in the previous section. The possibility that such pulses are transferred downstream, and so modify channel form progressively downstream, was also discussed in Chapter 7. It is apparent that processes such as avulsion, bar construction and channel division should be the most obvious manifestations of this transfer of sediment.

The best chance of observing the transfer of sediment pulses is in runs where the channel pattern is simple and the rate of change fairly slow. The time-lapse films of run 11 proved to be the best source of information and these observations are documented in Figure 8-23 and 8-24.

The first traceable pulse occurred at about 20 hours and this sediment was carried downstream to be deposited at point A [Figure 8-23(a)]. At about 21 hours the resultant deposit was dissected and accumulation commenced about 2 meters further downstream (B). This occurred in response to accumulation near the head of the flume (C) which starved the downstream area of bed material. When this upstream accumulation at 2-3 meters started to degrade, at about 23 hours, aggradation recommenced 1-2 meters further downstream (D), which was transferred a further 2 meters downstream about two hours later (E). Thus, between 20 and 26 hours two sediment pulses moved downstream, by successive aggradation and degradation, in steps of about two meters. Aggradation took the form of complex medial and/or lateral bars.

Two further examples of the movement of sediment pulses can be seen between 40 and 60 hours of run 11. Aggradation occurred first near the head of

Figure 8-23

Transfer of sediment pulses downstream during run 11. See text for explanation. Flow is from right to left and the black marks on the wall of the flume are one metre apart.

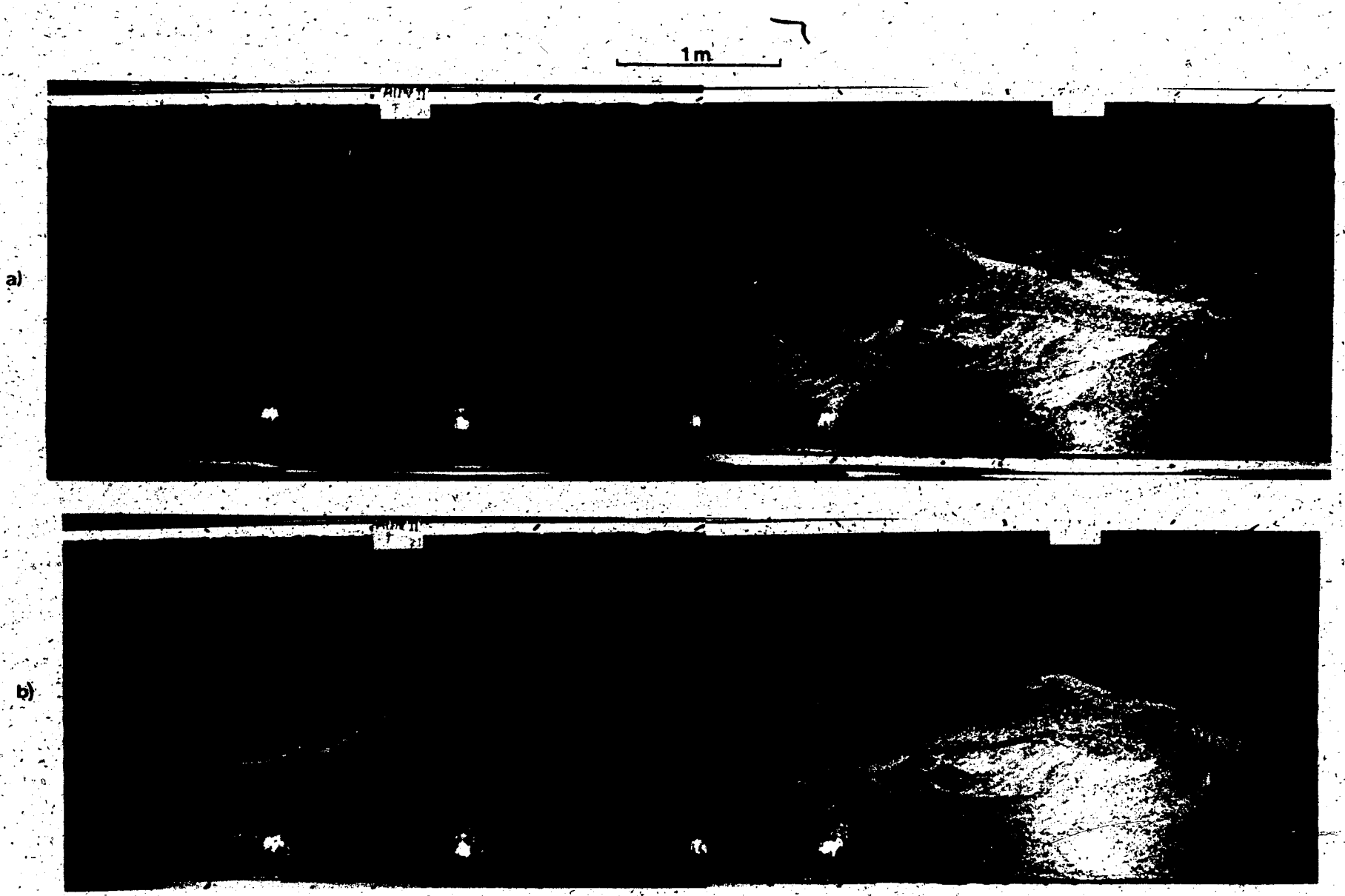
1m
a)
b)

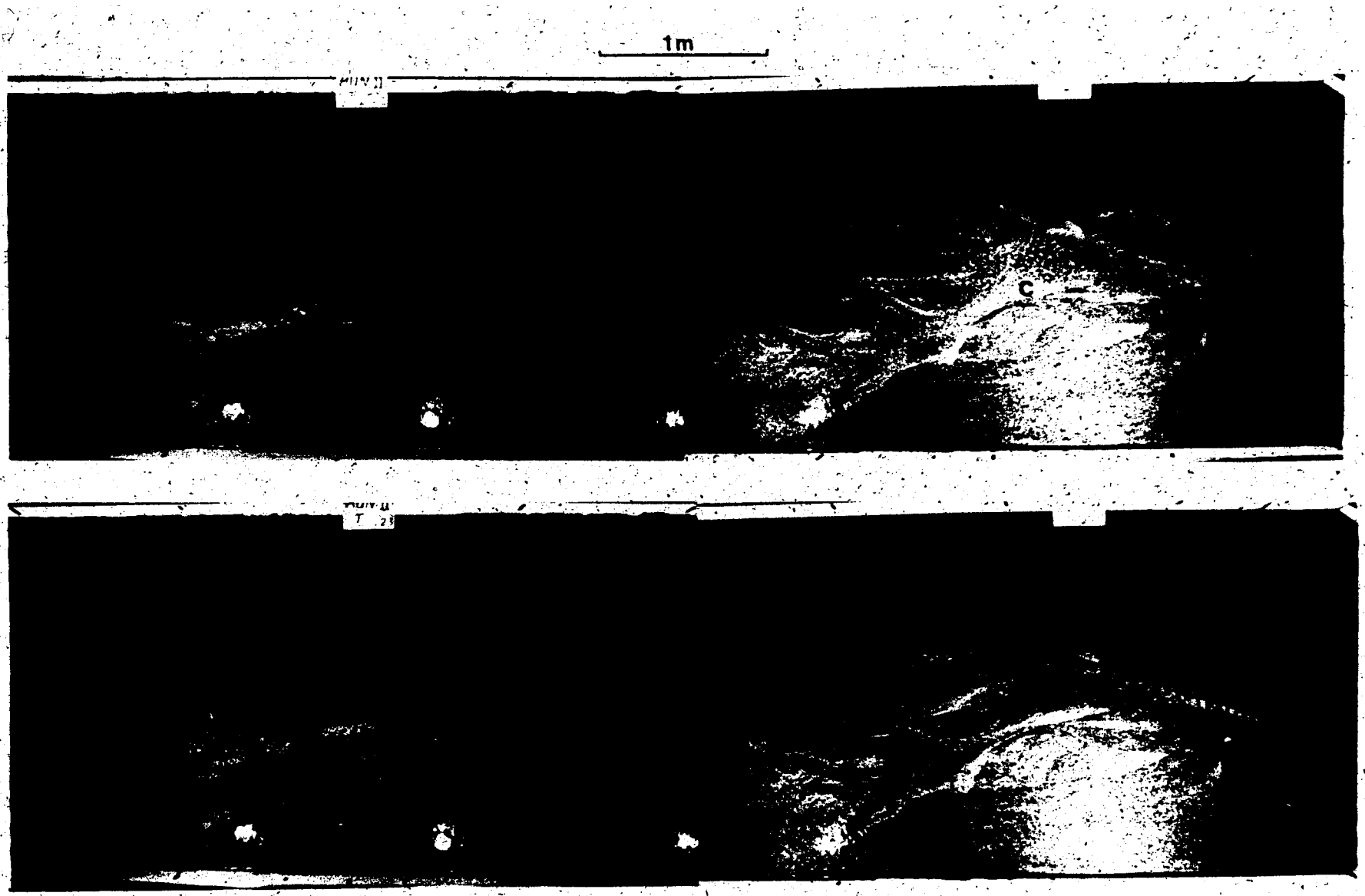
1m
c)
C
d)

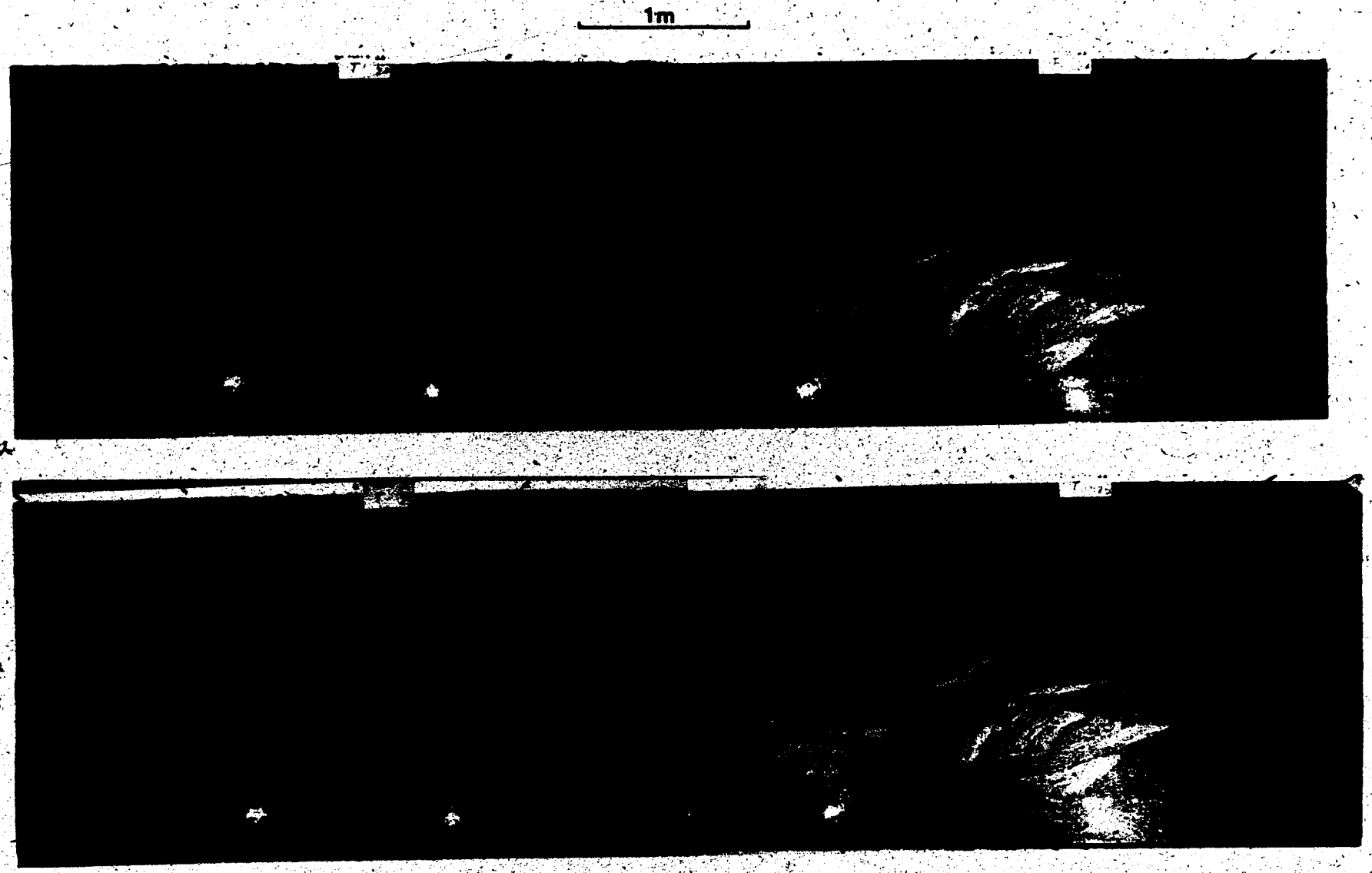
1m
a)
b)

Figure 8-24

Further examples of the downstream transfer of sediment pulses in run 11. See text for explanation. Flow is from right to left and the black marks on the wall of the flume are one metre apart.

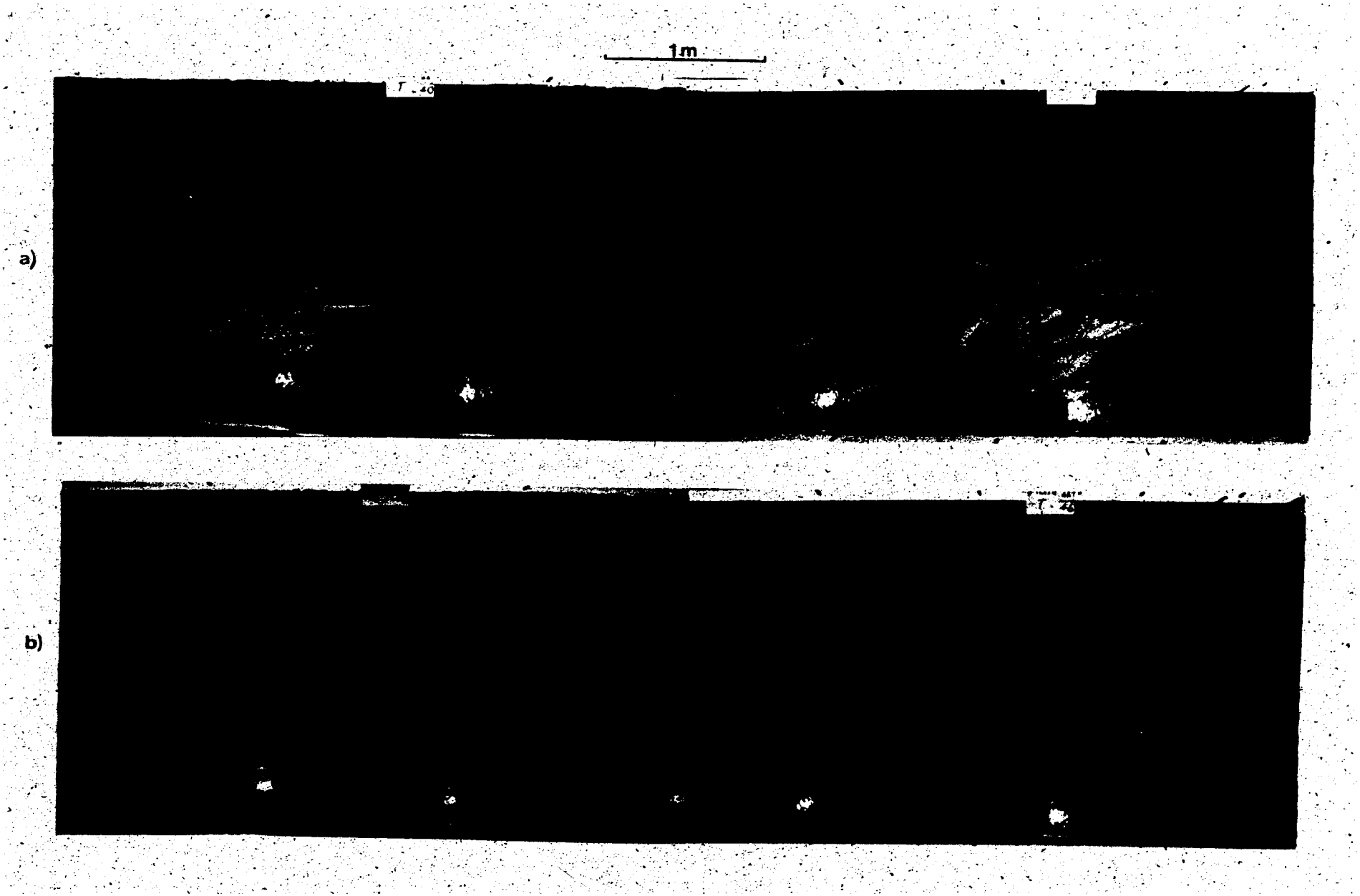
1m
a)
b)

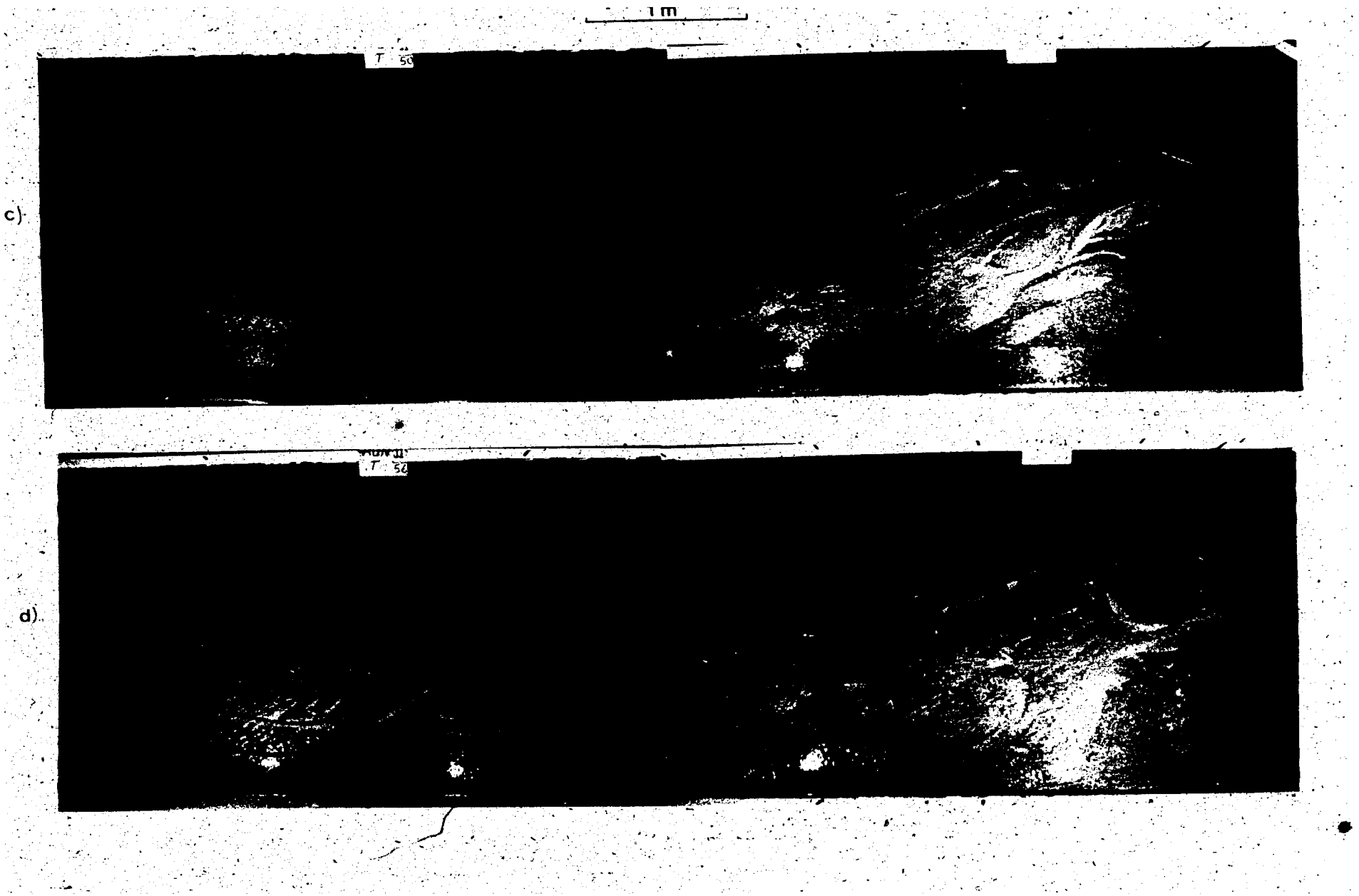
1 m
c)
d)

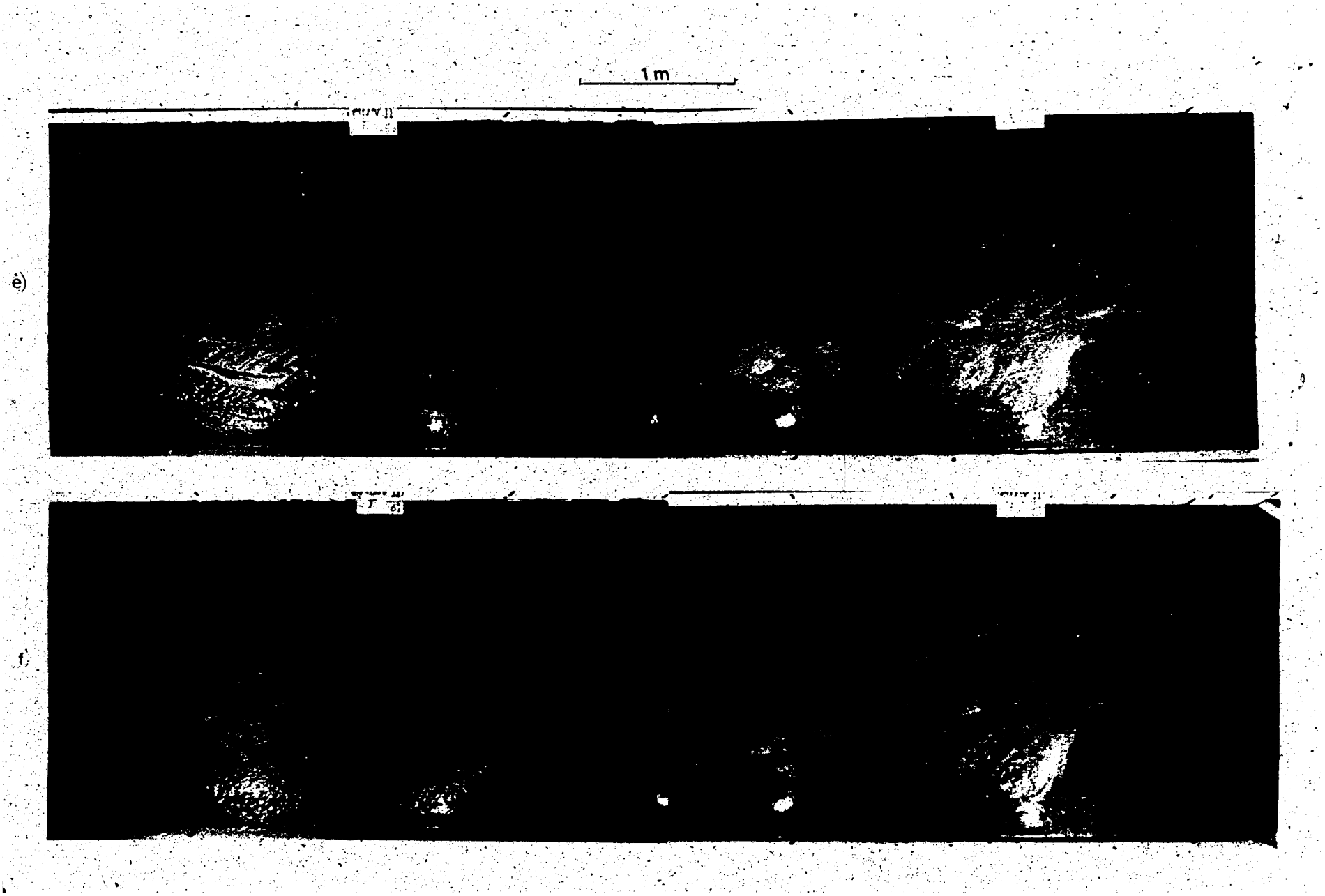
1m
e)
f)

the flume at about 40 hours (A, Figure 8-24). At 45 hours this area was dissected and aggradation began at 3-4 meters (B). The sediment in this deposit was transferred about one meter downstream at 48 hours (C) and a further two meters at 51 hours (D).

At about this time renewed aggradation was occurring at the head of the flume (E). This continued until about 56 hours when this accumulation was by-passed and fresh deposition commenced at 3 to 4 meters (F). Degradation in this area followed about two hours later when accumulation began in the vicinity of 6 meters (G). By about 61 hours this area had in turn been dissected and accumulation began at 8 meters (H).

The initiation of these pulses can be traced to the sediment input curves which show peaks just before aggradation commenced at the head of the flume. Since a new pulse formed before the previous one had passed completely through the flume then the process is more complex than the simple cycling of a single pulse through the system. This is encouraging with respect to the question of whether the sediment input pulses simply represent the repeated cycling through the system of the large sediment load generated in the unpaved, unconsolidated channel at the beginning of each run (see Chapter 5). The presence of at least two pulses passing through the flume at the same time suggests that there are other sources of the pulses apart from this initial activity.

The typical transfer distance in run 11 is roughly 1-2 meters. This distance (about 1.5 meters) corresponds to half the initial meander wavelength (i.e. the distance between successive point bars or alternating bars). The fact that the channel in run 11 rarely split up into more than two channels and was often a

single channel for some of its length, probably contributes to this regularity. Attempts to trace similar events in other runs were hampered by the more complicated channel patterns, the impingement of channels on the flume walls, and the rapidity of change. Nevertheless, it was possible to form a rough impression of similar events even in the high discharge runs. In run 9, for example, transfer distances seem to be about 4 meters so that there is only one intermediate depositional zone between the initial accumulation at the head of the flume and its passage into the tail box.

The temporal spacing of these aggradational events seems to coincide with the intermediate-term periodicities in sediment input (4-8 hours) discussed in Chapter 5, thus the physical nature of these pulses is now apparent. They appear as a series of lobes of sediment accreting in a small area of the flume to form lateral and medial complexes before being transferred downstream to another depositional site. Often an area of flow convergence intervenes between successive depositional sites (at which flow is generally divergent) and the configuration of the flow into the convergence controls the form of the junction and the location of the deposition downstream.

Observation of the films showed the large, infrequent (10-12 hour) pulses seen particularly in the high discharge runs to be the result of the main channel sticking close to the side of the flume near its downstream end. Why this should occur periodically is not known but it suggests a regularity in the timing of channel migration.

8-8 Evolution of a Complex Flat

Even though the main processes and bar forms responsible for the construction of complex flats in braided streams are now well known the developmental sequence producing such flats is still difficult to interpret from the final form of the complex. Often complexes of very similar appearance may be the result of completely different sequences of development. It is therefore instructive to follow the development of an area of the channel over several hours in the laboratory to show the kinds of events responsible for the complex forms usually visible. Bluck (1974, 1979), Cant and Walker (1978) and Ashmore (1982) have given some descriptions of the evolution of medial and lateral complexes but the intention here is to describe the development of a larger area which may encompass several such complexes. The example chosen is from run 4 and is illustrated in Figure 8-25. The following description identifies the main stages in the evolution of the complex in the top centre of the photograph in Figure 8-25 (g).

Development of the complex began between 17 hours and 18 hours when a large bar developed in the left-hand channel of the confluence at A. By 18 hours this channel had aggraded and migrated to the left resulting in avulsion to the left and almost complete cessation of flow into the confluence from the left. Some of the sediment deposited by this avulsing flow at B remained to form part of the core of the final complex. Between 18 hours and 19 hours this avulsion was abandoned in favour of the original channel in which considerable aggradation and bar building occurred (the sediment input record shows a pronounced peak between 17 hours and 19 hours). Sketches of the intermediate stages (18:30 hours

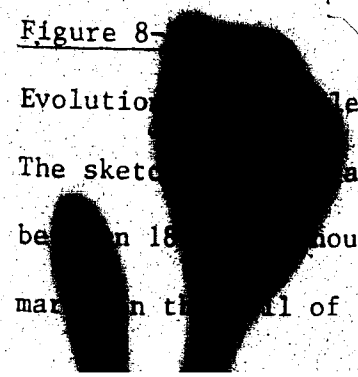

Figure 8-

Evolutio[illegible]lex flat in run 4. See text for explanation. The sket[illegible]ate the flow division in the vicinity of B be[illegible]n 18[illegible]hours. Flow is from right to left and the black mar[illegible]n t[illegible]l of the flume are one metre apart.


a)
C
18×40

and 18:40 hours) are shown in Figure 8-25. The sequence is very similar to the cut-offs described in an earlier section of this chapter. The large lateral complex developed at C contained two or three abandoned channels, cutting through the bar to the left into the slough channel, which by 19 hours had begun to capture some of the flow. The lateral complex at C was preserved in part to form a portion of the final complex. Between 19 hours and 20 hours further aggradation at the upstream end of the reach (due in large part to two large pulses of sediment) resulted in almost complete abandonment of the right-hand channel in favour of the slough channel. During this process several sheets of sediment were deposited in the left-hand (slough) channel and at one point a channel broke back to the right (D) before being abandoned in favour of the course visible at 20 hours. Between 20 hours and 21 hours the main channel shifted laterally in a series of steps each of which involved channel excavation followed by infilling, the remnants of which can be seen on the left-hand side of the final complex. The main feature of the final complex originating at this time is the abandoned channel at E. Note that for a short time some flow re-entered the right-hand main channel and deposited a small bar at the junction with the channel running along the flume wall. The final stage in development involved avulsion of the left-hand main channel back to the right near its downstream end, destroying some of the earlier deposits, and the reoccupation of the right-hand channel eroding part of the bar head and adding a single lateral sheet to the downstream end of the complex (F). The left-hand channel also deposited some lateral sheets (G) to give the complex its final form.

Many of the details of individual channel movements and bar migrations

have been left out of this description but the general course of events gives an impression of the way these small-scale features are linked to the larger-scale channel movements to produce the complex surface form visible in braided streams.

8-9 The Influence of Slope and Discharge on Channel Form

From the discussion at various points in this chapter it is apparent that channel form is visibly different at different discharges and slopes. For example, the distance between alternating bars at the beginning of each run increased with increasing discharge. At the same time the width of flume occupied by the braided channel similarly increased. The nature of this increase in width is not known because only at the lower discharges (less than 2 l s^{-1}.) did the channel remain free of the wall over most of the flume length throughout each run. The other obvious feature related to changes in slope and discharge is the rapidity with which channel changes occurred. For example, in run 11 the channel migrated across the flume perhaps 5 times throughout the run. In contrast the higher discharges repeatedly reworked their bed. This contrast in rates is a reflection of the differences in the sediment transport rate but is manifested in the rapidity with which the bedforms and channels developed and migrated. Diffuse sheets could be seen passing along the channels every two or three minutes in run 9, but only every fifteen to twenty minutes in run 7. The higher discharge runs also developed much more obvious unit bars with avalanche faces. In run 9 these were as much as 2 metres long and 0.5 wide with avalanche faces 10 to 20mm high. The lower discharge runs rarely developed avalanche-face bars. The result of this marked increase in activity is a much greater complexity in the

sedimentary forms. The bar complexes in run 7, for example, had a fairly simple history and a simple structure, but at higher discharges the events were much more complicated. The medial bar (Figure 8-26), one of the most complicated features developed in run 7, took 4-5 hours to form. An equivalent feature in run 10 was seen to develop in less than an hour. The changes in channel form therefore ranged from run 7 in which channel shifting and bar development occurred very slowly, in response to occasional increases in sediment input, and in which bar relief was very subdued, to run 9 in which large bars and sheets appeared in rapid succession sweeping downstream and laterally, creating complex bars which in some cases were developed and destroyed in the space of one or two hours. Between these two extremes, the intermediate discharges, with greater available flume width relative to their size, showed a greater tendency for channel migration across the flume and the appearance of more classical braided channel features.

8-10 Discussion

This descriptive account of sedimentation processes occurring in the laboratory model, supplemented by some examples from the Sunwapta River, has raised some important points about braided river mechanics.

It is apparent that the initial braiding mechanism itself varies with the initial conditions of channel shape and relative depth. Three different flow division mechanisms have been described; division round a mid-channel bar very similar to that described by Leopold and Wolman (1957), cut-off of low sinuosity meanders formed from an initial pattern of alternating bars, and dissection of the channel bed by shallow sheet flow into a network of 'proto-channels' which eventually combine to form a braided channel (Moss et al., 1980, 1982).

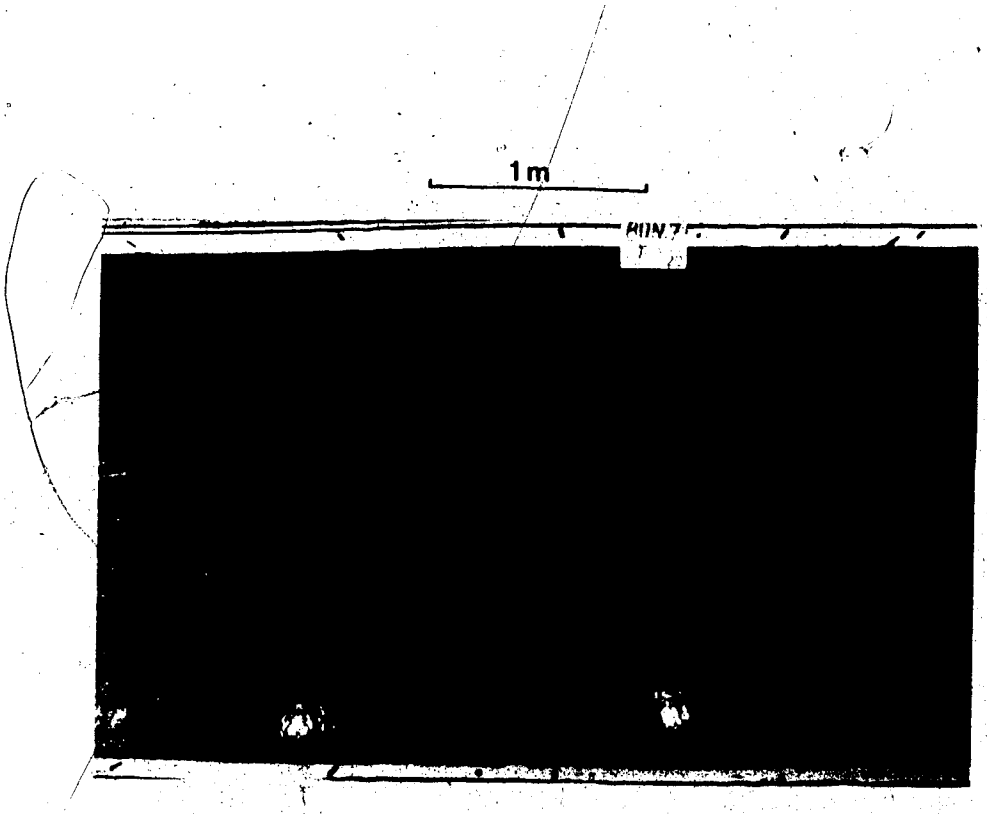

Figure 8-26

Complex bar in run 7. The sequence of development for this bar took several hours and is illustrated in part in figure 8-7. Flow is from right to left and the black marks on the wall of the flume are one metre apart.

In the experiments conducted here, runs 3 and 7 initially braided by a mechanism akin to that of Leopold and Wolman (1957), while the remainder of the runs braided by the meander cut-off process. Run B was used solely to reproduce the process described by Moss et al. (1980, 1982). Runs 3 and 7 were characterized by a relatively deep (0.012 m) channel but lower slope (0.01) than the other runs and as a result bed shear stress was only slightly above critical ($\tau^*/\tau^*_c \approx 1.5$). This low shear stress may, according to published data on alternating bar formation, be responsible for the absence of alternating bars, and therefore meanders, in these two runs. Run 6, at the same discharge, similar depth (0.011 m) but higher slope (0.015) than runs 3 and 7 developed pronounced alternating bars. The only explanation for this lies in the greater bed shear stress in run 6 as a result of the steeper channel slope ($\tau^*/\tau^*_c \approx 2.1$).

Braiding in runs 3 and 7 appeared, particularly in run 7, to be the result of a chance emplacement of a thin sheet of bed material the location of which was perhaps determined by the distance downstream from the confluence developed at the head of the flume. In other words, if flow competence decreases downstream from the confluence the threshold of movement has a spatial expression. It is interesting that the initial deposition of coarse material at this point seems to be the result of internal sorting in the diffuse gravel sheet which brings coarse material to its margin. This may also be true of Leopold and Wolman's (1957) experiment although they did not mention this fact. The mid-channel location of the bar results from the control of the form of the gravel sheet by the confluence upstream which was approximately symmetrical (the two confluent channels had approximately equal discharges). Thus, braiding in these two runs was the result

of slight local aggradation, the exact form of which was controlled from upstream. Whether or not Leopold and Wolman's (1957) observations fit those recounted here is difficult to say. The initial channel in their experiment plots outside Jaeggi's (1984) alternating bar criterion, apparently because it has an extremely low width/depth ratio (2.47) rather than low bed shear stress. It is possible, however, that initial channel widening reduced bed shear stress sufficiently to put the channel into a bedform regime similar to that of runs 3 and 7.

Run 4b is interesting in this context because of its failure to braid after the sediment load had been restored to normal values. Two points about this are significant. First, the channel became quite markedly paved (the D_{50} of the pavement was about 4mm, much greater than that of the other channels), something which did not occur in the other experiments, and secondly, the cross-sectional form of this channel was parabolic rather than trapezoidal, as it was at the beginning of the run. Jaeggi (1984) noted the tendency for armoured channels not to obey his criteria and indeed the pavement on the bed of this channel had D_{50} of greater than 4mm, which places it below the threshold for alternating bar development. The channel did, however, transport large quantities of finer sediment. The stability of the parabolic cross-section is interesting since this is the form adopted by stable gravel channels (Parker, 1978). It is possible that the use of an initially trapezoidal channel cross-section encourages mid-channel deposition and braiding; a situation from which most of the runs were unable to escape. This suggests that braiding initiation close to the threshold may be influenced by the cross-sectional shape of the channel, (although this is itself influenced by the sediment load delivered to the channel). Such considerations

clearly have implications for the simple channel pattern thresholds based on discharge, slope and particle size (Lane, 1957; Leopold and Wolman, 1957; Henderson, 1966; Schumm and Khan, 1972; Richards, 1982), and perhaps helps explain their failure to fully account for channel pattern variations, particularly in the case of natural rivers (rather than laboratory streams) (Carson, 1984 a and b).

Flow division in run B was quite different from both of the mechanisms discussed thus far. In this case initial bed shear stress was well below that necessary for alternate bar formation, and was only high enough to cause selective erosion of parts of the bed where local turbulence may have initiated sediment motion. Run A had the same slope and discharge but a much smaller width/depth ratio, and therefore higher depth and bed shear stress, than run B. These differences were sufficient to place it (run A) in the alternating bar regime. However, once the braided channels had developed in each of these runs their channel forms were indistinguishable from one another. Run B had therefore reduced its width/depth ratio and achieved an equilibrium form identical to that in run A. Thus, in similar bed material, and at the same slope and discharge, both runs tended towards the same equilibrium channel form regardless of their initial conditions. This conclusion seems to contradict that reached in the previous paragraph but the difference between the two situations is that run B was allowed to braid from a situation in which it was barely able to move its bed material. Run 4b, on the other hand, was prevented from braiding by its channel form. Presumably if it had been possible to force run 4b to braid, its form would have been similar to that of run 4a (which had the same slope and discharge).

The three flow division mechanisms therefore occur under different initial conditions. At very low relative depths the 'proto-channel' mechanism occurs, but, as depth and shear stress increase the mid-channel bar mechanism replaces this, and at higher shear stress again alternating bars develop and braiding takes place by the cut-off mechanism.

Two further points can be made with respect to flow division. First, confluence scours may exert an influence on the flow division mechanism occurring downstream by affecting the symmetry of sediment pulses (in the form of transverse bars or diffuse sheets) passing through the scour hole. Thus, where the confluent channels have fairly equal discharges, flow division occurs downstream by division round the central portion of the margin of the resulting symmetrical sheet or transverse bar. Where the confluent channels have unequal discharges, an asymmetrical bar is deposited downstream and may accrete laterally to form a point bar before being cut-off to form a flow division. Where sinuosity is very low, as in run 7, no cut-off occurs, so that the confluence actually influences not only the type of flow division but, also, in some cases whether division occurs or not.

Secondly, whether the channel divides because of the emplacement of a mid-channel bar or the cut-off of a low sinuosity meander, flow division occurs in an area of local aggradation represented by the bar. In some cases, such as run 7, this is the only such area in the channel, while in others several aggradational areas occur spaced, at least initially, at regular intervals along the channel.

The influence of confluence scour hole form on the nature of channel division downstream of the confluence has already been discussed but this begs

the question : why do deposition and channel division occur downstream of scour holes ? It is not true, of course, that this is the only location of flow division in braided channels; division around large unit bars also occurs in channels free of the influence of scour holes. However, the association between scour holes and bar formation downstream has been described in this chapter and noted in previous work (Smith, 1973; Hein, 1974; Moss et al., 1982).

Firstly, the appearance of large transverse bars downstream of scour holes, that are absent in the confluent channels, may be a reflection of the fact that the combined discharge of the two channels creates a deeper channel downstream of the scour hole and thus provides sufficient depth for slip-face development. It is common to observe, for instance, that as a large sediment pulse passes downstream some subdued bar development occurs in the confluent channels but much more obvious transverse bars are produced as the pulse emerges from the scour hole. The role of depth can be seen in situations where a flow division already exists downstream of the scour hole and therefore the depth of the thalweg declines as the division is approached. A slip-face bar prograding down such a channel often decreases in height as it approaches the flow division, until its slip-face disappears altogether, at least in the central part of the bar margin. The large transverse bars seem particularly prone to flow division on their surface as the divergent flow ceases to be competent to move bed material across the entire bar surface. Smith (1971a) suggested that on linguoid bars there is a limiting bar surface area that a given flow is capable of maintaining. Once the bar area exceeds this maximum value, part of the bar experiences a cessation of sediment movement and forms the nucleus of a flow division. A similar process may be operating in the case of transverse bars.

Secondly, the formation of the confluence itself may result in the production of a sediment load in excess of the capacity of the channel downstream. Whether or not this occurs may depend on the rapidity with which the scour develops. Often development is quite rapid (a few minutes or tens of minutes in the models) as a result of the avulsion of one channel across a bar surface to join another channel (for example, Figure 8-21). Such avulsions are often accompanied by the erosion of sediment from the bar surface which, together with sediment excavated from the scour hole, may be sufficient to cause aggradation and flow division downstream of the scour hole. Once the scour hole reaches equilibrium depth this spatial difference in sediment transport rate must disappear. Thus, the initial pulse of sediment produced during scour formation may be very important in initiating deposition and flow division downstream of a scour hole. In the light of this it seems likely that deposition would be less common downstream of low angle confluences or confluences with a large difference in discharge between the confluent channels, reflecting the fact that scour depth is lower and therefore the initial pulse of sediment smaller, under these circumstances. Controlled experiments in which these factors are varied one at a time would add to the understanding of the details of this situation.

Looked at in the context of the transfer of sediment pulses downstream, confluences represent areas of sediment transfer intervening between aggradational zones. If the confluence location shifts or the confluence changes in form, a former aggradational area may experience degradation and the sediment from that area is deposited further downstream (Figure 8-17).

The episodic nature of deposition is noticeable at several different scales

ranging from the diffuse gravel sheets accreting only a few minutes apart, to the long-term aggradation and degradation occurring over several hours. In each case this reflects temporal and spatial fluctuations in the sediment transport rate that are responsible for the simple sheets and bars as well as the more complex aggradational zones composed of many such unit bars.

The diffuse gravel sheets are a feature of gravel streams mentioned previously (Hein, 1974; Bluck, 1979). Bluck (1979) suggested that in single channel streams they originate in riffles from where they migrate downstream to be incorporated in the structure of the point bar. It is unclear whether the sheets observed in the present experiments are actually the same as features observed by Hein (1974) and Bluck (1979). One possibility is that they are actually artifacts of the flume imposed by, for example, the sediment return system. However, the fact that they were present at the commencement of each run, even before the sediment return system had begun to contribute sediment to the head of the flume, militates against the argument that they are artifacts of the flume. In addition, their regular spacing is reminiscent of very low amplitude alternating bars or dunes which are products of spatial fluctuations in the flow velocity, or bed shear stress (Yalin, 1977). Finally, their size and spacing seem to vary with the flow conditions, particularly discharge, which would not necessarily be expected of pulses produced by the sediment return system which is operating identically for each run (apart from the fact that the volume of sediment pumped in a given time varies between runs). The fact that similar features have been observed in the field is a further point in favour of the fact that they are reproductions of prototype features and not artificially produced by the flume.

The observation that sediment transport rate fluctuates in this fashion is significant. Mid-channel bar deposition in some of the runs appeared to be initiated by such a diffuse sheet and this can be regarded as a slight increase in sediment load which part of the channel is incompetent to transfer entirely. Similarly, division round transverse bars seemed to coincide with the arrival of diffuse sheets which accreted to the bar surface. The final sheet to be deposited before flow division commenced is essentially the extra minor sediment pulse which that portion of the channel is incapable of transporting. The fact that bar aggradation occurs in this fashion may explain the widespread presence of horizontally bedded, imbricate gravel in braided stream deposits (Hein and Walker, 1977).

The model of unit bar growth from diffuse gravel sheets suggested by Hein and Walker (1977) is difficult to substantiate. Observations discussed in this chapter and in Chapter 7 indicate that the development of an avalanche face depends largely on the depth of water into which the bar is prograding. In 'proximal' reaches, where relative depths are low, the potential for vertical growth of bars is limited. The rate of discharge of sediment, which Hein and Walker (1977) suggest is a major control on bar form, appears to be irrelevant. Indeed, it has the reverse effect of that proposed by Hein and Walker (1977); in the present experiments avalanche-face bars were most abundant in the runs with higher sediment discharge. An understanding of the conditions favouring the growth of avalanche-face bars awaits an analysis of the change of bedform height with shear stress and relative depth; data which Yalin and Karahan (1979) have pointed out

[redacted]nt. Yalin and Karahan (1979) were able to show that at relative

depths between 20 and 30, bedform steepness (height/wavelength) peaked at excess Shields stress of about 4. Beyond this value steepness declined again (that is, the bedforms were 'washed out') and only on this limb of the steepness - excess Shields stress curve might Hein and Walker's (1977) model fit with laboratory observations of the influence of depth and shear stress on bedform steepness. Yalin and Karahan's (1979) graphs show maximum steepness to be about 10^{-2} at relative depths of 20 to 30. Assuming a wavelength of 1 to 2 meters this indicates that maximum bar height would be 10 to 20 mm. Because relative depth in the streams reported here is usually about 10, and the excess Shields stress about 2, extrapolation of Yalin and Karahan's (1979) results to these experiments indicates that maximum height is likely to be less than 10 mm except where the bars prograde into unusually deep water. This agrees with the laboratory observations.

The observations reported here and in Chapter 7 suggest that the unit bars contain elements of both Jopling's (1964) 'rheologic fronts' and 'saltation fronts'. The former developed when a sudden small increase in depth occurred and the latter formed when the rate of sediment feed to the flume was temporarily increased. The fact that relative depth clearly exerts a control on bar form but that, in addition, they are common during the passage of sediment pulses, suggests that both local increases in depth and sediment load affect unit bar occurrence and form. It is possible that the effect of the extra sediment load is simply a response to the increased availability of finer, more mobile sediment (that is an increase in excess Shields stress) but, if not, then the role of excess Shields stress in bar development needs to be modified to recognise the influence

of excess sediment load in forming unit bars that are primarily 'saltation fronts'. Add this to the observation that braiding intensity is a dominant influence on the occurrence of avalanche-face bars, because of the importance of availability of local depth increases, and one is left with a series of controls on bar development and form which are to some extent mutually correlated. Little wonder that it is difficult to isolate the influence of each by statistical analysis (see Chapter 7). Clearly there is a need for experimental work on this problem to analyse the separate influences of each of these variables on bedforms in rough flows with low relative depths.

At the beginning of each run the large alternate bars, some of which had avalanche faces, could be seen to have smaller diffuse sheets migrating across their surfaces. Because of differences in the height of the bar margin, the rate of progradation of the margin would be slower, for a given rate of sediment transport, for the avalanche-face bars than the diffuse sheets. This explains the tendency for the diffuse sheets to migrate across the surface of the larger bars. It is extremely difficult to ascertain whether the larger bars are composed entirely of diffuse sheets, as Hein and Walker suggest (1977), or whether they are products of larger-scale sediment pulses to which the diffuse sheets contribute only the upper few layers of sediment. The resolution of this question requires more detailed time-lapse photography to provide more frequent observations of the transition from diffuse sheets to alternating bars at the beginning of each run.

It is apparent from the observations reported here that, in the laboratory, changes in channel configuration such as avulsion and deposition of complex bars occur in the space of a few hours. Sediment pulses may pass through one area of

the channel, causing aggradation and then degradation, within three or four hours. Other processes such as the deposition and dissection of a unit bar may occur in a matter of minutes. Some of these processes were observed occurring in the field and it is interesting to compare the time scale for these processes in the field with that of the laboratory streams.

The central portion of the reach of the Sunwapta River studied has a median grain size at the head of medial complexes of 30-40 mm (M. Dawson, pers. comm.) compared with a mean grain size in the model of 1.2 mm. Thus the geometric scale ratio λ_L is approximately 30. According to Froude modelling criteria the discharge scale ratio λ_Q is then about 5000, and the time scale λ_T about 5.5. Discharge in the model ranged from 0.0012 to 0.0045 m^3s^{-1}. Peak discharges in the Sunwapta River in the reach studied (Rice, 1979) are about $20m^3s^{-1}$ and a rough calculation shows that the discharge scale ratio is correct for the highest model discharges. The laboratory models are actually not strict Froude models of the Sunwapta River because of a difference in slope (0.01 - 0.015 in the model and 0.005 - 0.01 in the Sunwapta River).

It is possible to make approximate comparisons of the rates of channel change in the model and the field using some of the examples discussed previously. Daily peak flows during the high flow period on the Sunwapta River between August 6 and August 20, 1981, lasted about 6 hours, but peak daily flow increased gradually during that period so that daily low flows later in the month were actually higher than the daily high flows during the first few days of the month. A short-lived storm discharge occurred over the two days July 28 and 29, similar in magnitude to the peak flows caused by snow and glacier-melt in August (see Figure 4-7).

The two sequences of channel change appearing in Figure 8-19 (d) and (e) both showed some activity in the July storm at which time a channel was abandoned and a point bar constructed [Figure 8-19 (d)], and a unit bar migrated several meters downstream [Figure 8-19 (e)]. However, much more dramatic changes are apparent in Figure 8-15 where, over the course of two weeks in early August, major channel switches and bar construction occurred in this section of the channel. Indeed this reach changed from an aggradational to a degradational condition in those two weeks. It was noticeable, while carrying out scour hole measurements at this time, that channel migration was in some cases altering the configuration of the confluence during the one or two hours it took to survey the scour hole and measure the discharge of the confluent channels.

There is a problem with comparing rates of change produced by steady discharge in the laboratory and diurnally changing discharge in the field but if one estimates that, during summer melt, peak discharges equivalent to the 'channel forming' discharge in the laboratory occurred for 6 hours per day then appreciable channel switching, and bar accretion and destruction occurred over a period of perhaps 20 or 30 hours. At a time scale of 5.5 this reduces to about 5 hours in the flume which fits roughly with the laboratory observations. Similarly, small-scale changes in scour hole configuration, occurring in an hour or two in the field, would occur in ten or twenty minutes in the laboratory. This again fits with the rates of change observed in the laboratory.

8-11 Conclusions

The initial flow division causing braiding may occur by one of three distinct mechanisms. The first involves emplacement of a relatively coarse deposit in the

centre of the channel which grows in size and ultimately causes division. This is essentially the mechanism observed by Leopold and Wolman (1957) but in the experiments recounted here the initial coarse deposit was observed to be the downstream margin of a migratory diffuse gravel sheet which stalled in the centre of the channel. The second mechanism is one of cutting-off low sinuosity meander bends by chute cut-offs. The bends are initiated from lobate alternating bars and the channel forms in the laboratory experiments, in which division occurred by this process, resemble very closely the low sinuosity meanders in gravel described by Lewin (1976) in the River Ystwyth, Wales. The third mechanism, that of 'protochannel' development from a thin sheet flow, resembles the process of channelization by sheet flow described by Moss et al. (1980, 1982).

The circumstances under which each of these mechanisms operates are apparently controlled by the dimensions of the initial channel. In very shallow flows, with bed shear stress only locally high enough to produce sediment motion, the 'proto-channel' mechanism operates. At slightly higher shear stresses, but too low to produce alternating bars, the mid-channel bar process is prevalent and at still higher shear stresses the alternating bar process occurs. It should be possible to produce this sequence, and to establish the point at which the mechanism changes from one to another, by conducting a series of experiments at the same discharge and slope, but with different width/depth ratios for the initial channels. It remains to be determined under what conditions the alternating bar pattern breaks down to form a braided channel. In the experiments described here this occurred when sinuosity was only about 1.1 but it is likely to vary with bank stability (Carson, 1984 b).

The alternating bars are spaced at approximately regular intervals and have a wavelength equal to between 6 and 9 channel widths. The resultant meanders have slightly higher wavelengths, suggesting that the alternating bars may not be in exact equilibrium with the flow conditions. When the bends are cut off the distance between adjacent confluences in a simple braided system, with a maximum of two channels per cross-section, is very close to the wavelength of the meanders before the cut-off occurs. In more complex channel patterns such a consistent relationship is more difficult to establish because of the range of channel sizes involved.

Confluences are important elements of the channel pattern. The form of the unit bars deposited downstream is influenced by the relative discharges of the confluent channels. Avalanche-face transverse bars are common downstream of symmetrical confluences. A change in the relative discharge or the position of the confluent channels can have a great influence on the deposition downstream and may cause channel avulsion and the destruction of previously deposited medial bars.

Accretion of complex bars occurs in distinct stages associated with the arrival of individual unit bars or diffuse sheets, each of which accretes to the bar structure. The form of the unit bars and sheets themselves are controlled by the available depth. Where this increases, larger unit bars with slip-faces may develop. The larger unit bars are the product of sediment pulses migrating down the channel and are modified by the changing channel form that they encounter. The diffuse sheets often accrete vertically to these larger unit bars and this may account for the formation of horizontal stratification in shallow gravel rivers.

Much larger-scale sediment pulses, several hours apart, cause local aggradation and increased braiding activity. The occurrence of channel avulsions often coincides with the arrival of such pulses. Analysis of time-lapse films indicated that the pulses could, on occasion, be seen to migrate downstream in a series of steps from one aggradational zone to another. Thus, each area of the channel undergoes alternating phases of aggradation and degradation as a pulse passes. The length of steps, or the distance between adjacent aggradational zones, seems to bear some relation to discharge and perhaps to the braid wavelength in braided channels with only two or three active channels per cross-section.

The time scale of channel modification in the model corresponds approximately, assuming Froude modelling, with comparable processes in Sunwapta River, Alberta. Processes that occur in a matter of minutes in the flume occur in an hour or two in the field while those that take a few hours in the laboratory require twenty or thirty hours of high discharge in the field. In a flow regime such as that of a proglacial stream, in which discharge fluctuates daily during maximum summer melt, several days of high meltwater production are required to accumulate a total of twenty or thirty hours of high discharge.

Chapter 9 : Synthesis and Conclusions

9-1 Introduction

The preceding chapters have examined various aspects of braided stream form and process both qualitatively and quantitatively. The majority of the data and observations discussed were collected in the laboratory model, but wherever possible, comparisons with field data have been made in order to verify the model. In particular, quantitative analysis of the sediment transport rate in the model, compared with other model and prototype data, and direct comparison of field and laboratory data on confluence scour depths, served to verify the quantitative similarity of model and prototype. The intent here is to draw together the main conclusions of the preceding chapters and assemble a picture of the form of, and sedimentary processes in, braided streams. The common thread between these chapters is the role of sediment transport in determining channel form, and it is this transport process which is used as the basis for the synthesis of braided stream mechanics.

9-2 Gravel Braided Stream Form and Process

9-2-1 Channel Division and Unit Bar Form

Beginning from a straight channel of trapezoidal cross-section filled with water, braiding was initiated in the model streams by three essentially different mechanisms. Cut-off of bends initiated from alternating bars, mid-channel bar deposition, and incision of "protochannels" into the bed of a very shallow flow. The mechanism observed in the majority of the ten runs was the first of these in which lobate alternating bars, sometimes possessing avalanche faces at their margins, initiated a low sinuosity meandering pattern in the flow with scour of

the bed at alternate sides of the channel adjacent to each bar. Bank erosion adjacent to the scour holes was responsible for channel sinuosity and simultaneous deposition occurred at the bank on the opposite side of the channel to each scour hole. In this fashion each alternating bar was converted into a more complex point bar as bank erosion, and accretion at the opposite bank proceeded. The wavelength of these regular meanders was equal to about 8 to 10 times the width of the initial channel; a ratio similar to that found in river meanders of a wide range of sizes. The point bars grew both laterally and downstream and the result was the development of a slough channel between the original bank and the point bar. The pattern of development to this point is strikingly similar to that described by Bluck (1976) and Lewin (1976) from low sinuosity gravel rivers in Scotland and Wales. This includes the tendency for the coarsest particles to accumulate as thin sheets at the upstream end of the point bar and for the finer material to be carried round the bend and deposited in the downstream half of the point bar (Figure 8-3). Once channel sinuosity reached a value of about 1.1, flow began to spill over the head of the surface of the point bar, in part because downstream growth of the next point bar upstream forced the flow in that direction. Flow across the point bar entered the slough channel and the steep slope down into the slough channel was quickly degraded, so encouraging further flow in that direction. The first sign of this occurring was the deposition in the slough channel of a delta-like lobe of sediment eroded from the upstream portion of the point bar. These chute cut-offs gained further discharge until an obvious flow division occurred. Flow out of the slough channel into the bend downstream forced the flow in the bend away from the outside bank and a confluence scour

formed near the centre of the channel. The position of this confluence initially coincided with that at the bend apex of the previously meandering channel but lateral migration of the confluence caused erosion of the adjacent point bar. The result was that confluences were spaced about one meander wavelength apart and only every second point bar was converted to a medial bar by the cut-off process; the remaining point bars were eroded away by lateral migration of the scour hole in response to the increasing discharge and sediment load of the cut-off channel.

Once further subdivision of the channels occurred the obvious relationship between confluence spacing and meander wavelength broke down because the smaller channels each had different bend wavelengths which interfered with that of the main channels. However, in many cases it was possible to pick out the original braid wavelength provided the braiding pattern had only two or three active channels per cross-section.

Previous work on braiding thresholds suggests that the occurrence of chute cut-offs is governed by discharge and slope (Lane, 1957; Leopold and Wolman, 1957; Schumm and Khan, 1972; Richards, 1982); controls which Carson (1984a) recently refined by considering the rate of thalweg shoaling resulting from large sediment loads imposed by rapid bank erosion. However, the occurrence of cut-offs presupposes that alternating bars developed originally, to produce a sinuous channel. Criteria describing the occurrence of alternating bars have been investigated, although there is not exact agreement about the flow conditions under which alternating bars form. Jaeggi (1984) noted a rough agreement between the various criteria and in particular the lower limit of excess Shields stress (τ^*/τ^*_c) of about 1.7 is significant for the channels discussed here. The two

runs in which alternating bars were absent or poorly defined (runs 3 and 7) had excess Shields stress of about 1.5 which is below the lower limit for alternating bar formation for the bed material used in these experiments. This is also true of the paved channel in run 4b in which the bed material at the surface had a mean size of about 4mm and was barely at the threshold of motion. Most of the sediment load in run 4b consisted of finer material recirculating through the system. The initial channel of Leopold and Wolman's (1957) experiment, in which alternating bars were absent, had excess Shields stress quite close to Jaeggi's (1984) threshold of alternating bar formation when the sorting of the bed material is taken into account. The explanation of the conditions producing alternating bars is inadequate to fully explain the occurrence of braiding by the cut-off process. Further research is needed into the conditions under which alternating bars are cut-off.

It was suggested in Chapter 2 that relative depth might be an important control on the nature of the flow division mechanism. If one considers the alternating bar criterion discussed above, then at a given slope an increase in relative depth would be accompanied by an increase in bed shear stress, hence the apparent importance of relative depth. However, comparison of runs 6 and 7 which had very similar initial relative depths, but different values of bed shear stress because of the higher slope in run 6, makes it apparent that bed shear stress is the fundamental control. The higher bed shear stress in run 6 allowed the formation of alternating bars which were absent in run 7.

This conclusion about the role of excess shear stress and flow depth in controlling alternating bar development has implications for the form of unit bars

developed after braiding has occurred. If unit bar development is controlled initially by bed shear stress and if, as Yalin and Karahan (1979) suggest, for a given bar wavelength, bar height increases with increasing excess Shields stress, then not only the presence or otherwise of migrating unit bars, but also the extent to which they possess avalanche face margins, are controlled by excess Shields stress. However, as Yalin and Karahan (1979) have also shown, despite the influence of excess Shields stress the maximum bar height attainable, and the value of Shields stress at which this is reached, are controlled by the relative depth of the flow. An increase in Shields stress beyond this point results in a decline in steepness. However, one should be careful in applying Yalin and Karahan's (1979) findings directly to this problem because of their analysis in terms of steepness; a decrease in steepness need not be the result of a decrease in bar height, it could equally well be the result of a faster rate of increase in wavelength than height. Nevertheless, the point that relative depth may control bar form, and in particular limit the maximum height attainable, is a reasonable conclusion and suggests that the bars behave in a manner similar to Jopling's (1964) "rheologic fronts". The creation of the migratory unit bar in the first place is controlled by the bed shear stress. At very low relative depths the limit on bar height may be reached at very low values of excess Shields stress thus effectively limiting unit bars to sheet-like features without avalanche faces. This appears to be the situation in many gravel braided streams.

If this conclusion applies to migratory transverse and diagonal unit bars as well as alternating bars then some aspects of Hein and Walker's (1977) 'diffuse gravel sheet' model of unit bar development are brought into question,

particularly that part which suggests that discharge and sediment transport rate are the main controls on bar form and that avalanche face development is less likely as these two factors increase. Increasing discharge and sediment transport rate would presumably be accompanied by, and in the case of the sediment transport rate, would be the result of, increases in bed shear stress and relative depth. The foregoing discussion indicates that such circumstances ought to favour avalanche face growth, not discourage it. The only possible exception to this is the case of increasing shear stress beyond the optimum for bar steepness. Without measurements of bar dimensions at very low relative depths (10 or less) it is impossible to know whether this situation occurs in gravel braided streams or not. Regardless, this is a more rigorous approach than that employed by Hein and Walker (1977). These conclusions must be tempered by the fact that braiding intensity and local sediment load conditions are also important in controlling bar form (especially the occurrence of avalanche faces) making it clear that some qualification of the conclusion that shear stress and depth control bar form, is necessary.

In the initial channels that failed to satisfy the criteria for alternating bar development, channel division took place by one of the other two mechanisms. The first, very reminiscent of that described by Leopold and Wolman (1957) and reiterated many times since (for example, Ore, 1964; Miall, 1977), involves the deposition of the coarsest part of the bedload in the centre of the channel at a point where flow competence is reduced. This may occur at a widening of the channel, but in flume experiments the initiation is often the result of a decrease in shear stress downstream from the head of the flume. In the experiments described

here a confluence scour was often present near the head of the flume and it is possible that competence declined downstream from the scour hole until a section of channel incapable of transporting all the sediment that was delivered to it from upstream was reached. In fact the initial coarse-grained deposit appeared to be part of the margin of a thin migratory gravel sheet which ceased to migrate, and around which the flow was diverted. The initial coarse deposit acted as the nucleus for further bar growth by lateral accretion of subsequent migratory sheets. Eventually the bar reached a sufficient size that flow divided around its emergent surface. A markedly similar process occurred atop large transverse bars downstream of confluence scours in some of the other runs. In this case division was initiated by vertical accretion to the bar surface of thin sheets of bed material. In both cases division was initiated in the central part of the bar or sheet margin where the excess sediment load delivered from upstream was greatest.

The third mechanism observed occurred in very shallow sheet flow where bed shear stress was insufficient to transport bed material except in areas of locally intense turbulence. Once sediment transport was initiated, small, discontinuous "proto channels", often containing antidunes, were formed, at the downstream end of which the transported bed material was deposited in linguoid features. These depositional features helped concentrate the flow in other areas and so promoted the development of further "proto channels". These channels eventually integrated into a network at which point some enlarged at the expense of others and a braided channel was produced. This channel was indistinguishable from that developed from alternating bars in a separate

experiment that used the same discharge and slope but had an initial channel with a lower width/depth ratio than that in which "protochannels" developed. This "proto channel" development is similar to that described by Moss et al. (1980, 1982), although in their experiments the process was not allowed to develop to the final braided channel condition. Thus, at extremely low excess Shields stress not even subdued alternating gravel sheets can form. Instead, the spatial differences in sediment transport capacity are expressed by the chute-like "protochannels" with small lobate deposits at their downstream ends. This may be analogous to the process which Carson (1984a & b) refers to as "rutting" of the floodplain during flood discharges.

When the flow division process is examined there is a clear association between the mechanism of flow division and sediment mobility (as expressed by the excess Shields stress). Those runs with highest bed shear stress are those with the best developed alternating bars, and are also those with the highest sediment transport rate. Thus, the sediment transport rate is reflected in the channel form and flow division process and it is noticeable that once braiding develops the rapidity of channel migration, bar construction and other sedimentary processes are also a direct reflection of these differences in sediment mobility, as is the frequency of occurrence of migratory unit bars with avalanche faces. There is a clear contrast in such characteristics between, say, run 7 and run 9 because the latter has much higher values of each of these parameters.

Bar and sheet deposition are both manifestations of spatial changes in the sediment transport rate. In the case of alternating bars this variation apparently occurs at regular intervals along the channel, the spacing being a function of the

scale of the flow (as expressed by the channel width). The result is regularly spaced alternating bars which prograde downstream, hence altering the position of net aggradation and degradation areas. Such downstream migration requires a lag between the flow conditions causing the change in transport rate and the transport rate itself; this lag is a feature of all migratory bedforms although the direction of the lag may cause upstream migration is some cases (Vanoni, 1975, p.120-121). The scale of the spatial fluctuations in sediment transport rate causing the scour and deposition responsible for alternating bar formation is similar to that causing confluence scour and medial bar deposition in simple braided patterns with no more than two channels per cross-section. Thus, any repetitive alternation of areas of scour and deposition in the braided river as a whole (rather than within individual channels) can be traced back to the initial periodic scour and deposition responsible for alternating bar formation. In minor channels within the braided stream the same processes occur but the scale (wavelength of alternating scour and deposition) is accordingly smaller.

9-2-2 Channel Morphology

Once braiding has commenced the characteristics of the channel form can be related directly to stream power (as expressed by variations in discharge and slope) and hence indirectly to the sediment transport rate. Consider, for the moment, the average stream morphology (as measured by braiding intensity, mean width and depth and the frequency of occurrence of avalanche-face unit bars) under different conditions of slope and discharge. This constitutes a form of downstream hydraulic geometry of braided streams. As power increases the mean sediment transport rate increases also, as do the values of the stream morphology

parameters. Thus, there is an obvious increase in braiding intensity with stream power. Both increasing slope and increasing discharge result in an increase in the mean number of active channels per flume transect and the number of active channel segments per flume length (a segment is defined as the length of channel between two nodes in the braided channel network). Such a trend agrees with that observed in field streams (Howard et al., 1970; Maizels, 1979) and the intensity of braiding fits well with Parker's (1976) theoretical prediction which, as Parker (1976) demonstrated, works well for field conditions also.

The active width and depth also increase with increasing power and at a rate similar to that observed in single channel streams. The bed relief index, an indicator of the relative magnitude of bed elevation variation within the braided stream, also increases with stream power. Although discharge seems to have the most pronounced effect on this variable, an increase in slope seems to have little, or if anything a negative, influence on the bed relief index. This may be due to the fact that at a given discharge an increase in slope causes an increase in braiding intensity and channel width. This results in a decrease in depth and bed relief index in order to maintain a constant cross-section area. This suggests that the positive relationship between mean depth and stream power is really a correlation between depth and discharge which is modified by changing slope.

Finally, the frequency of occurrence of avalanche-face bars also correlates with stream power. Referring back to the discussion of alternating bars, since stream power and bed shear stress are closely related this relationship between stream power and avalanche-face bar development seems to fit the general argument that migratory unit bars will develop under conditions of greater

sediment mobility, although low relative depths may limit this development. The role of depth or bed relief index is an inconsistent one. In some cases relatively large numbers of avalanche-face bars occur in runs with relatively low depth and bed relief and these tend to be the runs at high slope (0.015) and relatively low discharge. This confirms the predominance of bed shear stress over depth in controlling avalanche face development (see section 9-2-1). This is complicated, however, by the observation that the occurrence of avalanche-face bars relates most consistently to the braiding intensity indexes to the extent that the correlation with stream power appears to be spurious and is caused by the dependence of braiding intensity on stream power.

The role of braiding intensity can be understood by considering that under conditions in which competence and depth vary downstream, as they do in braided rivers, the most common sites for avalanche-face bar development are areas of locally high depth. Elsewhere relative depth may be too low to allow such features to occur. Typically the areas of relatively high depth occur in the vicinity of confluence and bend scour holes and such sites become increasingly abundant as braiding intensity increases. This tendency towards avalanche-face bar development being limited to sites of relatively high depth concurs with Hein and Walker's (1977) field observations. Thus, once braiding has commenced, and mean flow depth is lower than in the initial channels, the limits on bar development imposed by relative depth may be more important than the control by bed shear stress. In the bed material used in the present experiments avalanche faces only developed when bar height reached at least 5mm and this sets an obvious lower limit on depth required for avalanche face development,

which in this case represents a relative depth of about 4. Even in flows with high excess Shields stress, pronounced transverse or diagonal unit bar development would therefore be severely limited in channels this shallow. Detailed observations at various slopes and relative depths would be required to set this lower limit more precisely, but it is obvious that many gravel braided streams are very close to this limit except in areas of locally high depth. It is, of course, possible that, in addition, excess Shields stress may be too low for transverse bar development.

Field observations of the differences in channel form between 'proximal' braided streams, with coarse sediment and low depths, and 'distal' braided streams with much higher relative depths, reflect the influence of sediment mobility and flow depth on unit bar form. The observations of Fahnestock (1969), Smith (1970), Boothroyd and Ashley (1975) and Hein and Walker (1977) bear this out. Although a decrease in channel slope without a change in discharge implies a downstream decrease in total stream power from proximal to distal sections of the same outwash, it is probable that dimensionless stream power (a measure of sediment mobility that accounts for differences in particle size) and excess Shields stress increase downstream. The result is greater braiding intensity, more rapid migration, accretion and destruction of bars, and more abundant avalanche-face bars. The sedimentological consequences of this have been particularly well documented by Boothroyd and Ashley (1975).

Refinement of this kind of approach presents the prospect of being able to classify various types of braided river channel on the basis of characteristics such as braiding intensity, sediment mobility, relative depth and dominant bar types

and to define the limits of relative depth, stream power and excess Shields stress for the occurrence of each type. The full range of types is not covered by the present experiments but it is clear that for these experiments excess Shields stress of less than 2, dimensionless stream power index ($\bar{\omega}'$) less than approximately 0.2 and mean relative depth of about 6, produces braided channels with low sediment mobility, few avalanche-face bars, low rates of bar migration, accretion and destruction, low rates of channel migration and infrequent avulsion. Above this limit, sediment mobility and the related processes all increase in rate of operation, and the number of migratory unit bars with avalanche-face bars begins to increase, initially in the vicinity of confluences because elsewhere relative depths were low enough (less than 10) to restrict avalanche face development. Increasingly, transverse or linguoid bars might develop in areas other than confluences and the extreme of this continuum of channel types controlled by relative sediment mobility would be sandy braided streams in which the bed is occupied by numerous overlapping linguoid bars (Collinson, 1970; Smith, 1971a; Cant and Walker, 1978). However, one must be wary of extending this idea too far because the boundaries of sandy streams are usually hydraulically smooth, so changing the conditions for sediment transport from those in gravel streams and allowing the formation of small-scale bedforms such as ripples.

It is unfortunate that suitable field data are unavailable to check the details of the laboratory findings discussed above, but the general trends are certainly similar to those found in the downstream transition from 'proximal' to 'distal' type braided streams. It is apparent from rough calculations based on Hein's (1974) observations on the Kicking Horse River, and from the author's and Rice's

(1979) observations on the Sunwapta River, that in both cases there is an increase in relative depth and a slight increase in excess Shields stress (the downstream decrease in grain size is counteracted by the decrease in slope) in the transition from 'proximal' to 'distal' areas of the outwash. It is not certain that these field measurements were made at a sufficiently high discharge but, for example, Rice's (1979) measurements of channel form suggest that Shields stress is barely above critical in the upstream reaches of the Sunwapta and only about 20 per cent above critical in the downstream reaches. This suggests that bed shear stress may be too low for transverse bar development and that their relatively greater abundance further downstream may actually be merely a reflection of the greater braiding intensity in that part of the stream rather than of any difference in sediment mobility.

9-2-3 Temporal Fluctuations in the Sediment Transport Rate and their Impact on Channel Form

Thus far the discussion of channel form has centred on average conditions of discharge, sediment transport rate and channel form. The sediment discharge measurements, and observation of the time-lapse films and of the channels and scour holes as the experiments were being carried out, revealed the presence of unsteadiness in the sediment transport rate at a variety of scales. These temporal fluctuations in the sediment transport rate have been shown to have an obvious impact on braided channel form , as do the spatial fluctuations discussed previously.

The thin migratory sheets of sediment observed, for instance, accreting to the surface of transverse bars, represent the smallest detectable fluctuations in

sediment transport rate. Such sheets were also present at the beginning of each run but were usually replaced by larger (or, at least, higher) unit bars within a few minutes. Only where bed shear stress was relatively low did this transformation not take place and in these cases the sheets often formed the nucleus of deposition that eventually evolved into a medial bar. Sediment sorting was present in these sheets with the coarse material concentrated around the margins and finer material towards the center. Such sorting could be the result of a slightly higher transport velocity of the coarse material than the finer material, caused by a relatively lower angle of internal friction for the coarse particles than finer particles moving over a relatively coarse grained bed (Meland and Norrman, 1966, 1969; Everts, 1973). It is conceivable that these sheets are the first stage in unit bar development and that their height is restricted by the prevailing flow conditions or simply because they have had insufficient time to grow to equilibrium height (this is likely the case at the beginning of each run). Hein (1974), Hein and Walker (1977) and Bluck (1979) have discussed in some detail features found in the field that are similar in form to those observed in the laboratory. Hein and Walker (1977) suggested that larger unit bars developed from these 'diffuse gravel sheets' by a process of winnowing out of the finer bed material and leaving behind a coarse lag. This would account for the downstream fining of bed material on the surface of such bars (Hein, 1974; Bluck, 1979). However, Ashmore (1979, 1982) observed that this sorting pattern was actually a consequence of vertical sorting on the avalanche face and resulted in the [illegible]al of coarser material as the bar prograded. The fact that the diffuse [illegible]ved in the present experiments tended to have relatively coarse-grained margins runs

counter to the bar development process proposed by Hein (1974), Hein and Walker (1977) and Bluck (1979). However, it is also true that after the coarse margins of such sheets ceased moving, they were often overridden by finer material transported from upstream. Regardless, the suggestion by Hein and Walker (1977) that the larger unit bars may be built by the vertical accretion of successive diffuse gravel sheets is borne out by the present observations. The details of sediment sorting during this process remain to be documented and the laboratory model is clearly potentially valuable for this purpose.

The periodic fluctuations in confluence scour depth observed several times during measurement of particular confluences are traceable to the passage of diffuse sheets or larger unit bars. The fact that the fluctuations in depth occurred over the course of a few minutes supports this conclusion, as does the observation that during aggradation larger particles appeared in the scour hole first, to be followed shortly afterwards by finer particles. Such a sequence of events would result from the downstream migration of a diffuse sheet or bar having coarser particles at its margin and finer material further upstream; this sorting pattern was visible in the diffuse sheets, as reported above. Thus, because of the migration of bedforms, the spatial variations in sediment transport rate that cause scour in some locations and deposition in others translate into temporal variations in the transport rate at a given location. The changes in scour depth through time at a given confluence are a reflection of this temporal variation.

The fact that pulses of sediment are periodically delivered to these scour holes has an impact on depositional processes downstream of the scour hole. Downstream of simple symmetrical scour holes (in which the discharges of the two

confluent channels are approximately equal) there is a tendency for large transverse or diagonal bars to form in the relatively deep channel formed as result of the combining of two channels into one and because of the effect of the strong secondary circulation on the channel shape. Away from the influence of the scour hole the channel tends to become wider and shallower. As a result, unless the slope increases, the bed shear stress, and hence the sediment transport capacity, decline. Ultimately the result is the reduction of the height of the avalanche face of the unit bar and finally the cessation of downstream progradation of the bar. At this point flow division occurs on the bar surface. In this manner the passage of sediment pulses, particularly the larger ones, through confluence scours and the resultant changes in form that such pulses may undergo, may be a significant part of the channel pattern changes occurring frequently in braided streams. In the case of asymmetric scour holes the sediment may accumulate downstream of the scour hole initially as a diagonal unit bar, which is subsequently enlarged by accretion to form a point bar and then experiences a chute cut-off similar to that described in connection with the development of braiding from alternating bars.

Flow division downstream of scour holes can therefore be interpreted as another example of local exceedance of bedload transport capacity resulting in mid-channel deposition. The initial extra load may not necessarily come from upstream of the scour, although confluence scour is often initiated by channel avulsion, a process which causes sediment erosion in the avulsing channel because of the increase in discharge in that channel. Rather, the source of sediment may be the scour hole itself.

The smaller-scale pulses in sediment transport rate (the unit bars and diffuse

sheets) are also important in the pattern of accretion of larger bar complexes. Bluck (1974, 1979) has described the processes by which individual unit bars are incorporated into the structure of complex lateral and medial bars and Smith (1974), Hein (1974) and Ashmore (1982) have provided similar descriptions with less sedimentological detail. In the present experiments it was possible to observe sediment pulses in the form of unit bars and sheets migrating downstream from the head of the flume, or an area of rapid erosion, and then being deposited at the accretionary margin of a complex bar. Each separate sheet or lobe of sediment in the complex bar was seen to be related to an individual migratory sediment pulse derived from further upstream. In some cases such accretion sequences were part of a general aggradation in that part of the channel associated with the passage of much larger sediment pulses, of which the unit bars are individual components. Accretion then occurred rapidly as regularly spaced bars or sheets migrated downstream and were deposited at the margin of the complex bars. For example, at the head of medial bars, particularly downstream of confluence scour holes, a rapid succession of thin sheets was observed on several occasions, each of which added a distinct unit to the head of the medial bar. While some of the structure of complexes can be explained in this fashion it is apparent from the description of the evolution of one particular complex bar that a sequence of channel migrations and avulsions, as well as accretion and dissection of bars, is responsible for the final form of most complexes.

These small-scale pulses in the sediment transport rate were visible but were too small and infrequent for analysis of the sediment transport rate measured at fifteen-minute intervals to reveal their presence. However, larger-scale, longer-

period fluctuations in the sediment transport rate were apparent from the regular (15-minute) measurements of the sediment transport rate. When analysed by autocorrelation it was apparent that some significant regular peaks occurred in these series, the most prevalent having a period of 6 to 8 hours although, particularly at higher discharges, periods of 2 to 4 hours and 10 to 12 hours were also detected. Similar periodicities have been reported from a model of Hilda Creek, Alberta, by Southard and Smith (1982) and from Hilda Creek itself (Kang, 1982). Southard and Smith (1982) attributed the longer-period pulses to "aggradation/degradation cycles" but were not precise about the physical characteristics of these "cycles". By examining the time-lapse films of each run it became apparent that the arrival of particularly large pulses at the head of the flume was often followed shortly afterwards by increased braiding activity in the upstream half of the flume. This increased activity was manifested physically by the appearance of migratory unit bars, rapid accretion of complexes, frequent avulsions and an increase in the intensity of braiding.

When the sediment transport data were compared with those channel morphology parameters which were measured sufficiently frequently (braiding intensity and the frequency of occurrence of avalanche-face bars) it was apparent that many of the increases in braiding intensity and the number of avalanche-face bars coincided with increases in the sediment input rate to the head of the flume, although there was often a lag of one or two hours between the arrival of the sediment pulses and the channel response. However, this correlation was not always present. There were cases of sediment pulses having little influence on the channel form and, more frequently, occasions when changes in channel form

occurred that were apparently unrelated to sediment input at the head of the flume. Cross-correlation of the time-series of the sediment transport rate, braiding intensity and frequency of occurrence of avalanche-face bars confirmed the visual impression given by the time-lapse films. The coincidence of the increase in braiding intensity and occurrence of avalanche-face bars was particularly noticeable in this analysis and confirms the importance of the number of sites with unusually high depths in encouraging avalanche face development. This may also be an indication that some of the transverse bars observed are "saltation fronts" (Jopling, 1964) whose appearance is due to an increase in the sediment supply rate but whose form is subject to the same control by shear stress and relative depth as other unit bars.

The lag between the sediment input and the channel response was two or three hours in some cases but in several runs the major peak in the cross-correlation function occurred at a higher positive or a negative lag. This could be caused by the fact that if the lag is three or four hours, and the sediment transport series is positively autocorrelated at six to eight hours, a strong spurious correlation of channel form with a future sediment pulse could occur. This is the danger of cross-correlating series which are themselves autocorrelated. However, there is a second explanation for this observation which relates to the manner in which the sediment pulses migrate downstream. Monitoring of the time-lapse film of run 11 revealed that each major peak in the sediment input produced aggradation and an increase in braiding intensity near the head of the flume. After a few hours, when the sediment input rate had declined, this accumulation was dissected and the sediment transferred some distance downstream to a new

site where the process of aggradation began again. This process was repeated three of four times before the pulse passed out of the system. It is possible that the large lags observed between the sediment input and the channel response are the result of aggradation several meters from the head of the flume caused by the downstream migration of a sediment pulse introduced to the flume several hours beforehand.

These observations indicate that the pulses themselves are the result of this alternation of aggradation and degradation in sections of the channel. This is perhaps the process referred to by Southard and Smith (1982). The fact that the pulses occur periodically presumably reflects the periodic nature of the aggradation and degradation and suggests that the temporal spacing of pulses in the sediment load has a spatial expression in the distance between adjacent aggradational zones. It is possible , at least in simple braided systems with only two or three channels per stream cross-section, that the sediment pulses are transferred from one medial bar to the next through an intervening confluence. Since the confluences in such a system are regularly spaced at an interval determined by the stream discharge (see section 9-2-1) the transfer distance for the sediment pulses is similarly determined. A further consequence of this is that the confluences are potentially important in directing the passage of sediment from one aggradation zone to the next.

It is apparent from monitoring of the sedimentation patterns downstream of confluences that they do indeed influence the position of the aggradational zones. The depth of the scour hole and its orientation are influenced by the angle of confluence, the total discharge through the confluence and the relative discharges

of the confluent channels (see Chapter 6). Thus, absolute scour depth is greatest when the entire discharge of the stream is concentrated into two channels of equal discharge with a confluence angle of 80° to 90°. Under such circumstances deposition downstream would probably be initiated by the development of a large, symmetrical unit bar around which flow would divide to form the nucleus of a medial bar.

Any change in the total discharge through the scour hole may result in upstream accretion of the bar head if discharge decreases, or erosion of part or all of the medial bar if total discharge increases. A change in the relative discharge of the confluent channels results in a reorientation of the scour hole so that its long axis more nearly parallels the trend of the larger channel. If the change in discharge results in a more equal distribution of discharge between the two channels then reorientation tends to bring the long axis of the scour hole into an alignment that bisects the confluence angle. In either case the location of bar deposition, and the nature of the bar growth (for example, whether or not a symmetrical or asymmetrical complex develops) will be affected by this reorientation. As the scour hole is reoriented, the channel immediately downstream migrates laterally and avulsion or abandonment of channels in the vicinity of the medial bar further downstream is a common result. If a confluence remains fixed in position for a period of time, but undergoes repeated reorientation and changes in size because of channel changes upstream, the aggradation zone undergoes repeated reworking by the flow issuing from the confluence. In confluences involving more than two channels the situation is obviously more complex, but the same principles apply.

9-3 Conclusions

Drawing on information from the foregoing synthesis and the previous chapters the following conclusions can be drawn :

1. The bedload transport rate in small-scale braided rivers increases with excess dimensionless stream power per unit width and excess Shields stress, at a rate comparable to that observed in other laboratory models of gravel rivers and prototype gravel rivers. The data from each of these sources and the present experiments coincide quite closely and accord with general empirical and theoretical bedload transport relations such as Meyer-Peter and Muller (1948), Einstein (1950) and Parker (1978). This is an important quantitative verification of the similarity of the model and field gravel streams and suggests that other aspects of sediment transport ought to be reliably modelled. One problem in the similarity analysis is the difference in the critical conditions for sediment motion between the various data sets, caused primarily by differences in the degree of sorting of the bed material. Further, the results suggest that the prediction of sediment transport rate in braided streams may not be as problematic as some have feared, provided sufficient cross-sections are measured over time at a given discharge to provide reliable average values of width, depth and bed shear stress. The results of this study suggest that between 50 and 100 such cross-sections are required.

2. For scours in simple confluences involving only two channels, the scour depth is determined primarily by the total discharge through the scour hole and the angle of confluence of the two channels. When the influence of discharge is eliminated by considering the scour depth relative to the depth of the confluent

channels, the angle of confluence is seen to be the dominant influence on scour depth, with the relative discharge exerting a minor effect unless the discharge of one channel is at least twice that of the other. Under circumstances of unequal discharge of the two channels, scour depth is severely limited. Field measurements of confluence scour confirmed these conclusions and showed relative depths to be similar in the field and laboratory at a given confluence angle and relative discharge. This is further quantitative verification of the model. The scour depth and confluence symmetry (relative discharge of the confluent channels) influence the development of unit bars and flow divisions downstream of the confluence so that an understanding of the functioning of the confluences in these terms is important for appreciating the sedimentary processes in braided streams.

3. Channel morphology responds to changes in imposed discharge and slope, and consequently to changes in the sediment transport rate. Braiding intensity increases with increasing discharge and slope, as do average active width, mean depth, the bed relief index and the frequency of occurrence of avalanche-face bars. Some of these trends have been verified qualitatively but the paucity of field data prohibits quantitative comparison of model and prototype, although the laboratory runs provide a crude typology of 'proximal' and 'distal' braided streams.

The average conditions of channel morphology are upset by the presence of unsteadiness in the sediment transport rate which causes phases of aggradation associated with an increase in the degree of braiding (through more frequent avulsion and channel division around unit bars) and a greater frequency of

occurrence of migratory avalanche-face bars. Degradation phases are associated with the reverse trends.

4. Unsteadiness and non-uniformity in the sediment transport rate are manifest at a variety of scales but in particular, small-scale features such as scour holes and migratory unit bars and sheets, and large-scale aggradation and degradation phases are the most obvious physical products of these characteristics of the sediment transport rate. The pulses in sediment load responsible for the smaller features are not detectable in the sediment transport measurements but the larger ones occurring quite regularly, several hours apart, are detectable in the auto-correlation function of the sediment transport time series from each run.

The smaller pulses cause temporary filling of scour holes and are also responsible for the unit-by-unit construction of large bar complexes. The larger pulses have an important influence on the channel pattern. It has been known for many years that externally generated sediment pulses can cause braiding or increased intensity of braiding; but the analysis here shows that internally generated pulses can achieve the same result and are probably a universal feature of braided streams.

The larger sediment pulses are transferred downstream in a step-like fashion from one complex to the next through an intervening transport reach which often includes a confluence. The spacing of confluences, and the distance from the confluence to the head of the medial complex downstream, are controlled by the scale of the flow; a larger discharge produces a greater spacing in the same manner that discharge and meander wavelength are related in single channel streams. Indeed, in simple braided patterns the distance between adjacent

confluence scour holes is similar to the meander wavelength of the initial single channel that precedes the onset of braiding.

5. Channel division occurs by at least three different processes : mid-channel bar deposition in the absence of obvious migratory unit bars but in the presence of diffuse sheets; cut-off of bends initiated from a pattern of alternating unit bars; and incision of "proto channels" into the bed by an initially shallow sheet flow. The first two mechanisms have also been described in the field and in other laboratory experiments, the third one has thus far been observed only in laboratory flumes (Moss et al., 1980, 1982). Each process occurs under different conditions of relative depth and bed shear stress but each is to some extent the result of local exceedance of bedload transport capacity. The occurrence of the cut-off process depends on the existence of appropriate conditions for alternating bar development. Most of the runs satisfied the published criteria but in those runs in which bed shear stress was too low the mid-channel bar process, first described by Leopold and Wolman (1957), occurred. "Proto-channel" development was limited to conditions of very low relative depth (less than 4) and only local exceedance of the threshold of motion of the bed material.

The cut-off process resulted in an initial braided channel developing medial bars from every second meander point bar, and confluence scour at every second meander bend apex. This explains the observation that the braid wavelength is very similar to the meander wavelength of the initial channel.

6. The development of avalanche-face bars is controlled primarily by the excess Shields stress but flow depth may also limit bar height. This helps to explain the trend towards increasing numbers of avalanche-face bars downstream,

from the proximal to distal areas of braided outwash. However, in many cases relative depth is so low that avalanche faces have the best opportunity to develop in the vicinity of local increases in depth, such as occur at channel confluences and bends. Hence there is a correlation between the abundance of avalanche-face bars and the braiding intensity, which is stronger than the correlation between stream power and the abundance of avalanche-face bars. It should also be pointed out that both braiding intensity and the abundance of avalanche-face bars are greatly influenced by the arrival of large sediment pulses. This might account for the apparent dominance of braiding intensity over stream power in explaining variations in the frequency of occurrence of avalanche-face bars. These bars appear to combine elements of the behaviour of both "rheologic" and "saltation" fronts (Jopling, 1964).

This analysis of the controls of bar height fits the conventional analysis of bedform steepness in shallow, gravel channels much better than Hein and Walker's (1977) "diffuse gravel sheet model". A re-examination of this model is required, along with field investigations of bar form and flow parameters, in order to fully comprehend the controls on bar type and hence the stratification of the sediment.

Two further, more general, conclusions can also be drawn :

1. Temporal and spatial fluctuations in the sediment transport rate, as well as the mean transport rate, play a significant role in sedimentary processes in braided streams. Braiding, initiation, bar accretion and aggradation/degradation cycles, all of which are fundamental aspects of braided river mechanics, are all intimately related to fluctuations in the sediment transport rate. In addition, the

average conditions of relative sediment mobility, and hence the mean bedload transport rate, have an influence on the division process, the occurrence of avalanche-face bars and the rapidity of the main sedimentary processes such as channel migration, avulsion, and bar accretion and erosion.

2. The model streams behave, in many respects, like prototype braided streams. Data on sediment transport rate and confluence scour depth illustrate the quantitative similarity of model and field data and more qualitative comparisons of the division processes, bar accretion and the influence of slope and discharge on channel form, provide further verification of the model. Rough calculations of the rates of operation of some sedimentary processes in the field and laboratory add further weight to this conclusion. Thus, the potential exists for model studies of braided streams to provide not only ideas on the mechanics of braided streams to be tested in the field, but reliable quantitative data on fluvial processes that can be extrapolated directly to prototype streams.

References

Allen, J. (1947) *Scale Models in Hydraulic Engineering*, London, Longman.

Allen, J.R.L. (1968) *Current Ripples: Their relation to patterns of water and sediment motion*, Amsterdam, North Holland Publishing Company.

Ashmore, P.E. (1979) *Laboratory modelling of braided streams*, M.Sc. Thesis, University of Alberta.

Ashmore, P.E. (1982) Laboratory modelling of gravel braided stream morphology, *Earth Surface Processes and Landforms*, 7, 201-225.

Ashmore, P.E. and Parker, G. (1983) Confluence scour in coarse braided streams, *Water Resources Research*, 19, 392-402.

Bagnold, R.A. (1973) The nature of saltation and of 'bed-load' transport in water, *Proceedings of the Royal Society of London, Series A*, 332, 473-504.

Bagnold, R.A. (1977) Bedload transport by natural rivers, *Water Resources Research*, 13, 302-312.

Bagnold, R.A. (1980) An empirical correlation of bedload transport rates in natural rivers, *Proceedings of the Royal Society of London, Series A*, 372, 453-473.

Bathurst, J.C. (1982) Theoretical aspects of flow resistance, in R.D. Hey, J.C. Bathurst and C.R. Thorne (eds.), *Gravel-bed Rivers*, Chichester, Wiley, 83-105.

Bégin, Z.B. (1981) Stream curvature and bank erosion: a model based on the momentum equation, *Journal of Geology*, 89, 497-504.

Bennett, R.J. (1979) *Spatial Time-Series*, London, Pion Ltd.

Blodgett, R.H. and Stanley, K.O. (1980) Stratification, bed forms and discharge relations of the Platte braided river system, *Journal of Sedimentary Petrology*, 50, 139-148.

Bluck, B.J. (1974) Structure and directional properties of some valley sandur deposits in southern Iceland, *Sedimentology*, 21, 533-554.

Bluck, B.J. (1976) Sedimentation in some Scottish rivers of low sinuosity, *Transactions of the Royal Society of Edinburgh*, 69, 425-456.

Bluck, B.J. (1979) Structure of coarse grained braided stream alluvium, *Transactions of the Royal Society of Edinburgh*, 70, 181-221.

Bluck, B.J. (1980) Structure, generation and preservation of upward fining, braided stream cycles in Old Red Sandstone of Scotland, *Transactions of the Royal Society of Edinburgh*, 71, 29-46.

Bluck, B.J. (1982) Texture of gravel bars in braided streams, in R.D. Hey, J.C. Bathurst and C.R. Thorne (eds.), *Gravel-bed Rivers*, Chichester, Wiley, 339-354.

Boothroyd, J.C. and Ashley, G.M. (1975) Process, bar morphology and sedimentary structures on braided outwash fans, northeastern Gulf of Alaska, in A.V. Jopling and B.C. McDonald (eds.), *Glaciofluvial and Glaciolacustrine Sedimentation*, Society of Economic Palaeontologists and Mineralogists Special Publication #23, 193-222.

Box, G.E.P. and Jenkins, G.M. (1970) *Time Series Analysis: forecasting and control*, San Francisco, Holden-Day.

Bray, D.I. (1982) Flow resistance in gravel-bed rivers, in R.D. Hey, J.C. Bathurst and C.R. Thorne (eds.), *Gravel-bed Rivers*, Chichester, Wiley, 109-133.

Brice, J.C. (1964) Channel patterns and terraces of the Loup Rivers in Nebraska, *United States Geological Survey Professional Paper* 422 D.

Bruun, P. (1967) Model geology: prototype and laboratory streams, *Bulletin of the Geological Society of America*, 77, 959-974.

Burrows, R.L., Parks, B. and Emmett, W.W. (1979) Sediment transport in the Tanana River in the vicinity of Fairbanks, Alaska, 1977-78, *United States Geological Survey Open-File Report*, 79-1539.

Cant, D.J. and Walker, R.G. (1978) Fluvial processes and facies sequences in the sandy braided South Saskatchewan River, Canada, *Sedimentology*, 25, 625-648.

Carson, M.A. (1984a) Observations on the meandering-braided river transition, the Canterbury Plains, New Zealand: Part One, *New Zealand Geographer*, 40, 12-17.

Carson, M.A. (1984b) The meandering-braided river threshold: a reappraisal, *Journal of Hydrology*, 73, 315-334.

Chang, H.Y., Simons, D.B. and Woolhiser, D.A. (1971) Flume experiments on alternate bar formation, *Journal of the Waterways and Harbours Division*, American Society of Civil Engineers, 97, 155-165.

Charlton, F.G., Brown, P.M. and Benson, R.W. (1978) The hydraulic geometry of some gravel rivers in Britain, *Hydraulics Research Station Report*, IT 180.

Chatfield, C. (1980) *The Analysis of Time Series*, London, Chapman and Hall.

Cheetham, G.H. (1979) Flow competence in relation to stream channel form and braiding, *Bulletin of the Geological Society of America*, 90, Part I, 877-886.

Chien, N. (1961) The braided stream of the Yellow River, *Scientia Sinica*, 10, 734-754.

Chow, V.T. (1959) *Open-Channel Hydraulics*, New York, McGraw-Hill.

Church, M. (1972) Baffin Island sandurs: a study of arctic fluvial processes, *Geological Survey of Canada, Bulletin* 216.

Church, M. (1983) Pattern of instability in a wandering gravel bed channel, in J.D.

Collinson and J. Lewin (eds.), *Modern and Ancient Fluvial Systems*, International Association of Sedimentologists Special Publication #6, 169-180.

Church, M. and Gilbert, R. (1975) Proglacial fluvial and lacustrine environments, in A.V. Jopling and B.C. McDonald (eds.), *Glaciofluvial and Glaciolacustrine Sedimentation*, Society of Economic Palaeontologists and Mineralogists Special Publication #23, 22-100.

Church, M. and Jones, D. (1982) Channel bars in gravel-bed rivers, in R.D. Hey, J.C. Bathurst and C.R. Thorne (eds.), *Gravel-bed Rivers*, Chichester, Wiley, 291-324.

Coleman, J.M. (1969) Brahmaputra River: channel processes and sedimentation, *Sedimentary Geology*, 3, 129-239.

Collinson, J.D. (1970) Bedforms of the Tana River, Norway, *Geografiska Annaler*, 52A, 31-55.

Cox, N.J. (1983) On the estimation of spatial autocorrelation in geomorphology, *Earth Surface Processes and Landforms*, 8, 89-93.

Crowley, K.D. (1983) Large-scale bed configurations (macroforms), Platte River Basin, Colorado and Nebraska: Primary structures and formative processes, *Bulletin of the Geological Society of America*, 94, 117-133.

Davies, T.R.H. and Tinker, C. (1981) Characteristics of regular stream meanders, *Abstracts, Second International Symposium on Fluvial Sedimentology*, Keele University, England.

Dawson, M. (1982) *Sediment variation in a braided reach of Sunwapta River, Alberta*, M.Sc. Thesis, University of Alberta.

Dodge, R.A. (1978) Sediment model verification for small diversions, *in Verification*

of Mathematical and Physical Models in Hydraulic Engineering, American Society of Civil Engineers, proceedings of the 26th Annual Hydraulics Division Specialty Conference, University of Maryland, 753-758.

Doeglas, D.J. (1951) Meandering and braided rivers, *Geologie en Mijnbouw*, 13, 297-299.

Einstein, H.A. (1950) The bed-load function for sediment transport in open channel flows, *U.S. Department of Agriculture, Soil Conservation Service, Technical Bulletin* No. 1026.

Einstein, H.A. and Li, H. (1958) Secondary flow in straight channels, *Transactions of the American Geophysical Union*, 39, 1058-1088.

Einstein, H.A. and Shen, H.W. (1964) A study of meandering in straight alluvial channels, *Journal of Geophysical Research*, 69, 5239-5247.

Emmett, W.W. (1976) Bedload transport in two large, gravel-bed rivers, Idaho and Washington. *Proceedings of the 3rd. Federal Interagency Sedimentation Conference*, Denver, Colorado, 4-101 - 4-114.

Engelund, F. and Skovgaard, O. (1973) On the origin of meandering and braiding in alluvial streams, *Journal of Fluid Mechanics*, 57, 289-302.

Evans, I.S. (1972) General geomorphometry, derivatives of altitude, and descriptive statistics, in Chorley, R.J. (ed.), *Spatial Analysis in Geomorphology*, London, Methuen, 17-90.

Everts, C.H. (1973) Particle overpassing on flat granular boundaries, *Journal of the Waterways and Harbours Division, American Society of Civil Engineers*, 99, 425-438.

Eynon, G. and Walker, R.G. (1974) Facies relationships in Pleistocene outwash

gravels, southern Ontario: a model for bar growth in braided rivers, *Sedimentology*, 21, 43-70.

Fahnestock, R.K. (1963) Morphology and hydrology of a glacial stream, White River, Mount Rainier, Washington, *United States Geological Survey Professional Paper* 422A.

Fahnestock, R.K. (1969) Morphology of the Slims River, in V.C. Bushnell and R.H. Ragle (eds.), *Icefield Ranges Research Project, Scientific Results*, volume 1, 161-172.

Fahnestock, R.K. and Bradley, W.C. (1973) Knik and Matanuska Rivers, Alaska: a contrast in braiding, in M. Morisawa (ed.), *Fluvial Geomorphology*, London, Allen and Unwin, 220-250.

Ferguson, R.I. (1973) Channel patterns and sediment type, *Area*, 5, 38-41.

Ferguson, R.I. (1975) Meander irregularity and wavelength estimation, *Journal of Hydrology*, 26, 315-33.

Ferguson, R.I. (1977) *Linear Regression in Geography*, Concepts and Techniques in Modern Geography no. 15, Norwich, Geo Abstracts.

Ferguson, R.I. (1981) Channel form and channel changes, in J. Lewin (ed.) *British Rivers*, London, Allen and Unwin, 90-125.

Ferguson, R.I. and Werritty, A. (1983) Bar development and channel changes in the gravelly River Feshie, Scotland, in J.D. Collinson and J. Lewin (eds.), *Modern and Ancient Fluvial Systems*, International Association of Sedimentologists Special Publication #6, 181-193.

Friedkin, J.F. (1945) A laboratory study of the meandering of alluvial rivers, *United States Waterways Experimental Station, Vicksburg, Mississippi.*

Galay, V. (1967) Observed forms of bed roughness in an unstable gravel river, *International Association for Hydraulic Research, Proceedings of the 12th Congress*, 1, 85-94.

Gilbert, G.K. (1914) The transportation of debris by running water, *United States Geological Survey Professional Paper* 86.

Gorycki, M.A. (1973) Hydraulic drag: a meander initiating mechanism, *Bulletin of the Geological Society of America*, 84, 175-186.

Griffiths, G.A. (1979) Recent sedimentation history of the Waimakariri River, New Zealand, *Journal of Hydrology (NewZealand)*, 18, 6-28.

Gupta, A. (1975) Stream characteristics in eastern Jamaica: an environment of seasonal flow and large floods, *American Journal of Science*, 275, 825-847.

Gustavson, T.C. (1974) Sedimentation on gravel outwash fans, Malaspina glacier foreland, Alaska, *Journal of Sedimentary Petrology*, 44, 374-389.

Gustavson, T.C. (1978) Bed forms and stratification types of modern gravel meander lobes, Nueces River, Texas, *Sedimentology*, 25, 401-426.

Hammer, K.M. and Smith, N.D. (1983) Sediment production and transport in a proglacial stream: Hilda Glacier, Alberta, Canada, *Boreas*, 12, 91-106.

Hammond, R.G. and McCullagh, P.S. (1974) *Quantitative Techniques in Geography*, Oxford, Clarendon Press.

Hein F.J. (1974) *Gravel transport and stratification origins, Kicking Horse River, British Columbia*, M.Sc. Thesis, McMaster University.

Hein, F.J. and Walker, R.G. (1977) Bar evolution and development of stratification in the gravelly, braided Kicking Horse River, British Columbia, *Canadian Journal of Earth Sciences*, 14, 562-570.

Henderson, F.M. (1961) Stability of alluvial channels, *Journal of the Hydraulics Division, American Society of Civil Engineers*, 87, 109-138.

Henderson, F.M. (1966) *Open Channel Flow*, New York, MacMillan.

Hickin, E.J. (1969) A newly-identified process of point bar formation in natural streams, *American Journal of Science*, 267, 999-1010.

Hollingshead, A.B. (1971) Sediment transport measurements in gravel rivers, *Journal of the Hydraulics Division, American Society of Civil Engineers*, 97, 1817-1834.

Hong, L.B. and Davies, T.R.H. (1979) A study of stream braiding, *Bulletin of the Geological Society of America*, 90, Part II, 1839-1859.

Hooke, R. Le B. (1968) Model geology: prototype and laboratory streams: Discussion, *Bulletin of the Geological Society of America*, 79, 391-394.

Hooke, R. Le B. (1975) Distribution of sediment transport and shear stress in a meander bend, *Journal of Geology*, 83, 543-566.

Howard, A.D., Keetch, M.E. and Vincent, C.L. (1970) Topological and geometrical properties of braided rivers, *Water Resources Research*, 1674-1688.

Hudson, H.R. (1983) *Hydrology and sediment transport in the Elbow River basin, S.W. Alberta*, Ph.D. Thesis, University of Alberta.

Hughes, D.A. (1982) An approach to the quantification of floodplain form, *Area*, 14, 285-291.

Ikeda, H. (1973) Bars in laboratory flumes and the conditions for their formation, *Geographical Review of Japan*, 46-7, 435-452.

Ingle, J.C. (1966) *The Movement of Beach Sand*, Amsterdam, Elsevier.

Jaeggi, M.N.R. (1984) Formation and effects of alternate bars, *Journal of the Hydraulics Division, American Society of Civil Engineers*, 110, 142-156.

Jenkins, G.M. and Watts, D.G. (1968) *Spectral Analysis and its Application*, San Francisco, Holden-Day.

Jones, M.L. and Seitz, H.R. (1980) Sediment transport in the Snake and Clearwater Rivers in the vicinity of Lewiston, Idaho, *United States Geological Survey Open-File Report*, 80-690.

Jopling, A.V. (1964) Interpreting the concept of the sedimentation unit, *Journal of Sedimentary Petrology*, 34, 165-172.

Kang, S. (1982) *Sediment transport in a small glacial stream: Hilda Creek, Alberta*, M.Sc. Thesis, University of Illinois at Chicago Circle.

Keller, E.A. (1971) Areal sorting of bed-load material: the hypothesis of velocity reversal, *Bulletin of the Geological Society of America*, 82, 753-756.

Kellerhals, R. (1982) Effect of river regulation on channel stability, in R.D. Hey, J.C. Bathurst and C.R. Thorne (eds.), *Gravel-bed Rivers*, Chichester, Wiley, 685-705.

Kellerhals, R. and Bray, D.I. (1971a) Comments on "An improved method for size distribution of stream bed gravel" by Luna B. Leopold, *Water Resources Research*, 7, 1045-1047.

Kellerhals, R. and Bray, D.I. (1971b) Sampling procedures for coarse fluvial sediments, *Journal of the Hydraulics Division, American Society of Civil Engineers*, 97, 1165-1180.

Kellerhals, R., Church, M. and Bray D.I. (1976) Classification and analysis of river processes, *Journal of the Hydraulics Division, American Society of Civil Engineers*, 102, 813-829.

Kellerhals, R., Neill, C.R. and Bray, D.I. (1972) Hydraulic and geomorphic

characteristics of rivers in Alberta, *Research Council of Alberta, River Engineering and Surface Hydrology Report*, 72-1.

Kennedy, J.B. and Neville, A.M. (1976) *Basic Statistical Methods for Engineers and Scientists*, (Second Edition), New York, Harper and Row.

Kinoshita, R. (1957) Formation of dunes on river beds - an observation on the condition of river meandering, *Proceedings of the Japanese Society of Civil Engineers*, 42.

Kinoshita, R. (1980) A model experiment using bedform similarity to study the consequences of removing the Ushio constriction on the Oi River, *Ministry of Construction, Central Regional Office*, Shizuoka, Japan.

Klassen, G.J. (1982) Discussion of "Gravel Bedload Transport Processes" by P.C. Klingeman and W.W. Emmett, in R.D. Hey, J.C. Bathurst and C.R. Thorne (eds.), *Gravel-bed Rivers*, Chichester, Wiley, 175-177.

Kleinbaum, D.G. and Kupper, L.L (1978) *Applied Regression Analysis and Other Multivariate Methods*, North Scituate, Massachusetts, Duxbury.

Klingeman, P.C. and Emmett, W.W. (1982) Gravel bedload transport processes, in R.D. Hey, J.C. Bathurst and C.R. Thorne (eds.), *Gravel-bed Rivers*, Chichester, Wiley, 141-179.

Knighton, A.D. (1976) Stream adjustment in a small rocky mountain basin, *Arctic and Alpine Research*, 197-212.

Kondratyev, N. Ye. and Popov, I.V. (1967) Methodological prerequisites for conducting network observations of the channel process, *Soviet Hydrology*, 6, 273-297.

Krigström, A. (1962) Geomorphological studies of sandur plains and their braided rivers in Iceland, *Geografiska Annaler*, 44, 328-346.

Krumbein, W.C. and Orme, A.R. (1972) Field mapping and computer simulation of braided-stream networks, *Bulletin of the Geological Society of America*, 83, 3369-3380.

Lane, E.W. (1957) A study of the shape of channels formed by natural streams in erodible materials, *United States Army Corps of Engineers, Missouri River Division, Omaha, Nebraska, Sediment Series* #9.

Lekatch, J. and Schick, A.P. (1983) Evidence for transport of bedload in waves: analysis of fluvial sediment samples in a small upland stream channel, *Catena*, 10, 267-279.

Leopold, L.B. (1970) An improved method for size distribution of stream bed gravel, *Water Resources Research*, 6, 1357-1366.

Leopold, L.B. and Maddock, T. (1953) The hydraulic geometry of stream channels and some physiographic implications, *United States Geological Survey Professional Paper* 252.

Leopold, L.B. and Wolman, M.G. (1957) River channel patterns, braided meandering and straight, *United States Geological Survey Professional Paper* 262B.

Lewin, J. (1976) Initiation of bed forms and meanders in coarse-grained sediment, *Bulletin of the Geological Society of America*, 87, 281-285.

Lewin, J. (1978) Floodplain geomorphology, *Progress in Physical Geography*, 2, 408-437.

Lewis, G.W. and Lewin, J. (1983) Alluvial cutoffs in Wales and the Borderlands, in J.D. Collinson and J. Lewin (eds.), *Modern and Ancient Fluvial Systems*, International Association of Sedimentologists Special Publication #6, 145-154.

Lewis, W.V. (1944) Stream trough experiments and terrace formation, *Geological Magazine*, 81, 241-253.

Lisle, T. (1979) A sorting mechanism for a riffle-pool sequence, *Bulletin of the Geological Society of America*, 90, Part II, 1142-1157.

Mackin, J.H. (1956) Cause of braiding by a graded river, *Bulletin of the Geological Society of America*, 67, 1717-1718.

Maizels, J.K. (1979) Proglacial aggradation and changes in braided channel patterns during a period of glacier advance: an Alpine example, *Geografiska Annaler*, 61A, 87-101.

Martini, I.P. (1977) Gravelly flood deposits of Irvine Creek Ontario, Canada, *Sedimentology*, 24, 603-622.

Maxwell, W.H C. and Weggel, J.R. (1969) Surface tension in Froude models, *Journal of the Hydraulics Division, American Society of Civil Engineers*, 95, 677-701.

Meland, N. and Norrman, J.O. (1966) Transport velocities of single particles in bed-load motion, *Geografiska Annaler*, 48A, 165-182.

Meland, N. and Norrman, J.O. (1969) Transport velocities of individual size fractions in heterogeneous bedload, *Geografiska Annaler*, 51A, 127-144.

Meyer-Peter, E. and Muller, R. (1948) Formulas for bed-load transport, *Proceedings of the International Association for Hydraulic Research, 3rd Annual Conference, Stockholm*, 39-64.

Miall, A.D. (1977) The braided river depositional environment, *Earth Science Reviews*, 13, 1-62.

Miall, A.D. (1978) Lithofacies types and vertical profile models in braided river deposits: a summary, in A.D. Miall (ed.), *Fluvial Sedimentology*, Canadian Society of Petroleum Geologists Memoir #5, 597-604.

Milhous, R.T. (1973) *Sediment Transport in a Gravel-Bottomed Stream*, Ph.D. Thesis, Oregon State University.

Miller, J.P. (1958) High mountain streams: effects of geology on channel characteristics and bed material, *New Mexico Bureau of Mines and Mineral Resources, Memoir* 4.

Miller, T.K. and Onesti, L.J. (1979) The relationship between channel shape and sediment characteristics in the channel perimeter, *Bulletin of the Geological Society of America*, 90, Part I, 301-304.

Mosley, M.P. (1976) An experimental study of channel confluences, *Journal of Geology*, 84, 535-562.

Mosley, M.P. (1977) Stream junctions - A probable location for bedrock placers, *Economic Geology*. 72, 691-697.

Mosley, M.P. (1981) Scour depths in branch channel confluences, Ohau River, *Water and Soil Science Centre, Ministry of Works and Development, Christchurch, New Zealand, Report* WS 395.

Mosley, M.P. and Zimpfer, G.L. (1978) Hardware models in geomorphology, *Progress in Physical Geography*, 2, 438-461.

Moss, A.J., Walker, P.H. and Hutka, J. (1980) Movement of loose, sandy detritus by shallow water flows: an experimental study, *Sedimentary Geology*, 25, 43-66.

Moss, A.J., Green, P. and Hutka, J. (1982) Small channels: their experimental formation, nature and significance, *Earth Surface Processes and Landforms*, 7, 401-415.

Nakagawa, T. (1983) Boundary effects on stream meandering and morphology, *Sedimentology*, 30, 117-127.

Nordseth, K, (1973) Fluvial processes and adjustments on a braided river, the islands of Koppangsoyene on the River Glomma, *Norsk Geografisker Tidsskrift*, 27, 77-108.

Ore, H.T. (1964) Some criteria for the recognition of braided stream deposits, *Contributions to Geology*, 3, 1-14.

Østrem, G. (1975) Sediment transport in glacial meltwater streams, in A.V. Jopling and B.C. McDonald (eds.), *Glaciofluvial and Glaciolacustrine Sedimentation*, Society of Economic Palaeontologists and Mineralogists Special Publication #23, 101-122.

Parker, G. (1976) On the cause and characteristic scales of meandering and braiding in rivers, *Journal of Fluid Mechanics*, 76, 457-480.

Parker, G. (1978) Self-formed straight rivers with equilibrium banks and mobile bed, Part 2. The gravel river, *Journal of Fluid Mechanics*, 89, 127-146.

Parker, G. (1979) Hydraulic geometry of active gravel rivers, *Journal of the Hydraulics Division, American Society of Civil Engineers*, 105, 1185-1201.

Parker, G. and Anderson, A.G. (1975) Modelling of meandering and braiding rivers, *in Symposium on Modelling Techniques, Waterways, Harbours and Coastal Engineering Division of the American Society of Civil Engineers, Second Annual Symposium*, San Francisco, volume 1, 575-591.

Parker, G. and Klingeman, P.C. (1982) On why gravel-bed streams are paved, *Water Resources Research*, 18, 1409-1423.

Parker, G., Klingeman P.C. and McLean, D.G. (1982) Bedload and size distribution in paved gravel-bed streams, *Journal of the Hydraulics Division, American Society of Civil Engineers*, 108, 544-571.

Parker, G. and Peterson, A.W. (1980) Bar resistance of gravel-bed streams, *Journal of the Hydraulics Division, American Society of Civil Engineers*, 106, 1559-1575.

Pickup, G. and Higgins, R.J. (1979) Estimating sediment transport in a braided gravel channel - The Kawerong River, Bougainville, Papua New Guinea, *Journal of Hydrology*, 40, 283-297.

Rajaratnam, N. and Berry, B. (1977) Erosion by circular turbulent wall jets, *Journal of Hydraulic Research*, 15, 277-290.

Raudkivi, A.J. and Ettema, R. (1977) Effect of sediment gradation on clearwater scour, *Journal of the Hydraulics Division, American Society of Civil Engineers*, 103, 1209-1213.

Reid, I., Layman, J.T. and Frostick, L.E. (1980) The continuous measurement of bedload discharge, *Journal of Hydraulic Research*, 18, 243-249.

Rice, R. (1979) *The Hydraulic Geometry of the Lower Portion of the Sunwapta River Valley Train, Jasper National Park, Alberta*, M.Sc. Thesis, University of Alberta.

Richards, K.S. (1979) *Stochastic processes in one-dimensional series; an introduction*, Concepts and Techniques in Modern Geography no. 23, Norwich, Geo Abstracts.

Richards, K. (1982) *Rivers: form and process in alluvial channels*, London, Methuen.

Romashin, V.V. (1967) Some characteristics of the morphological process in a mountain stream, *GGI Trudy*, 144, 67-76.

Rouse, H. (1940) Criteria for similarity in the transportation of sediment, *Proceedings of the 1st Hydraulic Conference, State University of Iowa*, Bulletin 20, 33-49.

Rubey, W.W. (1952) Geology and mineral resources of the Hardin and Brussels Quadrangles, *United States Survey Professional Paper* 218.

Rundle, A.S. (1976) *Morphology of Braided Streams*, Ph.D. Thesis, Macquarie University.

Rust, B.R. (1978a) A classification of alluvial channel systems, in A.D. Miall (ed.), *Fluvial Sedimentology*, Canadian Society of Petroleum Geologists Memoir #5, 187-198.

Rust, B.R. (1978b) Depositional models for braided alluvium, in A.D. Miall (ed.), *Fluvial Sedimentology*, Canadian Society of Petroleum Geologists Memoir #5, 605-625.

Sahu, B.K. (1964) Transformation of weight frequency and number frequency in size distribution studies of clastic sediments, *Journal of Sedimentary Petrology*, 34, 768-773.

Schumm, S.A. (1960) The shape of alluvial channels in relation to sediment type, *United States Geological Survey Professional Paper* 352 B.

Schumm, S.A. (1963) A tentative classification of alluvial river channels, *United States Geological Survey Circular* 477.

Schumm, S.A. and Khan, H.R. (1972) Experimental study of channel patterns, *Bulletin of the Geological Society of America*, 83, 1755-1770.

Schumm, S.A. and Lichty, R.W. (1963) Time, Space and Causality in Geomorphology, *American Journal of Science*, 263, 110-119.

Shen, H.W. (1979) *Modelling of Rivers*, New York, Wiley.

Shen, A.W. and Vedula, S. (1969) A basic cause of a braided channel, *International Association for Hydraulic Research, Proceedings of the 13th Congress*, Kyoto, Japan, 5-1, 201-205.

Smith, D.G. (1973) Aggradation of the Alexandra - North Saskatchewan River, Banff

Park, Alberta, in M. Morisawa (ed.), *Fluvial Geomorphology*, London, Allen and Unwin, 201-219.

Smith, D.G. and Smith, N.D. (1980) Sedimentation in anastamosed river systems: examples from alluvial valleys near Banff, Alberta, *Journal of Sedimentary Petrology*, 50, 157-164.

Smith, N.D. (1970) The braided stream depositional environment: comparison of the Platte River with some Silurian clastic rocks, North Central Appalachians, *Bulletin of the Geological Society of America*, 81, 2993-3014.

Smith, N.D. (1971a) Transverse bars and braiding in the Lower Platte River, Nebraska, *Bulletin of the Geological Society of America*, 82, 3407-3420.

Smith, N.D. (1971b) Pseudo-planar stratification produced by very low ampltitude sand waves, *Journal of Sedimentary Petrology*, 41, 69-73.

Smith, N.D. (1974) Sedimentology and bar formation in the upper Kicking Horse river, a braided meltwater stream, *Journal of Geology*, 82, 205-223.

Smith, N.D. (1978) Some comments on terminology for bars in shallow rivers, in A.D. Miall (ed.), *Fluvial Sedimentology*, Canadian Society of Petroleum Geologists, Memoir #5, 85-88.

Smith N.D. and Southard, J.B. (1982) Field investigations of braiding and gravel transport in a small outwash stream, *International Association of Sedimentologists, Abstracts, 11th International Congress on Sedimentology*, Hamilton, Ontario.

Southard, J.B. and Smith, N.D. (1982) Model experiments on braiding and gravel transport in a small outwash stream, *International Association of Sedimentologists, Abstracts, 11th International Congress on Sedimentology*, Hamilton, Ontario.

Southard, J.B., Smith, N.D., Drake, T.G. and Kuhnle, R.A. (1981) Field and laboratory studies of braiding in shallow gravel-bed streams, *Abstracts, Second International Symposium on Fluvial Sedimentology*, Keele University, England.

Stebbings, J. (1964) The shape of self-formed model alluvial channels, *Proceedings of the Institution of Civil Engineers*, 25, 485-510.

Steel, R.J. and Thompson, D.B. (1983) Structures and textures in Triassic braided stream conglomerates ('Bunter' Pebble Beds) in the Sherwood Sandstone Group, North Staffordshire, England, *Sedimentology*, 30, 341-368.

Sukegawa, N. (1973) Criterion for alternate bar formation, *Proceedings of the Japan Society of Civil Engineers*, 126.

Sundborg, A. (1956) The River Klarälven - a study of fluvial processes, *Geografiska Annaler*, 38, 127-316.

Tanner, W.F. (1960) Helicoidal flow, a possible cause of meandering, *Journal of Geophysical Research*, 65, 993-995.

Vanoni, V.A. (ed.) (1975) *Sedimentation Engineering*, American Society of Civil Engineers Manual on Engineering Practice #54.

Walker, R.G. and Cant, D.J. (1979) Sandy fluvial systems, in R.G. Walker (ed.), *Facies Models*, Geoscience Canada Reprint Series 1, 23-31.

White, W.R. and Day, T.J. (1982) Transport of graded gravel bed material, in R.D. Hey, J.C. Bathurst and C.R. Thorne (eds.), *Gravel-bed Rivers*, Chichester, Wiley, 181-213.

Williams, P.F. and Rust, B.R. (1969) The sedimentology of a braided river, *Journal of Sedimentary Petrology*, 39, 649-679.

Wolman, M.G. (1954) A method of sampling coarse bed material, *Transactions of the American Geophysical Union*, 35, 951-956.

Wolman, M.G. and Brush, L.M. (1961) Factors controlling the size and shape of stream channels in coarse, non-cohesive sand. *United States Geological Survey Professional Paper* 282 G.

Wright, L.D., Coleman, J.M. and Erickson, M.W. (1974) Analysis of major river systems and their deltas: morphologic and process comparisons, *Coastal Studies Institute, Louisiana State University, Technical Report*, No. 156.

Yalin, M.S. (1971) *Theory of Hydraulic Models*, MacMillan, London.

Yalin, M.S. (1977) *Mechanics of Sediment Transport (Second Edition)*, Oxford. Pergamon.

Yalin, M.S. and Karahan, E. (1979) Steepness of sedimentary dunes, *Journal of the Hydraulics Division, American Society of Civil Engineers*, 105, 381-392.

APPENDIX 1

Channel Dimensions and Flow Properties of Field and Laboratory Channels

(a) Field Data

Width (m)	Mean Depth (m)	Mean Velocity (ms^{-1})	Mean Particle Size (mm)	Froude Number	Relative Depth
8.6	0.21	0.76	20.4	0.53	10.3
7.0	0.25	0.76	24.6	0.48	10.2
6.4	0.13	0.88	38.3	0.78	3.4
6.0	0.18	1.15	45.6	0.86	3.9
6.4	0.19	1.28	52.3	0.94	3.6
9.4	0.19	1.10	37.9	0.81	5.0
8.9	0.20	1.12	49.9	0.80	4.0
13.4	0.25	1.02	59.5	0.65	4.2
4.2	0.14	1.09	59.4	0.93	2.4
6.4	0.19	1.26	68.7	0.92	2.8
7.0	0.11	0.90	43.3	0.87	2.5
4.2	0.14	1.07	56.0	0.91	2.5
3.8	0.23	1.05	32.2	0.70	7.1
7.6	0.16	1.01	35.8	0.81	4.5
3.8	0.18	1.10	30.7	0.83	5.9
6.0	0.12	0.84	32.5	0.77	3.7
4.4	0.13	0.98	41.4	0.87	3.1
6.8	0.29	0.98	33.6	0.58	8.6
3.7	0.15	1.20	55.0	0.96	2.9
4.6	0.20	1.01	58.0	0.72	3.4
3.6	0.19	0.90	19.3	0.66	9.8
9.0	0.18	0.54	14.8	0.41	12.2
4.0	0.20	0.89	27.4	0.63	7.3
3.0	0.12	0.64	21.8	0.59	5.5
3.7	0.30	1.43	30.7	0.83	9.8
9.0	0.16	0.81	32,5	0.65	4.9
4.7	0.20	1.38	42.6	0.98	4.7
4.4	0.17	1.39	38.1	1.08	4.5
5.6	0.13	0.92	38.6	0.81	3.4
4.4	0.19	0.94	30.4	0.69	6.3
5.2	0.21	0.81	37.1	0.56	5.7
6.4	0.22	1.46	28.7	0.99	7.7
6.4	0.13	0.86	38.7	0.76	3.4
8.4	0.16	1.01	23.5	0.81	6.8
8.4	0.24	1.18	47.2	0.77	5.1
4.0	0.20	1.10	41.6	0.78	4.8
7.8	0.23	1.30	45.0	0.87	5.1
6.9	0.16	0.97	33.1	0.77	4.8
4.4	0.15	1.13	40.6	0.93	3.7
3.0	0.21	1.22	47.0	0.85	4.5
2.8	0.13	1.05	52.6	0.93	2.5
5.8	0.23	1.49	40.3	0.99	5.7
9.8	0.19	1.32	39.2	0.97	4.9
5.6	0.25	1.69	46.4	1.08	5.4
4.0	0.20	1.39	57.0	0.99	3.5
3.4	0.09	0.77	47.8	0.82	1.9

(b) Laboratory Data

Width (m)	Mean Depth (mm)	Mean Velocity ($m\ s^{-1}$)	Mean Particle Size (mm)	Froude Number	Particle Reynolds Number	Relative Depth
0.23	9.6	0.243	1.75	0.79	65.8	5.5
0.20	11.3	0.235	1.22	0.71	49.7	9.3
0.22	7.7	0.211	1.81	0.77	49.7	4.3
0.26	9.5	0.194	1.28	0.63	39.1	7.4
0.19	8.3	0.209	1.86	0.73	53.1	4.5
0.21	9.1	0.240	2.33	0.80	69.6	3.9
0.36	10.7	0.279	2.67	0.86	86.5	4.0
0.35	14.1	0.345	1.75	0.93	65.1	8.1
0.39	12.4	0.265	1.57	0.76	54.8	7.9
0.39	14.5	0.277	1.44	0.73	54.3	10.1
0.34	13.5	0.255	1.32	0.70	49.0	10.2
0.31	22.1	0.282	1.71	0.61	79.6	12.9
0.14	11.4	0.211	2.48	0.63	101.6	4.6
0.26	13.1	0.252	1.58	0.70	69.4	8.3
0.09	7.2	0.223	2.26	0.84	73.6	3.2
0.17	7.5	0.172	1.08	0.63	35.9	6.9
0.10	6.8	0.226	1.13	0.88	35.7	6.0
0.16	8.1	0.211	1.61	0.75	55.6	5.0
0.24	8.1	0.180	1.95	0.64	67.3	4.2
0.20	11.4	0.214	1.74	0.64	71.3	6.5
0.28	13.0	0.261	1.70	0.73	74.3	7.7
0.32	13.4	0.261	1.00	0.72	44.4	13.4
0.23	7.3	0.165	1.13	0.62	37.0	6.5
0.24	10.7	0.209	2.40	0.64	95.2	4.5
0.17	9.4	0.207	1.48	0.68	55.0	6.4
0.20	8.9	0.165	1.97	0.56	71.3	4.5
0.17	7.8	0.187	1.39	0.68	47.1	5.6
0.18	10.7	0.205	1.64	0.63	65.1	6.5
0.19	8.7	0.183	1.15	0.63	41.1	7.6
0.22	11.5	0.231	2.51	0.69	103.2	4.6
0.32	10.9	0.212	2.56	0.65	102.5	4.3
0.38	10.5	0.202	2.53	0.63	99.4	4.2
0.20	11.7	0.230	1.17	0.68	49.6	10.0
0.29	12.6	0.227	1.27	0.65	54.7	9.9
0.24	10.2	0.210	1.62	0.66	62.8	6.3
0.21	8.0	0.235	1.49	0.84	51.1	5.4
0.26	13.5	0.242	1.59	0.66	70.9	8.5
0.33	12.0	0.217	1.63	0.63	68.5	7.4
0.19	11.5	0.236	1.22	0.70	50.2	9.4
0.19	12.8	0.242	1.06	0.68	46.0	12.1

APPENDIX 2

Sediment Transport Data for Laboratory and Field Rivers.

Notation

Q	Discharge
S	Water surface slope
B	Channel width
d	Mean depth
g_b	Mass rate of sediment transport per unit width
ω'	Stream power index per unit width
τ^*	Shields stress
$\bar{\omega}'$	Dimensionless stream power index per unit width
q^*_b	Dimensionless bedload discharge per unit width
τ^*_c	Critical Shields stress
$\bar{\omega}'_c$	Critical dimensionless stream power index per unit width

	τ^*_c	$\bar{\omega}'_c$	$(R g D_{50})^{\frac{1}{2}} D_{50}$
Laboratory data	0.03	0.100	1.67×10^{-4}
Schumm and Khan (1972)	0.03	0.128	7.45×10^{-5}
Leopold and Wolman (1957)	0.04	0.300	9.10×10^{-5}
Wolman and Brush (1961)	0.03	0.128	7.00×10^{-5}
Snake River	0.08	0.400	1.79×10^{-2}
Clearwater River	0.08	0.400	9.72×10^{-3}
Elbow River	0.08	0.400	1.59×10^{-2}
Oak Creek	0.08	0.400	1.14×10^{-2}
Tanana River	0.03	0.100	7.39×10^{-3}

Laboratory data (present study)

Q	S	B	d	g_b	$\omega' \times 10^5$	τ^*	$\bar{\omega}'$	q^*_b	τ^*/τ^*_c	$\bar{\omega}'/\bar{\omega}'_c$
0.00300	0.015	0.975	0.0086	0.0093	4.62	0.065	0.277	0.02101	2.17	2.77
0.00300	0.015	0.950	0.0087	0.0097	4.74	0.066	0.284	0.02192	2.20	2.84
0.00150	0.010	0.640	0.0106	0.0022	2.34	0.053	0.140	0.00597	1.77	1.40
0.00150	0.015	0.728	0.0085	0.0045	3.09	0.064	0.185	0.01017	2.13	1.85
0.00150	0.015	0.378	0.0121	0.0145	5.95	0.092	0.356	0.03276	3.07	3.56
0.00150	0.015	0.680	0.0079	0.0037	3.31	0.060	0.198	0.00836	2.00	1.98
0.00150	0.010	0.460	0.0109	0.0020	3.26	0.055	0.195	0.00452	1.83	1.95
0.00450	0.010	1.060	0.0110	0.0075	4.25	0.056	0.254	0.01695	1.87	2.54
0.00450	0.015	1.050	0.0100	0.0200	6.43	0.076	0.385	0.04519	2.53	3.85
0.00225	0.015	0.880	0.0083	0.0054	3.84	0.063	0.230	0.01220	2.10	2.30
0.00120	0.015	0.570	0.0077	0.0020	3.16	0.058	0.189	0.00452	1.93	1.89

Schumm and Khan (1972)

Q	S	B	d	g_b	$\omega' \times 10^5$	τ^*	$\bar{\omega}'$	q^*_b	τ^*/τ^*_c	$\bar{\omega}'/\bar{\omega}'_c$
0.0042	0.0015	0.518	0.0270	0.0029	1.22	0.035	0.164	0.0147	1.17	1.64
0.0042	0.0028	0.649	0.0180	0.0028	1.82	0.044	0.244	0.0142	1.47	2.44
0.0042	0.0039	0.655	0.0190	0.0032	2.44	0.063	0.327	0.0162	2.10	3.27
0.0042	0.0040	0.664	0.0175	0.0038	2.56	0.061	0.344	0.0193	2.03	3.44
0.0042	0.0010	0.353	0.0500	0.0057	1.19	0.043	0.160	0.0289	1.43	1.60
0.0042	0.0017	0.655	0.0270	0.0034	1.09	0.040	0.146	0.0172	1.33	1.46
0.0042	0.0021	0.670	0.0260	0.0037	1.32	0.047	0.177	0.0187	1.57	1.77
0.0042	0.0150	1.550	0.0053	0.0079	4.06	0.069	0.545	0.0400	2.30	5.45
0.0042	0.0160	1.610	0.0045	0.0085	4.17	0.062	0.560	0.0431	2.07	5.60
0.0042	0.0180	1.670	0.0039	0.0092	4.53	0.061	0.608	0.0466	2.03	6.08
0.0042	0.0200	1.720	0.0034	0.0097	4.88	0.059	0.655	0.0491	1.97	6.55
0.0042	0.0026	0.945	-	0.0044	1.19	-	0.154	0.0172	-	1.54
0.0042	0.0043	1.160	-	0.0035	1.56	-	0.209	0.0177	-	2.09
0.0042	0.0059	1.220	-	0.0048	2.03	-	0.272	0.0243	-	2.72
0.0042	0.0064	1.250	-	0.0052	2.15	-	0.289	0.0263	-	2.89
0.0042	0.0075	1.370	-	0.0050	2.30	-	0.309	0.0253	-	3.09
0.0042	0.0085	1.430	-	0.0050	2.50	-	0.335	0.0253	-	3.35
0.0042	0.0100	1.430	-	0.0059	2.94	-	0.395	0.0299	-	3.95
0.0042	0.0130	1.490	-	0.0063	3.70	-	0.497	0.0319	-	4.97

Leopold and Wolman (1957)

Q	S	B	d	g_b	$\omega' \times 10^5$	τ^*	$\bar{\omega}'$	q^*_b	τ^*/τ^*_c	$\bar{\omega}'/\bar{\omega}'_c$
0.00178	0.0085	0.268	0.016	0.00634	5.60	0.103	0.615	0.0263	2.58	2.05
0.00241	0.0133	0.488	0.011	0.00430	6.56	0.111	0.721	0.0178	2.78	2.40
0.00241	0.0095	0.363	0.014	0.00578	6.31	0.101	0.693	0.0240	2.53	2.31
0.00241	0.0104	0.421	0.012	0.00475	5.96	0.094	0.655	0.0197	2.35	2.18
0.00241	0.0079	0.402	0.013	0.00498	4.73	0.078	0.520	0.0207	1.95	1.73
0.00241	0.0081	0.393	0.015	0.00513	5.00	0.092	0.549	0.0213	2.30	1.83
0.00241	0.0157	0.579	0.008	0.00345	6.53	0.095	0.718	0.0143	2.38	2.39
0.00241	0.0093	0.366	0.015	0.00546	6.12	0.106	0.672	0.0227	2.65	2.24

0.00085	0.0135	0.219	0.008	0.00594	5.25	0.082	0.577	0.0246	2.05	1.92
0.00085	0.0114	0.171	0.010	0.00702	5.67	0.086	0.623	0.0291	2.15	2.08
0.00150	0.0111	0.244	0.014	0.00738	6.80	0.118	0.747	0.0306	2.95	2.49
0.00263	0.0165	0.655	0.009	0.00733	6.63	0.112	0.729	0.0304	2.80	2.43
0.00263	0.0095	0.387	0.015	0.01240	6.46	0.108	0.710	0.0[illegible]5	2.70	2.37
0.00113	0.0115	0.235	0.012	0.00723	5.53	0.104	0.608	0.0300	2.60	2.03
0.00028	0.0103	0.107	0.008	0.00748	2.72	0.062	0.299	0.0310	1.55	1.00
0.00113	0.0175	0.207	0.013	0.01160	9.56	0.172	1.051	0.0481	4.30	3.50
0.00113	0.0113	0.207	0.016	0.01160	6.18	0.137	0.679	0.0481	3.43	2.26
0.00244	0.0068	0.299	0.019	0.00401	5.55	0.098	0.610	0.0166	2.45	2.03
0.00244	0.0041	0.305	0.019	0.00393	3.28	0.059	0.360	0.0163	1.48	1.20
0.00093	0.0133	0.201	0.010	0.00458	6.17	0.101	0.678	0.0190	2.53	2.26
0.00093	0.0103	0.201	0.010	0.00458	4.79	0.078	0.526	0.0190	1.95	1.75
0.00093	0.0148	0.232	0.009	0.00396	5.95	0.101	0.654	0.0164	2.53	2.18
0.00093	0.0117	0.204	0.010	0.00451	5.34	0.089	0.587	0.0187	2.23	1.96
0.00093	0.0112	0.201	0.012	0.00199	5.22	0.102	0.574	0.0083	2.55	1.91
0.00093	0.0105	0.201	0.011	0.00463	4.88	0.087	0.536	0.0192	2.18	1.79
0.00093	0.0105	0.201	0.010	0.00955	4.83	0.079	0.535	0.0396	1.98	1.79
0.00093	0.0109	0.204	0.011	0.01430	5.00	0.091	0.549	0.0597	2.28	1.83

Wolman and Brush (1961)

Q	S	B	d	q_b	$\omega' \times 10^5$	τ^*	$\bar{\omega}'$	q^*_b	τ^*/τ^*_c	$\bar{\omega}'/\bar{\omega}'_c$
0.00030	0.0041	0.128	0.0096	0.000485	0.961	0.035	0.138	0.00261	1.18	1.38
0.00057	0.0039	0.204	0.0100	0.001020	1.103	0.035	0.158	0.00550	1.18	1.58
0.00110	0.0039	0.283	0.0130	0.003530	1.505	0.045	0.216	0.01903	1.51	2.16
0.00057	0.0038	0.177	0.0110	0.001250	1.232	0.038	0.176	0.00674	1.26	1.76
0.00054	0.0064	0.213	0.0110	0.012300	1.624	0.063	0.233	0.06631	2.11	2.33
0.00113	0.0068	0.378	0.0096	0.009230	2.032	0.059	0.291	0.04976	1.96	2.91
0.00071	0.0071	0.247	0.0120	0.006070	2.041	0.077	0.292	0.03272	2.56	2.92
0.00062	0.0035	0.204	0.0115	0.000691	1.064	0.036	0.152	0.00210	1.21	1.52
0.00096	0.0042	0.265	0.0160	0.001660	1.521	0.061	0.218	0.00895	2.02	2.18
0.00116	0.0023	0.247	0.0200	0.000385	1.482	0.041	0.212	0.00207	1.38	2.12
0.00178	0.0025	0.344	0.0160	0.000988	1.314	0.037	0.188	0.00533	1.22	1.88
0.00091	0.0028	0.219	0.0160	0.000826	1.164	0.040	0.167	0.00445	1.35	1.67
0.00074	0.0018	0.241	0.0140	1.88×10^{-6}	0.544	0.022	0.078	0.00001	0.74	0.78
0.00139	0.0018	0.253	0.0220	0.000375	1.012	0.036	0.145	0.00202	1.22	1.45
0.00110	0.0021	0.241	0.0180	0.000324	0.963	0.034	0.138	0.00175	1.14	1.38
0.00110	0.0019	0.232	0.0180	0.000168	0.909	0.031	0.130	0.00091	1.04	1.30
0.00140	0.0017	0.271	0.0200	0.000299	0.889	0.031	0.127	0.00161	1.03	1.27
0.00140	0.0017	0.232	0.0199	0.000354	1.056	0.031	0.151	0.00191	1.05	1.51
0.00068	0.0027	0.195	0.0140	0.000410	0.959	0.035	0.137	0.00221	1.16	1.37
0.00025	0.0038	0.146	0.0099	0.001090	0.651	0.034	0.093	0.00588	1.13	0.93
0.00062	0.0029	0.177	0.0130	0.000904	1.028	0.034	0.147	0.00487	1.15	1.47
0.00062	0.0032	0.189	0.0120	0.000847	1.048	0.035	0.150	0.00457	1.15	1.50
0.00062	0.0035	0.201	0.0120	0.000796	1.080	0.038	0.155	0.00429	1.26	1.55
0.00062	0.0037	0.192	0.0115	0.000833	1.208	0.039	0.173	0.00449	1.29	1.73
0.00034	0.0048	0.152	0.0093	0.000566	1.086	0.041	0.155	0.00305	1.35	1.55
0.00195	0.0019	0.363	0.0171	0.000545	1.030	0.030	0.148	0.00294	0.99	1.48
0.00082	0.0032	0.244	0.0150	0.001030	1.090	0.044	0.156	0.00555	1.46	1.56

Snake River, James and Seitz (1980)

Q	S	B	d	q_b	$\omega' \times 10^5$	τ^*	$\bar{\omega}'$	q^*_b	τ^*/τ^*_c	$\bar{\omega}'/\bar{\omega}'_c$
1124	0.00068	166	3.81	0.0161	0.0046	0.058	0.259	0.00034	0.73	0.65
1467	0.00077	172	4.17	0.0576	0.0052	0.072	0.369	0.00122	0.90	0.92
1909	0.00088	180	4.60	0.0771	0.0093	0.091	0.524	0.00163	1.14	1.31
2453	0.00101	186	5.00	0.1531	0.0133	0.113	0.748	0.00325	1.41	1.87
2509	0.00102	187	5.06	0.0949	0.0137	0.116	0.769	0.00201	1.45	1.92
3059	0.00112	192	5.42	0.0931	0.0178	0.136	1.002	0.00197	1.70	2.51
2750	0.00107	187	5.21	0.1046	0.0157	0.125	0.875	0.00222	1.56	2.19
2138	0.00094	183	4.78	0.0513	0.0110	0.101	0.617	0.00109	1.26	1.54
2569	0.00105	189	5.15	0.0503	0.0148	0.121	0.830	0.00107	1.51	2.08
3002	0.00112	192	5.36	0.0781	0.0175	0.135	0.984	0.00166	1.69	2.46
2600	0.00103	187	5.12	0.0452	0.0143	0.118	0.804	0.00096	1.48	2.01
2812	0.00108	190	5.24	0.0958	0.0160	0.127	0.898	0.00203	1.59	2.25
2685	0.00105	189	5.18	0.3102	0.0149	0.122	0.838	0.00658	1.53	2.10
2322	0.00098	184	4.91	0.2814	0.0124	0.108	0.695	0.00597	1.35	1.74
2379	0.00099	186	4.97	0.0781	0.0127	0.110	0.711	0.00166	1.38	1.78
3257	0.00116	195	5.55	0.0497	0.0194	0.144	1.099	0.00105	1.80	2.75
2744	0.00107	189	5.21	0.0356	0.0155	0.125	0.873	0.00075	1.56	2.18
1846	0.00087	178	4.54	0.1473	0.0090	0.089	0.507	0.00312	1.11	1.27
1626	0.00082	177	4.33	0.0937	0.0075	0.080	0.423	0.00199	1.00	1.06
2274	0.00098	184	4.88	0.1503	0.0121	0.107	0.680	0.00319	1.34	1.70
2172	0.00094	183	4.82	0.1131	0.0112	0.102	0.627	0.00240	1.28	1.57
2285	0.00098	184	4.88	0.1086	0.0122	0.107	0.684	0.00230	1.34	1.71
2175	0.00094	183	4.82	0.0491	0.0112	0.102	0.628	0.00104	1.28	1.57
2132	0.00094	183	4.78	0.0878	0.0110	0.101	0.615	0.00186	1.26	1.54

Clearwater River, Jones and Seitz (1980)

Q	S	B	d	q_b	$\omega' \times 10^5$	τ^*	$\bar{\omega}'$	q^*_b	τ^*/τ^*_c	$\bar{\omega}'/\bar{\omega}'_c$
1812	0.00040	143	5.06	0.0386	0.0051	0.068	0.522	0.00150	0.85	1.31
2266	0.00047	145	5.30	0.0139	0.0073	0.084	0.757	0.00054	1.05	1.89
4117	0.00062	149	5.67	0.2579	0.0130	0.118	1.336	0.01004	1.48	3.34
1543	0.00035	142	4.88	0.0144	0.0038	0.058	0.395	0.00056	0.73	0.99
2294	0.00049	146	5.30	0.0309	0.0077	0.087	0.794	0.00120	1.09	1.99
1575	0.00036	142	4.91	0.0267	0.0040	0.059	0.412	0.00104	0.74	1.03
1747	0.00039	142	5.00	0.0316	0.0048	0.066	0.495	0.00123	0.83	1.24
1552	0.00035	142	4.88	0.0288	0.0038	0.058	0.399	0.00112	0.73	1.00
2348	0.00050	143	5.33	0.0733	0.0082	0.090	0.846	0.00285	1.15	2.12
2749	0.00056	146	5.52	0.0592	0.0105	0.104	1.083	0.00230	1.30	2.71

Elbow River, Hollingshead (1971)

Q	S	B	d	q_b	$\omega' \times 10^5$	τ^*	$\bar{\omega}'$	q^*_b	τ^*/τ^*_c	$\bar{\omega}'/\bar{\omega}'_c$
109.0	0.00745	48.8	1.16	0.486	0.0166	0.209	1.046	0.01153	2.61	2.62
82.1	0.00745	45.8	0.95	0.274	0.0134	0.171	0.841	0.00650	2.14	2.10
53.8	0.00745	41.5	0.67	0.264	0.0097	0.121	0.607	0.00627	1.51	1.52
46.2	0.00745	40.1	0.55	0.043	0.0086	0.099	0.539	0.00102	1.24	1.35
44.2	0.00745	39.7	0.52	0.112	0.0083	0.094	0.522	0.00266	1.18	1.31
41.6	0.00745	39.1	0.49	0.085	0.0079	0.088	0.498	0.00202	1.10	1.25
35.4	0.00745	37.7	0.46	0.006	0.0070	0.083	0.440	0.00014	1.04	1.10
42.2	0.00745	39.3	0.55	0.090	0.0080	0.099	0.503	0.00214	1.24	1.26
39.7	0.00745	38.7	0.46	0.016	0.0076	0.083	0.480	0.00038	1.04	1.20
38.8	0.00745	38.5	0.46	0.017	0.0075	0.083	0.472	0.00040	1.04	1.18
82.1	0.00745	45.8	0.80	0.512	0.0134	0.144	0.841	0.0121	1.80	2.10
90.6	0.00745	46.8	0.83	0.463	0.0144	0.150	0.907	0.01099	1.88	2.27
68.0	0.00745	43.8	0.76	0.604	0.0116	0.137	0.727	0.01433	1.71	1.82
62.3	0.00745	42.9	0.73	0.310	0.0108	0.132	0.680	0.00736	1.65	1.70
63.7	0.00745	43.2	0.74	0.417	0.0110	0.134	0.692	0.00989	1.68	1.73
95.2	0.00745	47.3	0.84	0.507	0.0150	0.152	0.942	0.01203	1.90	2.36
90.1	0.00745	46.7	0.83	0.803	0.0144	0.150	0.903	0.01906	1.90	2.26
85.0	0.00745	46.1	0.81	0.502	0.0137	0.146	0.863	0.01191	1.83	2.16
82.1	0.00745	45.8	0.80	0.739	0.0134	0.144	0.841	0.01754	1.80	2.10
69.4	0.00745	44.0	0.76	0.304	0.0118	0.137	0.738	0.00721	1.71	1.85
62.3	0.00745	42.9	0.73	0.262	0.0103	0.132	0.680	0.00622	1.65	1.70
59.5	0.00745	42.5	0.72	0.102	0.0104	0.130	0.656	0.00242	1.63	1.64
59.5	0.00745	42.5	0.72	0.127	0.0104	0.130	0.656	0.00301	1.63	1.64
62.3	0.00745	42.9	0.73	0.073	0.0108	0.132	0.680	0.00173	1.65	1.70

Oak Creek, Parker et al. (1982)

Q	S	B	d	q_b	$\omega' \times 10^5$	τ^*	$\bar{\omega}'$	q^*_b	τ^*/τ^*_c	$\bar{\omega}'/\bar{\omega}'_c$
2.61	0.0097	3.66	0.399	0.0486	0.00692	0.117	0.607	0.00161	1.46	1.52
2.61	0.0097	3.66	0.399	0.0367	0.00692	0.117	0.607	0.00121	1.46	1.52
2.63	0.0097	3.66	0.399	0.0297	0.00697	0.117	0.612	0.00098	1.46	1.53
2.83	0.0098	3.66	0.418	0.0292	0.00758	0.124	0.665	0.00097	1.55	1.66
3.40	0.0099	3.66	0.445	0.1034	0.00920	0.134	0.807	0.00342	1.68	2.02
1.90	0.0100	3.66	0.341	0.0077	0.00519	0.103	0.456	0.00025	1.29	1.14
1.81	0.0100	3.66	0.329	0.0069	0.00495	0.100	0.434	0.00023	1.25	1.09
1.76	0.0100	3.66	0.326	0.0040	0.00481	0.099	0.422	0.00013	1.24	1.06
1.70	0.0100	3.66	0.320	0.0016	0.00464	0.097	0.408	0.00005	1.21	1.02
1.53	0.0100	3.66	0.314	0.0009	0.00418	0.095	0.367	0.00003	1.19	0.92
1.76	0.0100	3.66	0.357	0.0033	0.00481	0.108	0.422	0.00011	1.35	1.06
2.04	0.0101	3.66	0.369	0.0068	0.00563	0.113	0.494	0.00023	1.41	1.24
2.61	0.0102	3.66	0.387	0.0364	0.00727	0.120	0.638	0.00120	1.50	1.60
2.21	0.0108	3.66	0.372	0.1108	0.00652	0.122	0.572	0.00367	1.52	1.43
1.53	0.0105	3.66	0.341	0.0099	0.00439	0.109	0.385	0.00033	1.36	0.96
1.33	0.0104	3.66	0.326	0.0048	0.00378	0.103	0.332	0.00016	1.29	0.83
1.02	0.0102	3.66	0.308	0.0014	0.00284	0.095	0.249	0.00005	1.19	0.62
1.08	0.0102	3.66	0.305	0.0014	0.00301	0.094	0.264	0.00005	1.17	0.66
1.44	0.0100	3.66	0.335	0.0059	0.00393	0.102	0.345	0.00020	1.27	0.86
1.76	0.0100	3.66	0.357	0.0197	0.00481	0.108	0.422	0.00069	1.35	1.06
2.10	0.0100	3.66	0.372	0.0397	0.00574	0.113	0.504	0.00131	1.41	1.26

Tanana River, Burrows et al. (1979)

Q	S	B	d	q_b	$\omega' \times 10^5$	τ^*	$\bar{\omega}'$	q^*_b	τ^*/τ^*_c	$\bar{\omega}'/\bar{\omega}'_c$
750	0.00047	204	2.02	0.0187	0.00173	0.048	0.234	0.00198	1.60	2.34
1325	0.00050	350	2.27	0.2482	0.00189	0.047	0.255	0.01270	1.57	2.55
1167	0.00050	320	2.22	0.0656	0.00182	0.046	0.247	0.00335	1.53	2.47
1079	0.00049	290	2.18	0.0933	0.00182	0.046	0.247	0.00476	1.53	2.47
1269	0.00050	341	2.25	0.0452	0.00186	0.046	0.251	0.00231	1.53	2.51
1679	0.00052	424	2.39	0.1595	0.00206	0.048	0.279	0.00814	1.60	2.79
1458	0.00051	381	2.32	0.1241	0.00195	0.047	0.264	0.00634	1.57	2.64

APPENDIX 3

Sediment Transport Measurements from the Laboratory Runs

Time	Run									
(hours & tenths)	1	2	3	4	6	7	8	9	10	11
00.25	775	330	135	490	460	32	440	890	240	14
00.50	300	550	230	180	156	96	1020	700	320	16
00.75	100	520	150	230	165	94	510	950	210	10
1.00	125	280	200	240	104	134	540	1510	370	60
1.25	125	340	36	70	94	82	490	900	430	106*
1.50	150	460	170	100	200	95	505	1220	350	152*
1.75	170	600	200	68	216	56	370	500	132	198*
2.00	210	280*	100	140	234	48	290*	645*	128	244
2.25	230*	245	100	111*	148	44	210*	790	300	238
2.50	250	210	128	82*	132	71*	130*	600	460	108
2.75	340	210	104	54	60	98	50	620*	400	148
3.00	640	350	60	54	76	92	395	640	146	174
3.25	680	370	70*	50	103*	105	389*	830	104	144
3.50	340	600	80	102	130*	72	382*	740	245	196
3.75	580	260	56	88	157*	40	376*	660	124	202
4.00	530	530	20	178	184	30	370	690	96	198
4.25	790	360	22	54	110	12	470	620	143*	132
4.50	545*	590	24	148	38	15	210	790	190	130
4.75	330	420	12	94	30	28	210	880	270	96
5.00	330	500	54	76	14	50	150	750	170	84
5.25	280	550	76	134	16	55	200*	530	200	86
5.50	230	340	68	210	14	58	550	570	240	48
5.75	230	318*	36	146	130	58	470	450	230	74
6.00	250	296*	70	108	80	32	350	680	250	64
6.25	230	278*	50	102*	38	44	340	620	176	61*
6.50	180	252*	40	96*	48	84	230	560	164*	58
6.75	280	230	20	90	58	58	410	810	152*	62
7.00	250	440	22	72	42	35	330	690	140	66
7.25	425*	200	22	120	44	56	340	1590	220	58
7.50	600	260	24	120	52	64	367*	950	184	86

* indicate missing values calculated by linear interpolation

Note: Sediment transport rates are measured in cm^3 per minute.

Time	Run									
(hours & tenths)	1	2	3	4	6	7	8	9	10	11
7.75	400	180	36	166	222	46	395*	560	320	66
8.00	610	350	22	280	212	51	422*	740	350	92
8.25	440	350	32	172	188*	75	450	760	168	104
8.50	470	420	30	250	165*	60	470	710	242	84
8.75	270	250	46	152	141*	66	370	730	150	64
9.00	480	120	68	100	118	80	300	810	185	66
9.25	50	560	68	126	132	34	150	650	204	66
9.50	240	380	42	140	184	28	310	780	116	64
9.75	220	230	74	134	122	26	190	710	240	36
10.00	160	270	134	112	164	20	190	1040	94	22
10.25	330*	340	132	86	120	30*	292*	950	126	12
10.50	500	220	116	160	100	40	395	640	70	48
10.75	170	270	98	128	106	24	330	820	84	24
11.00	570	260	82	96	114	42	260	990	52	18
11.25	570	90	84	128	120	18	270	600	36	46
11.50	250	300	90	68	76	60	260	680	116	52*
11.75	320	200	70	204	118	36	290	730	111*	58
12.00	400	320	132	142	94	64	240	420	106	74
12.25	200	450	82	164	174	35	490	1160	142	54
12.50	220	420	40	214	130	62	450	1035*	108	78
12.75	250*	340	76	64	122	28	480	850	116	52
13.00	280	290	52	380	42	36	310	1210	60	86
13.25	250	265*	46	136	26	36	390	940	106	162
13.50	220	240	80	122	154	28	270	880	80	50
13.75	225*	190	52	218	110	20	360	990	66	16
14.00	230	170	46	180	85	35	370	630	112	10
14.25	230	230	35	187*	44	43*	335	880	146	8
14.50	210	277*	34	194*	28	50	380	530	120	46
14.75	470	324*	34*	201*	94	40	405	730	152	76
15.00	380*	370	35	208*	78	48	200	1770	238	102

Time	Run									
(hours & tenths)	1	2	3	4	6	7	8	9	10	11
15.25	290	300	22	216	82	98	180	520	196	58
15.50	220	360	44	70	94	92	220	840	168	50
15.75	300	420	28	160	156	60	190	810	120	78
16.00	390*	330	120	148	114	38	130	960	202	60
16.25	380	420	142	130	114	60	260	1300	176	48*
16.50	325	200	72	96	46	28	230	1100	112	36
16.75	270	240	65*	88	94	14	250	840	149*	16
17.00	180	270	60*	126	25	12	170	790	186*	52
17.25	420	260	55*	162	66	42	250	900	222	40
17.50	290	230*	50	150	84	54	280	800	234	64
17.75	130	260	20	260	82*	28	220	740	186	34
18.00	280	550	30	260	80*	42	225	980	255	24
18.25	270	570	130	310	78*	60	255	1010	260	24
18.50	267*	350	170	110	76*	52	270	600	174*	16
18.75	263*	450	72	72	74*	41*	215	590	88	48
19.00	260	390	126	96	72	30	260	390	130	34
19.25	320	500	54	150	56	21	290	700	116	20
19.50	230	500	170	100	68*	12	320	300	142	30
19.75	390	280	78	92	80*	22	135	540	104	26
20.00	870	280	116	126	92*	28	420	1040	74	48
20.25	810	310	54	82	104*	38	360	710	104	162
20.50	440	450	46	182	116	40	340	310	78	82
20.75	330	390	36	146	132	33	340	1050	255	84
21.00	170	430	134	138	86	24	340	670	110	98
21.25	460	440	108	136	160	12	260	1060	495	96
21.50	310	470	94	160	162	20	225	950	330	60
21.75	250	610	68	116	76	8	200	730	320	48
22.00	410	510	48	110	80	14	240	740	325	44
22.25	400	590	30	52	70	5	250*	980	170	30
22.50	310	600	40	68	50	11	260	910*	166	16

Time (hours & tenths)	Run 1	2	3	4	6	7	8	9	10	11
22.75	380	450	64	196	65	10	290	840*	104	24
23.00	410	610	96	188	112	9	290	770	146	24
23.25	350	510	76	208	144	24	280	700	390	22
23.50	200	1260	103*	98	96	33*	280	960	301*	8
23.75	350	450	130	138	86	42	430	750	212	68
24.00	310	425*	68	124	65	28	400	1020	230	52
24.25	380	400	60	214	102	28	680	830	200	24
24.50	220	390	64	124	92	26*	390	1040	270	62
24.75	320	250	67*	142	100	24	260	400	218	58
25.00	320	400	70	136	102	15	280	710	250	78
25.25	310	480	154	136	73	25	355	730	192	80
25.50	700	480	76	200	66	24	400	940	168	140
25.75	140	510	83	200	66	25	350	950	104	204
26.00	340	280	122	146	14	36	390	770	148	204
26.25	380	420	86	154	20	48	330	520	152	154
26.50	380	330	102	120	32*	44	445	510	162	106
26.75	320	300	87	120	44*	32	360	920	62	90
27.00	510	200	98	74	56	21	360	1090*	154	88
27.25	310	220	48	60	96	22	290	1260	130	100
27.50	350	230	39*	70	125	8	290	690	166	36
27.75	290	260	30*	96	102	10	290	760	144	130
28.00	260	310	22	102	76	14	265	970	96	76
28.25	280	310	41	160	50	8	220	1030	158	28
28.50	460	390	24	94	108	23	320	590	248	20
28.75	395*	320	22	84*	162	72	220	790*	198	132
29.00	330	230	28	74	208	28	220	990*	106	24
29.25	260	480	18	70	190	46	150	1190	184	40
29.50	240	440	32	62	163	64	60	1250	270	46
29.75	230	370	118	102	114	78	70	800	196	32
30.00	405*	350	130	112	112	50	60	860	350	32

Time (hours & tenths)	Run 1	2	3	4	6	7	8	9	10	11
30.25	580	260	62	74	92	22	190	450	160	54
30.50	680	220	108	100	114	48	100	400	330	22
30.75	410	190	116	72	78	50	240	600	330	40
31.00	400	430	54	52	85	30	320	560	200	30
31.25	370	430	90	88	162	44	260	620	320	42
31.50	310	290	56	210	92	18	250	1120	180	50
31.75	450	430	72	182	91*	42	180	690	220	124
32.00	430	580	70	180	90	33*	110	670	96	124
32.25	410	475*	68	210	78	24	160	920	185	76
32.50	420	370	102	102	98	32	200	450	140	56
32.75	430	300	50	98	98	33*	275	470	124	40
33.00	370	250	50	158	98	34*	180	620	100	50
33.25	540	480	74	170	108	35*	280	490	48	54
33.50	450	430	54	162	68	36*	320	410	58	54
33.75	540	230	80	96	124	36	260	480	185	50
34.00	100	200	54	182	72	62	240*	670	194	34
34.25	640	220	60	250	84	48	220	1730	120	26*
34.50	670	500	74	166	62	46	375	1310	104	18*
34.75	340	270	60	112	122	42	425	1520	136	10
35.00	330	450	72	164	60	34	530	1200	230	16
35.25	230	110	74	250	52	56	270	780	255	22
35.50	180	490	68	216	30	92	300	920	280	16
35.75	210	180	52	335	30	66	300	690	295	12
36.00	200	300	68	184	78	48	260	1440	400	16
36.25	260	240	86	285	92	96	205	1170	385	16
36.50	370	590	64	275	156*	40	275	690	270	16
36.75	400	440	74	290	220	93	380	1440	210	12
37.00	680	300	54	270	192	67	310	1150	270	24
37.25	430	500	28	170	104	70	500	1050*	270	20
37.50	360	160	68	205*	76	88	450	1050*	230	18

Time (hours & tenths)	Run 1	2	3	4	6	7	8	9	10	11
37.75	180	320	60	240	98	36	490	960	320	16
38.00	290	200	64	215	146	52	480	1550	310	12
38.25	310*	300	108	230	112	16	500	1300	190	24
38.50	330*	320	85	210	125	10	520	1150	152	20
38.75	350	370	62*	230	175	12	460	660	158	46
39.00	330	470	36	180	94	10	630	700	126	26
39.25	290	250	84	260	134	54	650	490	126	24
39.50	200	230	94	244*	150	50	570	1040	160	52
39.75	240	205*	44	228*	96	68	380	910	128	42
40.00	430	180	34	212*	40	40	450	1260	320	30
40.25	440	180	40	196*	26	114	380	1170	285	34
40.50	740	260	28	180	76	24	560	870	390	26
40.75	480	240	18	188	102	36	530	870	190	20
41.00	510	310	8	220	88	40	370	730	300	14
41.25	390	300	28	170	64	16	520	980	240	14
41.50	290	250	76	144	66	22	490	610	410	10
41.75	280	220	82	170	112	61	420	760	144	10
42.00	240	360	78	260	78	74	330	1140	136	14
42.25	630	380	81	290	110	40	420	900	110	18
42.50	570	420	84*	260	88	62	380	1160	230	18
42.75	420	300	120	270	170	66	370*	1150	126	30
43.00	420	310	78	180	104	58	360	970	128	18
43.25	430*	280	130	190	152	82	380	340	250	26
43.50	440	240	100	96	106	78	383*	520	196	24
43.75	460	180	114	97*	105	65	386*	640	138	24
44.00	430	280	84	93*	50	59	390*	1100	96	31*
44.25	620	520	102	98*	130	55	393*	840	188	38
44.50	660	320	104	98	98	58	396*	610	234	46
44.75	470	520	112	117*	68	32	400	720	220	42
45.00	330	480	80	136	65	45	410	800	204	28

Time (hours & tenths)	Run 1	2	3	4	6	7	8	9	10	11
45.25	260	280	52	220	140	28	320	900	166	30
45.50	570	290	78	226	124	20	180	940	84	52
45.75	490	280	50	330	104	12	200	720	204	68
46.00	350	480	30	230	66	12	205*	750	118	74
46.25	480	540	15	198	55	24	210	580	550	56
46.50	360	500	8	202	80	40	200	740	500	70
46.75	390	480	28	212	50	35	250	950	360	64
47.00	310	500	10	206	68	102	280	610	355	38
47.25	390	440	12	220	114	68	280	760*	377*	39*
47.50	200	370	20	250	75	34	350	910	400	40
47.75	230	420	70	178	79	42	240	1050	310	44
48.00	305*	380	20	132	114	24	250	1070	200	28
48.25	380	560	22	136	133	35	300	740	270	26
48.50	340*	430	24	160	123*	27*	310	1065*	202	24
48.75	300	450	16	200*	113*	20	190	1390	290	34
49.00	300	680	36	240	104	20	200	1070	310	30
49.25	[illegible]	340	46	280	112	30	420	620	330	30
49.[illegible]	[illegible]	[illegible]60	30	330	94	10	190	990	285	24
49.[illegible]	[illegible]	390	12	280	84	16	200	600	240	18
50.00	[illegible]	440	22	310	38	32	180	330	210	50
50.25	[illegible]	620	24	240	172	32	190	880	130	34
50.50	[illegible]	460	54	250	250	20	250	770	230	48
50.75	[illegible]	350	148	218	330	22	210	840	230	32
51.00	[illegible]	550	200	220	180	30	250	670	110	48
51.25	[illegible]	570	154	220	170	28*	280	590	250	30
51.50	[illegible]	380	92	212*	110	27*	275	550	178	22
51.75	[illegible]	360	102	204	84	25*	230	1020	206	31
52.00	[illegible]0	720	80	280	95	24	320	950	280	33*
52.25	[illegible]0*	720	70	340	198	20	235	620	174	36
52.50	[illegible]30	480	80	270	167*	26	320	780	300	32

Time	Run									
(hours & tenths)	1	2	3	4	6	7	8	9	10	11
52.75	200	140	52	265*	135*	26	390	950	170	60
53.00	160	240	44	260	104	28	510	850	230	106
53.25	520	680	66	230	112	22	400	790	260	64
53.50	250	300	24	250	60	32	270	1140	170	40
53.75	160	270	52	250	66*	32	360	400	192	14
54.00	350	450	58	250	72	30	308*	730	176	26
54.25	230	388*	30	230	52	20	559	770	178	16
54.50	360	326*	36	280	84	42	810	200	158	26
54.75	240	264*	8	170	92	30	390	1320	110	20
55.00	440	200	28	200	172	44	420	730	112	47*
55.25	610	270	34	360	190	10	530	770	232	74
55.50	600	530	36	200	105	28	480	810	132	30
55.75	360	330	24	130	168	18	250	510	138	24
56.00	280	420	46	220	225	32	350	350	106	16
56.25	700	630	32	210	155	39*	210	360	190	14
56.50	670	520	30	220	232	46	150	1110	120	8
56.75	590	810	20	205	172	22	210	915*	138	12
57.00	590	490	28	305	116	28	180	720	92	11*
57.25	575*	450	16	280	156*	22	190	1070	152	10
57.50	560	300	12	275	64	10	215*	845*	570	22
57.75	440	190	16	255	95	48	240	620	240	42
58.00	240	600	5	220	75*	35	180	850	230	58
58.25	510	900	34	220	55*	32*	150	1070	170	66
58.50	660	595*	22	245	36	30	200	790	68	156
58.75	750	290	40	170	178	34	180	1120	184	250
59.00	640	330	30	270	250	28	400	940	134	190
59.25	470	480	38	240	265	60	540	1020	126	90
59.50	690	460	24	220	250	24	480	1380	124	128
59.75	430	280	26	230	250	42	590	800	104	68
60.00	370	230	34	250	116	32	490	980	106	

Time (hours & tenths)	Run 1	2	3	4	6	7	8	9	10	11
60.25			40			34				
60.50			28			14				
60.75			46			10				
61.00			44			16				
61.25			18			24				
61.50			10			44				
61.75			42			26				
62.00						36				
62.25						36				
62.50						28				
62.75						34				
63.00						38				
63.25						30				
53.50						28				
63.75						16				
64.00						18				
64.25						24				
64.50						20				
64.75						13				
65.00						28				

APPENDIX 4

Confluence Scour Dimensions and Flow Characteristics.

h_s	Absolute scour depth
h_r	Relative scour depth
Q_T	Total discharge
θ	Confluence angle
ε	Relative discharge
Fo	Sediment mobility no.

(a) Sunwapta River

h_s (m)	h_r	Q_T ($m^3 s^{-1}$)	θ (Degrees)	ε	Fo
1.35	5.87	2.70	40	0.030	-
1.20	7.74	1.97	80	0.518	1.318
1.45	7.63	3.52	60	0.239	1.423
1.30	5.78	5.41	100	0.521	1.169
0.52	3.15	2.17	60	0.820	1.255
0.49	3.98	1.32	50	0.091	1.164
1.10	5.64	2.15	80	0.288	1.474
1.10	7.33	1.36	60	0.221	1.406
1.10	5.24	2.50	60	1.102	1.315
0.80	4.44	1.64	100	0.265	1.207
0.61	3.30	1.49	50	0.350	1.248
0.60	3.68	0.94	50	1.021	1.579
0.75	3.26	2.75	50	0.313	1.567
0.80	4.37	2.34	60	0.221	1.851
0.60	3.75	1.46	40	0.160	1.344
0.64	2.98	2.10	60	0.316	1.204
0.48	3.31	2.08	45	0.619	1.435
0.80	3.64	2.54	75	1.172	1.460
0.90	4.61	3.39	55	0.743	1.565
0.40	2.22	1.51	50	0.036	1.504
0.47	2.61	2.37	30	1.350	1.706
0.90	4.09	4.83	50	0.040	1.901
0.65	4.48	1.35	55	1.302	1.423

(b) Laboratory Model

h_s (m)	h_r	Q_T (m^3s^{-1} x 10^3)	θ (Degrees)	ε	Fo
0.019	2.40	0.958	75	0.687	1.607
0.036	3.46	1.066	60	0.010	1.527
0.036	4.21	0.838	35	0.292	1.232
0.040	4.58	0.788	60	0.327	1.226
0.067	5.40	2.777	90	0.451	1.671
0.058	4.31	2.850	65	0.198	1.738
0.060	3.37	3.101	65	0.489	1.728
0.044	3.59	1.197	55	0.873	1.301
0.033	4.49	0.363	75	0.403	1.151
0.033	4.44	0.426	85	0.558	1.447
0.031	3.19	0.835	50	0.332	1.145
0.025	1.89	2.071	20	0.160	1.760
0.039	3.65	0.814	55	0.636	1.125
0.031	3.37	0.627	40	0.119	1.103
0.032	3.44	0.643	40	0.461	1.258
0.030	2.98	0.887	45	0.640	1.232
0.038	3.56	1.543	45	0.089	1.016
0.036	2.96	1.368	30	0.421	1.621
0.036	3.94	0.912	50	0.270	1.387
0.033	2.59	1.710	25	0.014	1.418
0.033	2.72	1.103	30	0.131	1.746
0.037	4.53	0.500	55	0.404	
0.049	4.28	1.254	60	0.046	
0.024	2.57	0.950	30	0.656	
0.029	2.48	1.256	40	0.968	
0.030	2.11	1.456	25	0.343	
0.029	2.43	1.763	25	0.775	
0.039	2.43	1.725	45	0.225	
0.050	4.65	1.220	60	0.114	
0.033	2.75	1.980	25	0.328	
0.030	3.21	0.911	30	0.281	
0.034	2.46	1.814	35	0.616	
0.044	3.48	1.587	75	1.142	
0.042	3.58	1.562	80	1.033	
0.027	2.71	0.744	25	0.172	
0.039	4.15	1.225	55	0.342	
0.038	3.13	0.999	55	0.329	
0.038	2.89	1.531	35	0.592	

APPENDIX 5

Time Series of Sediment Load, Braiding Intensity and Abundance of Avalanche-face Bars in Laboratory Runs.

Notation

T = Time in hours from the beginning of the run

Q_b = Bedload in cm^3 per minute

P = Mean number of active channel segments per flume length

M = Mean number of avalanche-face bars per flume length

T	Run 2			Run 3			Run 4		
	Q_b	P	M	Q_b	P	M	Q_b	P	M
10	280	15	0	83	10	1	111	14	2
11	207	19	1	93	–	–	117	8	3
12	323	24	1	49	–	–	170	18	3
13	298	8	0	79	4	1	193	17	0
14	197	17	0	86	4	0	195	14	2
15	331	13	0	97	8	0	208	14	3
16	390	13	0	99	4	0	146	19	1
17	256	14	1	75	7	0	125	23	3
18	287	15	1	31	7	1	277	15	1
19	513	18	0	23	6	0	106	17	2
20	290	14	1	103	3	0	100	11	1
21	417	9	0	87	9	1	140	7	3
22	570	12	0	70	6	0	93	11	2
23	523	14	0	58	6	0	197	10	1
24	425	13	1	65	1	0	159	20	3
25	377	21	1	69	6	0	138	13	1
26	403	19	2	69	6	0	167	13	2
27	240	13	3	52	6	0	85	18	1
28	293	9	1	77	6	0	119	12	2
29	343	13	0	61	6	0	76	3	1
30	327	10	1	39	9	2	96	5	1
31	350	10	0	18	6	1	71	5	0
32	495	12	2	80	9	0	191	3	0
33	343	23	5	109	4	0	142	3	0
34	217	14	3	100	4	0	176	3	0
35	277	16	0	81	7	0	175	3	0
36	240	14	1	32	4	1	268	5	0
37	413	7	1	17	6	2	243	5	0
38	273	14	0	37	12	1	228	1	0
39	363	14	1	33	6	0	223	1	0
40	215	14	1	19	3	1	212	–	–
41	283	9	0	167	1	0	193	6	1
42	320	14	0	84	4	1	240	3	0
43	297	10	0	54	4	0	213	7	2
44	327	9	0	47	9	4	98	–	–
45	426	10	1	23	15	2	158	1	0
46	433	15	2	34	9	0	253	1	0
47	473	21	3	21	9	0	213	4	1
48	453	18	1	18	15	0	149	4	0
49	490	15	0	36	9	0	240	1	0
50	483	10	0	33	6	0	277	1	0
51	490	9	2	36	4	0	219	1	0
52	600	25	3	26	4	0	275	1	0
53	353	14	2	–	–	–	252	1	0
54	369	11	0	–	–	–	243	1	0
55	245	7	2	21	3	0	243	1	0
56	460	10	1	–	7	2	187	1	0
57	583	5	1	127	4	0	263	1	0
58	563	6	2	47	4	0	232	1	0
59	367	10	3	53	4	0	227	4	0
60	255	13	1	–	4	0	240	4	0

T	Run 6 Q_b	P	M	Run 7 Q_b	P	M	Run 8 Q_b	P	M
10	128	6	0	62	6	0	340	11	6
11	103	17	1	53	6	0	393	7	1
12	133	17	1	23	6	0	355	20	4
13	74	19	1	43	3	1	262	11	1
14	52	18	2	21	3	1	193	8	1
15	85	20	2	29	3	2	223	8	2
16	91	16	3	23	6	0	233	8	1
17	58	17	4	9	6	0	255	8	1
18	-	-	-	14	6	0	305	6	2
19	72	9	4	33	6	0	313	9	3
20	-	-	-	21	9	0	240	11	1
21	136	11	1	36	6	0	287	6	0
22	67	11	0	25	9	0	503	3	0
23	117	10	0	11	6	0	298	3	0
24	86	8	0	28	6	0	357	3	0
25	80	10	0	50	9	0	337	3	0
26	14	13	1	41	9	0	258	3	0
27	92	6	0	-	-	-	197	6	0
28	78	10	0	-	-	-	107	9	3
29	187	6	0	49	3	0	273	11	1
30	106	4	0	44	3	0	150	11	2
31	113	10	1	70	6	0	245	19	2
32	89	22	1	77	5	0	240	14	2
33	91	12	1	35	5	1	408	14	2
34	73	9	2	25	3	0	255	20	2
35	47	6	0	74	3	0	397	10	1
36	78	8	0	31	3	0	480	6	2
37	124	15	1	58	3	0	580	9	0
38	128	15	1	69	11	0	403	9	1
39	126	9	1	60	19	4	473	6	0
40	47	21	0	35	12	2	390	9	0
41	73	14	1	16	9	2	360	8	1
42	92	15	0	68	6	1	390	-	-
43	121	6	0	34	9	2	377	17	1
44	93	7	1	23	12	0	205	17	1
45	110	9	0	27	9	0	270	13	5
46	67	8	1	30	6	0	263	16	2
47	86	9	4	24	3	0	270	20	2
48	114	6	2	25	3	0	190	25	1
49	103	3	1	27	8	0	247	14	0
50	153	3	0	28	4	3	262	19	0
51	153	6	3	32	9	4	433	16	1
52	95	9	3	24	6	3	308	9	3
53	92	6	1	35	9	2	443	9	4
54	69	8	1	41	9	2	270	13	3
55	156	12	3	55	6	1	193	19	5
56	204	3	1	35	6	1	180	14	3
57	110	4	1	51	12	2	373	5	1
58	75	11	2	53	9	0	490	9	2
59	255	6	-	38	6	1			
60	116	13	3	28	6	0			

T	Run 9 Q_b	P	M	Run 10 Q_b	P	M	Run 11 Q_b	P	M
10	900	11	0	153	13	0	81	7	0
11	803	18	1	57	13	4	71	4	0
12	770	19	3	106	14	0	41	6	0
13	1000	14	2	94	11	2	30	5	2
14	833	12	0	108	13	0	58	7	1
15	1007	9	0	195	13	0	72	10	2
16	1023	18	2	166	17	1	25	3	0
17	843	18	1	186	18	1	75	4	0
18	910	6	0	234	8	0	63	4	4
19	560	11	1	111	8	0	35	4	1
20	763	17	2	94	6	1	41	1	0
21	927	16	1	287	3	0	33	6	1
22	817	18	0	272	3	1	35	11	0
23	770	9	0	213	14	5	88	3	3
24	867	12	0	214	17	2	51	8	2
25	613	12	0	220	22	2	21	9	0
26	747	16	0	135	14	1	43	6	0
27	1090	17	3	115	19	2	66	13	0
28	920	19	3	133	15	1	183	9	0
29	990	14	1	163	27	0	95	15	3
30	703	14	1	235	9	0	81	9	3
31	593	15	2	283	18	1	25	13	2
32	760	16	1	167	19	1	37	8	0
33	527	14	2	91	21	2	31	6	0
34	960	14	2	166	16	4	99	6	0
35	1167	9	3	207	9	2	49	3	0
36	1100	18	2	360	12	0	46	3	0
37	1150	9	0	250	23	6	10	5	0
38	1270	13	1	273	14	2	15	3	0
39	617	24	3	137	24	3	17	3	2
40	1113	8	1	244	19	0	15	3	0
41	860	15	4	243	14	1	31	8	0
42	933	13	0	130	16	1	41	8	0
43	687	12	1	168	17	0	20	9	0
44	860	20	1	141	13	0	11	8	2
45	807	6	1	197	11	0	22	6	1
46	683	15	3	291	11	1	24	8	0
47	610	14	1	355	18	1	39	6	0
48	953	12	0	260	15	1	65	6	0
49	1027	11	2	310	18	0	57	9	0
50	603	24	4	193	21	0	37	9	0
51	700	17	3	197	17	0	29	6	0
52	863	17	1	220	12	1	31	14	1
53	863	17	4	220	8	2	43	3	0
54	633	26	1	182	10	2	30	9	0
55	940	12	3	151	12	0	66	3	0
56	407	18	3	145	13	2	27	12	1
57	720	11	3	127	11	1	20	3	0
58	847	13	2	213	9	0	23	10	1
59	1027	9	0	148	5	0	12	1	0
60	980	9	0	106	8	2	41	1	0
61							199	1	0
62							68	6	0